

SURVEY OF CHEMICAL INHIBITION IN FLAMES

Raymond Friedman

Atlantic Research Corporation, Alexandria, Virginia

When a fire is extinguished by addition of a third substance to fuel and air, the mechanism of the effect obviously may be either blanketing, i.e. separation of the fuel from the air, or cooling, i.e. reducing the flame temperature to the point where flame kinetics is too slow to maintain combustion. However, either of these effects would depend on the specific nature of the third substance only through the generally well known physical and especially thermal properties of that substance. Practical experience has shown that some extinguishing agents are significantly more effective than can be accounted for on this basis, and this finding has led to the belief that chemical inhibition may play a key role in fire extinguishment. Evidence for this view will be briefly reviewed here. A more detailed review made in 1957 is available (1).

The most widely known agents believed capable of chemical inhibition of flames of organic fuels fall in two classes: (a) volatile substances containing bromine or iodine; (b) alkali metal salts (except lithium). While one might think it would be relatively simple to demonstrate the superiority of these over other chemical substances, if such superiority exists, by making comparative pan-fire extinguishment tests, this has not proven to be so. One difficulty is the notoriously poor reproducibility of pan-fire experiments, probably largely due to the random nature of the free convective gas motion around such fires. Another complication is that the bromine compounds may themselves be fuels (e.g. methyl bromide) or oxidants (e.g. elemental bromine). In the case of salts, there are problems of knowledge of surface area and degree of dispersion, and the difficulty of knowing the number of salt particles present per unit volume of burning gases. These problems notwithstanding, results of many fire-extinguishment studies tend to show the superiority of the above-mentioned classes of compounds over other substances of similar physical properties.

The combustion scientist, however, would prefer more than statistical evidence from model fire studies. He has made detailed measurements over the past eighty years of flammability limits, burning velocities, and quenching distances of premixed combustible gases at rest or in steady streamline flow, and he has at least partially reliable theories which qualitatively relate these flame properties to the "first principles" of chemical kinetics and gas kinetics. It is only in the past few years that measurements of this kind have been utilized systematically to examine the question of flame inhibition.

Let us first consider flammability limits. For example methane-air mixtures containing less than roughly five or more than roughly fourteen per cent methane are not flammable, the stoichiometric composition lying in the middle of this range. Upon adding additional nitrogen to any flammable methane-air mixture, a point is reached where it is no longer flammable. Finally, thirty-eight per cent additional nitrogen is enough to render all methane-air mixtures nonflammable. While the mechanism causing such a limit is not rigorously known, most combustion scientists would accept the following explanation. Addition of excess diluent, fuel, or oxidant reduces the flame temperature, and hence the rate of heat generation by chemical reaction, according to the Arrhenius law. The rate of heat loss from the flame to the cold surroundings also decreases, but not as much. Thus, heat-loss rate tends

to overtake heat-generation rate as the flame is diluted. The effect is amplified by the fact that as the chemical reaction time increases, in the cooler flame, there is now more time for heat loss from the reaction zone to occur. Thus a finite limit of flammability is predictable mathematically, governed primarily by the magnitudes of the chemical reactivity and the heat-loss rate. (The relative importance of convective and radiative heat loss is not yet well understood.)

Now, if elemental bromine vapor (2) is added to methane-air, 2.45 mole per cent is sufficient to render all mixtures nonflammable, compared with 38 mole per cent nitrogen for the same effect. On this basis bromine is some 15 times as effective as nitrogen in extinguishment on a molecular basis, a result which cannot be explained except as a specific chemical effect, presumably inhibition. It follows from the above finding that one bromine molecule can prevent the combustion of four methane molecules. Many other examples of narrowing of the flammability range by additives have been reported.

Let us now consider burning velocity, which is the idealized rate at which a flat combustion wave would propagate through an initially stationary combustible mixture. This velocity may be deduced, to an accuracy of a few per cent, from the knowledge of the shape of a stabilized laminar flame in a known flow field, as a Bunsen burner provides. The magnitude of the burning velocity is determined by the interaction of two important parameters, the chemical reactivity in the flame and the transport properties of the mixture. Since the latter are influenced only slightly by small additions of possible inhibitors, we have a convenient means of measuring inhibition of the chemical reactivity quantitatively by observing burning velocity.

Consider the data below, which show systematic measurements of reduction in burning velocity by a series of volatile bromine and other halogen compounds:

**ADDITIVE REQUIRED FOR 10% REDUCTION OF
STOICHIOMETRIC METHANE-AIR BURNING VELOCITY (3)**

additive	number of halogen atoms	molecules additive required per 100 molecules CH ₄
HBr	1	1.8
CH ₃ Br	1	1.6
CF ₃ Br	1	1.2
Br ₂	2	0.83
CH ₂ Br ₂	2	0.81
CF ₂ Br ₂	2	0.85
CHBr ₃	3	0.55
CH ₃ Cl	1	4.9
CH ₃ Br	1	1.6
CH ₃ I	1	1.7

Note that one molecule of bromine added to 100 molecules of methane (and 900 molecules of air) is more than enough to produce a ten per cent reduction in burning velocity. It can be shown that the burning velocity varies with the square root of chemical reactivity, so this corresponds to a reduction of 21 per cent in chemical reactivity. Such a small addition could not affect the flame temperature significantly, so the effect must be a chemical inhibition. Note that all seven of the bromine compounds show similar effects, the strength of the inhibition being almost directly proportional to the number of bromine atoms per molecule. Note further that iodine is comparable with bromine while chlorine is much less effective.

Consider now the greater variety of chemical substances tested in another investigation:

**ADDITIVE REQUIRED FOR 30% REDUCTION OF
STOICHIOMETRIC HEXANE-AIR BURNING VELOCITY (4)**

Additive	molecules required per molecule hexane
CO ₂	4.05
N ₂	4.05
Cl ₂	1.54
Br ₂	0.33
TiCl ₄	0.09
PCl ₃	0.07
Pb(C ₂ H ₅) ₄	0.034
Fe(CO) ₅	0.033

Here the fuel vapor is hexane instead of methane and data are reported on the basis of a 30 per cent instead of a 10 per cent reduction in burning velocity. Note that the most effective substance, iron pentacarbonyl, is more than 100 times as effective as the least effective substances, carbon dioxide and nitrogen. Bromine occupies an intermediate position in this list. New data (5) show that iron pentacarbonyl is such a powerful inhibitor that one molecule, added to 10,000 molecules of a stoichiometric methane-air mixture, reduces the burning velocity by 25 per cent.

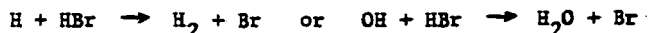
It must be mentioned that pure iron pentacarbonyl is flammable in air, so it would hardly be capable of extinguishing an open fire unless used in combination with some other agent. Nevertheless the powerful inhibiting effect produced by traces is highly suggestive.

We turn now to the third premixed flame property frequently measured by combustion scientists, quenching distance. This is the closest distance of approach of a flame to a cold wall, and is readily determined to about one per cent accuracy by observing the minimum width of a rectangular or circular channel through which a flame can propagate. As does burning velocity, quenching distance depends on transport properties and chemical reactivity. The minimum pressure at which a flame would propagate through a stoichiometric propane-air mixture in a 3.73-diameter tube has been reported (6) to increase from 46 mm Hg to 80 mm Hg upon addition of 0.1 mole per cent methyl iodide, or one molecule of inhibitor per 40 molecules of propane. Since quenching distance of propane-air is nearly inversely proportional to pressure, this result is about equivalent to an 80/46 increase in quenching distance at constant pressure. Similar effects were observed with bromine-containing agents, while carbon tetrachloride was much less effective. Another investigator (7) has measured the depth of flame penetration into a tapered tube of gradually decreasing diameter, the diameter of the tube at the position of furthest flame penetration being taken as the quenching distance. An 8 per cent increase in quenching distance is reported to be produced by addition of one molecule of bromotrifluoromethane per 1000 molecules of stoichiometric methane-air, hydrogen bromide being not quite as effective.

The above examples, based on precise measurements of flammability limits, burning velocities, or quenching distances of premixed hydrocarbon-air mixtures, clearly show that trace quantities of certain gaseous substances can substantially reduce flame reactivity and thus make extinguishment easier. Similar data, although not so quantitative, are available for effects of suspended sodium and potassium salts on flames.

Let us now examine what is known about the chemical mechanisms by which these agents act, a necessary preliminary to rational development of more potent or less toxic agents.

Considering first the bromine and iodine inhibition, we note that the effectiveness of a variety of carrier molecules correlates well with the number of halogen atoms per molecule, so it is reasonable to assume that breakdown to some simple halogen-containing molecule occurs in the flame, the latter being responsible for the inhibition. In the case of bromine inhibition, Br_2 will not exist at flame temperature, so Br and HBr are the candidates. However, to inhibit the flame, it seems probable that the inhibitor must deactivate the most abundant chain-carrying radicals present, H and OH. Monatomic Br could not do this except by slow three-body processes while HBr can easily react by a rapid two-body process, e.g.,



with inhibitor regeneration by hydrogen abstraction:



The radical R must be presumed less reactive (or less capable of upstream diffusion) than the H or OH it replaces. Since H has the unique ability to lead directly to chain-branching via



any inhibiting mechanism capable of removing H (or OH, since $\text{OH} + \text{CO} \rightleftharpoons \text{H} + \text{CO}_2$, is rapid) looks promising. The reaction of H with HBr to form H_2 , however is not a satisfying explanation of inhibition since the H_2 would rapidly oxidize, giving more H atoms. Thus OH radicals may be the key species inhibited by HBr. This kind of speculation was first published by Rosser *et al.* (3), and others who have considered the problem generally utilize this approach as a working hypothesis. However, neither the theory of chain-reaction-governed flames nor knowledge of individual rate constants is sufficiently advanced to permit a theory like this to be proved. Rosser *et al.* (3) have observed that the 3064 Å emission line from excited OH decreased in intensity as bromine was added, but confirmatory evidence obtained by observing unexcited OH in absorption would be highly desirable.

According to the above ideas, HI should behave similarly to HBr, and HCl and HF are too stable to react rapidly with free radicals, so the behavior of the entire halogen family is accounted for if one accepts the foregoing type of mechanism.

Considering now the inhibition produced by other substances, especially metal compounds, we find much less understanding. The mere fact that powerful inhibition can occur is good evidence that chain carriers are being taken out of circulation, and the further fact that hot fuel-oxygen flames are less susceptible to inhibition than cooler fuel-air flames is readily attributed to the much higher radical concentrations believed present in the hotter, faster-burning flames, making them harder to inhibit. To progress beyond this point to specific mechanisms is difficult. Metal atoms might react with O, OH, or H to form oxides, hydroxides, or hydrides, or metal atoms might remove energy from active species by becoming electronically excited and then radiating. When the metal-containing substance is added in dispersed condensed-phase form, there is a choice between assuming surface reaction or vaporization. A paper in this symposium (8) suggests that vapor reactions are the important ones. Much more research is needed in this area.

Finally, attention must be given to the problem of relating information on inhibition of chemical reactivity in a premixed flame to the extinguishment of a fire, which is more nearly a diffusion flame. The rate of combustion in a

diffusion flame is determined by fuel-air mixing rate for a gaseous fuel, or by rate of heat transfer from flame to fuel supply for a slowly volatilizing liquid or solid fuel, and does not depend on chemical kinetics, generally speaking. Thus, introduction of an inhibitor which would cause a moderate reduction of reactivity in a premixed flame would be expected to have no measurable effect on a diffusion flame. Nevertheless, a gaseous diffusion flame as maintained on any of several types of laboratory burners can be extinguished when a sufficient concentration of inhibitor is mixed with the air supply, the necessary concentration of inhibitor being roughly that which would extinguish a premixed flame of the same fuel. This gaseous diffusion-flame extinction process may be attributable to the presence of one or more local regions in the flame, generally at the base, which serve to anchor or stabilize the flame. Such a region, which might be very small, could contain fuel and air which mix before they burn, while in the bulk of the flame, mixing and burning are simultaneous. The inhibitor may exert its entire action in this small region. Detailed studies of this effect have apparently not been made.

A potential method for studying effects of inhibitors on diffusion flames is Potter's experiment (9) in which coaxial opposing jets of fuel and air of equal flow rates meet at a flame surface. At sufficiently high flow rates, the flame ruptures, as indicated by appearance of a hole. Effects of inhibitors on this process have not yet been reported, but such experiments are currently under way in our laboratory.

In conclusion, the fundamental knowledge of flames and inhibition thereof is sufficient to show promise that practical methods of fire control may evolve from this approach, but such knowledge is as yet quite fragmentary, and more basic research is required.

References

1. R. Friedman and J. B. Levy, WADC Technical Report 56-568, "Survey of Fundamental Knowledge of Mechanisms of Action of Flame Extinguishing Agents." 1957. Available from U.S. Dept. of Commerce, Office of Technical Services, as PB 121853.
2. R. F. Simmons and H. G. Wolfhard. T. Faraday Soc. 51, 1211-1217 (1955).
3. W. A. Rosser, Jr., H. Wise, and J. Miller, Seventh Symposium (International) on Combustion, Butterworths, London, 1959, pp. 175-182.
4. G. Lask and H. G. Wagner, Eighth Symposium (International) on Combustion, Williams and Wilkins, Baltimore, in press.
5. U. Bonne, W. Jost, and H. G. Wagner, this symposium.
6. F. E. Belles and C. O'Neal, Jr., Sixth Symposium (International) on Combustion, Reinhold, New York, 1957, pp. 806-813.
7. W. A. Rosser, Jr., S. H. Inami, and H. Wise, WADC Technical Report 59-206, "Study of the Mechanism of Fire Extinguishment of Liquid Rocket Propellants," 1959. Available from U.S. Dept. of Commerce, Office of Technical Services, as PB 151962.
8. W. A. Rosser, Jr., S. H. Inami, and H. Wise, this symposium.
9. A. E. Potter, Jr., S. Heibel, and E. Anagnostou, Eighth Symposium (International) on Combustion, Williams and Wilkins, Baltimore, in press.

IRON PENTACARBONYL IN $\text{CH}_4 - \text{O}_2$ AND AIR FLAMES

U. Bonne, W. Jost, H. Gg. Wagner
Institute of Physical Chemistry, University of Göttingen

Investigating the influence of additives on the propagation velocity and other flame characteristics of laminar flames we tested several substances which showed very pronounced effects on the propagation velocity. One of these was $\text{Fe}(\text{CO})_5$.

In the course of our investigations of reaction rate in low-pressured flames we tried to find the mode of action of $\text{Fe}(\text{CO})_5$ in hydrocarbon-air and hydrocarbon-oxygen flames. To this purpose the pressure dependence of the influence of $\text{Fe}(\text{CO})_5$ was first investigated. In fig. 1 the burning speeds (λ) of methane oxygen mixtures are shown as function of composition. Contrary to other observations (including our own with carbon-monoxide in mixtures with oxygen) but in agreement with our measurements with C_2H_4 and C_2H_6 the burning speed is practically independent of pressure (near the value of maximum flame velocity) down to pressures of about 1 at. Below 0.1 at. the flame speed starts to increase with decreasing pressure.

Fig. 2 gives the influence of iron pentacarbonyl on the burning speed of the stoichiometric $\text{CH}_4 - \text{O}_2$ mixtures at the corresponding pressures. (The $\text{Fe}(\text{CO})_5$ concentration is given in volume percent of the whole mixture). Small inhibitor concentrations have a distinct, but not strong influence. The influence decreases with decreasing pressure (the $\text{Fe}(\text{CO})_5$ concentration is proportional with pressure). In methane-air mixtures (fig. 3) (as well as in other hydrocarbon-air mixtures) the influence of $\text{Fe}(\text{CO})_5$ is much more pronounced. 0.01 % of $\text{Fe}(\text{CO})_5$ causes a decrease in burning speed by 25 % at atmospheric pressure. If one compares the influence of $\text{Fe}(\text{CO})_5$ not in volume percent of the total mixture but in volume percent of the fuel it still remains three times more active in mixtures with air than in those with oxygen. As in CH_4 -oxygen mixtures the additive becomes less active with decreasing pressure. This still holds if the absolute $\text{Fe}(\text{CO})_5$ concentration in molecules per cm^3 remains the same. For comparison fig. 4 shows the influence of added bromine and iron pentacarbonyl on the burning speeds of hydrogen-air (37% H_2) and stoichiometric n-hexane air, for higher percentages of added bromine and chlorine. As was to be expected, the influence of bromine is stronger than that of chlorine, and, less easily expected, benzene is more susceptible to the action of additives than hexane. The effectiveness of $\text{Fe}(\text{CO})_5$ in every case is much more pronounced than that of the halogenes and hydrogenated hydro-carbons.

$$\lambda^* = [\text{O}_2] / [\text{C}_i]_{\text{stoch}}$$

- 2 -

Though the influence of $\text{Fe}(\text{CO})_5$ markedly decreases with decreasing pressure the investigation of the action of this additive on low-pressure flat flames seemed to be useful for learning something about the specific action of the inhibitor on the chemical reaction. The following results may be considered as preliminary ones.

CH_4 -air flames were investigated in some detail with and without additives. The flames were kept burning on flat-flame burners with 12 and 20 cms. diameter, mostly at 60 mm Hg pressure. Temperatures were measured by several independent methods: surface protected platinum-platinum-rhodium thermocouples with compensation for radiation losses, rotational temperatures of OH-bands and occasionally line reversal temperatures.

In fig. (6) the flame temperatures (thermocouple) is plotted versus distance above burner (centimeters) for three different mixtures (1.1 CH_4 +10 air, CH_4 +10 air, 0.9 CH_4 +10 air) burning at 60 mm Hg with a burning speed $v_n = 0.33$ m/sec without additive. Flame temperature and burning speed under these circumstances, of course, depend on the flow conditions chosen. For comparison some rotational temperature values determined from the absorption spectrum of OH are plotted in the same curves.

With added $\text{Fe}(\text{CO})_5$, 0.001 % by volume in the mixture, the thermocouple measurements are no longer reliable, due to iron oxide deposit. This changes radiation losses, and, in addition, may give rise to heterogeneous reactions. From former investigations there is no doubt, that OH radicals play an important role in the propagation of all flames of hydrogen containing compounds. In Fig. 8 OH-concentration and temperature for the stoichiometric CH_4 -air flame are plotted as function of distance from the burner. The decrease of OH concentration in the "burned" gas is mainly due to diffusion losses. In fig. 9 the decrease of OH absorption (as measure for concentration, but not corrected for finite optical thickness) in the burned gases is plotted for the pure mixture of methane with air, for 0.001 % $\text{Fe}(\text{CO})_5$ and 0.005 % $\text{Fe}(\text{CO})_5$ added to the mixture. The concentration decrease of OH itself would be somewhat steeper. The initial increase in OH concentration and its maximum value are hardly influenced by added $\text{Fe}(\text{CO})_5$. Only the position where OH absorption increases is shifted away from the burner with increasing $\text{Fe}(\text{CO})_5$ concentration, and the flames become less stable. If one plots the logarithm of the OH concentration in the zone of nearly constant temperature, for flames with $\text{Fe}(\text{CO})_5$ added, as function of the height above the burner, straight lines are obtained. This points to a decay reaction of first order in the radical concentration.

- 3 -

For very low $\text{Fe}(\text{CO})_5$ concentrations the rate is proportional to the $\text{Fe}(\text{CO})_5$ concentration, while for increasing $\text{Fe}(\text{CO})_5$ concentration its relative influence seems to decrease.

From the experimental results obtained till now we cannot decide whether the recombination reaction of OH is homogeneous or heterogeneous, but it seems that at relatively high $\text{Fe}(\text{CO})_5$ concentrations a heterogeneous decay reaction is dominant while at very low concentrations a homogeneous reaction may become important. In order to achieve further information, spectra of the flames were taken. (The middle of the flame was focused on the slit of the spectroscopy). No. 1, in fig. 10 shows the emission of a stoichiometric CH_4 -air flame at 60 mm Hg around the maximum of OH emission (0.14- 0.9 cms. above the burner). No. 2 shows the emission of the same flame at 2.6 to 3.4 cms. above the burner. The Nos. 3-6 show emission spectra of the same flame, but with 0.005 % $\text{Fe}(\text{CO})_5$ added. No. 3 represents the zone 0.1-0.9 cms. above the burner (two different exposure times). The exposure time of all spectra was identical, while in No. 4, 5, 6 the weaker spectra correspond to 1/15th of the normal exposure time. In the flames with $\text{Fe}(\text{CO})_5$ iron lines and the emission of FeO is seen, but there is no pronounced continuous emission. In the following pictures the emission of different particles measured by a high resolution monochromator are plotted as function of the height above the burner. (fig. 11, 12, 14) As in other cases maximum emission of OH, maximum concentration of OH as well as maximum emission of C_2 and CH do not coincide at all. The emission maximum of OH may be linked to a maximum of reaction rate as the emission maxima of C_2 , CH Fe and the first maximum of FeO. A measure for the concentration of iron atoms is given by fig. 14 where the absorption of the 3659.91 Å iron line is plotted for different $\text{Fe}(\text{CO})_5$ concentrations, (see Fig. 13). While in the flame zone the emission of OH, C_2 , CH and Fe has a pronounced maximum and then decreases very rapidly, the emission of FeO shows a different behavior. It has a second maximum about 3 cms above the burner, in a zone, where OH concentration and Fe absorption decrease rapidly. Then the intensity decreases in a zone where the temperature is still high. Fe, of course, forms solid particles in the flame, but the decrease in radiation intensity does not seem to be connected with the decay of FeO concentration but the second emission maximum of FeO, as well as the first one, seems to be due to chemiluminescence, to the decay of radicals in that zone.

The results, reported, concerning the investigation of the influence of $\text{Fe}(\text{CO})_5$ (and other additives) on the reaction in low pressure flames were made to obtain first impression of the action of this very active inhibitor on the chemical reaction. The investigations are still in progress.

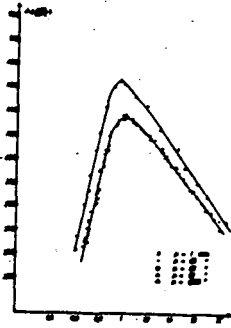


Fig.1 Influence of mixture composition and pressure on the flame velocity of $\text{CH}_4\text{-O}_2$ -flames.

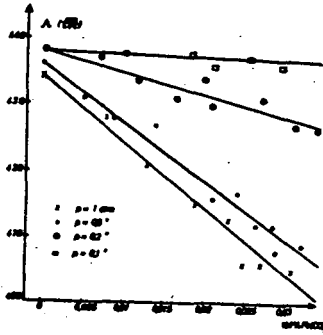


Fig.2 Influence of $\text{Fe}(\text{CO})_5$ and pressure on flame velocity of stoich. $\text{CH}_4\text{-O}_2$ -flames.

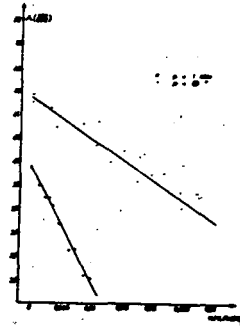


Fig.3 Influence of $\text{Fe}(\text{CO})_5$ and pressure on the flame velocity of stoich. $\text{CH}_4\text{-air}$ -flames.

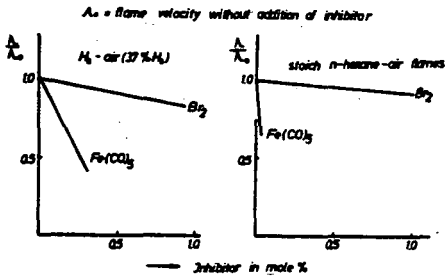


Fig.4 Influence of Br_2 and $\text{Fe}(\text{CO})_5$ on the flame velocity.

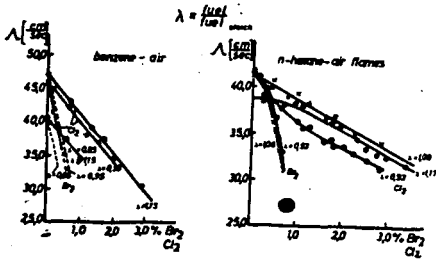


Fig.5 Influence of Br_2 and Cl_2 on the flame velocity.

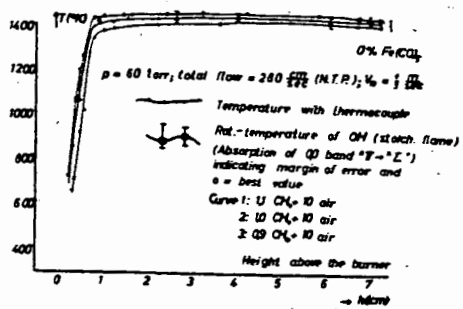


Fig. 6 Temperature in CH_4 -air-flames (Pt-Pt 10% Rh-thermocouple)

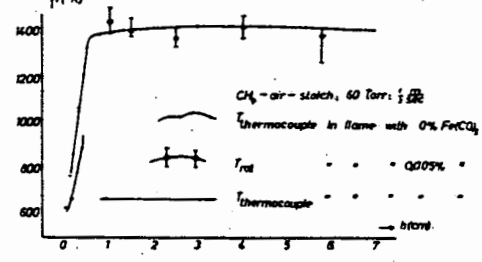
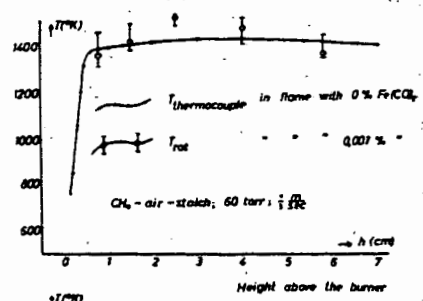


Fig. 7a, 7b Influence of $\text{Fe}(\text{CO})_5$ on CH_4 -air-flames I. Comparison of temperatures.

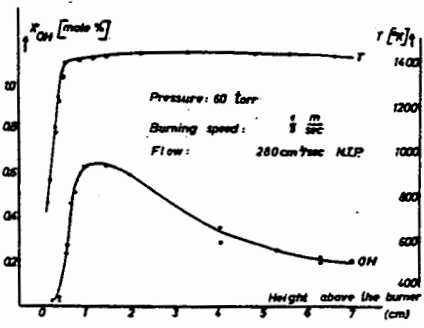


Fig. 8 Temperature and OH-concentration in a stoich. CH_4 -air-flame without $\text{Fe}(\text{CO})_5$.

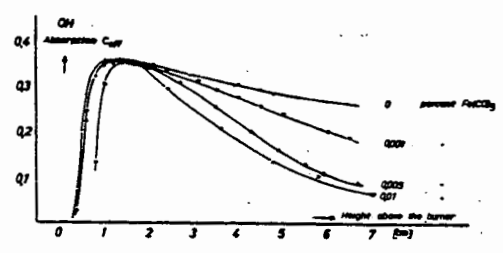


Fig. 9. Influence of $\text{Fe}(\text{CO})_5$ on CH_4 -air-flames.

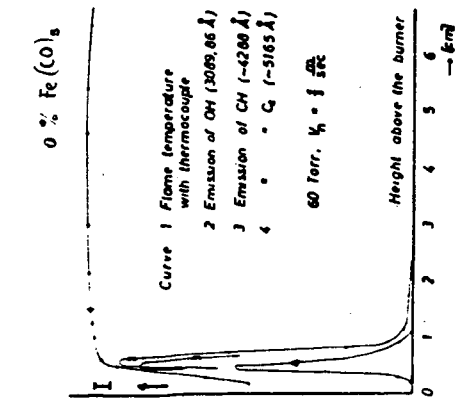


Fig. 11 Influence of $\text{Fe}(\text{CO})_5$ on stoich. CH_4 -air-flames.

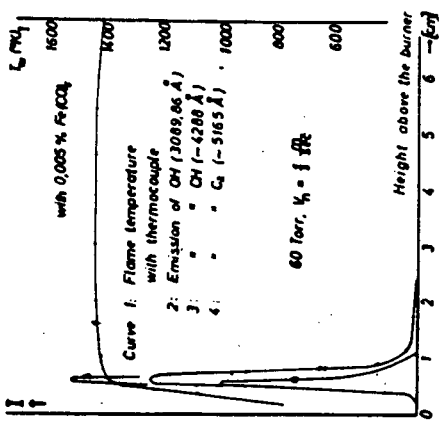


Fig. 12 Influence of $\text{Fe}(\text{CO})_5$ on stoich. CH_4 -air-flames.

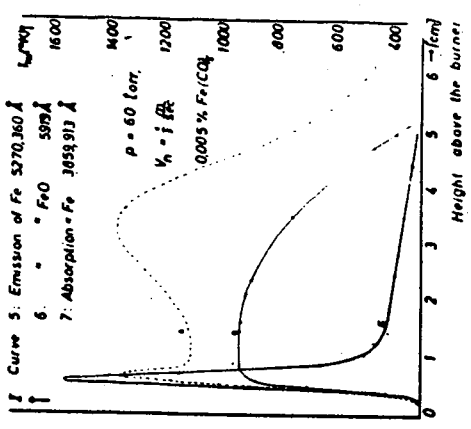


Fig. 13 Influence of $\text{Fe}(\text{CO})_5$ on CH_4 -air-flames. Course of Fe and FeO.



No.	Height above the burner	Remarks
6	6,0 - 6,8 cm	FeO
5	3,1 - 3,9 "	max. of $\text{Fe}(\text{O})_5$ Emission
4	1,1 - 1,9 "	max. of OH Emission
3	0,1 - 0,9 "	max. of OH Emission
2	2,6 - 3,4 "	0
1	0,1 - 0,9 "	0

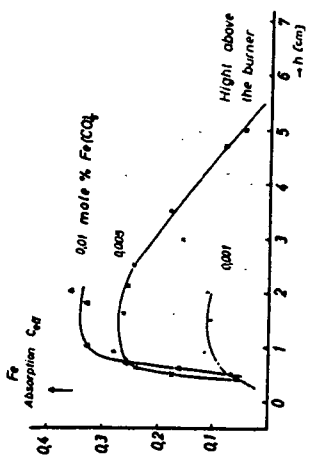


Fig. 14 Influence of $\text{Fe}(\text{CO})_5$ on stoich. CH_4 -air-flames Fe-concentration (C_{Fe} of Fe 3859,913 Å)

The Effect of Powders on Premixed Hydrocarbon-Air Combustion*

Willis A. Rosser, Jr., S. Henry Inami and Henry Wise

Stanford Research Institute, Menlo Park, California

I. Introduction

It has long been known that finely powdered salts such as NaHCO_3 can be used to extinguish fires or to prevent ignition of combustible gaseous mixtures. Various studies (Ref. 1) of combustion inhibition have revealed that powdered materials vary widely in their ability to inhibit combustion, that alkali metal salts are generally effective inhibitors, and that the effectiveness of at least some powders is proportional to the specific surface area of the material (Ref. 2). The available data do not permit identification of the significant processes which result in inhibition. The present study of combustion inhibition by finely divided powders was undertaken in order to elucidate the mechanism of flame inhibition.

II. Experimental Details and Results

A. Materials

Various gases were used as obtained from commercial sources. These included C.P. CH_4 , C_3H_8 , NH_3 , and A from the Matheson Co., industrial grade O_2 , commercial dry N_2 from General Dynamics Corp. Compressed laboratory air was dried prior to use by passage through a bed of granular CaCl_2 .

All the powders used were C.P. anhydrous materials. Some were of sufficient fineness to be used as received; most, however, required some size reduction. These were wet milled with acetone in a small laboratory ball mill. After milling, the powder was first air dried under a heat lamp to remove the bulk of the acetone and then oven dried at about 110°C . The dry powder cake was pulverized by brief ball milling and then sieved through a 250 or a 325 mesh stainless steel screen. Most of the test powders were used without further treatment.

Milled powders contained a wide range of particle sizes. Two methods of size separation were tried, sieving and gas elutriation. Attempted sieving by means of micromesh screens was unsuccessful because the screens plugged quickly. Gas elutriation with dry N_2 was inefficient and slow except at high gas flow rates. Some size reduction could be obtained but not as much as desired. Consequently, gas elutriation was used only for special purposes and not as a standard procedure.

B. The Dispersal of Powder in a Combustible Gas

A dispersing device was assembled for the introduction of powders into combustible gas mixtures which performed adequately for most cases. The powder

*This paper is based on research supported by the Wright Air Development Division, Air Research and Development Command, United States Air Force, under Contract AF 33(616)-6853.

generator (Fig. 1) consisted of a Pyrex cylinder (6 cm i.d.) fitted at each end with large rubber stoppers. The generator was provided with five jets through which gas could enter the system, a four-bladed propeller to agitate the powder bed, and an exit tube for the gas-powder mixture. The propeller was driven by a 1500 RPM electric motor. Four of the gas jets were made from glass tubing and had an opening of about 1 mm in diameter. The fifth jet, used only to obtain high powder concentrations, was made from brass tubing with a hemispherical cap through which five holes 0.015 inch in diameter had been drilled. One of these holes was on the axis of the tube, the other four were arranged symmetrically around it. The gas emerging from these holes was very effective in picking up powder from the powder bed.

In order to introduce the powder into the gas mixture a steady flow of pre-mixed fuel and oxidizer of known composition from a conventional gas handling system was split by means of needle valves into two streams; one passed directly to the vertical output tube of the powder generator, and the other entered the powder generator through the glass jets. The concentration of powder in the final mixture could be changed by varying the relative amounts of the two gas streams up to the point when all of the gaseous mixture passed through the generator. If even higher powder concentrations were desired, it was again necessary to split the gas flow, this time into a fraction which entered the generator through the four glass jets and the remainder through the metal jet. In this manner it was possible to obtain powder concentrations up to about 10% by weight of the gas flow.

C. Measurement of the Effect of Powder on Combustion

The effectiveness of the powder was determined from the change in flame propagation velocity as measured in the apparatus shown in Fig. 1. A long glass cylinder, about 2 cm in diameter, was inserted a short distance into the generator. The gas-powder mixture from the generator flowed vertically upward through the tube and was vented to the atmosphere at the top. After a steady flow of gas-powder mixture had been established, the powder output was measured by collecting on a glass filter paper* the powder content of the gases. A collection time of 30 or 60 seconds was usually sufficient to give a weighable amount of powder on the filter. The weight concentration of powder in the gas was calculated from the collection time, the weight of collected powder, and the flow rate of the gas stream. Immediately after a powder sample had been collected, the flow of gas was stopped, the damper valve closed, the side vent opened to the atmosphere, the top of the tube capped with a rubber stopper, and the mixture ignited by spark. The time required for the flame to travel between two fixed points on the tube was measured by phototubes. The phototube signals were displayed on an oscilloscope face and photographed by Polaroid camera. The average propagation velocity of the flame was calculated from the known distance between the phototubes and the measured time of transit.

In the absence of powder the flames were approximately hemispherical in shape; after the first few inches of travel, they moved through the tube at an apparently uniform rate. Slight tilting of the flame was sometimes observed. The presence of powder at times resulted in irregular flame shapes. Because the propagation velocity v is related to flame speeds by $v = SA_f/A_t$ (where A_f = the area of the flame and A_t = cross-sectional area of the tube), these perturbations of flame shape are a source of error. In extreme cases the flames were extremely long and highly tilted, as a result of nonuniform powder distribution in the tube.

* Mine Safety Appliance Co.

D. Measurement of Particle Size and of Specific Surface Area

Specific surface area of the experimental powders was measured by an optical method (Ref. 3). About 20 mg of powder was thoroughly dispersed in about 300 ml of acetone contained in an optical cell and the optical density of the mixture measured. The total specific area of the powder, A^* , was calculated from the approximate relation

$$A^* = \frac{-4 \ln \xi_1}{2cl} \quad (1)$$

where ξ_1 = the initial optical transmission, c = the powder concentration in gms/cc, and l = optical path length (5 cm in this case).

When size analysis was desired, the optical density was recorded for a period of time sufficient for settling of the powder suspension. The distribution of particle sizes can be derived from the chart record of $-\ln \xi$ vs. time (Refs. 3 and 4).

The specific surface data listed in Table I were obtained in the manner described. The average particle size, \bar{d} , is defined by Eq. 2

$$\bar{d} = \frac{6}{\rho A^*} \quad (2)$$

where ρ is the density of the powder material. One gram of powder containing only particles of diameter \bar{d} would have the same surface area as one gram of the actual powder. Size analysis revealed that \bar{d} is only a crude measure of powder fineness. All powders listed in Table I, even the coarse ones, contained a substantial number of particles with diameters of only 2 or 3 microns. For example, the weight distribution of NaF particles passed through a maximum at about 3.5μ although $\bar{d} = 6.5\mu$.

The data in Table I refer to samples collected at the exit of the flame tube. Comparison of that data with surface data for the powder initially present in the generator revealed little or no difference for fine powders ($A^* \approx 10,000 \text{ cm}^2/\text{gm}$). For coarse powders the material collected at the burner tube was finer than the original powder charge. It appears that the generator also functioned to some extent as an elutriation device. To avoid error from such elutriation only a few per cent of the initial powder charge in the generator was used in a related series of measurement.

E. The Effect of Powders on Premixed Flames

Several of the powders tested were not effective inhibitors of premixed CH_4 -air combustion. About 5 wt % of CaF_2 , talc, CaCO_3 , or $\text{Ca}(\text{OH})_2$ was required to reduce by 10% the speed at which a stoichiometric CH_4 -air flame propagated through a tube. Heat and momentum loss by the flame are sufficient to account for that degree of reduction. On the other hand, the remainder of the powders tested, NaF, NaCl, NaBr, CuCl, K_2SO_4 , NaHCO_3 , KHCO_3 , and Na_2CO_3 were effective inhibitors of CH_4 -air combustion to a degree which indicates chemical interference with the combustion process.

As shown in Fig. 2, relatively little Na_2CO_3 is required to produce a significant reduction in the propagation velocity of a stoichiometric CH_4 -air flame. These following features should be noted: (a) the weight concentration of powder when expressed in mg/cc is very nearly the same as the weight fraction; (b) the scatter in the data is primarily due to perturbations of flame shape; (c) the ratio of flame area to tube, apart from erratic perturbations, increases from about 2 at zero inhibitor concentration to about 4 at concentrations corresponding to points on the nearly horizontal portion of the curve; (d) the powder concentration corresponding to the intersection of the dotted straight lines may be used as

a measure of inhibitor effectiveness. The lower this critical concentration, the more effective the inhibitor. For fine Na_2CO_3 this intercept concentration is about 0.6 wt % whereas for the coarser Na_2CO_3 the intercept concentration is about 1.1 %. Comparison of these values with the specific surface area of the two powders indicates that powder effectiveness is approximately proportional to specific surface area.

As shown in Fig. 3, similar results were obtained using NaHCO_3 . Because of flame perturbations for low concentrations of NaHCO_3 , the relation between powder effectiveness and A^* could not be determined with precision. However, a size effect is clearly evident. In view of the fact that NaHCO_3 decomposes to Na_2CO_3 at relatively low temperature, it is probable that the observed effectiveness of NaHCO_3 merely reflects the effectiveness of Na_2CO_3 . The data shown in Figs. 2 and 3 are consistent with this interpretation. The effect of KHCO_3 , $A^* = 12,400 \text{ cm}^2/\text{gm}$, on propagation velocity is shown in Fig. 4. Comparison with the data for NaHCO_3 , $A^* = 11,900 \text{ cm}^2/\text{gm}$, reveals that KHCO_3 powder is twice as effective as NaHCO_3 powder. It is noteworthy that KHCO_3 has been found to be twice as effective as NaHCO_3 as a fire extinguisher (Ref. 5). Because both NaHCO_3 and KHCO_3 decompose readily to the respective carbonates, the effective inhibitor in both cases is probably the alkali carbonate. The effectiveness of NaHCO_3 for non-stoichiometric CH_4 -air mixtures (CH_4 from 8 to 12 % by volume) was comparable with or slightly greater than for the stoichiometric flame.

The effect of NaBr , NaCl , NaF , CuCl , and K_2SO_4 on stoichiometric CH_4 -air flames was also measured. Precise results were obtained for NaCl and CuCl (Figs. 5 and 6). Qualitatively NaBr , NaF , and K_2SO_4 were also effective inhibitors, but because of extreme flame instability precise data could not be obtained. This instability is apparently associated with poor dispersibility of the powder.

Flame inhibition by dispersed powder is affected by oxidizer concentration. A stoichiometric CH_4 - O_2 flame diluted with N_2 so that $\text{O}_2/(\text{O}_2 + \text{N}_2) = 0.25$ required 1.7 wt % of fine Na_2CO_3 to reduce the linear speed from 142 cm/sec to the intercept point which in this case occurs at about 20 cm/sec. The increase in powder requirement reflects primarily the higher initial propagation velocity. Support for this view is provided by another experiment using a CH_4 - O_2 - A mixture with an initial propagation velocity very nearly the same as that for a stoichiometric CH_4 -air flame, 65 cm/sec. The effectiveness of KHCO_3 in the two cases was much the same, about 0.6 wt % powder. In contrast, the presence of about one per cent by volume of CH_3Cl in a stoichiometric CH_4 -air mixture considerably reduced the effectiveness of Na_2CO_3 , although the CH_3Cl itself has very little effect on the initial propagation velocity of the mixture (see Fig. 7).

The effectiveness of Na_2CO_3 (or NaHCO_3) was found to vary with the nature of the fuel. About 2.5 wt % of Na_2CO_3 , $A^* = 10,800 \text{ cm}^2/\text{gm}$, was required to reduce the propagation velocity of a stoichiometric C_3H_8 -air flame from 80 cm/sec to 20 cm/sec, compared to about 1 wt % for a stoichiometric CH_4 - O_2 - N_2 mixture of the same initial propagation velocity. The noncarbonaceous system NH_3 - O_2 - N_2 was found to be only slightly affected by powdered NaHCO_3 . For a near stoichiometric composition with an oxidizer concentration $\text{O}_2/(\text{O}_2 + \text{N}_2) = 0.4$, two wt % of NaHCO_3 , $A^* = 11,980 \text{ cm}^2/\text{gm}$, only reduced propagation velocity from 62 cm/sec to 52 cm/sec.

III. The Temperature History of Small Particles Exposed to a Premixed Flame

During passage through a flame the individual particles of a dispersed powder will be heated and may partially evaporate. The heat transferred from the flame gases to the particles may not represent a significant thermal drain on the flame,

but the evaporated material may effect the combustion reactions. Two problems must be considered: the degree of heating of small particles by the flame, and the extent of evaporation resulting from this heating. The two problems are coupled and in their entirety are extremely difficult to solve. However, with some simplifying assumptions it is possible to obtain solutions which are adequate for our purposes.

The actual temperature profile through a premixed flame is replaced by the profile shown in Fig. 8, which has been divided into three zones: a preheat zone in which the temperature of the unburned gas rises exponentially with distance, a reaction zone in which the temperature rises linearly with distance, and a post-combustion zone of uniform temperature. The assumed temperature profile has been terminated at a definite position $x = \delta$, because where strong chemical inhibition occurs it must occur where the reaction rate is high, that is, in or near the visible flame. The reactions which take place in the post flame gases do so gradually over a distance large compared with the thickness of the visible flame. Particles in the region $x > \delta$ may affect these processes and will eventually reach thermodynamic equilibrium with the hot combustion gases. In this analysis, however, the region $x > \delta$ will not be considered. In addition, because the observed sensitivity of flame speed to the presence of some powders is far greater than can be accounted for by heat loss alone, the effect of the powder on T_a , the adiabatic flame temperature, has been neglected.

In the preheat zone the reaction rate is taken to be zero. Consequently, the temperature profile has the form (Ref. 6)

$$\frac{T_1 - T_i}{T_0 - T_i} = \exp\left(\frac{c\rho_i Sx}{\lambda}\right) \quad (3)$$

where

- ρ_i = the initial gas density
- T_1 = the gas temperature at a point x
- T_i = the initial gas temperature
- T_0 = an ignition temperature
- c = the average heat capacity of the gas
- λ = the average thermal conductivity of the gas
- S = the flame speed

The preheat zone ends at the point $x = 0$, where $T_1 = T_0$. For mathematical convenience T_0 is taken as the average of T_i and the adiabatic flame temperature T_a . The quantities c and λ should be values averaged over the temperature interval $T_0 - T_i$. Because c and λ also appear in calculations for the reaction zone, it is more convenient to evaluate c and λ at T_0 and use those values for both the preheat and the reaction zones.

The gas temperature in the reaction zone increases linearly from T_0 to T_a and can be represented by the expression

$$\frac{T_1 - T_0}{T_0 - T_i} = \frac{x}{\delta} \quad (4)$$

where $\delta = \frac{\lambda}{c\rho_i S}$. Equation 4 is the tangent to Eq. 3 at the point $x = 0$. As shown in Fig. 8, the parameter δ is the thickness of the reaction zone, about 0.2 mm for a stoichiometric CH_4 -air flame.

In both the preheat and the reaction zones the time rate of temperature increase of nonevaporating spherical particle has been represented by Eq. 5.

$$\rho_s c_s V \frac{dT}{dt} = 2\pi d \lambda (T_1 - T) \quad (5)$$

where

V_s	=	volume of the particle
d	=	diameter of the particle
T_1	=	the gas temperature
T	=	the particle temperature
c_s	=	specific heat of the particle material
ρ_s	=	density of the particle

The most important assumptions implied by Eq. 5 are:

- (1) The thermal conductivity of the particle material is very large, consequently the temperature within the particle is uniform and equal to the surface temperature
- (2) The course of particle heating may be regarded as a succession of incremental steady states
- (3) The Nusselt number for heat transfer equals 2.

These plausible assumptions simplify the mathematical problem but may introduce some error. The first of these assumptions is the least serious. A rigorous treatment of a related problem, the temperature history of a small particle of similar physical properties suddenly immersed in a large quantity of a hot gas, indicated that no significant error resulted from the assumption of uniform particle temperature.

A certain length of time is required to attain a steady state for either heat transfer or diffusion. For heat transfer, a measure of this time is the quantity $l^2/2\alpha$, where l is some characteristic distance, and α is the thermal diffusivity of the gas. Similarly, for diffusion a measure of the time is the quantity $l^2/2D$ where D is the diffusion constant of the evaporating material through the surrounding medium. For this problem α and D are of comparable magnitude, a few cm^2/sec . The characteristic distance l may be taken as the radius of the particle. For particles with radii less than 5 microns the time required for attainment of a steady state (for either diffusion or heat transfer) is found to be less than 10^{-7} sec, compared to the transit time through the flame greater than 10^{-4} sec. It may be concluded that the steady state assumption involves little or no error.

The applicability of the steady state assumption for heat transfer is implied when using a value of two for the Nusselt number. In addition, only conductive heat transfer is taken into consideration. For the very small particles with which we are concerned this is probably the case.

The velocity of a particle being swept along by a moving gas will always differ from that of the gas itself. The importance of this lag can be estimated by comparing the relaxation time associated with velocity lag to the transit time of the particle through the flame. The relaxation time for velocity lag is given by the expression $\tau_v = \frac{2r^2\rho}{9\eta}$ where r = radius of the particle, ρ = density of the particle, η = viscosity of the surrounding gas. This time τ_v is the time required for a particle initially at rest in a quiescent gas to accelerate as a consequence of gravitational pull to $(1 - \frac{1}{e})$ of the terminal velocity. The lag time τ_v was evaluated for various values of r , with $\rho = 2$ gms/cc, and $\eta = 490$ μpoises (this value of η corresponds to air at about 1000°C). For

$r = 1\mu$, $\tau_v = 0.9 \times 10^{-5}$ sec, and for $r = 5\mu$, $\tau_v = 2.3 \times 10^{-4}$ sec. The transit times of interest are in the range 10^{-4} to 10^{-3} sec. It appears that velocity lag is not a serious perturbation for small particles ($r \sim 1$ or 2μ) but will occur to some extent for larger particles ($r \sim 5\mu$). The effect of velocity lag will be to lengthen the time of exposure of the particle to the flame. The rate of heat transfer will not be significantly affected because of the low Reynolds number associated with small particles and the relatively low gas velocities used. In these semi-quantitative calculations the effect of evaporation on drop and heat transfer is not taken into account.

Equation 5 may be converted to a form involving distance rather than time by means of the relation

$$\frac{dT}{dt} = \bar{v} \frac{dT}{dx} \quad (6)$$

where \bar{v} is the average velocity of the gas-powder mixture. The use of a single average velocity for both gas and powder requires that the particles be small enough to follow the gas flow.

The integral of Eq. 6 for values of $x < 0$ is given by

$$\frac{T - T_i}{T_o - T_i} = \frac{\phi \delta e^{x/\delta}}{1 + \phi \delta} \quad (7)$$

where

$$\phi = \frac{12 \lambda}{\bar{v} c_s \rho_s d^2} \quad (8)$$

Based on the conservation of mass equation the average flow velocity of the gas-powder mixture, \bar{v} , is approximately equal to $4S$ for near-stoichiometric CH_4 -air flames. For values of $x > 0$, the integral of Eq. 6 is given by

$$T = T_o + (T_o - T_i) \left[\frac{e^{-\phi \delta (x/\delta)} + \phi \delta (x/\delta) - 1}{\phi \delta} - \frac{e^{-\phi \delta (x/\delta)}}{1 + \phi \delta} \right] \quad (9)$$

and at $x = \delta$,

$$T_w = T_o + (T_o - T_i) \left[\frac{e^{-\phi \delta} + \phi \delta - 1}{\phi \delta} - \frac{e^{-\phi \delta}}{1 + \phi \delta} \right] \quad (10)$$

The particle temperature within the reaction zone is seen to depend on the product parameter $\phi \delta$ and on the dimensionless distance-ratio x/δ . The particle temperature at the end of the reaction zone is a function of $\phi \delta$ alone.

The temperature T_w has been calculated as a function of particle size for these specific values: $c_s \rho_s = 2/3$ and 1 , $\bar{v} = 4S$, $\lambda = 2 \times 10^{-4}$ cal cm^{-1} sec^{-1} deg^{-1} , $\rho_i = 1 \times 10^{-3}$ gms cm^{-3} , $c = 1/4$ cal gm^{-1} deg^{-1} , and $S = 40, 25, 15$, and 10 cm sec^{-1} . The cited values for $c_s \rho_s$ are applicable to NaCl and NaF, respectively. It is clear from the variation of T_w with particle size (Fig. 9) that the degree of particle heating can be great and that particle temperature can rise high enough to result in evaporation of materials not usually considered volatile.

In an isothermal system the steady state molar rate of flow, ψ_M , of material M diffusing away from a sphere of radius r may be represented by

$$\psi_M = -4\pi D r n \ln \left(1 - \frac{n_1}{n} \right) \quad (11)$$

where n = total molar concentration
 n_1 = molar concentration of "M" at the surface of the sphere
 D = diffusion constant of "M"

If the ratio $n_1/n \ll 1$, Eq. 11 may be approximated by

$$\psi_M = 4\pi D r n_1 \quad (12)$$

Relative to unevaporated material the enthalpy flow ψ_L associated with the molar flow, ψ_M , is given by

$$\psi_L = 4\pi D r n_1 L \quad (13)$$

where L is the molar heat of evaporation. In a nonisothermal system, such as a flame, the material diffusing away from a particle will be further heated as it diffuses. This enthalpy increase, however, is small compared with L which is about 40 to 50 kcal/mole for the materials we will consider and, therefore, it will be neglected. The diffusion and heat transfer processes are then coupled only at the surface of the particle. As in the case of heat transfer alone, it is assumed that steady state expressions can be used to describe the rate at which mass and heat are transferred.

Evaporation (an endothermic process) is limited by, and can proceed only to, the extent that heat is provided to maintain the process. The rate of conductive heat transfer, q , from the flame gases to the particles is given by

$$q = 2\pi d \lambda (T_1 - T) \quad (14)$$

Initially, $q \gg \psi_L$, and both the particle temperature and n_1 increase. Eventually there may arrive a time when $q = \psi_L$ and evaporation may be regarded as having begun at that time. Further addition of heat to a particle will result primarily in evaporation and only secondarily in an increase in particle temperature. This temperature increase is not thermally significant but is important in that n_1 is a strongly varying function of particle temperature. The temperature at which evaporation may be considered to have begun can be obtained by equating Eqs. 13 and 14.

$$\lambda (T_1 - T) = n_1 L D \quad (15)$$

The quantity n_1 is related to particle temperature by

$$n_1 = A e^{-L/RT} \quad (16)$$

Equation 16 when substituted in Eq. 15 results in

$$T_1 - T = \frac{A e^{-L/RT} D L e}{\lambda} \quad (17)$$

The initial evaporation temperature is that temperature T_e consistent with Eqs. 4, 9, and 17 (for $x > 0$).

By graphical methods T_e was determined as a function of particle size for NaCl and NaF. The necessary thermodynamic data were obtained from Ref. 7 and used to derive expressions of the type Eq. 16 for n_1 . For NaCl these data were used: B.P. = 1738°K, L at B.P. = 41 kcal/mole, $D = 4 \text{ cm}^2/\text{sec}$. The quantity n_1 was represented by

$$n_1 = 0.924 \times 10^{-8900/T} \text{ moles/cc} \quad (18)$$

For NaF these data were used: B.P. = 1977°K, $L = 48 \text{ kcal/mole}$, $D = 4 \text{ cm}^2/\text{sec}$, and n_1 was represented by

$$n_1 = 1.12 \times 10^{-10,400/T} \text{ moles/cc} \quad (19)$$

In both cases the diffusion constant D is an estimated value.

The variation of T_e (initial) with particle size was determined graphically. Because S and r enter into the parameter ϕ in the same way, once T_e is shown as a function of particle size for a given flame speed, T_e can readily be calculated as a function of size for other flame speeds. For either NaCl or NaF the initial evaporation temperature increases with increasing particle size up to a maximum value, $T_e(\max)$. The temperature of an evaporating particle cannot exceed (although it will reach) $T_e(\max)$ at $x = \delta$ unless the particle evaporates completely during passage through the flame. For NaCl, $T_e(\max) = 1480^\circ\text{K}$, and for NaF, $T_e(\max) = 1650^\circ\text{K}$.

Equation 12 implies that a particle evaporating under steady state conditions will decrease in size at a rate described by the expression

$$d^2 = d_0^2 - \frac{8 M D n_1 t}{\rho_s} \quad (20)$$

where M = molecular wt of material.

A similar steady state expression can be derived for a particle evaporating in a flame

$$d^2 = d_0^2 - \frac{8 M \lambda}{\rho_s L} \int_0^t (T_1 - T) dt \quad (21)$$

In Eq. 21, n_1 has been eliminated by means of Eq. 15. Time is measured from the onset of evaporation as previously defined. Let x_e be the point in the flame corresponding to this time. In the cases we will consider, $x_e > 0$. This distance will be traversed in a time $\tau = (\delta - x_e)/\bar{v}$.

$$\frac{d_w^2}{d_0^2} = 1 - \frac{8 M \lambda}{\rho_s L} (\overline{T_1 - T}) \tau \quad (22)$$

where d_w = diameter of the particle at $x = \delta$

$(\overline{T_1 - T})$ = the average temperature difference between the gas and the particle in the interval $\delta - x_e$.

Further, $\bar{v} = 4S$, and after substitution for τ and \bar{v} and some manipulation, Eq. 22 can be transformed into Eq. 23, a form suitable for determining the degree of evaporation.

$$\frac{d_w^2}{d_0^2} = 1 - \frac{2 M c_s (\phi\delta)_0}{3'L} \left(1 - \frac{x_e}{\delta}\right) (\overline{T_1 - T}) \quad (23)$$

The parameter $(\phi\delta)_0$ is the value of $\phi\delta$ appropriate to d_0 and to an assumed value of the flame speed. The quantity $1 - \frac{x_e}{\delta}$ can be obtained from a graph of $(T_1 - T_e)_i$ as a function of $(\phi\delta)_0$, the value of $(\phi\delta)_0$, and Eq. 4. The quantity $(\overline{T_1 - T})$ may be taken without significant error as the average of $(T_1 - T_e)_i$ at $x = x_e$ and $(T_1 - T_e)_f$ at $x = \delta$. For NaCl, $(T_1 - T_e)_f = 720^\circ\text{K}$ and for NaF, $(T_1 - T_e)_f = 550^\circ\text{K}$.

Proceeding as indicated, we calculated the fractional degree of evaporation, $f = 1 - \frac{d_w^3}{d_0^3}$, for NaCl and NaF. The results are shown in Fig. 10. The product Sd_0 is constant for a given degree of evaporation. Consequently, the variation of f with particle size for any flame speed can be easily obtained once the variation is known for a single flame speed.

The calculation of degree of evaporation carried out for $x = \delta$ can be done for other selected values of x . For the purpose of demonstrating that small

particles of materials such as NaCl and NaF will partially evaporate during passage through a flame, the results shown in Fig. 10 for $x = 8$ are sufficient.

The mathematical analysis just described can only be successfully applied to materials for which there is available a relation between the vapor pressure and the temperature of the material. Substances such as Na_2CO_3 which decompose during evaporation cannot be treated. Therefore, the relative volatility of several such materials was determined in the following way. A small quantity of material was fused by flame onto the end of a platinum wire until a small bead about 1 mm in diameter had been formed. The bead and wire were suspended in a Meker burner flame about 1 cm above the primary cones. By stopwatch, the time was measured from the appearance of color in the flame gases to the disappearance of that color. The results of such measurements are shown in Table II.

Consideration of the data in Table II reveals a number of interesting facts. NaF and Na_2CO_3 have roughly the same volatility. Consequently, the degree of evaporation derived for NaF can be expected to apply roughly to Na_2CO_3 as well. Next, K_2CO_3 is seen to be about twice as volatile as Na_2CO_3 . This is also about the same as the ratio of inhibition effectiveness for these two materials. Lastly, all the test substances except Na_2CO_3 are more volatile than NaF and small particles of these substances would be expected to evaporate during passage through a flame to an even greater extent than NaF particles of the same size. Powders of all but two of the materials listed in Table II were tested experimentally and found to be effective inhibitors of CH_4 -air combustion. Materials which were not effective inhibitors, talc, CaCO_3 , $\text{Ca}(\text{OH})_2$, and CaF_2 are not volatile at the flame temperatures encountered in our system and would not be expected to evaporate to a significant extent during passage through a CH_4 -air flame although CaCO_3 and $\text{Ca}(\text{OH})_2$ might decompose to CaO. It appears that evaporation and inhibition effectiveness are companions and that the observed inhibition is due to evaporated materials. With increasing flame temperature some of these less volatile materials may exhibit a higher degree of effectiveness.

IV. Discussion

The theoretical analysis presented in Section III revealed that a significant amount of evaporation will occur for those powders which were found to be effective inhibitors. The extent of evaporation will depend on the temperature history of the powder particles and on the volatility of the material. The calculated results for NaCl and NaF shown in Fig. 10 indicate a high degree of evaporation by the end of the reaction zone. The average extent of evaporation in the reaction zone will be lower. For all but the very finest powders the degree of evaporation for the spectrum of particle sizes present in the powder is probably much less than one. Under such conditions one would expect a proportionality between powder effectiveness and specific surface area. An increase in specific surface area will result in greater fractional evaporation. Evaporation can, of course, be completed in the post flame gases, but we are not concerned with that region -- only with the reaction zone itself.

Two essential tasks remain: to identify the species responsible for inhibition and the reactions involved. To that end, consider first the relatively simple case of NaCl. The condensed material will evaporate at high temperatures primarily as NaCl molecules. The NaCl in diffusing through the hot reaction gases may be converted to Na by reactions such as



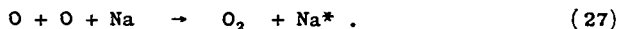
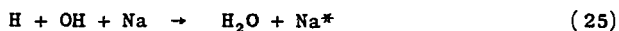
Experimental observation of flames in which Na and Cl were both present indicates that the conversion will not be complete (Ref. 8). Consequently, both Na

and NaCl must be accepted as major species involving Na. Traces of NaOH can also be present, as well as minute concentrations of sodium hydride or sodium oxides. However, the oxides have never been observed spectroscopically in flames which also contained sodium (Ref. 9). Inasmuch as only minute concentrations are required to give observable emission spectra, the presence of significant quantities of these compounds is unlikely. As far as NaCl is concerned, the major species to consider are Na and NaCl.

Consider next the more complicated case of Na_2CO_3 which evaporates with decomposition. Depending on the circumstances one may initially have Na, Na_2O , Na_2O_2 , etc. The initial spectrum of products in the course of diffusing away from the particle will be altered. The major species to be expected at some distance from the particle is the Na atom. The presence of chlorine species in the gas will convert a portion of that sodium into NaCl. The observed decrease in powder effectiveness as observed in the presence of Na_2CO_3 powder and CH_3Cl (see Fig. 7) indicates that NaCl is relatively inactive and that inhibition is associated with the sodium atom. By implication the overall effectiveness of a sodium compound depends not only on volatility but also on the availability of the atom after evaporation. By analogy other alkali metal compounds would behave similarly. The ability to inhibit combustion is probably not limited to the alkali metal atoms in view of the similar results obtained with NaCl and CuCl: The two are of comparable volatility and both would yield some metal atoms, Na in the one case and Cu in the other. Further, both $\text{Pb}(\text{C}_2\text{H}_5)_4$ and $\text{Fe}(\text{CO})_5$ strongly inhibit hexane-air flames (Ref. 10). A metal atom mechanism may be operative in those cases too, although both Fe and Pb may be partially converted to oxides or hydroxides.

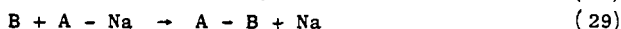
The second task is to identify a mechanism of inhibition which depends on the presence of metal atoms. A number of possible mechanisms were considered. Of these, three were found to be consistent with the obtained results.

It is possible that metal atoms increase the rate of recombination of the radicals directly associated with flame propagation -- H, O, and OH. Recombination reactions limit the concentration of radicals in the flame and insure their removal in the post flame gases. Consequently, an increase in recombination rate can be expected to reduce flame speed. A metal such as Na, which we will use as an example, can affect recombination rate by acting as a third body which is efficient in absorbing a portion of the energy of recombination.



The efficiency of Na as a third body in reactions 25 and 26 has been measured in flame gases (Ref. 11) but is not greater than that of other flame components present in far larger concentrations. Therefore, little direct effect can be expected. However, Na does remove at least 50 kcal of energy, the excitation energy for the transition $\text{Na}(^2\text{S}) \rightarrow \text{Na}^*(^2\text{P})$. This excitation energy may then be radiated as light or degraded into heat by collision with other molecules. On the other hand, such third bodies as the product molecules H_2O , H_2 , or O_2 may absorb all or a portion of the energy released in recombination reactions of the type shown in Eqs. 25, 26, and 27. Such molecules with excess energy may be of unusual chemical reactivity. However, in the case of vibrationally excited product molecules collisions with other molecules will lead to rapid loss of this energy. The mechanism cited cannot be definitely ruled out on the basis of our present knowledge about the state of excitation of the products resulting from recombination reactions.

A metal such as Na can also alter a rate of recombination by a two-step process like that shown formally in Eqs. 28 and 29.



in which A and B are H, O, and OH, and M is a third body. The collision-stabilized complex Na-A need not be a major species but it must have a sufficient lifetime to react with B. Such a mechanism has recently been advanced as an explanation of third-body efficiencies and negative temperature coefficients (Refs. 12 and 13). If the product molecule Na-A does survive this length of time and if reaction 29 is exothermic, the rate of reactions 28-29 relative to the direct recombination



will be about equal to the ratio Na/B. In order to evaluate the feasibility of this mechanism the cited ratio must accordingly be known.

The equilibrium mole fractions of H, OH, O in the post flame gases of a one-atmosphere stoichiometric CH₄-air flame are known (Ref. 14).

$$T_a = 2214^\circ\text{K}$$

$$\text{Equilibrium Mole Fraction} \begin{cases} \text{H} & = 3.57 \times 10^{-4} \\ \text{OH} & = 27.8 \times 10^{-4} \\ \text{O} & = 2.11 \times 10^{-4} \end{cases}$$

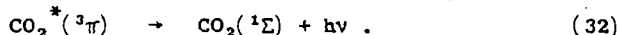
In the flame zone itself the mole fractions of these three species are undoubtedly much higher, consequently the cited values represent lower limits. The concentration of Na in an inhibited flame can be estimated from the data shown in Fig. 2 for fine Na₂CO₃. About 0.003 mg/cc reduces propagation velocity by about half of the original value. The mole fraction of Na corresponding to that concentration is about 1.5×10^{-3} . If the average degree of evaporation in the flame is about 10%, the mole fraction of Na in the gas will be 1.5×10^{-4} . A higher degree of evaporation is unlikely in view of the proportionality between specific surface area and powder effectiveness. Comparison of the mole fraction of Na in the flame with the lower limit values for H, OH, and O indicates that the ratio Na/B in the flame is probably much less than one. In the post flame gases, the degree of evaporation is much higher and the concentration of radicals lower. In that region the mechanism is a feasible one, although it is apparently not feasible in the reaction zone unless the estimates of concentration are badly in error.

Finally, Na may deactivate energetically excited species such as O₂^{*}, CO₂^{*}, C₂^{*}, CH^{*}, OH^{*}. The concentration in the flame of each of the cited species is not known but is probably low. These species may in addition be sideshow performers not directly involved in flame propagation. Consider for instance C₂^{*} and CH^{*}. Emission intensities from C₂^{*} and CH^{*} increases with the addition of bromine inhibitors (Ref. 15), although flame speed decreases. Both C₂^{*} and CH^{*} are apparently unrelated to flame speed. On the other hand, emission intensity of OH^{*} decreases with increasing concentration of bromine inhibitor (Ref. 15). However, OH^{*} is deexcited on virtually every collision with flame gases (Ref. 16). Consequently, a minor constituent can have little further influence on the deactivation of OH^{*}. The decrease in emission intensity is probably associated with a diminution in the rate of production of OH^{*} upon the addition of an inhibitor rather than its removal by reaction with HBr (Ref. 15).

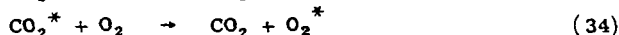
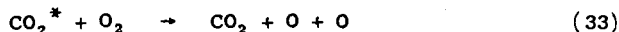
Inhibition can result from the deactivation of CO_2^* . The reactants necessary to form CO_2^* are present in the flame, such as



Moreover, CO_2^* is metastable with respect to radiation because of the multiplicity change associated with the radiative transition (Ref. 17),

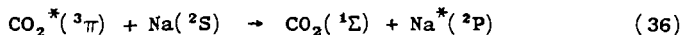


Excited CO_2^* can therefore exist for a time and be available for reactions such as those shown (Ref. 17)



Oxygen atoms produced by reactions 33 and 35 may by further reaction produce H and OH.

If Na (or other metal atom) is present in the flame the deexcitation reaction



could remove the energy required for reaction 33. The excitation energy of $\text{Na}^*(^2\text{P})$ may be radiated or eventually degraded into thermal energy by collision. The excited O_2^* formed in reaction 34 can also lose its energy of excitation by collision with Na, especially if the O_2 is only vibrationally excited (Ref. 18). This mechanism of inhibition, the removal of excitation energy by metal atoms, provides a qualitative explanation for metal inhibition. So far as know, it is consistent with fact. The mechanism does require that CO_2^* be an important intermediate in the combustion of hydrocarbons.

BIBLIOGRAPHY

1. Friedman, R. and J. B. Levy, "Survey of Fundamental Knowledge of Mechanisms of Action of Flame-Extinguishing Agents," WADC Technical Report 56-568, January 1957.
2. Dolan, J. E. and P. B. Dempster, J. Appl. Chem. (London), 5, 510 (1955).
3. Rose, H. E., J. Appl. Chem., 2, 80 (1952).
4. Rose, H. E., "The Measurement of Particle Size in Very Fine Powders," Lecture III, Chemical Publishing Co., Inc., New York (1954).
5. Fire Research Abstracts and Reviews, p 61, Vol. 1, Jan. 1959, abstract of NRL Report 5183 (Aug. 1958).
6. Gaydon, A. G. and H. G. Wolfhard, "Flames, Their Structure, Radiation and Temperature," 2nd Edition Revised, p 91 Chapman and Hall Ltd., London (1960).
7. Kubaschewski, O. and E. L. Evans, "Metallurgical Thermochemistry," J. Wiley and Sons, Inc., New York (1956).
8. Phillips, L. F., and T. M. Sugden, "Some Observations on the Radiative Combination of Atomic Hydrogen with Atomic Halogens in Burner Flames," paper presented at a Symposium on Some Fundamental Aspects of Atomic Reactions, held at McGill Univ., Montreal, 6 and 7 Sept. 1960.
9. Gaydon, A. G., "The Spectroscopy of Flames," p 224, Chapman and Hall Ltd., London (1957).

BIBLIOGRAPHY (Continued)

10. Lask, G., and H. G. Wagner, "Influence of Additives on the Propagation Velocity of Laminar Flames," p 55 of Abstracts of Papers presented at the 8th Symposium (International) on Combustion, Calif. Inst. of Technology, Aug. 1960.
11. Padley, P. J., and T. M. Sugden, "Seventh Symposium (International) on Combustion," p 235, Butterworths, London (1959).
12. Bunker, D. L., and N. Davidson, JACS, 80, 5085 (1958).
13. Porter, G., and J. A. Smith, Nature, 184, 445 (1959).
14. Clingman, W. H., R. S. Brokaw, and R. N. Pease, "Fourth Symposium (International) on Combustion," p 310, The Williams and Wilkins Co., Baltimore (1953).
15. Rosser, W. A., H. Wise, and J. Miller, "Seventh Symposium (International) on Combustion," p 175, Butterworths, London (1959).
16. Carrington, T., J. Chem. Phys., 30, 1087 (1957).
17. Ref. 9, pp 108-111.
18. Gaydon, A. G., and I. R. Hurle, "Measurement of Times of Vibrational Relaxation and Dissociation behind Shock Waves in N_2 , O_2 , air, CO, CO_2 , and H_2 ," p 70 of Abstracts of Papers presented at the 8th Symposium (International) on Combustion.

Table I
SPECIFIC AREA OF POWDERS USED

Powder	A*(cm ² /gm)	\bar{d} (μ)
talc	12,600	2.4
Ca(OH) ₂	9,000	2.9
CaCO ₃	2,000	11
NaBr	2,000	9
CaF ₂	3,500	5.4
NaF	3,300	6.5
CuCl	3,000	5.7
NaCl	4,500	6.0
K ₂ SO ₄	5,200	4.3
NaHCO ₃	7,760	3.5
NaHCO ₃	11,900	2.3
KHCO ₃	12,400	2.2
Na ₂ CO ₃	4,940	4.9
Na ₂ CO ₃	10,800	2.2

$$\bar{d} = \frac{6}{\rho A^*}$$

\bar{d} = average particle diameter
 ρ = density of material
A* = specific surface area

Table II
RELATIVE VOLATILITY OF VARIOUS SOLIDS

Substance	τ (sec)	B.P. ($^{\circ}$ K)
NaI	~ 1	1577
KCl	~ 2	1680
CuCl	~ 2	1639
NaBr	~ 2	1666
NaCl	3	1738
K ₂ CO ₃	7
K ₂ SO ₄	10
Li ₂ CO ₃	11
NaF	13	1977
Na ₂ CO ₃	16

τ = lifetime of 1 mm bead of material when exposed to a Meker flame

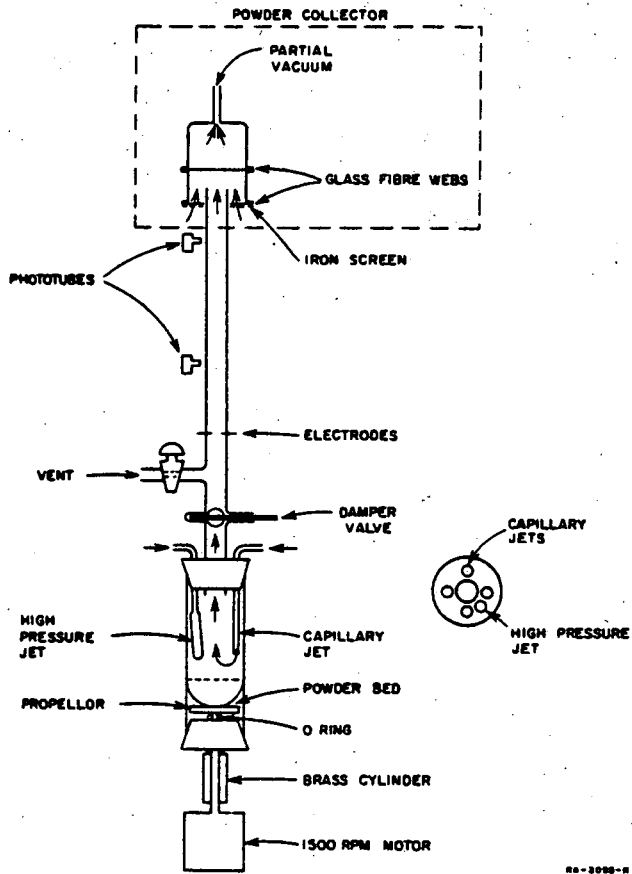


FIG. 1
POWDER GENERATOR AND FLAME TUBE
SCHEMATIC DIAGRAM

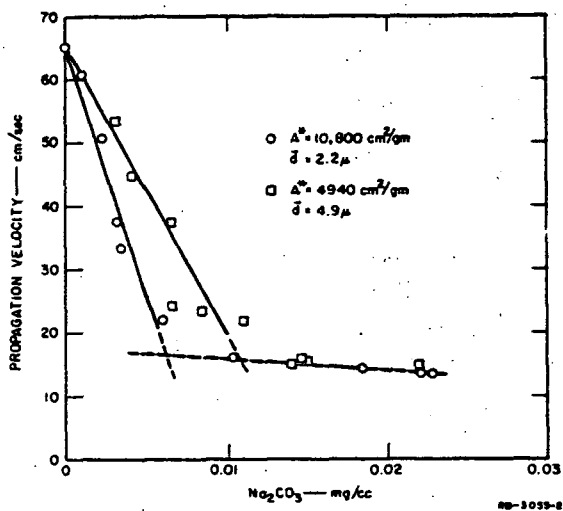


FIG. 2

STOICHIOMETRIC CH_4 -AIR: THE EFFECT OF Na_2CO_3
ON THE PROPAGATION VELOCITY.

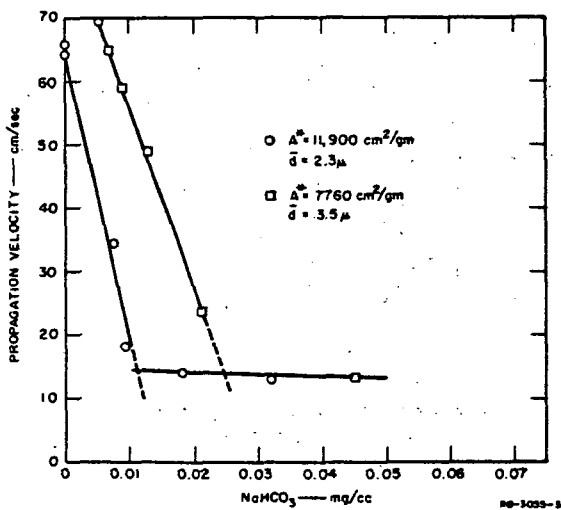


FIG. 3

STOICHIOMETRIC CH_4 -AIR — EFFECT OF NaHCO_3
ON PROPAGATION VELOCITY

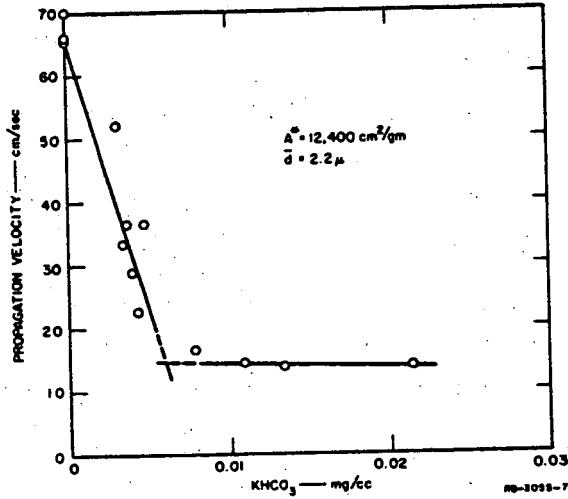


FIG. 4

STOICHIOMETRIC CH_4 -AIR — EFFECT OF KHCO_3
ON PROPAGATION VELOCITY

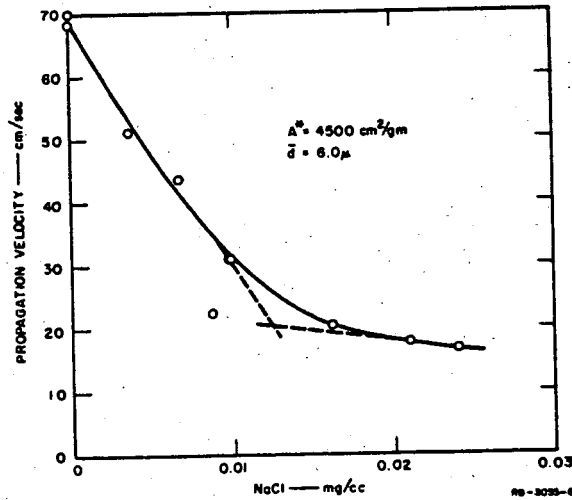


FIG. 5

STOICHIOMETRIC CH_4 -AIR — EFFECT OF NaCl
ON PROPAGATION VELOCITY

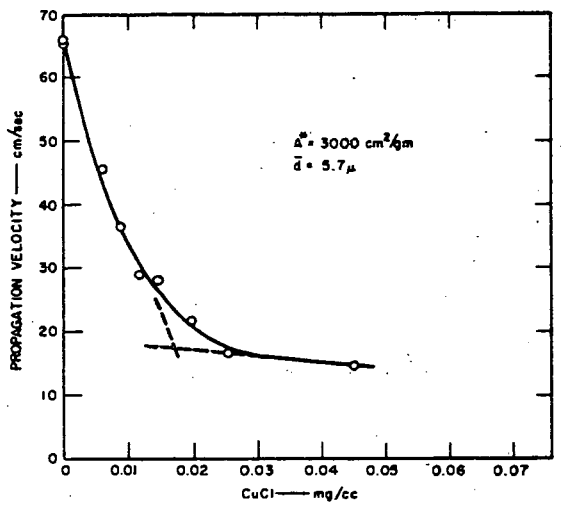


FIG. 6

STOICHIOMETRIC CH_4 -AIR — EFFECT OF CuCl
ON PROPAGATION VELOCITY

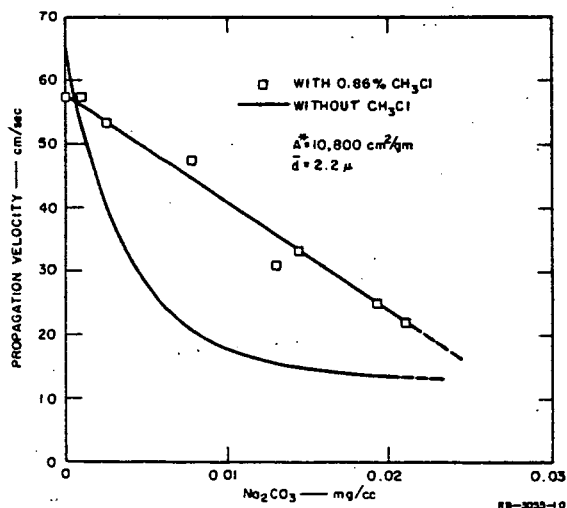


FIG. 7

STOICHIOMETRIC CH_4 -AIR — THE EFFECT OF CH_3Cl
ON THE EFFECTIVENESS OF Na_2CO_3

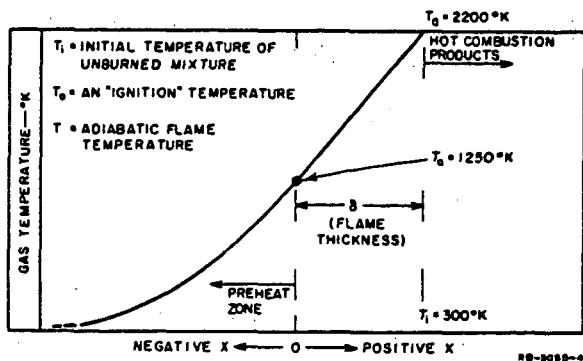


FIG. 8

ASSUMED TEMPERATURE PROFILE FOR A STOICHIOMETRIC CH_4 -AIR FLAME

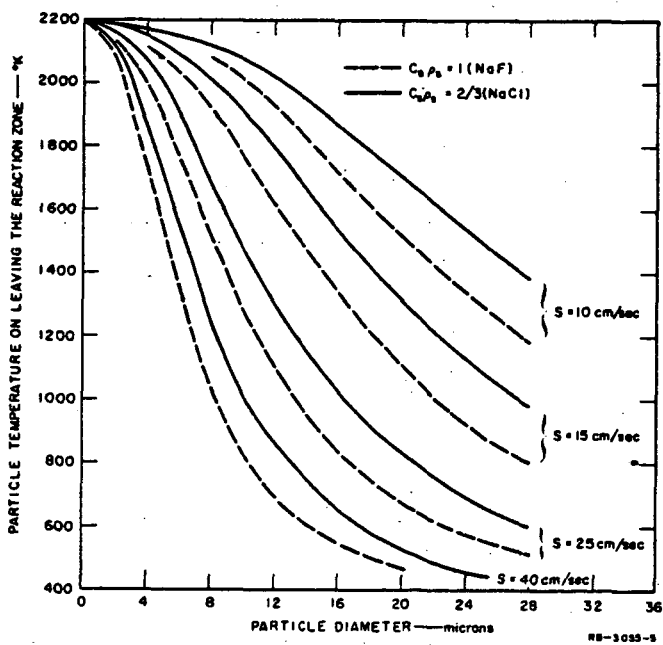


FIG. 9

THE TEMPERATURE REACHED BY SMALL NONEVAPORATING PARTICLES DURING PASSAGE THROUGH A STOICHIOMETRIC CH_4 -AIR FLAME

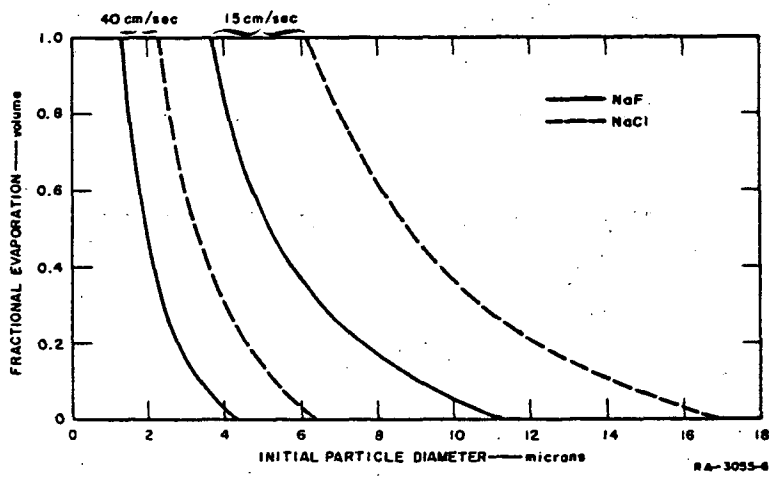


FIG. 10
FRACTIONAL EVAPORATION OF NaCl AND OF NaF
ON LEAVING THE REACTION ZONE

RA-3055-6

STUDY OF VARIOUS INFLUENCES ON THE EXTINGUISHING OF METHANE-
OXYGEN DETONATIONS BY FINE POWDERS

BY

P. Laffitte, R. Delbourgo, J. Combourieu and J. C. Dumont
Laboratoire de Chimie Generale - Sorbonne - PARIS

Since our last contribution to this subject (1) a considerable impulse has been given, especially in the United States, to the Study of flame extinction, inhibition and related phenomena and an important effort has been made to coordinate investigations carried out in this field, to promote further research and to bring to the knowledge of workers throughout the world all possible information on the topic.

The existence of an extensive and exhaustive Survey Report on the Action of Flame Extinguishing Agents by R. FRIEDMAN and J.B. LEVY (2) together with the regular publication by the Fire Research Committee under the Sponsorship of the National Research Abstracts and Reviews (3) will authorize us to cut short any historical development on this subject and refer the reader in search of such information to references 2 and 3.

/Research Council, of Fire .../

Experimental:

All our experiments were carried out on the mixture $\text{CH}_4 + 2 \text{O}_2$ whose detonation velocity is well determined and of the order of 2300 m/s. Whereas previous investigations had been carried out with various mixture concentrations and in some cases with hydrocarbons other than methane we have this time extensively studied the behaviour of stoichiometric methane oxygen mixture at atmospheric pressure. The lay out of the apparatus allows for mixtures to be made out under constant volume in a mixing vessel where each constituent is introduced under its own partial pressure. Methane used is pure grade 99% and is desiccated before admission. Oxygen is delivered from commercial cylinders and is also treated by phosphorus pentoxide. The new and interesting part of the apparatus consists of the detonation tube and this will be described in some detail.

The detonation tube is made of perspex, sheathed by a plastic vinyl tubing. This device has proved effective in the sense that the tube is not shattered to pieces as was the case with glass tubes; reproducible and well defined conditions prevail at each experiment. The tube itself consists of two parts separated by a specially built slide valve which is mechanically triggered open synchronously with the ignition device. The tube is vertical with an inside diameter of 16 mm. The top part is 40 cm long and the bottom part 200 cm. The ignition is started at the bottom by a small detonator and the detonation travels upward.

The slide valve (figures 1 and 2) consists mainly of a thin glucinium bronze blade $\frac{3}{10}$ th of a mm thick which either shuts the communication between the two tubes or instantaneously sets the complete aperture open. The shutter mechanism has a certain number of advantages mainly in the sense that being extremely thin the sudden opening of the slide introduces as little as possible perturbation to the mixture contained in the tube, also that the aperture of the

valve being exactly the tube diameter it therefore does not introduce any diameter variation at its passage, thirdly that it has been possible to use this device to introduce the pulverised material into the mixture by setting the weighed sample on the slide prior to any other step in the experiment then allowing the two parts of the tube to be first evacuated (the slide valve being vacuum tight through the use of O rings) then filled with the combustible mixture at the same pressure. In triggering the valve open and in setting the ignition started, the powder is set free to fall and disperse facing the detonation front travelling upward towards it.

The luminous phenomenon is recorded by the classical rotating drum camera on a Kodak Trix film and different recordings are given in figures 3 to 12. In particular it can be seen in figure 3 which relates to the detonation of $\text{CH}_4 + 2 \text{O}_2$ mixture with no powder at all that important fundamental conditions are met with, namely that the detonation is well established and stable throughout the propagation and also that the slide valve which has been set open at the ignition instant has not introduced any perturbation.

The pulverised substance studied has been potassium bitartrate which has previously proved to be a good inhibitor and which has the advantage of being easily prepared in fine fractions and of not being too hygroscopic. Silica was also investigated in some cases in order to confirm previous results obtained with it and also to draw a parallel between the two samples.

The sample is first crushed mechanically and then sieved down to a fraction passing through 450 mesh. This fraction is further reduced by passing through a Roller Air Elutriator and two fractions can be obtained in this way, one with an average diameter $< 10 \mu$ and another with an average diameter $< 20 \mu$. In each case the specific surface area has been measured by the Rigden air permeability method.

A relay, conveniently energised, is able to introduce a delay between the opening of the valve and the ignition of the mixture. This enables the operator either to obtain a simultaneous ignition and opening of the shutter setting the powder falling, or on the contrary to start the powder falling a few fractions of a second prior to ignition.

In acting in this way on the delay between the opening of the valve and the ignition one in fact acts upon the dispersion of the sample which if of course better dispersed if the delay is longer. In this way a powder (potassium bitartrate) of average particle size $< 10 \mu$ is likely to disperse from 0 to 68 cm when the delay introduced varies from 0 to 0,6 sec.

Table I summarizes the results obtained with such a sample where r (average radius) is $< 10 \mu \approx 3,25 \mu$ and where S is the specific surface area of the sample in cm^2/g ; in this case $S = 4680 \text{ cm}^2/\text{g}$.

TABLE I

t	0	0,15	0,2	0,3	0,4	0,48	0,5	0,6
m	015	510	675	1050	1320	1590	1640	1970
n	10,2	2,59	3,43	5,33	6,70	8,07	9,32	10,0
Σ	9430	2390	3160	4910	6180	7440	7680	9220
h	-	10	14	24	37	51	54	68
σ	-	119	112	101	83	73	71	68
λ	-	1,29	1,22	1,10	0,901	0,787	0,767	0,732

m is the extinguishing mass, expressed in mg, i. e. the minimum weight of material to obtain the complete quenching of a detonation.

h is the height in cm attained by the falling powder.

Σ is the total extinguishing surface area in cm^2 , i. e. m. S.

$\frac{\Sigma}{V}$ is the average extinguishing density expressed in surface of the powder by volume unit of the cloud at the extinction point.

$$= \frac{\Sigma}{V}, \quad (V = \text{volume of the dust cloud} = h \times \text{area of the cross-section of the tube}).$$

This table shows a certain number of characteristic features:

1. The minimum quantity in weight necessary for extinction is that obtained with a delay of 0,15 sec, that is after the cloud has dispersed 10 cm downwards; if the delay is longer, the powder is more and more dispersed and the quantity necessary for extinction increases. A minimum dispersion is therefore necessary and is more effective than none. When dispersion increases over this critical value then the density of the cloud becomes smaller and a larger quantity becomes necessary to obtain the same effect.

2. Except in the case where $t = 0$, i. e. no dispersion, there seems to be a relation of the form:

$$m = k t$$

between the extinguishing mass and the delay.

The larger particles together with the smaller ones fall with respective velocities v and v' which are rapidly attained, the height of dispersion of the falling cloud being.

$$h = (v - v') t$$

$$\therefore m = kt \rightarrow \frac{m}{h} = \frac{k}{v - v'} = \text{cte}$$

Therefore the minimum extinguishing density would be constant.

This has led us to photograph the falling of the sample by recording the diffracted light along a slit parallel to the tube. Such a photograph is shown in figures 13 and 14.

Using the values of h we have calculated the average extinguishing densities per unit volume of combustible mixture expressed in number of millimoles γ per cc n being the total number of millimoles of powder contained in the tube.

3. The density σ decreases rapidly when t increases, reaching however a limit value.

Table II shows the experimental data obtained with a coarser sample, $< 20 \mu$ the average diameter in this case is $8,4 \mu$, the specific area S is $1820 \text{ cm}^2/\text{g}$.

TABLE II

t	0	0,15	0,2	0,3	0,4	0,48	0,5	0,6
m	2000	1000	1100	1570	2100	2725	2950	4000
n	10,2	5,08	5,58	7,97	10,7	13,8	15,0	20,3
Σ	3640	1820	2000	2860	3820	4960	5370	7280
h	-	12	14,5	28	38	50	53	72
σ	-	75,4	68,6	50,8	50,0	49,4	50,4	50,3
γ	-	2,11	1,91	1,42	1,40	1,38	1,41	1,40

These results show that the limit value of the density is attained with $t \approx 0,3$ sec. Comparing Tables I and II one can see that m increases when h is increased, σ however decreases and tends towards a limit which is more rapidly

reached with a coarser particle than with a fine one.

Table III concerns a sample passing a 450 mesh without further reduction. The average radius is $r \approx 10\mu$ and the specific surface area is $1570 \text{ cm}^2/\text{g}$

TABLE III

t	0	0,15	0,2	0,3	0,4	0,48	0,5	0,6
m	3045	1460	2875	3400	4240	4775	4825	5440
n	15,4	7,41	14,6	17,3	21,5	24,2	24,5	27,6
Σ	4760	2290	4510	5340	6660	7500	7580	8540
h	-	13,5	29	48,5	70	79	80	90
σ	-	84,4	77,4	53,7	47,3	47,2	47,1	47,2
γ	-	2,73	2,50	1,74	1,53	1,52	1,52	1,53

Compared with Table II this sample which is coarser than sample II shows an increase in m, minimum quantity necessary for extinction, h, the dispersion height is also greater, σ and γ decrease when t increases, the limit values being reached as early as 0,3 sec.

Table IV summarizes the results obtained with silica, passing a 450 mesh, the specific area being $S = 6,11 \text{ m}^2/\text{g}$

TABLE IV

t	0	0,15	0,2	0,6
m	2235	2155	2920	3250
Σm^2	13,7	13,2	17,8	19,9
h	-	-	-	100
$\sigma \text{ m}^2/\text{cc}$	-	-	-	1990

In order to compare the experimental data obtained we have calculated the limit velocity of the dust particles, assuming each particle to be spherical and falling independantly. This has led us, for a delay of 0,6 sec, that is for the greater possible dispersion to a value of

$$r \leq 83 \mu$$

in order to attain a point situated 1 m below the shutter in 0,6 sec. The powder therefore forms clusters of an average radius of 83 microns.

Discussion:

A certain number of useful comments can be made by the careful observation of the photographic recordings.

Figure 3: shows a detonation free of powder passing through the slide valve (black space at the upper part) without any disturbance. The interval between two black marks at the top represents 10 cm.

Figure 4: shows a detonation with 2000 mg of potassium bitartrate $\langle 10 \mu \rangle$ - no delay between the opening of the shutter and the ignition. Practically all the powder is still at the level of the slide valve when the detonation front reaches it, an attenuation of the velocity is apparent passed the valve before the detonation carries on its way.

Figure 5 : Same conditions with 2015 mg instead of 2000 mg. Extinction is practically obtained at the valve, a small flame is seen to propagate at a reduced velocity after the passage of the valve.

Figure 6 Delay 0,3 sec between opening the shutter and ignition, $m = 1040$ mg; the luminous part of the recording immediately before the slide valve coincides with the position of the dust front as measured by the diffracted light method (fig. 14). This is immediately followed by a dark zone where the velocity is seen to be reduced. The quantity m being less than that necessary for extinction the wave passes through the shutter and is seen to propagate at the upper part of the tube with a reduced velocity before the detonation is reformed.

Figure 7 shows the same phenomena, 10 mg over the 1040 mg used in figure 6, extinction is obtained. The same luminosity and velocity reduction as in figure 6 are observed.

Figures 8, 9 and 10 are a series with a delay of 0,4 sec where the luminosity is seen to appear earlier in the recording (the delay being longer the powder has travelled further) the same velocity reduction is observed before extinction is obtained (fig. 10).

Figure 11 concerns a still longer delay (0,5 sec) the luminosity starts earlier.

Figure 12 concerns silica, 2150 mg, 0,2 sec. This recording is interesting in the sense that two re-ignitions are observed none of them leading to the reformation of a true detonation before the end of the tube is reached.

Figures 13 and 14 are relevant to powder samples falling along the tube (diffracted light photographs) each black interval is 10 cm distant from the next one. Figure 13 has been obtained with a delay of 0,6 with potassium bitartrate $\langle 450 \mu \rangle$. The density of the cloud appears to be maximum towards the centre. Figure 14 is for a delay of 0,3 s, the powder has reached 50 cm, the distribution is better than in figure 13.

Conclusion:

The general conclusions that can be drawn from the observation of the data presented are the following.

1. Extinction always precedes through the same reproducible film of events. A reduction of velocity is always observed after the wave has travelled for some length through the dust cloud. During this propagation a strong excitation of the luminosity is observed. This is immediately followed by an important reduction in luminosity (probably due to the cooling effect). According to whether the dust quantity is sufficient or not to produce extinction the wave will either proceed with a reduced velocity and reform a detonation further along the tube or proceed as an unstable deflagration or else become completely extinguished.

These events are perfectly reproducible and the inhibition mechanism is one of dissociation of the combustion and detonation waves, the effect being to reduce the flame velocity either operating as an important heat sink, reducing the temperature or by ~~any~~ other mechanism such as a chain breaking one (4), to the point where the flame cannot reaccelerate enough to reform the detonation.

2. The effect of dispersion shows that a minimum dispersion is necessary to obtain minimum quantities of material. In the case of our experiments a time lag of 0,15 sec has proved to be optimum. This corresponds to a height of dispersion of 10 cm below the slide valve.

Table I II and III show that the ratio $\frac{\Sigma}{V}$, the average extinguishing density $\sigma \text{ cm}^2/\text{cm}^3$ tends towards a limit value, more or less rapidly attained according to the average particle size.

3. The fine particles remain nearest the slide valve while the coarser ones fall more rapidly. Extinction is only obtained if propagation through the cloud can reach the fine portion of the sample.

4. Potassium bitartrate is definitely a better inhibitor than silica with which too large quantities are necessary to be significant.

We have in this work endeavoured to obtain definite experimental conditions and reproducible results. In studying one sole mixture (Stoichiometric methane oxygen) and in extensively examining the behaviour of one sole inhibitor (namely potassium bitartrate) we have willingly limited this paper to the influence of dispersion on the extinguishing phenomenon. Other factors will be studied systematically in the near future.

The authors' thanks are due to R. FOULATIER, Collaborateur technique au CNRS, for his help and ingenuity in building the slide valve and other parts of the equipment used.

References

1. P. LAFFITTE and R. BOUCHET
Seventh Symposium (International) on Combustion, Butterworths London, P.504,
1959.
 2. R. FRIEDMAN and J.B. LEVY
Survey of fundamental Knowledge of mechanisms of action of Flame extinguishing
Agents.

Wright Air Development Centre Technical Report 56-368 (1957)
Supplement I (1958) Supplement II (1959)
 3. Fire Research Abstracts and Reviews - Quarterly Reviews National Academy of
of Sciences-National Research Council.
 4. A. Van TIGGELEN
Colloque sur la combustion et la cinétique des réactions en phase gazeuse
CNRS 1948 p.159.
-

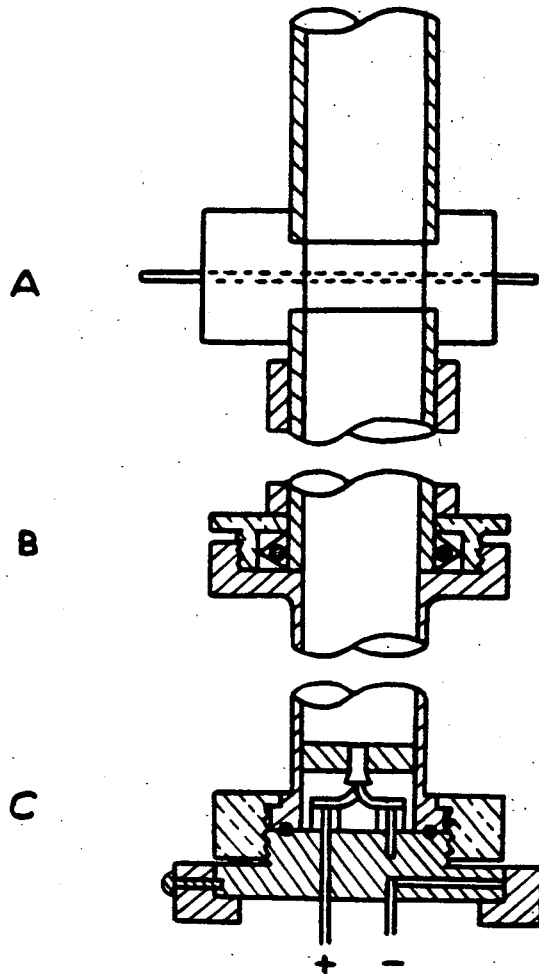


Figure 1

- A. Slide Valve
- B. Tube Connection
- C. Ignition Plug

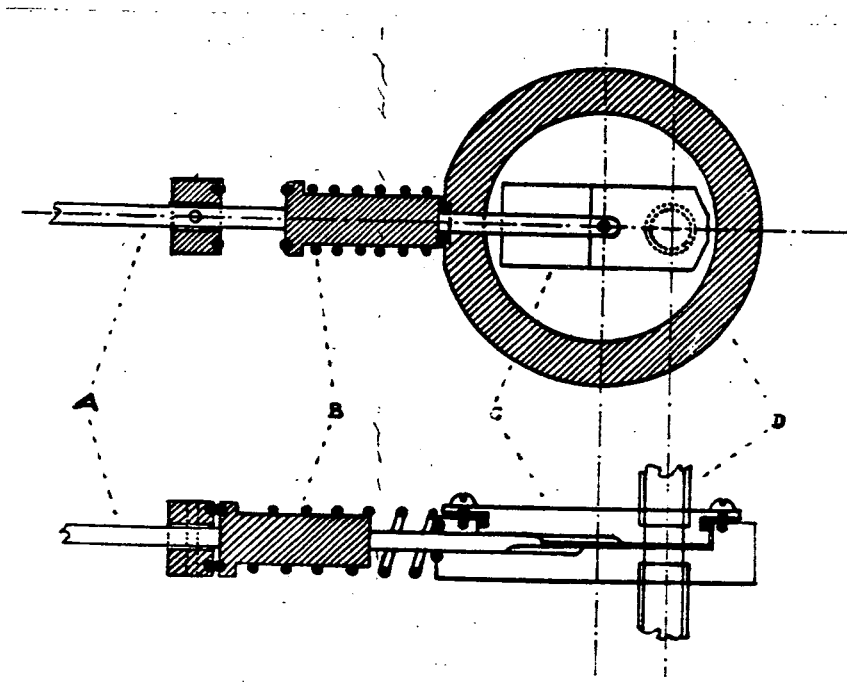
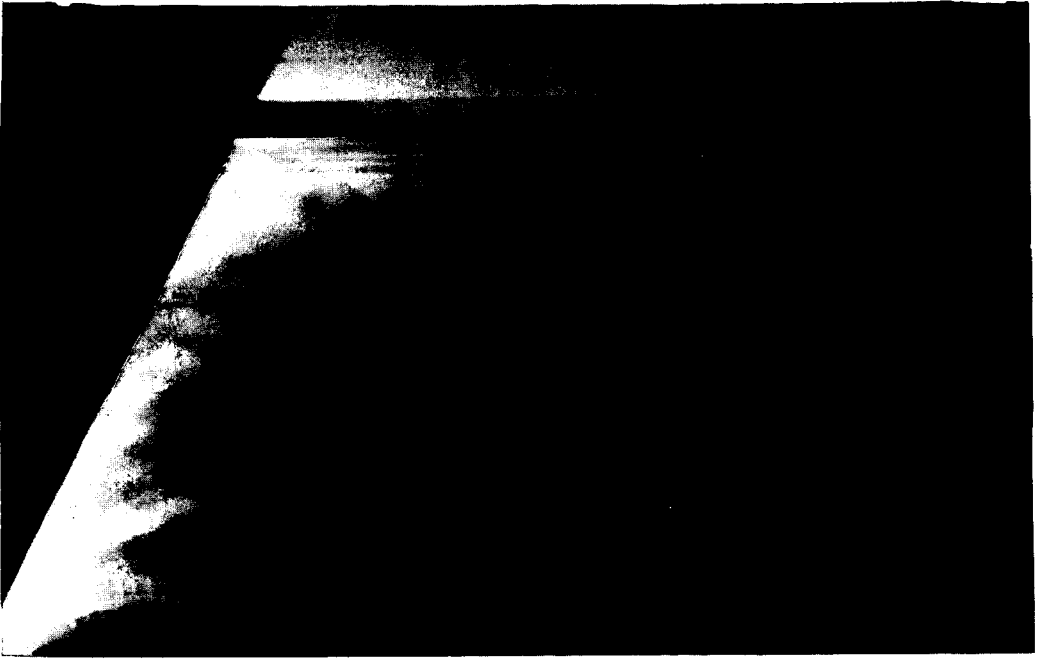


Figure 2

SLIDE VALVE

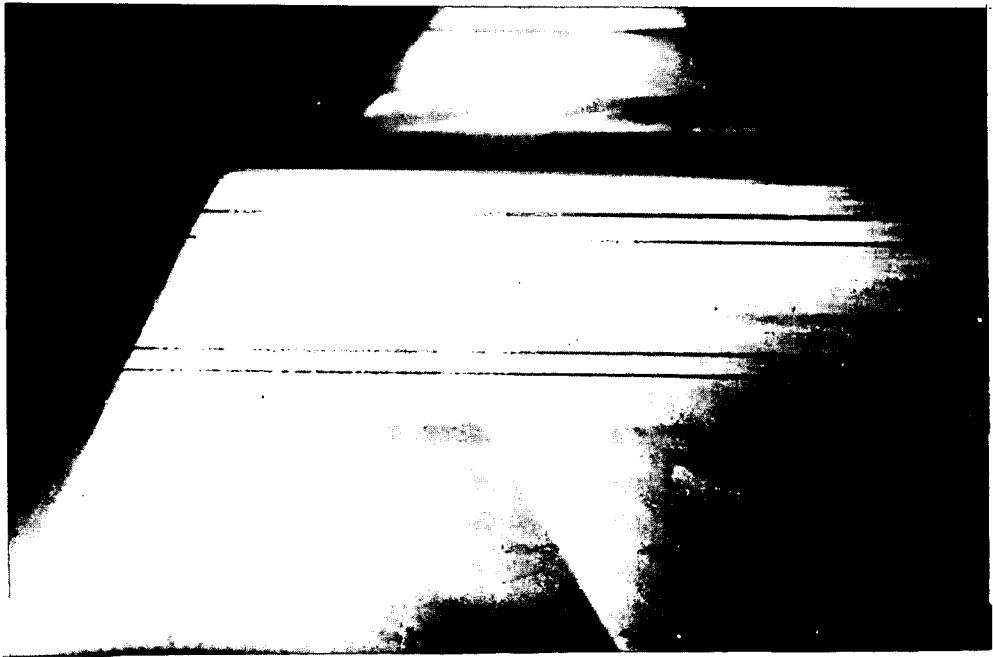
- A. Connecting Rod
- B. Spring
- C. Slide Shutter
- D. Detonation Tube

Space ↑



Bottom
Figure 3
Top

Time →

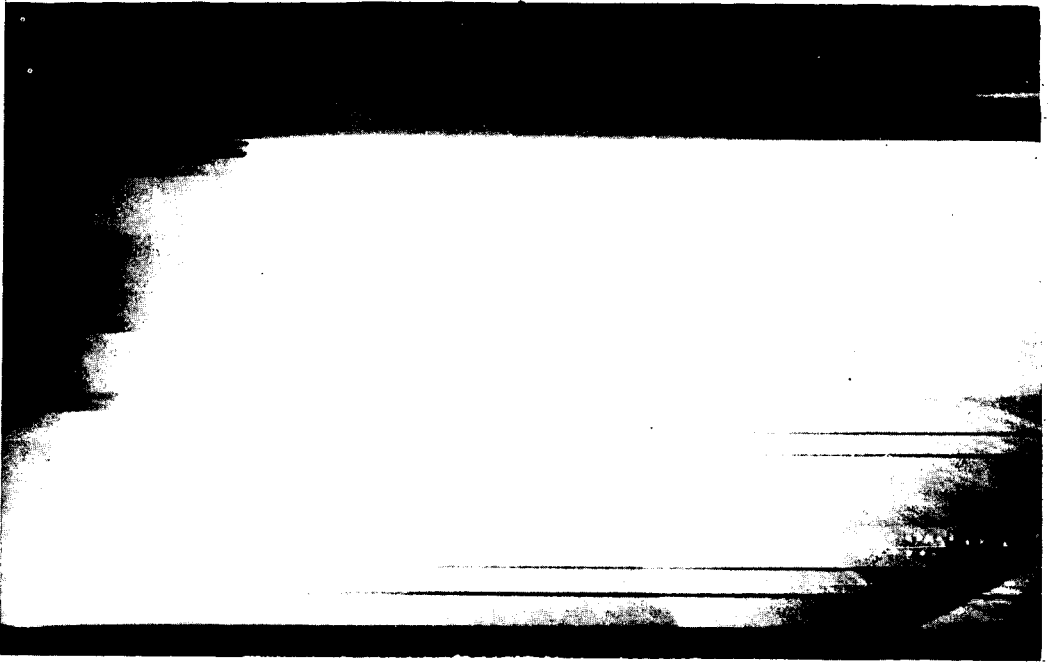


Bottom
Figure 4

Top

44.

↑
Space



Bottom
Figure 5
Top

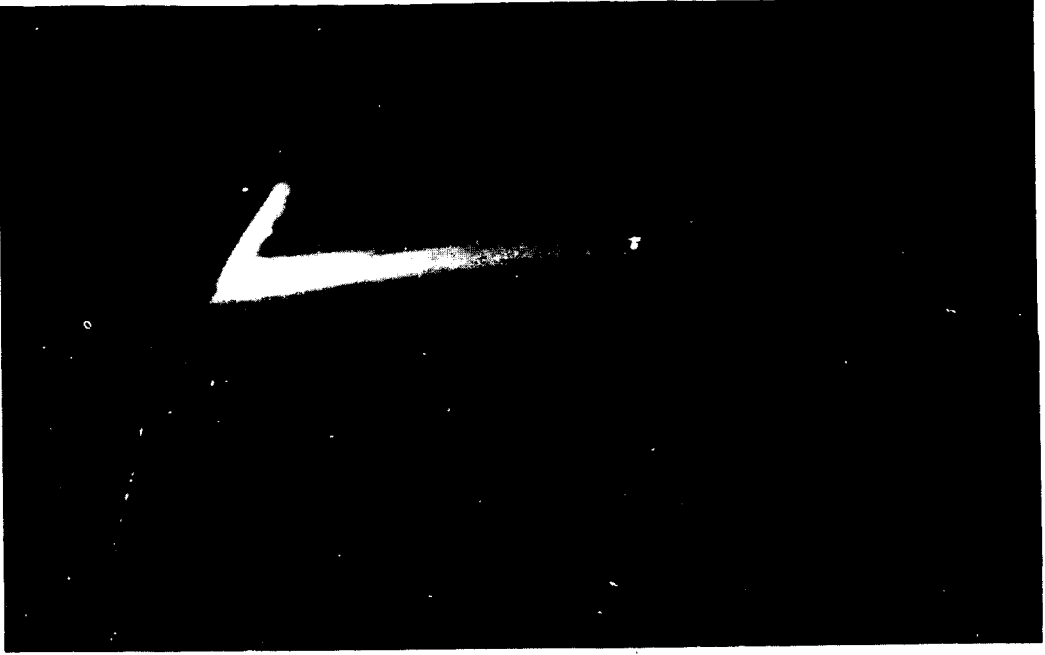
Time →



Bottom
Figure 6

~

Space ↑



Bottom
Figure 7
Top

Time →



Bottom
Figure 8

↑
Space



Bottom
Figure 9
Top

Time →



Bottom
Figure 10

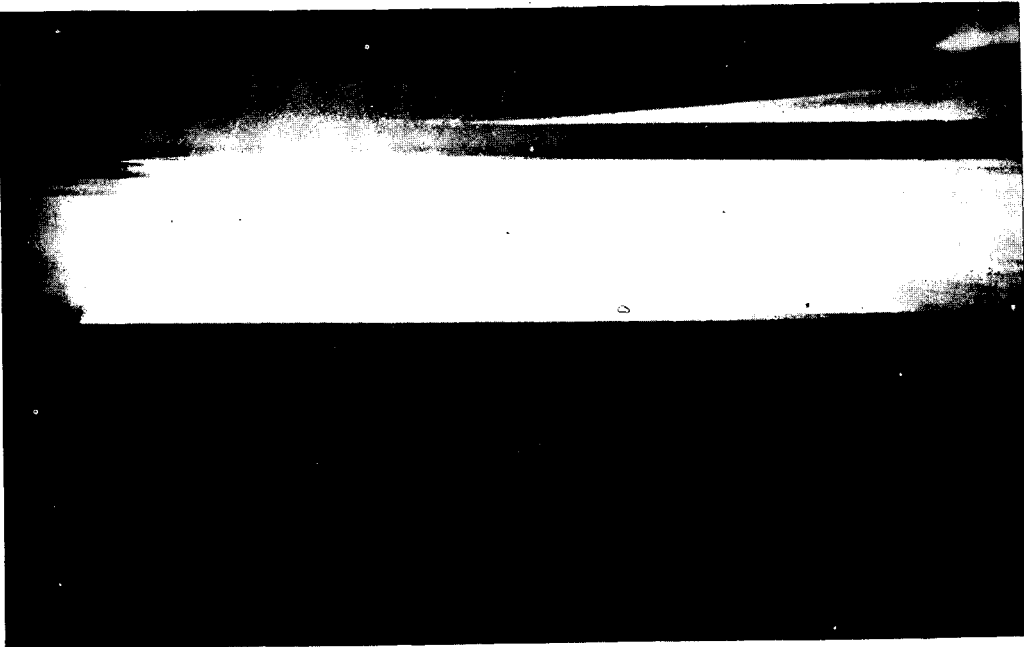
Top

↑
Space

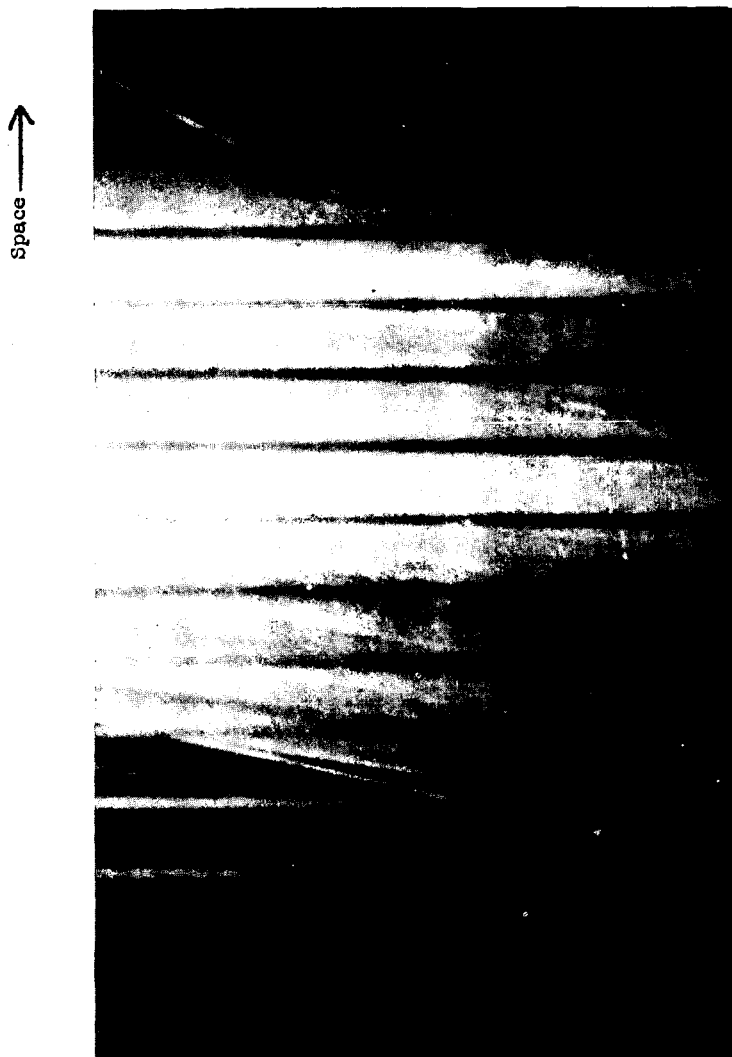


Bottom
Figure 11
Top

Time →



Bottom
Figure 12



Bottom

Time →

Figure 13

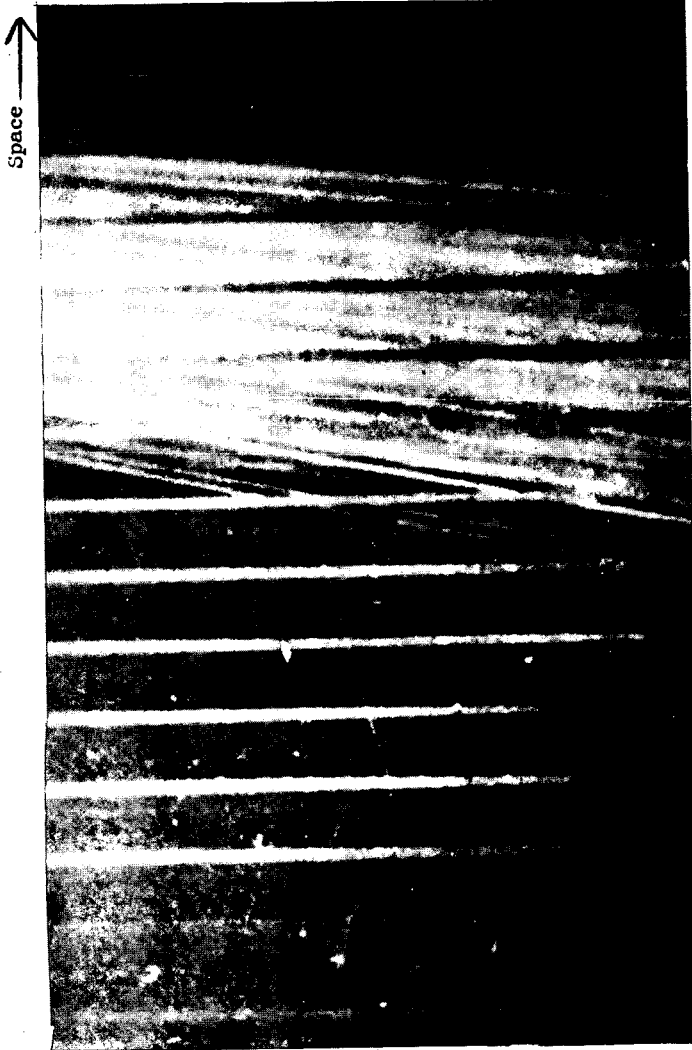
Bitartrate K
450 Mesh

$M = 5440 \text{ Mg}$

$\Sigma = 8570$

$t = 0.6 \pm 0.1 \text{ Sec.}$

Top



Bottom

Time →

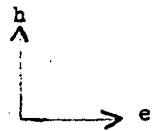


Figure 14

Bitartrate K
450 Mesh
 $t \approx 0.3$ Sec.

The Extinction of Fires by Water Sprays

by

D. J. Rasbash

Department of Scientific and Industrial Research and Fire Offices' Committee
Joint Fire Research Organization

Fire Research Station, Station Road, Boreham Wood, Herts.

INTRODUCTION

Water spray has long been widely used for the extinction of fires in both liquid and solid fuels. Although there have been numerous *ad hoc* investigations on the effect of sprays from various nozzles on fires of different types, it is only in recent years that any systematic study has been made using sprays and fires with controlled and measured properties. Work of this nature has been carried out for about ten years at the Joint Fire Research Organization. In this work attention has been paid in particular to the ability of spray to penetrate to the seat of a fire, the mechanism of extinction and the properties of sprays required to extinguish fires of various types. To some extent the work has also permitted an approach to be made to defining critical heat transfer criteria for extinguishing fire. In this paper these aspects of the problem will be discussed and illustrated by experimental results obtained at the above organization and elsewhere. The results of the experiments also suggest certain broad principles on which fire fighting operations should be based, and these will be outlined.

PENETRATION OF SPRAY TO THE SEAT OF A FIRE

In order for a spray to be able to exert a useful effect on a fire it is usually necessary for the spray to be able to penetrate to the seat of the fire, particularly to the burning fuel. To do this the spray must be either formed near the fuel or it must have sufficient forward force to prevent too much of the spray being either deflected by or evaporated in the flame and hot gases associated with the fire.

The factors which control the penetration of spray to the seat of a fire are the drop size and thrust of the spray, the thrusts of the flames and wind, gravity and the evaporation of spray in the flames. When sprays are applied to fires by hand the effects of the thrust of the flames and the wind, and the evaporation of spray in the flames are usually minimized by applying the spray directly through the base of the flames to the fuel from the upwind side of the fire; the reach of the spray, which is determined mainly by gravity and the forward thrust of the spray, usually controls the penetration to the seat of the fire under these conditions. When spray is applied downward to a fire all the above factors are of importance but particularly the relative thrusts of the spray and the flames. Little information is available from the literature on either of these two factors but work carried out at the Joint Fire Research Organization indicates that they may be estimated from readily measured properties of the spray and the flame. The thrust within a spray is a function of the reaction at the nozzle and the width of the spray; there is also evidence that at some distance from the nozzle it is approximately equal to the thrust of the entrained air current. The latter depends on the flow rate of spray per unit area and the pressure at the nozzles. The thrust of flames is proportional to the buoyancy head. Further information

on these relationships is given in the appendix.

Experimental information on the penetration of sprays to burning fuel is available for fires in kerosine burning in a 30 cm diameter vessel using downward application of spray(1). The results were scattered mainly because the penetration was very sensitive to the pattern of the spray at the fire area, a factor which was very difficult to control experimentally. Broadly, however, the penetration decreased as the pattern of the spray became more peaked in the centre of the vessel and as the thrust and the drop size of the spray decreased. The effect of the latter two factors are illustrated in fig. 1 which refers to sprays in which the peak of the spray distribution was contained in the central half of the vessel but in which not more than one fourth of the area of the vessel was covered by a flow rate less than one half of the peak value. In spite of the scatter of the points, the effect of spray thrust, as calculated from the entrained air current, and the drop size on the penetration is clearly seen. There is, however, an indication that at drop sizes greater than about 0.8 mm the penetration was independent of the thrust. If the peak was outside the central area of the vessel the penetration was usually considerably greater.

In the tests referred to in fig. 1 the height of the flame as judged visually was 150 cm before the application of spray and was reduced to mean values between 80 and 140 cm during the application of the spray. These heights correspond to upward flame thrusts of 34 and 18 - 30 dynes/cm² (see appendix). It will be seen from fig. 1 that the thrusts of the spray required to give a 50 per cent penetration for the finer sprays is comparable to these values.

It was observed during the tests that as the thrust of the spray was increased above 20 dynes/cm² the flames became increasingly unstable. Sprays with higher thrusts than represented in fig. 1 often caused stabilization of the flame as a relatively flat flame above the vessel after a period of instability. The minimum spray thrust at which this phenomenon occurred was 77 dynes/cm². It would be expected that under these conditions the bulk of the spray, even if it were fine and of a peaked pattern at the fire area, would penetrate to the burning fuel; this might also be inferred by extrapolation of the results in fig. 1. This critical thrust, T_c might be related to x , the height of the flames as judged visually prior to the application of spray, by equation 1.

$$T_c = 0.5 \rho_a g x \quad \dots\dots(1)$$

ρ_a = density of air, g = acceleration due to gravity.

It would be expected that since equation 1 represents the thrust in the air current of the spray required to overcome the buoyancy head of the flames, T_c should scale with flame height for larger sizes of fire than the fire tested.

For a given flow rate of spray in the absence of fire, and for a given pressure, the thrust of the spray in these experiments was approximately independent of the drop size. Therefore, as the drop size decreased the penetration decreased. However, as the drop size decreased the efficiency of unit mass of spray in reducing the rate of burning increased since the finer spray cooled the liquid more efficiently. As a result of these two phenomena a drop size occurred at which there was a minimum rate of burning for a given flow rate and pressure. This drop size depended on the spray thrust, and decreased from 0.8 to 0.33 mm as the thrust increased from 6 to 26 dynes/cm².

MECHANISM OF EXTINGUISHMENT

There are two main ways of extinguishing a fire with water spray:

(1) cooling the burning fuel and (2) cooling the flame. The mechanism of smothering the flame with steam is one aspect of cooling the flame and will be dealt with under that heading.

Cooling the fuel

To reduce the temperature of the fuel the spray must be capable of abstracting heat from the fuel at a rate greater than the rate at which the fuel will take up sensible heat. Heat will normally reach the fuel by heat transfer from neighbouring hot bodies and from the flame. Information on heat transfer from bodies may be obtained from texts on heat transfer although there are many important cases, for example, on the flow of films of fluid over hot surfaces where information is lacking. There is evidence, which will be given later, that radiation from the flame to the fuel that is being cooled does not normally play a large part in determining critical conditions for extinction, although if only a part of the fire is being extinguished at any one time, radiation from the rest of the flames might become an important factor. In this paper, therefore, particular attention will be paid to estimating critical conditions when the surface receives heat mainly by convective or conductive transfer from the flame. Such estimates may be obtained from known relationships between the rate of burning and the heat transferred from the flame to the surface. The method used may be best illustrated by an example. Equation 2 was found by Spalding to give the rate of burning of liquid fires flowing over surfaces with a vertical dimension (d)(7)

$$\dot{m}'' = \frac{0.45k}{dc} B^{\frac{3}{4}} 4 \sqrt{\frac{gd^3}{\kappa^2}} \dots\dots(2)$$

where \dot{m}'' is the average rate of vaporization per unit surface area,

d is the linear dimension of the surface,

k, c, κ are thermal conductivity, specific heat and thermal diffusivity of air at room temperature,

g is the acceleration due to gravity,

B is a transfer number equal to $\frac{m_{O_2} H / r + c(T_g - T_s)}{Q}$

where Q is the heat transfer to the fuel surface per unit mass of fuel vaporized,

m_{O_2} is the concentration of oxygen in air (by weight),

H is the heat of combustion of the fuel,

T_g is the ambient gas temperature and T_s the surface temperature,

r is the stoichiometric ratio (weight of oxygen/weight of fuel).

Normally, under steady conditions, the value of Q in the transfer number is equal to λ_f the heat required to vaporize unit mass of fuel. However, when a spray is acting on the fuel and heat is being removed from the fuel, Q will be greater than λ_f .

For most liquid hydrocarbons, equation 2 may be reduced with little error to

$$\dot{m}'' = \frac{0.17}{d^{0.25} Q^{0.75}} \dots\dots(3)$$

(\dot{m}'' in $g\ cm^{-2}\ s^{-1}$; d in cm; Q in cal/g.)

The rate at which heat reaches unit area of the burning liquid from the flame is $Q \dot{m}^n$; the rate at which heat needs to be transferred to vaporize the fuel is $\lambda_f \dot{m}^n$. Therefore, a steady condition as expressed in equation 3 will be maintained if the spray removes from the liquid a quantity of heat γ given by

$$\gamma = (Q - \lambda_f) \dot{m}^n \quad \dots\dots(4)$$

Combining equations 3 and 4 gives either

$$\gamma = \frac{0.17}{d^{0.25} Q^{0.75}} (Q - \lambda_f) \quad \dots\dots(5)$$

or

$$\gamma = \left(\left(\frac{0.17}{d^{0.25} \dot{m}^n} \right)^{4/3} - \lambda_f \right) \dot{m}^n \quad \dots\dots(6)$$

If the spray is capable of removing heat at a greater rate than γ the temperature of the fuel will be reduced. This will result in a smaller value of \dot{m}^n and a correspondingly larger value of Q and γ . The reduction in temperature will also bring about a reduction in the rate at which spray can remove heat from the fuel.

In a burning fuel in which the temperature of the fuel has reached steady conditions, $Q = \lambda_f$ and $\gamma = 0$. The application of spray with a lower temperature than the fuel will therefore result in the fuel being cooled. This will continue until either a steady burning condition is established at a particular temperature or one of the two following critical conditions for extinction is reached.

- (1) The value of Q may reach the maximum value, Q_c which the flame is capable of imparting to the surface without becoming extinguished.
- (2) The value of \dot{m}^n may reach a minimum value, \dot{m}_c^n below which a flame cannot continue to exist above the surface.

The rate γ at which the spray must abstract heat from the fuel at the particular fuel temperature at which these critical conditions occur will be given by one of the equations (5) and (6), and if Q_c and \dot{m}_c^n are assumed independent of the linear dimension of the burning surface, then γ_c will be expected to decrease slowly as this dimension increases.

By a similar argument to that developed above it is possible to put forward equations giving γ_c for a wide range of conditions, indeed for all conditions for which there is a known relationship between the Nusselt number for heat transfer from a gas and other relevant dimensionless groups, e.g. the Reynolds, Grashof and Prandtl numbers. By these means it may be shown that above a certain dimension of the surface γ_c will cease to decrease with increase in d , and if the wind is sufficiently strong γ_c will be proportional to the square root of the wind velocity and inversely proportional to the square root of d .

A certain amount of information is available for the critical value of Q . Thus for flame quenching in channels⁽³⁾ and in flame arresters⁽⁴⁾ it has been found that for stoichiometric hydrocarbon flames the maximum amount of heat a flame can impart to a surface before it is extinguished is 23 per cent of the heat of combustion of the fuel, i.e. about 2,500 cal/g. Spalding⁽²⁾ carried out experiments on the circulation of kerosine burning on the surface of a sphere and here again it was found that the fire was extinguished when the heat transferred to the burning surface by the flame was 2,500 cal/g of fuel vaporized. Spalding's experiment is analogous to extinguishing a fire by cooling with water spray, the only difference being that heat was removed by

excess fuel rather than by water spray. It would be expected that the conditions under which the maximum fraction of the heat of combustion can reach the surface of the burning fuel would occur when a stoichiometric mixture burns very close to the liquid surface. The temperature of the surface should therefore be near to the value corresponding to equilibrium with a stoichiometric mixture. For kerosine this temperature is 15°C higher than the temperature at which the surface is in equilibrium with the lower limit mixture and is approximately equal to the fire point.

Using $2,500 \text{ cal/g}$ as the value for Q_c the following values for γ_c may be calculated for fires burning under conditions of natural convection.

$$\text{Pool or spill fires} \quad \gamma_c = 0.6/d^{0.25} \quad \dots\dots(7)$$

$$\text{Fires on tubes} \quad \gamma_c = 1.2/d^{0.25} \quad \dots\dots(8)$$

$$\text{Fires on vertical surfaces} \quad = 1.2/l^{0.25} \quad l < 100 \text{ cm} \quad \dots\dots(9)$$

$$= 0.4 \text{ for } l > 100 \text{ cm} \quad \dots\dots(10)$$

γ_c is in $\text{cal/cm}^2\text{s}$; d , l characteristic dimension in cm.

There is little information on the minimum value of m'' below which a flame will not be sustained. It might be postulated that m_c'' should be not less than the value required to sustain a lower limit flame at its appropriate burning velocity over the whole surface; this would give m_c'' equal to about $1.5 \times 10^{-4} \text{ g/cm}^2\text{s}$ for fires in hydrocarbon liquids. On the other hand experiments on the extraction of heat from laminar propane-air flames(5) indicate that a stoichiometric mixture may continue to burn close to a surface to which it is imparting heat at a rate similar to Q_c when the combustion rate is as low as $2.6 \times 10^{-4} \text{ g/cm}^2\text{s}$. The above figures for m_c'' are about one-tenth of the rate of combustion of pool fires under steady conditions; they imply that γ_c may depend on critical rate of vaporisation when the dimension of the fire is greater than 30 cm, for fires burning in a natural draught.

The analysis so far has dealt only with burning liquids. There are difficulties in applying a similar analysis to wood. The main difficulty as far as the extinction of flaming combustion is concerned is that the heat required to produce unit mass of volatiles is not known. The slow decomposition of wood is an endothermic process, i.e. λ_f is negative, but Klason(6) showed that as the rate of decomposition increases the process changes from being exothermic to endothermic. There is evidence that for the rates of decomposition required to sustain a flame over a wood surface, the decomposition is indeed highly endothermic. For the extinction of glowing combustion the analysis would have to be modified to take into account the loss of heat from the surface by radiation and the effect of surface temperature on the combustion rate.

The above considerations are concerned with the rate at which heat must be removed from the fuel in order that the fire may be extinguished by cooling the fuel. The ability of the spray to remove this heat will depend on the properties of the spray and the fuel; this aspect of the problem will be referred to when experimental results are discussed.

Extinction of the flame

The criterion of extinction of a flame by heat abstraction inside the flame is that the combustion products as they leave the reaction zone should not exceed the temperature they would have for lower limit flames; this

temperature is about 1580°K for a wide range of flammable vapours and gases. A decrease in temperature approximately to this value is obtained when extinction is obtained by adding nitrogen, water vapour, carbon dioxide or inert dust to flames in stoichiometric mixtures.

The amount of heat which it is necessary to remove from the flame to accomplish this is the difference in heat of combustion of stoichiometric and lower limit mixtures. For most flammable organic compounds and probably also for the volatiles from some common dry woods this is about 45 per cent of the heat of combustion of the fuel. Since with diffusion flames it would be expected that there would be a zone between the fuel and the atmosphere where the stoichiometric mixture occurs, the heat which has to be removed from the flame as a whole is 45 per cent of the heat of combustion of the fuel. It is important, however, that this heat be removed either from the reactants or the reaction zone. If the heat is removed from the combustion products the heat removal will not substantially affect the temperature of the products leaving the reaction zone. In a turbulent diffusion flame it is very difficult to differentiate between the reactants, the reaction zone and the combustion products. However, it would be expected that if a spray is capable of removing all the heat of combustion from the flame, then the flame will be extinguished.

It is interesting to note that the heat removal required to extinguish the flame by cooling the flame is twice as great as the heat which an extended surface on the reactant side of the flame may abstract from the flame before the flame is extinguished. This might be explained by a different balance of heat release and heat loss rates for a vitiated flammable mixture and a stoichiometric flammable mixture close to an extended surface⁽⁸⁾. Owing to the intractability of defining the position and properties of the reaction zone in a turbulent diffusion flame the approach to estimating critical conditions for extinction of the flame by water spray has been made on the basis of heat transfer taking place within the whole flame. If V is the volume of the flame, Z the mass rate of burning and H the heat of combustion of the fuel, then I , the mean rate of the heat production per unit volume of flame, assuming complete combustion of the fuel, is $\frac{ZH}{V}$. If the capacity for heat transfer of the spray within the flame is defined as X , the rate of heat transfer per unit volume of flame to the spray, then three critical criteria for X may be put forward.

- (1) Removal of all the heat in the flame neglecting the production of steam as a result of heat transfer to the spray

$$X_1 = I \quad \dots(11)$$

- (2) Removal of heat only from the reaction zone and the reactants, but also neglecting steam formation

$$X_2 = 0.45 I \quad \dots(12)$$

- (3) Removal of heat only from the reaction zone and the reactants, but assuming that all the heat transfer for the drops result in steam formation. This will only be the case if the drops enter the flame at the wet bulb temperature (about 75°C). It may be assumed that the steam formed will contribute to the cooling of the flame a quantity β per unit mass of steam equal to the whole of the sensible heat of steam from 370 - 1580°K . The ratio of β to λ , the latent heat of steam, is 1.23 . This gives

$$X_3 = \frac{\lambda}{\beta + \lambda} 0.45 I = 0.195 I \quad \dots(13)$$

A fourth criterion may also be put forward if steam is formed outside the flame either at the burning surface or at surrounding hot bodies. Under these conditions the latent heat of vaporization does not contribute to cooling the flame but the sensible heat of steam up to 1580°K does. If the steam is formed at or sufficiently near to the burning surface to accompany the reactants into the flame then the critical flow rate, W , of water required would be

$$W = 0.45 \frac{ZH}{\beta} \dots(14)$$

If the steam is formed well away from the burning surface and is heated by the combustion products, then W may rise to values equal to $\frac{ZH}{\beta}$.

The quantity I in equations (11) - (13) is an intensity of combustion and depends on the conditions of combustion, particularly the air current in which the flame is burning. For petrol, kerosine, benzole and alcohol fires 30 cm diameter burning under conditions of natural draught, I was found to be independent of the fuel or the rate of burning and equal to 0.45 to 0.50 cal cm⁻³s⁻¹ (9).

The entrained air current in a spray not only affects the intensity of combustion but also affects the critical heat transfer rate required to extinguish flame. There is very little information to allow the assessment of this factor on a quantitative basis, but an indication of what might be expected may be obtained from work on the blow out of flame at obstacles. For example, if the assumption is made that the fundamental burning velocity of the flame decreases in proportion to the heat transfer capacity of the spray, then on the basis of relationships between the blow out velocity and the fundamental burning velocity(10) it may be expected that

$$V_{BO} = 93 - bX^{1.5} \text{ to } 2d^{0.5} \text{ to } 1 \dots(15)$$

Where V_{BO} is the velocity of the entrained air current that will cause a blow out when the spray has a flame heat transfer capacity X , d is a characteristic dimension of the system and a_3 and b are constants.

It is of interest to compare critical heat transfer rates for extinction by cooling the flame and cooling the fuel. It follows from equations (11) to (14) that the critical heat transfer rate for cooling the flame is greater than 20 per cent of the total heat of combustion of the fire. Equation (4) and subsequent remarks indicate that for cooling the fuel the critical heat transfer is less than 25 per cent of the much smaller rate of combustion that would occur under critical conditions. On this basis much lower critical flow rates would be expected for extinguishing the fire by cooling the fuel than by cooling the flame. As opposed to this, however, it is feasible that unit mass of water can, under critical conditions, be the sink of a much greater amount of heat from the flame (about 1300 cal/g) than it can from a solid or liquid fuel (45 cal/g for kerosine and 750 cal/g for wood).

EXPERIMENTAL INVESTIGATIONS ON THE EXTINCTION OF FIRE

In order to examine the relevance of the above analyses of extinction mechanism, experimental investigations have been divided into two groups covering investigations in which there is substantial evidence that extinction was by cooling the fuel and the flame respectively. For investigations on the extinction of fires in rooms, however, there has not usually been sufficient evidence to decide on the mechanism of extinction and these investigations will be dealt with separately.

Cooling the fuel

Critical flow rate of spray for extinction of pool fires. Evidence has been obtained from experiments with pool fires that the critical heat transfer rate for extinction of the fire by cooling the fuel is controlled mainly by convection from the flame to the liquid rather than by radiation from the flame. This evidence may be summarised briefly as follows:

- (1) With sprays at less than the critical rate a steady fire condition could be established with a temperature near the liquid surface not greatly in excess of the fire point, with a flame size very much less than the size of the flame if no spray were applied, and with the flame reaching down to the surface of the liquid⁽¹⁾. In these fires the predominant mechanism of heat transfer to the fuel surface was by convection.
- (2) The effect of scale on the critical flow rate was as may be expected if convection controlled the critical heat transfer rate rather than radiation.

The reason for the above phenomenon is that when radiation is the predominant mechanism of heat transfer from the flame to the surface, the bulk of the heat reaching the surface is taken up as latent and sensible heat of the vapour leaving the surface and does not manifest itself as sensible heat in the remaining fuel. There is thus little resistance to the cooling of the fuel by water spray. The temperature of the surface is also much higher than the fire point and the capacity of the water spray for taking up heat is correspondingly much greater. Fig. 2 shows critical rates to extinguish kerosine and transformer oil fires by cooling the fuel plotted against the mass median drop size for fires burning in vessels 11, 30 and 24.3 cm diameter. The curves for the 30 and 11 cm diameter kerosine fires were obtained by extrapolating to the fire point relationships between the flow rate of spray reaching the fuel and the resulting steady temperature near the fuel surface, for sprays of different drop size; the spray was applied in a downward direction⁽¹⁾. The curves obtained separate tests in which extinction took place by cooling from tests in which no extinction occurred. Although for both fires the critical rate was approximately proportional to the drop size, for a given drop size the rate was slightly less for the 30 cm diameter fire than for the 11 cm diameter fire. If radiation controlled the critical heat transfer rate, the critical flow rate for extinction would be expected to be 100 per cent greater for the 30 cm diameter fire but if convection controlled about 15 per cent smaller. The difference between the points for tests with horizontal application of spray to a kerosine fire 30 cm diameter and for hand application of spray to a fire 24.3 cm diameter may be accounted for by the different drop sizes of the spray. If radiation controlled the critical heat transfer rate, a ratio of 2.5 would be expected in the critical rate. After taking into account the probable effect of drop size there was in fact no difference in the critical rates. However, the critical rate for horizontal application for the 30 cm diameter fire was about half that for vertically downward application. A possible reason for this difference is that the spray pushed the flame sideways; as a result the drops did not become heated in the flame and have a greater cooling capacity when they reached the liquid.

The effect of radiation is likely to be much greater with pool fires in which the burning surface can "see" all the flame than with other fires. Since radiation from the flame of the fuel being extinguished has a minor effect on the critical rates for extinguishing pool fires by cooling, it is reasonable to neglect it for other fires.

The effect of drop size on the critical rate follows from the fact that the drops are in the liquid for only a limited time and their size is a controlling factor in the rate at which heat is transferred. It would be expected⁽¹¹⁾ that the heat transfer from the body of the liquid to the drops would be proportional to $D^{-4/3}$. However, the transfer of heat from the surface of the liquid to the interior would be expected to increase as the eddy conductivity caused by the turbulent eddies set up by the motion of the drops on the liquid; this is estimated to increase as D^{+3} . The actual effect of drop size results from a combination of these two factors.

The driving force for heat transfer in the liquid may be represented by ΔT , the difference in temperature between the surface of the liquid under critical conditions (for practical purposes the fire point) and the temperature of the drops (for practical purposes ambient temperature). It would, therefore, be expected that for a given drop size the critical rate should be inversely proportional to ΔT . Measurements of critical rate indicated in fig. 2 for downward application of spray to a transformer oil fire 30 cm diameter and hand application of spray to a fire 24.3 cm diameter support this.

Extinction time for pool fires. As long as the flow rate of spray is greater than the critical value, then extinction will take place in a time which depends on the amount of heat present in the burning fuel which must be removed by the spray to reduce the surface temperature to the fire point. With most pool fires this heat content increases as the preburn time increases up to about 10-20 minutes but for hot zone forming liquids, e.g. heavy fuel oils, this heat content may increase indefinitely. Experiments⁽¹²⁾⁽¹³⁾ on extinction of pool fires using fixed nozzles sited vertically above the burning liquid (see plate 1) and for hand extinction of an 8 ft diameter fire (plate 2) gave the following relationships.

Fixed nozzle

$$t = 5,800 (D/M)(Y/\Delta T)^{1.75} \dots(16)$$

Hand application for 8 ft diameter vessel

$$t = 121,600 D^{0.85} F_1^{-0.68} Y^{0.39} \Delta T^{-1.67} L^{-0.33} \dots(17)$$

where D is the mass median drop size of the spray in mm
 M is the flow rate of spray in gallons ft⁻²min⁻¹
 Y is the preburn time in minutes
 ΔT is the difference between fire point and ambient temperature °C.

F_1 is the total flow to the fire in gallon/min.

L is the total number of tests carried out by the operator

t is the extinction time, sec.

The influence of drop size and of flow rate of spray are as may be expected from considerations of heat transfer between the liquid and the drops. The influence of ΔT , however, is greater than may be expected from a heat transfer basis alone. A reason for this may be that the higher the value of ΔT the greater was the temperature of the surface of the liquid in excess of 100°C, particularly when application of water spray commenced, and the greater was the steam formation in the liquid during the extinction process. This steam probably accelerated the cooling of the liquid surface by stirring the

* "gallon" refers to imperial gallon in this paper - 1 Imp. gall = 1.2 U.S.Gall.

bulk liquid. An increase in the preburn time increased the extinction time although to a lesser extent for hand application than for fixed application. The experience of the operator as expressed by the factor L in equation (17) was also an important factor in the extinction of fire by hand application.

Both the equations (16) and (17) presume that the bulk of the spray reaches the burning liquid. If the downward thrust of the spray was less than the upward thrust of the flames and if the flames could burn vertically upwards against the spray, then the extinction time was prolonged. In this connection it is noteworthy that the size of the flames in the first few seconds of application were usually considerably greater than the size before application of spray, as indicated in plate 1. This was due to the sputtering of fuel into the flame. However, for tests on fires 3 ft and 4 ft diameter in a large roofless structure, the ambient wind was usually sufficient to blow the flames away from the upright position and the force of the spray was not a significant factor in extinction of the fire; if the spray was much wider than the fire. With hand application of spray to an 8 ft diameter fire there was no difficulty in enabling even fine sprays of low thrust to reach the burning liquid, since the fire could be approached on the upwind side and applied directly to the base of the flames. A complicating factor in all these tests was the occurrence of splash fires with coarse sprays; burning fuel was splashed into the flame by the spray and a vigorous flame maintained even though the liquid was cooled well below the fire point. If, when a splash fire was established, the spray were taken away the fire often went out. An example of this is shown in plate .

Fires in oil running over metal work. When sprays are applied to a pool fire which has been burning for some time, there is an initial upsurge of flame and the flames then reduce in size gradually within the extinction time. When burning liquids are flowing over a surface the liquid layer is very thin and the sensible heat in the liquid which needs to be removed is very small. Providing the flow rate of water spray is near the critical rate the flames are reduced in size almost immediately after turning on the water spray and thereafter are reduced in size much more slowly. This is illustrated in plate 4 which shows a fire in transformer oil flowing over a test rig consisting a bank of tubes 5 cm diameter. The rate of flow required to extinguish the fire in a given time depended on the preburn time in this case since during the preburn period the tubes themselves were heated and acted as a reservoir of heat during the application of spray. The effect of the temperature of the tubes on the rate of flow required to control and extinguish the fire is given in Fig. 3. The relationships in Fig. 3 were obtained for sprays projected directly downwards from 5 ft above the point in the tube rig where oil was injected (6 in below the top), but tests in which the sprays were projected from a similar distance from the side of the rig did not give significantly different results, nor was there any difference if the tube bank was horizontal rather than vertical. The drop size of the spray was found to have no significant effect in the range tested (mass median 0.6 to 3.0 mm); there was evidence, however, that an increase in drop velocity increased the efficiency of the spray⁽¹⁴⁾ and the effect of the drop size may have been masked by the fact that the ratio of drop size to drop velocity was constant for the sprays referred to in Fig. 3. The tests covered a wide range of ambient wind conditions. However, Fig. 3 indicates that the critical rate for these varying conditions increased as the temperature of the tubes increased. These critical rates may be taken as lying between curves (1) and (3) in Fig. 3.

A large number of tests have been carried out in the United States in which water spray has been applied to oil fires on sheet metal structures simulating transformers⁽¹⁵⁾⁽¹⁶⁾. A comparison between the results of these tests and those carried out on the tube rig in England has indicated that to

obtain a given extinction performance under given conditions of nozzle pressure, oil fire point and preburn time, a mean flow to unit area of the envelope of the tube rig on the average 2.3 times as great as that to the large sheet metal simulated transformers was required. Equations 8 and 10 indicate that the ratios of critical heat transfer rates to the surface would be about 1.8, the expected ratio of flow rates to the envelopes of the two rigs would be between 1.8 and 2.8. If the wind velocity controlled the critical heat transfer rate the expected ratio would be greater. It is unlikely that the condition for heat transfer to the drops in the oil would differ between the oil running down tubes and a vertical surface although it would be expected that the accessibility of spray to the surfaces would be easier for a flat surface than for a nest of tubes. Broadly, however, the comparison does support the theoretical approach.

Critical rate for extinction of a wood fire. Bryan⁽¹⁷⁾ has measured the critical rate for a wood fire consisting of pieces 2 in square section and a total surface area of 80 ft². The minimum rate at which he obtained extinction with water was 0.16 gallons/minute corresponding to a rate of 0.01 g/cm²min. Bryan concluded from other observations that extinction was by cooling the wood. Under the conditions he used it may be assumed that the water was entirely vaporized; this would correspond to a heat transfer of 0.1 cal/cm²s at the wood surface. From information on the heat of combustion of wood volatiles and assuming that critical criteria as described above may be applied to burning wood, it may be estimated that 0.8 cal/cm²s would have been transferred from the flame to the wood surface under critical conditions. The difference between the measured and estimated values might be taken to indicate that a substantial heat transfer, of the order of 800 cal/g, was required to cause the evolution of sufficient volatiles for combustion.

Direct extinction of flame

To examine the relevance of the theory developed above it is necessary to have an estimate for X , the heat transfer capacity for the sprays. These estimates were obtained using equation 18, a modification of the Ranz and Marshall relationship for heat transfer from gases to drops⁽¹⁸⁾ which was found to hold for water drops evaporating in a bunsen flame⁽¹⁹⁾.

$$\frac{hD}{k} = 1/1 + 0.39 \frac{c\mu}{\lambda} \left(2 + 0.6 \left(\frac{c\mu}{k} \right)^{0.4} / \left(\frac{V_D D \rho}{\mu} \right)^{0.5} \right) \dots (18)$$

c, μ, k, ρ, β specific heat, viscosity, thermal conductivity, density in boundary layer;

D drop size, V_D drop velocity relative to gas stream;

h heat transfer coefficient;

β enthalpy increase per unit mass of vapour between surface and flame temperature;

λ heat required to vaporize unit mass of the liquid.

In estimating X it was assumed that the concentration and velocity of the drops in the flame were the same as in the approaching spray, and that the contribution of the individual fractions of the different drop sizes could be added. Since the surface area of drops of size D present per unit volume of space through which the drops are passing is proportional to $M_D/V_D D$ where M_D is the flow rate per unit area, it follows from equation 18 that

$$X \propto M D_r^{-(1.5 \text{ to } 2.0)} V_r^{-(0.5 \text{ to } 1.0)} \dots (19)$$

where M is the total flow rate per unit area, D_r and V_r are a representative

drop size and drop velocity.

The extinction of fire by water spray by extinguishing the flame has been studied with fires in kerosine petrol and benzole in a vessel 30 cm diameter⁽²⁰⁾(1). Extinction of the flame differed from extinction by cooling the fuel in that there was a sudden clearance of a comparatively large volume of flame which led to extinction.

When the spray was applied in a downward direction the flames of the petrol and kerosine fires were not extinguished unless the downward thrust of the spray was greater than 60 and 40 dynes/cm² respectively. These forces are comparable with the upward force of the flames before the spray was applied. With sprays of greater downward force the flames were extinguished as long as the heat transfer capacity of the spray was greater than about 0.15 cal/cm³s, and as long as the preburn time was not very short. The above value is intermediate between those expected from equations 12 and 13, if I is taken to refer to the upward moving flames before spray application.

For a given type of spray the most important factor in the heat transfer capacity is the drop size of the spray (equation 19) and in the thrust of the spray the rate of flow per unit area of the fire. If the drop size of the spray is plotted against the critical rate of flow for extinction at that drop size, the above phenomenon of critical thrust manifests itself as a flow rate below which the fire is difficult to extinguish with sprays of any drop size. Critical flow rates for extinction of a flame have been plotted in this way in Fig. 4 for the kerosine and petrol fires; points for extinction and non-extinction are shown for the petrol fire. For comparison critical flow rates for the extinction of the kerosine fire by cooling the liquid have been included. Similar relationships obtained by the author for sprays produced by hypodermic needles acting on a kerosine fire 11 cm diameter⁽²¹⁾, and by the National Board of Fire Underwriters for sprays acting on a petrol fire 15 cm diameter⁽²²⁾ have been given elsewhere. The critical flow rate below which extinction was difficult was smaller in both cases than those shown in Fig. 4 for the 30 cm diameter fires. This may be mainly attributed to the smaller dimension of the fires and the resulting smaller upward force of the flames, but different conditions of test and different patterns of spray at the fire area also probably played a part. Extinction of the flame has been found to be easier if the peak concentration of the spray is near or even outside the edge of the vessel, since after a clearance of part of the flame, the remnants of flame from which a flash back may occur are at the edge⁽²⁰⁾. This phenomenon may account also for comparatively low flow rates for extinction of flame reported by Y. Yazl⁽²³⁾.

During the tests the flames were usually wild with frequent partial clearance and flashbacks. However, with petrol and benzole fires when the preburn time was very short (less than 10 sec) and when sprays with high downward thrust were used, the spray pushed the flame immediately into a flat flame close to the liquid surface which was very difficult to extinguish. The appearance of the flame depended on the drop size and heat transfer capacity of the spray; a spray with a value of I equal to 0.44 cal/cm³s gave thin blue flames near the inside edge of the vessel (plate 5); with a value of I of 0.14 cal/cm³s; a belt of yellow flame covered the whole vessel. Flames stabilized close to the liquid surface were also obtained if spray were applied to the surface at an angle less than 30° to the horizontal. It was estimated that the value of I for flames stabilized in this way was about 2.5 cal/cm³s. It would, therefore, be expected that a value of I equal to about 0.5 to 1 cal/cm³s would have been required to extinguish these flames reliably.

Regression analyses on the extinction time for the kerosine and petrol fires⁽²⁰⁾ indicated that for sprays with a given value of X the entrained air current had a powerful effect on the extinction time. This effect was much more powerful than might be expected from a relation such as is given in equation 15. This may be attributed to two reasons. Firstly, the entrained air current helped to present the spray to all parts of the flame; associated with this reason it also helped the spray penetrate to the burning liquid, cooling the latter and thus reducing the size of the flame. Secondly, the entrained air current tended to blow away the thick vapour zone which was usually established after burning for about 10 seconds and thus render the flames unstable.

EXTINCTION OF FIRES IN ROOMS

Tests have been carried out by many authorities on the extinction of solid fuel fires in rooms. It is not yet clear, however, whether these fires are more efficiently controlled by cooling of the fuel or by the formation of steam which cools the flames.

Kawagoe⁽²⁴⁾ has found that the rate of burning in room fires is, on the average, directly proportional to the ventilation, and the constant of proportionality indicates that the ratio of air to fuel volatiles is the stoichiometric ratio. When fires in rooms are attacked with sprays from an opening in the wall, then additional air would be entrained into the room comparable with the normal ventilation rate through the opening. Under these conditions it may, therefore, be expected that the fire is burning with excess air when extinction is commenced. The critical amount of steam required to smother the flames would then be governed by equation(14). It may be estimated using equation 14 that if steam is obtained by the impact of spray on the burning surface, the critical flow rate of water to form sufficient steam to extinguish the flames is 10 to 15 times greater than that found by Bryan⁽¹⁷⁾ to be necessary to extinguish a wood fire by cooling. However, conditions in practical fire fighting may still frequently be such that steam extinction would require the use of a smaller total quantity of water.

From the intrinsic nature of extinction of the flame by steam and extinction by cooling the fuel, the qualitative effect of various factors on the efficiency of control (i.e. critical flow rate and quantity of water required) may be deduced. These effects are compared in Table 1.

Table 1

Effect of various factors on control of room fires
by cooling and by steam formation

Factor	Cooling the fuel	Steam formation
1. Increase in preburn time	Critical flow rate increased somewhat. Quantity increased approximately in proportion to preburn time.	No effect
2. Decrease in ease of access of water spray to burning surfaces.	Quantity increased	No substantial effect if walls are hot.
3. Increase in the fraction of incombustible surface present; total area of combustibles remaining the same.	Critical flow rate increased (due to radiant heat falling onto burning surfaces).	No substantial effect if incombustible surfaces are hot.
4. Increase in ventilation	No effect	Critical flow rate and quantity increased.
5. Linear dimension d	Critical rate proportional to d^2	Critical rate proportional to $d^{3/2}$

Available test results have been summarised by Hird et al⁽²⁵⁾ but owing to the lack of a systematic investigation of the above factors, at least on the full scale, it is not possible to give a firm opinion on the extinction mechanism. Amounts of water used to control the fires varied from 2 to 15 gallons/1000 ft³. The above workers also carried out a comprehensive series of tests in which sprays of varying pressures from 80 to 500 lb/in² and with flow rates from 5 to 25 gallons/minute were used against a standard fully developed fire in a room of volume 1750 ft³. The tests are illustrated in plate 7. The quantity of water required to control and extinguish the fire was 7 and 17 gallons respectively, and within the variance of the results, was independent of the pressure, the flow rate and whether jets or sprays were used.

USE OF WATER SPRAYS IN PRACTICAL FIRE FIGHTING

The following broad principles may be put forward on the basis of the experimental work carried out at the Joint Fire Research Organization and elsewhere.

(1) In general the best way of putting a fire out is that spray should be made to reach and cool the burning fuel. The rate at which the spray need absorb heat in doing this is generally far less than the rate of production of heat by the fire. Experimental results are available giving information on critical rates for a few systems. On the basis of equations 7 to 10 or other relationships developed in similar manner, it is possible to extrapolate

these results to other systems as long as heat transfer between the spray drops and the fuel behaves in a similar way. Perhaps the most important consequence of equations 7 to 10 is that critical flow rates per unit area for a given type of system should not increase as the scale increases; under some conditions they may in fact decrease.

(2) If sprays are applied downwards to a fire with a flame moving steadily upwards then for the bulk of the water to reach the burning fuel the downward thrust of the spray should be comparable to the upward thrust of the flame. These two thrusts may be calculated as indicated in the paper. If the sprays are applied laterally or by hand from the windward side of a fire, a much smaller thrust is necessary.

(3) Water sprays in current use are unreliable in extinguishing a fire that cannot be extinguished by cooling the fuel. However, extinction may frequently be obtained with available fire sprays produced by pressure nozzles (mass median drop size 0.2 - 0.4 mm) particularly if there is no change to stable burning in the air current of the spray. When extinction is not obtained, a large reduction in the size of flame may be achieved.

(4) For most of the fires for which water sprays are useful, e.g. fires in solids and fires in high boiling liquids flowing over solid surfaces, the drop size of the spray is not usually an important practical factor. However, for fires in deep pools of high boiling liquids the efficiency of the spray increases as the drop size is reduced.

(5) The pressure at a nozzle influences a number of factors that affect the extinction of fire. However, where sprays may be reliably used for extinction of fire, an increase in pressure about 100 lb/in² with a given flow rate of spray has not been found to confer any extra efficiency on the spray providing that the water can reach the seat of the fire. The choice of pressure for a pump, therefore, depends rather on operational factors, in particular the length and diameter of hose line and the flow rate which it is desired to give the operator, than on intrinsic efficiency of the spray in fighting the fire. It should be added here that an increase in flow rate, or a decrease in cone angle, has a greater effect on increasing the throw of a spray^(26,27) than an increase in pressure, and that an increase in pressure has a smaller effect on reducing the drop size of a spray when the pressure is above 100 lb/in² than when it is below 100 lb/in².

Finally, it is instructive to compare quantities of water which have been found necessary to extinguish experimental fires with those actually used in practical fire fighting. For fires in rooms it has been found experimentally that about 10 gallons per 100 ft² of floorarea is required and, according to the drop size of the spray, from 5 to 15 gallons may be used to extinguish a gas oil pool fire of the same size. According to information provided by Mobius⁽²⁸⁾ the minimum quantity of water to extinguish fully developed room fires under operational conditions is about 100 gallons. Thomas⁽³⁰⁾ made an analysis of the amount of water used at large fires based on the number of pumps called to the fire. It may be estimated from this analysis that for large fires approximately 1000 gallons of water is used for 100 ft² of the fire. Thus, either wastage or operational difficulties in applying water to fires is by far the most important factor governing the amount of water used, and this would appear to be a direction where a substantial research effort is worthwhile.

ACKNOWLEDGMENT

The work described in this paper forms part of the programme of the Joint Fire Research Organization of the Department of Scientific and Industrial Research and Fire Offices' Committee; the paper is published by permission of the Director of Fire Research. The author would like to express his thanks to Dr. F. E. T. Kingman for advice and criticism in the preparation of the paper.

APPENDIX

THRUST OF FLAMES AND SPRAYS

Thrust of flames

A complete analysis of the movement of flame has not yet been made, but as this movement is controlled by the buoyancy of the flame, it would be expected that the upward thrust would be proportional to the flame height. Analysis of buoyant columns rising from small heat sources indicate (30,31) that the thrust at the centre of the column is given by

$$\rho_z V_z^2 = 1.5 \text{ to } 2.0 (\rho_0 - \rho_z) g z \quad \dots(20)$$

where ρ_z is the density of the column at a point z above the source and ρ_0 is the density of the ambient air.

In Fig. 5 some calculated thrusts based on measurements of the upward velocity of flames and the flame temperature (9) are plotted against the buoyancy head $(\rho_0 - \rho_z) g z$ for fires in different liquids burning in a vessel 30 cm diameter; ρ_z is the density of the flame and z the height of the point in the flame for which the thrust was estimated. The velocity measurements were made by observing the upward motion of the top of the flame and eddies at the side of the flame as recorded by a cine camera; the calculation of the thrust was made for the mean time of burning and the mean height of the flame at which measurements were made. The temperature on which ρ_z was based was a mean temperature across the flame as measured by the Schmidt method. The straight line relation (equation 21) obtained

$$\rho_z V_f^2 = 0.27 (\rho_0 - \rho_z) g z \quad \dots(21)$$

confirms the proportionality expected and indicates that thrust is independent of the nature of the burning fuel. The constant, however, is considerably less than would be expected from equation (20).

On the basis of equation (21) it is possible to calculate the upward thrust of the flame knowing the flame heights. The latter has been related by Thomas to the rate of burning and the main dimension of the fuel layer for solid fuel fires (32).

Thrust of a spray

A spray after leaving a nozzle very soon becomes a suspension of drops moving in an air stream. The air stream is generated by the transfer of momentum from the drops and is of importance in determining the velocity of the drops and the motion of the spray as a whole. The total forward thrust of a spray may be measured by the reaction at the nozzle. Measurements of the entrained air current of sprays directed downward from a number of nozzles (33) have shown that for sprays of mass median drop size less than 1.0 mm the bulk of the thrust is transferred into momentum of the airstream by the time the spray has reached a plane 6 ft below the nozzle; most of the remaining thrust may be accounted for by momentum of the drops moving at the velocity of the air stream. For very coarse sprays (mass median drop size 1.5-3.5mm) about 50 per cent of the initial thrust is converted into momentum of the air current.

The reaction of a jet is the product of the flow rate and the velocity at the nozzle, both these factors being proportional to the square root of the pressure. The reaction of a spray nozzle, however, is less than the product mentioned above due mainly to the presence of lateral motion in the spray. Fig. 6 shows the ratios of the reaction of a number of spray nozzles to that of corresponding perfect jets and indicates the extent to which the reaction is reduced as the cone angle increases and as the spray pattern becomes less

peaked in the centre. Knowing the reaction at the nozzle, an approximate estimate of the mean forward thrust in a plane is given by R/A where A is the cross-sectional area of the spray in the plane, and if the assumption is also made that the thrust has been entirely converted into movement of the entrained air stream then the air velocity v_a may be given by:-

$$\int_0^R v_a^2 = \frac{R}{A} = a_1 \int_0^R P^{0.5} \frac{F}{A} \quad \dots(22)$$

where a_1 is a constant depending on the nozzle
 P is the nozzle pressure
 F is the flow rate

Equation (22) gives, of course, a mean value of v_a . There is evidence, however, that the distribution of entrained air velocity in a plane perpendicular to the spray axis, when both entrained air velocity and distance from the axis are expressed in dimensionless terms, is approximately independent of the distribution of flow rate within the spray. In addition the distribution of the entrained air velocity is similar to the distribution found in a turbulent air jet. These points are illustrated in Fig. 7 which shows an almost identical distribution of the entrained air for two sprays with widely different spray pattern. The radius of the spray referred to in this figure were radii where the entrained air velocity and water flow rate were respectively $1/100$ of the values in the centre of the spray.

For sprays with a similar pattern over a given area it follows from equation (22) that for a given part of the spray

$$v_a \propto P^{0.25} M^{0.5} \quad \dots(23)$$

where M is the local flow rate per unit area. A relation similar to this has been found to hold for a wide range of values of P and M for sprays projected downward from a battery of impinging jet nozzles (26).

REFERENCES

1. RASBASH, D. J. and ROGOWSKI, Z. W. Department of Scientific and Industrial Research and Fire Offices' Committee Joint Fire Research Organization, Boreham Wood, Hertfordshire, England. F. R. Note No.58/1953,
2. SPALDING, D. B. 4th International Symposium on Combustion 1952, p.347.
3. POTTER, A. E. and BERLAD, A. L. Sixth International Symposium on Combustion, 1956, p.27.
4. PALMER, K. N. Seventh International Symposium on Combustion, 1958, p.497.
5. BOTHA, J. P. and SPALDING, D. B. Proc. Roy. Soc. 1954, 225, 71.
6. KLASON, P. J. Prakt Chem. 1914, 20, 413.
7. BURGOYNE, J. H. and RICHARDSON, J. F. Fuel 1949, 27, 150.
8. BERLAD, A. L. and YANG, C. H. Combustion and Flame 1960, 4, 325.
9. RASBASH, D. J., ROGOWSKI, Z. W. and STARK, G.W.V. Fuel 1956. 35, 94.
10. SPALDING, D. B. Some Fundamentals on Combustion, Butterworths, London. 1955, p.192.
11. RASBASH, D. J. F. R. Note 290, 1957. (See ref.1).
12. RASBASH, D. J. and ROGOWSKI, Z. W. Combustion and Flame 1957, 1, 453.
13. RASBASH, D. J. and STARK, G.W.V. F. R. Note No. 304, 1959. (See ref.1).
14. RASBASH, D. J. and STARK, G.W.V. F. R. Note No. 303. (See ref.1).
15. Factory Mutual Laboratories Research Project 12549, 1954.
16. Automatic Sprinkler Corporation of America. Transformer Fire Protection Programme.
17. BRYAN, J. Engineering 1945, 159, 457.
18. RANZ, W. E. and MARSHALL, W. R. Chem. Engng. Progr. 1952, 48, 141-6, 173-80.
19. D. J. RASBASH and STARK, G.W.V. F. R. Note No. 26, 1952. (See ref.1)
20. RASBASH, D. J., ROGOWSKI, Z. W. and STARK, G.W.V. Combustion and Flame, 1960, 4, 223.
21. Annual Report. Joint Fire Research Organization, 1950. Her Majesty's Stationery Office.
22. National Board Fire Underwriters Research Report No. 10. 1955.
23. YAZI, Y. Bull. of Fire Prevention Soc. of Japan 1960, 2, (No.2) 58.
24. KAWAGOE, K. Building Res. Inst. Japan. Research Report No. 27.
25. HLED, D., PICKARD, R. W., FITTES, D. W. and NASH, P. F.R. Note No.388. (See ref. 1).

26. RASBASH, D. J. F. R. Note 181, 1955. (See Ref. 1).
27. THOMAS, P. H. and SMART, P.M.T. F. R. Note No. 168. 1955 (see Ref.1)
28. MORIUS, K. V. F. D. B. 1956, 5, (2) 33 - 42.
29. THOMAS, P. H. Quart. J. Inst. Fire Eng. 1959, 19, 130-2.
30. YEKOI, S. Report of Building Research Inst. Japan No. 34, Nov.1960.
31. YIH, C. S. Prot. 1st U.S. NAT. CONGRESS APP.MECH. 1952, 941-7.
32. THOMAS, P. H. Combustion and Flame 1960, 4, 381.
33. RASBASH and STARK, G.W.V. F. R. Note No. 445, 1960. (See ref.1).
34. GOLDSTEIN, S. Modern Developments in Fluid Dynamics, Clarendon Press, 1952, p.596,

Symbols

a_1, a_2, a_3, b	-	constants
c_p	-	Specific heat in gas boundary layer
d	-	Linear dimension
g	-	Acceleration due to gravity
h	-	Heat transfer coefficient
k	-	Thermal conductivity
l	-	Linear dimension
M_{O_2}	-	Concentration of oxygen in the air
\dot{m}''	-	Rate of burning per unit area per unit time
r	-	Stoichiometric ratio (weight of air/weight of fuel)
t	-	Time
U_a, U_D, U_{30}	-	Velocity of entrained air, of spray drops, and velocity to blow out flame.
U_f, U_z	-	Upward velocity in flame, in buoyant hot column.
x	-	Height of flame
z	-	Height of buoyant column.
A	-	Cross sectional area of spray.
B	-	Transfer number (after Spalding)
D	-	Drop size.
F	-	Total flow rate of spray
H	-	Heat of combustion
I	-	Intensity of combustion in flame
M, M_D	-	Total flow rate of spray per unit area, flow rate of drops size D .
L	-	Number of tests carried out by operator.
P	-	Pressure to produce spray with pressure nozzles.
Q, Q_c	-	Heat transfer to fuel surface per unit mass of fuel vaporised, critical value of Q .
R	-	Reaction of nozzle.
T, T_s	-	Gas temperature, surface temperature.
ΔT	-	Difference in temperature between fire point and ambient.
V	-	Volume of flame
W	-	Critical flow rate of water to extinguish flame by steam formation.
X_1, X_2, X_3	-	Critical values of X .
X	-	Heat transfer to spray within unit volume of flame in unit time.
Y	-	Preburn time
Z	-	Rate of fuel consumption in fire.
α	-	Thermal diffusivity
β	-	Sensible heat of steam or vapour.
γ	-	Heat taken up as sensible heat in fuel per unit area of surface per unit time.
λ, λ_f	-	Heat required to vaporize unit mass ^{of} liquid, of fuel.
μ	-	Viscosity in boundary layer.
$\rho, \rho_f, \rho_o, \rho_2$	-	Density in boundary layer, in flame, ambient air, in buoyant column.
T_c	-	Thrust of spray
δ_c	-	Critical value of δ

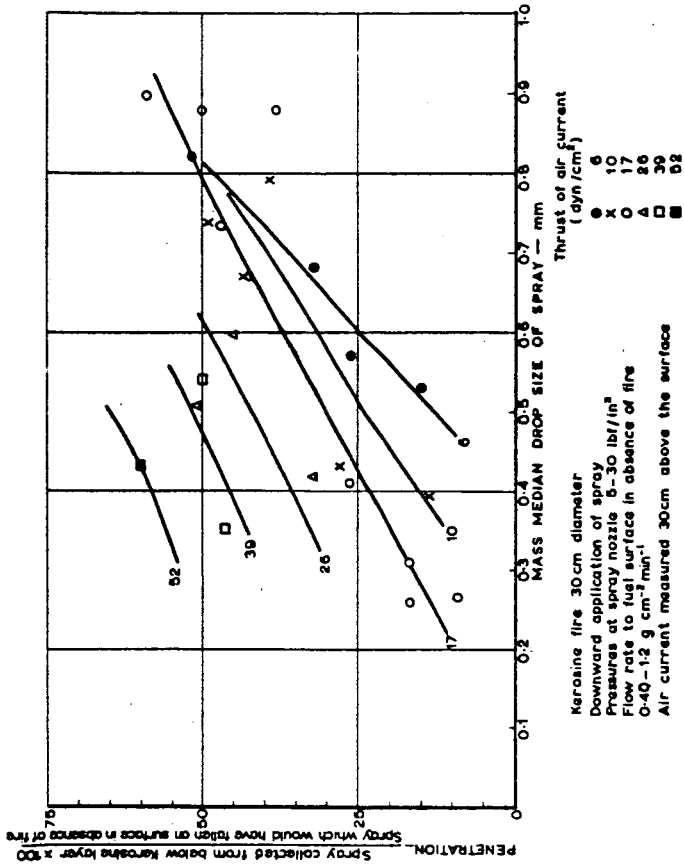


FIG. 1. PENETRATION OF SPRAY TO THE FUEL OF A FIRE

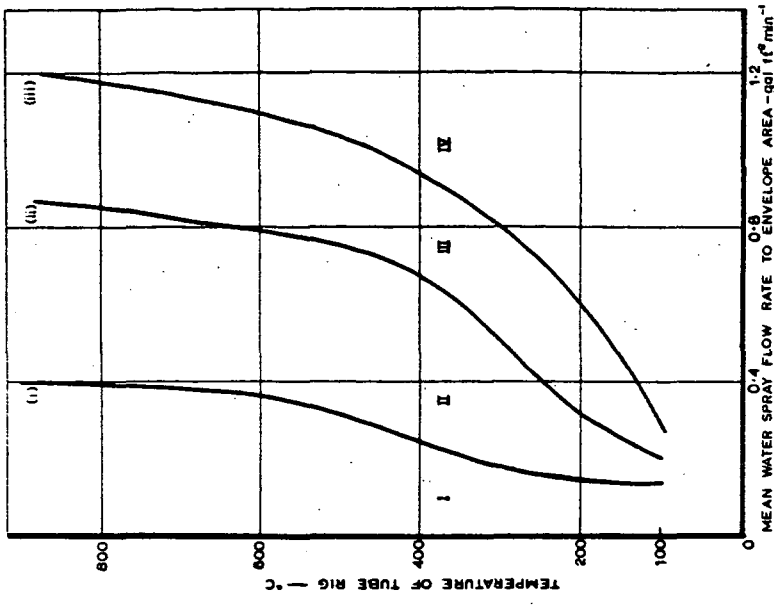


FIG. 3. CONTROL AND EXTINCTION OF OIL FIRES ON TUBE RIG

I No control
 II More than 50 per cent of rig cleared of flame in 30s
 III More than 50 percent chance of complete extinction in 45s
 IV Estimated certain extinction in 45s

Spray pressure 90 lb/in²
 Drop size 0.6 - 3.0 mm
 Envelope area of rig 90 ft²
 Transformer oil - flow rate 5.25 gal/min

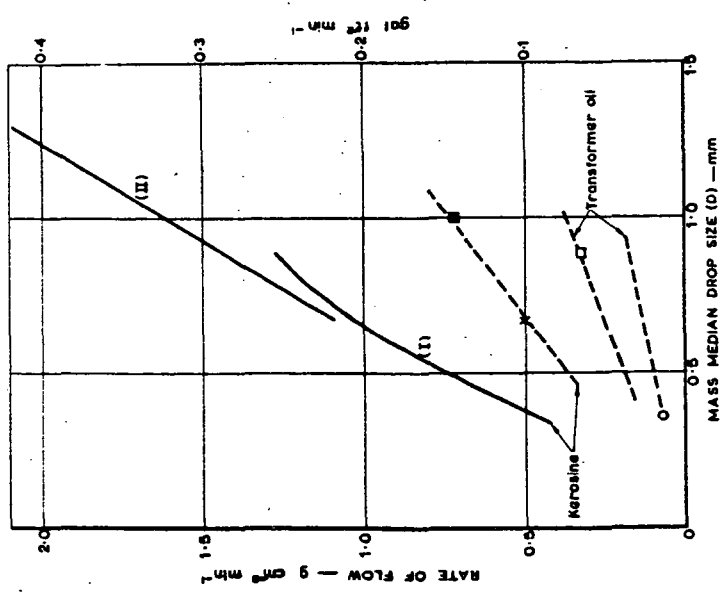
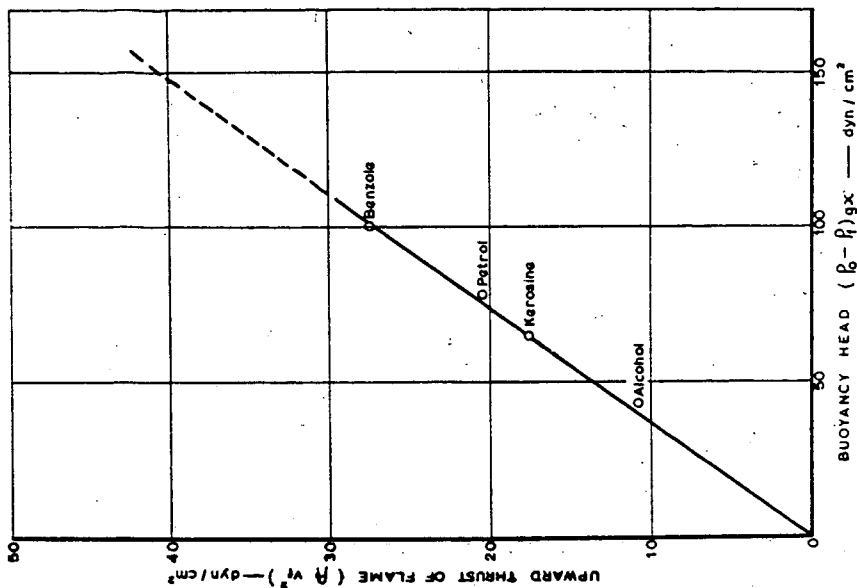


FIG. 2. CRITICAL FLOW RATES FOR EXTINCTION OF POOL FIRES BY COOLING THE LIQUID

(I) 30cm diameter Kerosine fire spray applied downwards
 (II) 11cm diameter Kerosine fire spray applied downwards
 x. 30cm diameter Kerosine fire spray applied 10° to horizontal
 ■ 243cm diameter Kerosine fire spray applied by hand
 □ 30cm diameter transformer oil fire spray applied downwards
 ○ 243cm diameter transformer oil fire spray applied by hand



NB X refers to the height in the flame at which v_1 was measured and not maximum height of flame.

FIG. 5. RELATION BETWEEN UPWARD THRUST OF FLAMES AND BUOYANCY HEAD—FREELY BURNING LIQUID FIRES 30cm DIAMETER

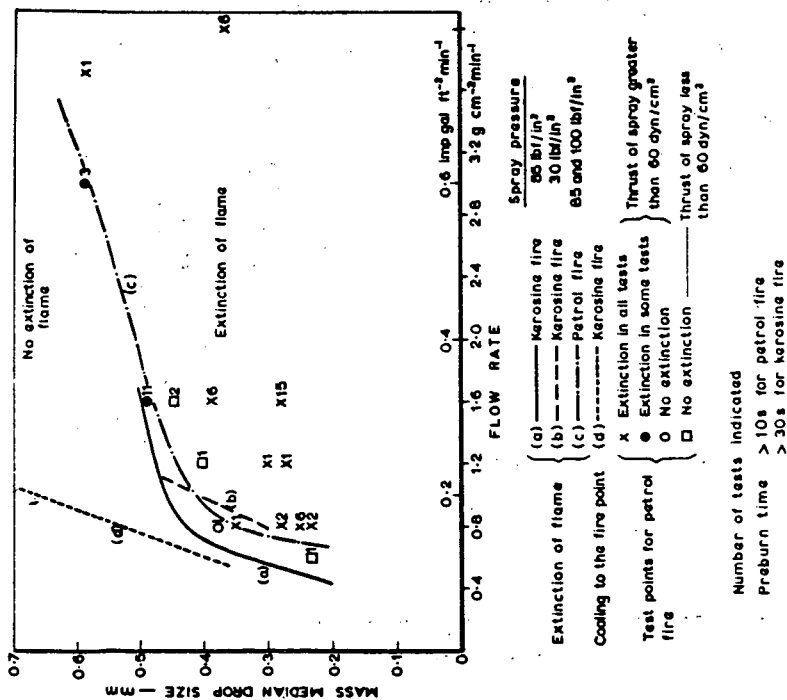


FIG. 4. CRITICAL FLOW RATES FOR EXTINCTION OF KEROSENE AND PETROL FIRES 30cm DIAMETER, DOWNWARD APPLICATION OF SPRAY

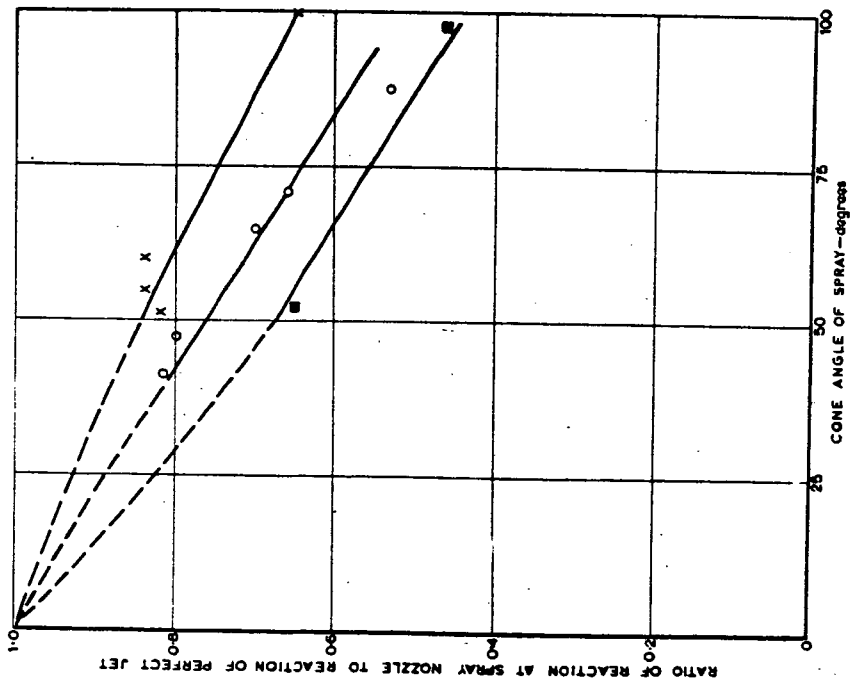


FIG. 6. REACTION OF SPRAY NOZZLES

* N.B. Fig.7 gives pattern of a spray falling into this category

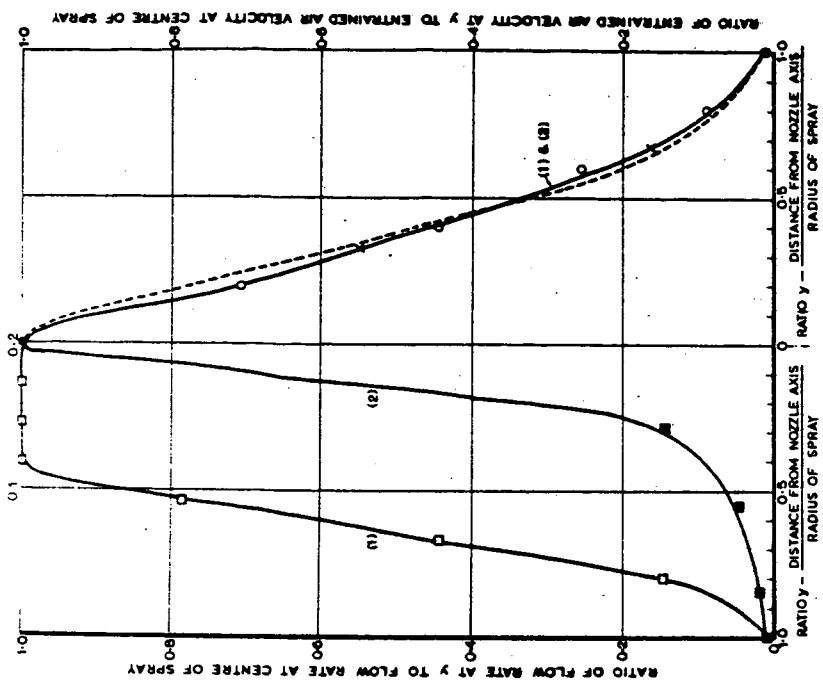
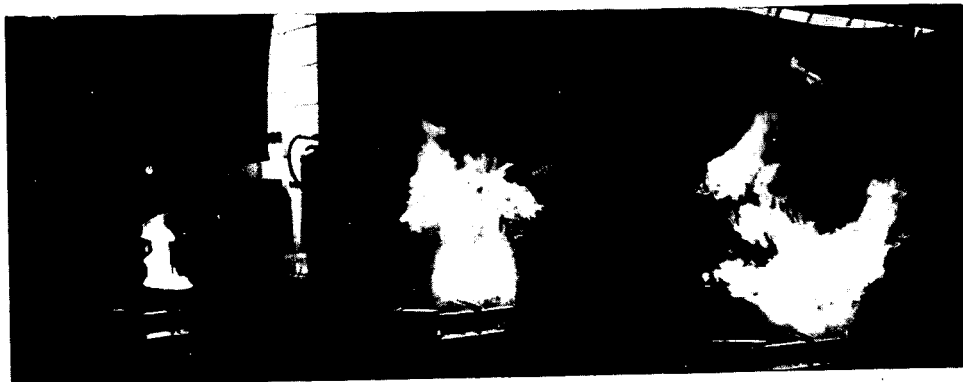


FIG. 7. COMPARISON OF DISTRIBUTION OF ENTRAINED AIR CURRENT AND WATER FLOW IN SPRAYS FROM GIVEN NOZZLES

□ Nozzle (1) uniform pattern
 ■ Nozzle (2) peaked pattern
 --- Curve for free air jets*
 * See reference 34

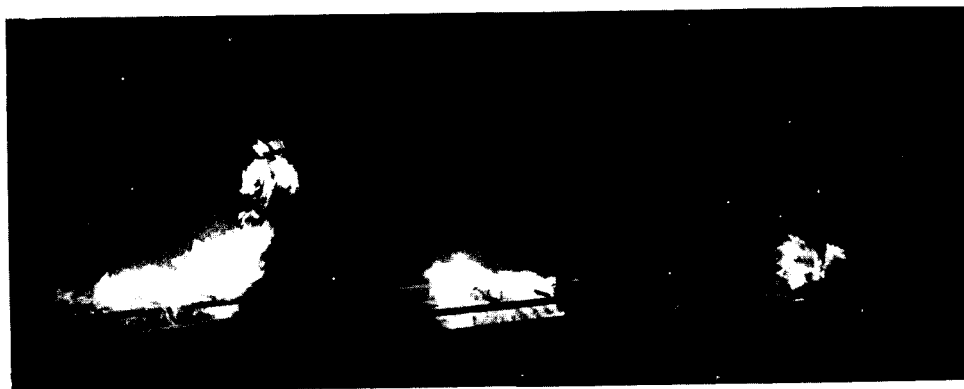
FLOW RATE PATTERN 7:0' BELOW NOZZLE
 ENTRAINED AIR VELOCITY PATTERN 6:0' BELOW NOZZLE



BEFORE SPRAY
APPLICATION

$\frac{1}{2}$ s

1 s



4 s

6 s

8 s

EXTINCTION OF FIRE IN TRANSFORMER OIL BY
DOWNWARD APPLICATION OF SPRAY FROM FIXED
NOZZLE (EXTINCTION TIME 8.8 s)

PLATE I



BEFORE SPRAY APPLICATION



EXTINCTION AT NEAR SIDE OF RIM



FIRE UNDER CONTROL



JUST BEFORE EXTINCTION

EXTINCTION OF FIRE IN HEAVY FUEL OIL BY
HAND APPLICATION OF WATER SPRAY. SPRAY
FLOW RATE 1.4 GAL/MIN.

PLATE 2



BEFORE APPLICATION OF SPRAY



SPLASH FIRE DURING APPLICATION
OF SPRAY



1 SECOND AFTER REMOVAL OF
SPRAY

SPLASH FIRE CAUSED BY THE ACTION OF A COARSE
SPRAY ON BURNING DIESEL OIL

PLATE 3



APPLICATION



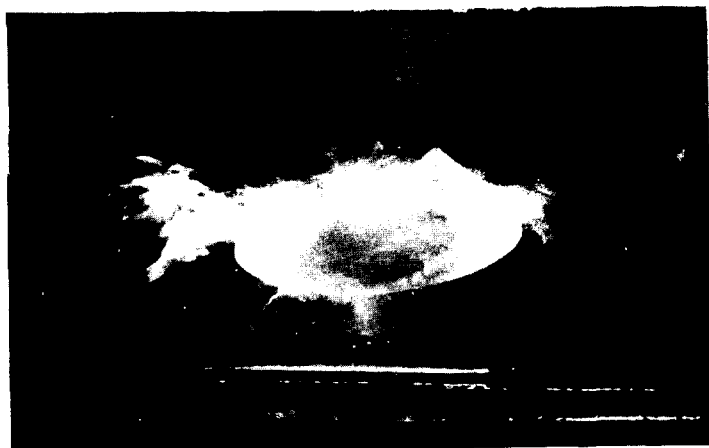
5 s



30 s

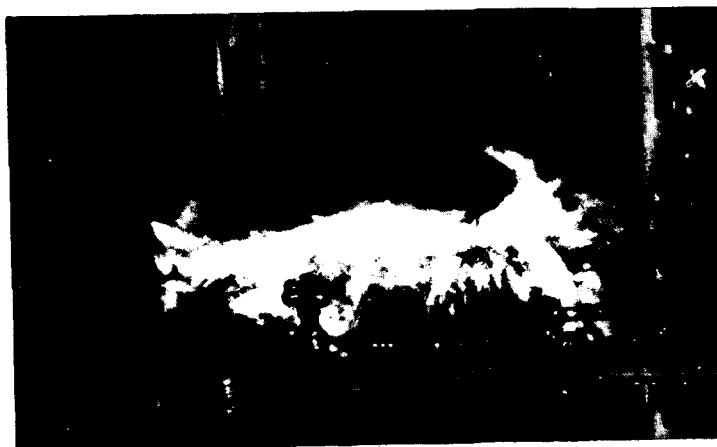
CONTROL OF FIRE IN TRANSFORMER
OIL ON A BANK OF TUBES

PLATE 4



STABLE FLAME CAUSED BY ACTION OF FINE
SPRAY ON PETROL FIRE. DROP SIZE OF SPRAY
0.28 mm. FLOW RATE $1.6\text{g cm}^{-2}\text{ min}^{-1}$

PLATE 5



STABLE FLAME CAUSED BY ACTION OF SPRAY
ON PETROL FIRE. DROP SIZE OF SPRAY
0.28 mm. FLOW RATE $1.6\text{g cm}^{-2}\text{ min}^{-1}$

PLATE 6



ATTACK WITH A WATER JET ON A FULLY DEVELOPED
FIRE IN A ROOM

PLATE 7

Improving the Effectiveness of Water for Fire Fighting

C. S. Grove, Jr. and A. R. Aidun

Syracuse University, Syracuse 10, New York

INTRODUCTION

Fire is of great benefit to mankind. It furnishes the heat for his cooking and for warmth of his shelters. Until the relatively recent advent of nuclear power, some form of combustion process, that is fire, provided the major source of energy for his power.

However, along with its tremendous value, fire has also proved a terrible enemy of mankind. Few people need to be convinced of the heavy annual waste resulting from uncontrolled fires in the civilized world, as well as in areas where civilization has progressed more slowly.

Uncontrolled fires have caused frightening physical, mental and financial losses to local communities. For example, from 1948 to 1952, the average annual fire loss according to the National Fire Protection Association in the United States amounted to \$814,957,000. Even this figure cannot possibly take into account the lost lives, the destroyed businesses and the disruption of production.

This paper discusses a new method to help mitigate this terrible toll of fire waste. Ideally, the best way to combat the problem of fires is to prevent them. Unfortunately, this approach appears to be one of the most difficult to implement. Another way to combat this problem is to increase the rapidity with which fire extinguishing agents function.

Research scientists in fire fighting are constantly working toward this goal. If an improved extinguishing agent can be developed, the fire loss can be decreased. Scientists at Syracuse University have been working toward such a goal for the past fourteen years. From 1947 to 1957, the primary concern was with methods to increase the effectiveness of fire fighting foams. During the past four years, these researches have been concentrated on methods to improve the fire fighting characteristics of water.

The original fire research conducted at Syracuse University dealt with fire fighting foams. The major objectives during this work were to develop better foam formulations, foam generation techniques and foam extinguishing systems. These studies were largely carried out under the auspices of the Navy and Army. Early experimental work was partially responsible for the development of the high expansion foam used to envelop an aircraft crash fire. Other uses of foam in air disasters are for covering a runway for a "belly landing", blanketing a gasoline spillage to prevent fires from starting, and even for calming wave action in sea rescue operations. Syracuse University conducted much of the fundamental research on these uses, while the government facilities were concentrating on pertinent applications. Foams are probably the best methods available for extinguishing Class B fires.

During this work there was also some experimentation with the extinguishment of Class A fires which are normally attacked by water. The studies on foams led to the belief that some of their outstanding qualities, such as blanketing ability and high viscosity, might be obtainable in water through the use of certain additives. The present study was thus initiated to determine whether additives improve the fire fighting characteristics of water, and if so, which formulation is most effective.

Water in its natural state has been used to extinguish fires for many centuries. It has three great advantages because of its cooling properties, low cost and almost universal availability. Before the great trend toward urbanization in the United States and other parts of the world, these three qualities were sufficient to offset some of the limitations of water as a fire fighting agent. However, today when a city fire is feared not only because of the damage inflicted to one building but also because of the possibility of damage to a great area, these limitations can not be completely neglected. There is also a further danger that with the current population explosion, the supply of water may be extremely limited in some areas.

The limitations of water are essentially three fold. First, because of its low viscosity, water forms a thin film which rapidly runs off the burning structure. This may allow the fire to reignite. Secondly, water's continued blanketing ability is limited. Third, water has relatively poor reflective powers. If the radiant energy of the fire can be separated from the source of fuel, more rapid extinguishment of the flame is possible. The reflection of the radiant energy away from the adjacent buildings will help to prevent the spread of the fire.

EXPERIMENTAL PROCEDURE

The approach to this problem has been to prepare solutions of various additives and water and to test these new solutions for fire fighting effectiveness. Basically, the experimentation has been with two major groups of additives: viscosity additives and opacifier additives. Detergents have been used in limited amounts to improve the initial spreading of the viscous water. Viscosity additives are utilized to improve the blanketing and run-off properties of water. The opacifier additives are employed to reflect radiant energy away from the burning and/or adjoining structures.

Work to date has been primarily directed toward the evaluation of viscosity additives and these additives have generally been the most effective. However, experience with opacifiers has also been accumulated. Samples have been received from many major manufacturers of viscosity, opacifier and detergent additives. Essentially, the basic approach is to screen these additives in the laboratory and then test the more promising ones on small and large scale fires.

The viscosity additives, are tested on a run-off simulator apparatus (ROSA) which was designed and built in the Syracuse University laboratories. This apparatus was designed to simulate the actual run-off properties of the fire fighting solution. It measures the fluid film time, temperature drop, and volume of the liquid evaporated.

The more promising additives are subjected to a small scale fire test. All small scale fire tests are conducted in a small laboratory built expressly for this purpose. The test site itself is constructed such that the tests can be conducted in a controlled environment. Such variables as rain, snow and wind velocity do not affect the test conditions (7). Both the small and large scale fire tests are conducted in an enclosed fire room. This room consists of a Butler building which is approximately 13' x 12' x 12' and which is constructed of galvanized sheet metal. A window has been inserted on one side of the enclosure so that the performance of the solution as it is sprayed on the burning surface can be observed. Exhaust facilities

have been provided to permit adequate control of ventilation or draft.

The fuel generally used for both large and small scale fires is California clear pine which has been presoaked in kerosene, for approximately 30 seconds. For the small scale tests, eight pieces of the wood, 1" x 3" x 10", are arranged in two tiers. A single nozzle (Fulljet 1/8 GG8, manufactured by Spraying Systems Company) is located at the height of 6 feet above the fire. The wood is ignited and the fire is allowed to burn four minutes before extinguishment is started. Through use of thermocouples and a radiometer, it has been found that almost all of the test fires reach their maximum intensity at this time interval. In studying the effect of viscosity on extinguishment, a uniform preburn time of four minutes was used. On the small scale fire test, the sample solution was sprayed on the burning structure at a rate of 1.G.P.M.

After the various solutions of additives are tested on the small scale fires, the surviving promising ones are further tested on larger scale fires. In this test the wood, which is 2" x 4", is arranged in three tiers. The first tier is comprised of 13 pieces each 36" long spaced one inch apart. The second tier is comprised of 12 pieces each 35" long, and the top tier consists of 12 pieces each 34" long. This is shown in Figure 1. Thus, a type of truncated pyramid structure is obtained. Only the wood in the first tier is presoaked in kerosene. In this test, four nozzles (Fulljet 1/4 GG nozzles, manufactured by Spraying Systems Company) are used for extinguishing the fire. The nozzles are equally spaced at a distance of 1.4 ft., from the center of the fire crib, and approximately 12 ft., above the wood arrangement. In the larger scale fire tests, varied preburn times are used but the sample solution is sprayed on the burning structure at a rate of 3.6 G.P.M., 19 psi.

After ignition, the intensity of the large scale fire continually increases until it reaches a maximum after about three minutes. (Figures 2 and 3). The preburn times for the large scale fire tests are varied in order to permit thorough analysis of the effects of various additives on extinguishment. Each formulation is tested on the larger scale fire and the results are compared with corresponding data obtained using water alone.

Recent work has been concentrated on transferring the optimum formulation results from the laboratory to field fire tests. In these efforts, local county fire departments have cooperated. Several series of field fire tests have been run in cooperation with the Navy Fire School at Norfolk, Virginia on cribs of seasoned 2" x 4" pine wood, measuring approximately 8 feet on a side and 4 feet in height.

In addition to these relatively controlled tests, close liaison has been maintained with the U. S. Department of Agriculture, Forest Service, Division of Forest Fire Research, Berkeley, California. Mr. Carl C. Wilson, Chief of the Division, and associates ran operational studies in the summer of 1960 and are running additional operational studies at this time utilizing viscous water on some of the tank fire trucks for fighting forest fires.

RESULTS AND DISCUSSION

Studies to date have yielded some quite significant results. A number of viscosity increasing additives have been found which improve the effectiveness of water as a fire fighting agent. Some additives are more effective than others. Opacifiers have been shown to decrease the radiant energy transfer. Further study on opacifiers has been delayed since over 75% of the total improvement was attributable to increased viscosity. Viscous water without opacifiers offers less attendant storage problems.

(a) Initial Control: One of the important factors in fighting Class A fires is the "knock-down" or initial control. This is a very difficult parameter to measure quantitatively due to the differences in fire fighting personnel and procedures. However, experience in the laboratory fire tests (Figure 4) and in the field fire tests has shown that viscous water "knocks down" the fire much more rapidly than plain water. The fire fighters can advance up to or into the structure for rapid control and later for final "clean-up". As a further advantage, more rapid initial control means less fire damage and in some cases, preserves life.

A rather vivid illustration of this phenomenon was reported (1) from some tests run by the Los Angeles City and County Fire Departments at the Van Nuys, California Airport. "A previously exposed building was ignited and one room allowed to become completely involved. The fire was then knocked down in 15 to 20 seconds with viscous water at an application rate of 30-40 G.P.M. The demonstration was repeated several times. Finally, the building was allowed to burn until it was completely involved and about half of the roof had caved in. At this point one of the Los Angeles City Mountain Battalion Crews attempted to extinguish it. They used a small pumper with a capacity of about 35 G.P.M. They made little, if any, progress and gave up after one of the firemen received minor burns. The viscous water crew next took over with about the same application rate and were able to knock the fire down and bring it under control in about four minutes".

(b) Extinguishment Time: Small fire tests were conducted on cribs consisting of eight pieces (1" x 3" x 10") of California clear pine arranged in two tiers, four pieces in each tier, with one inch spacing. The viscous water was applied at a rate of one G.P.M. after a preburn time of four minutes. The extinguishment time decreases as the viscosity is increased. Figure 5 illustrates this effect by two different viscosity additives, Monsanto DX-840-91 and bentonite clay, Volclay (2). Volclay reaches its peak of effectiveness at a viscosity of five centipoises, while Monsanto DX-840-91 reaches its peak at ten centipoises. The reason for this difference is not fully explainable.

Larger scale fire tests were run as previously described. The results (3) of a series of tests comparing extinguishment time for water and for viscous water, obtained from the addition of Dow ET-460-4 are shown in Figure 6. Certain uncontrollable variables, such as the chemical and physical properties of the wood and the difficulty of obtaining a perfectly reproducible test fire, cause a scattering of the data. However, it can be clearly seen that the use of viscous water gives a marked reduction in extinguishment time when plotted as a function of minutes of preburn time. For example, at a preburn time of four minutes, water took about 8 minutes for complete extinguishment, while viscous water (5.5 cp.) averaged about 1 1/2 minutes. With water, the wood collapsed during extinguishment for a preburn time of five to six minutes. On the other hand with viscous water, extinguishment was so rapid that it was possible to obtain preburn times of as much as nine minutes, with no wood collapse. Other additives for increasing viscosity, e.g. sodium alginates, were tested with results of the same general magnitude.

The results on extinguishment time for Dow ET-460-4, Carboxymethyl Cellulose (CMC) and water are shown in Figure 7, with preburn time as a parameter. Each viscosity additive reduces extinguishment time, although at the same viscosity Dow ET-460-4 appears to be more effective than CMC.

Field fire tests at the Navy Fire School in Norfolk have confirmed the reduction in extinguishment time when viscous water is used. The percentage reduction is not as marked as in the laboratory but control and reproducibility of open field fires are much more difficult; scatter of data is wide.

Based upon laboratory results, fire fighting agencies in California and Nevada

pooled their efforts in 1960 to conduct a series of suppression and retardant tests to determine whether the chemical additives could be used to help control forest fires with ground equipment. A report (5) on this effort from the U. S. Department of Agriculture, Forest Service, Division of Forest Fire Research states: "Viscous water reduced suppression time under many conditions and was outstanding in keeping fires from rekindling. The residual film of algin thickened water seemed to be particularly effective in extinguishing usually difficult-to-extinguish fires in fuels such as baled hay and sawdust. Although there were operational difficulties such as spoilage and slight corrosion of metal parts, most problems have or can be solved. The dry powder that makes the water thick can be mixed on the fireline in 1 to 5 minutes using the jet-type mixer which is easily installed on the truck".

(c) Reignition: A common problem in Class A fire fighting is the reignition of the fire after it has been extinguished, due to the residual heat. Many such experiences have been presented in fire fighting annals. One of the outstanding characteristics of the viscous water extinguishment is the almost universal lack of reignition after the fire is "out". This is quite evident in the controlled laboratory test fires. A large number of detailed tests have been reported (3,4) which show that fires extinguished with water reignited from one to four times after initial extinguishment, while most of the comparable fires extinguished with viscous water did not reignite. It was also quite evident that water extinguished fires retained much more residual heat, necessary for reignition, than viscous water extinguished fires.

Comparable results on reignition have been observed in various field fire tests at Norfolk and at Mariposa Airport, California. Reignition occurs at times even with extinguishment with viscous water; however, it is much delayed and is more easily controlled. Davis (6) stated in regard to the Mariposa Airport tests: "The chemicals also had a noticeable effect on rekindling of the charred cribs that remained after the initial suppression. Although cribs sprayed with viscous chemicals did reignite, rekindling was slower in starting and cribs that rekindled, burned at a lower rate than those sprayed with water".

(d) Reduced Water Consumption: In many tests, it has been shown that the rate of extinguishment with viscous water is many times greater than with plain water. This means that a given fire can be fought with reduced water consumption; the water actually used is much more effective. While in many parts of the world, water is available in unlimited quantities for fighting fires there are many other places on the globe where water is very scarce. A good example of this is Southern California.

Where fires need to be fought in isolated places and all fire fighting water must be brought in by trucks, it becomes of grave importance to utilize fully every bit of water. If one assumes a five fold increase in rate of extinguishment for viscous water, it is easy to see that one tank truck of viscous water can control as much fire as five tank trucks of plain water.

(e) Reduced "Run-Off": An obvious disadvantage of poor utilization of water is the rapid "run-off" so that only a portion of the water is effective. A large number of laboratory fire tests have shown that viscous water is more effectively used for extinguishment. A group (3) of comparative tests were run to check this point under controlled conditions. Plain water applied at a rate of 3.6 G.P.M. averaged three pounds per minute of "run-off"; for CMC at a viscosity of 5.5 cp., the "run-off" was only 1.5 pounds per minute; and for Dow ET-460-4 the rate was less than 1 pound per minute of 5.5 centipoise viscous water.

A corollary to the more effective use of viscous water is the reduced water damage to structures, contents, and adjoining facilities. Every one recalls the large fire several years ago in lower New York, in which the old Wannamaker store building was destroyed, but, does every one recall that the adjacent subways were flooded out of service for many hours? Frequently, firemen complain that water damage to the contents of a structure is as great as the fire damage.

(f) Logistics of Chemical Additives: The amount of chemical additives required to achieve an optimum viscosity of water for fire fighting varies with the characteristic of the chemical. Satisfactory viscosity can usually be achieved with less than 0.2% of a chemical additive. This percentage would require about 16 pounds for treatment of 1,000 gallons of water.

Some of the chemical additives are only in pilot plant production, so costs per pound are not firm. Others, such as CMC and Keltex FF, are in full production. At a price of \$0.50 per pound for chemicals, it would cost less than one cent per gallon to raise the viscosity of the water to a satisfactory point. This would not be considered prohibitive under many conditions of fire fighting.

Davis and Phillips (5) state that for fighting forest fires even a higher cost per gallon for chemical additives is not prohibitive. "The price per gallon is reasonable for all of these chemicals, only 3 to 14 cents per gallon".

CONCLUSIONS

1. Viscous water produces much more rapid initial control of Class A fires.
2. The rate of extinguishment of Class A fires is more rapid with viscous water.
3. The danger of reignition is markedly reduced when Class A fires are extinguished with viscous water.
4. A lower amount of viscous water is required for extinguishment of Class A fires.
5. Markedly reduced "run-off" of viscous water mitigates water damage.
6. Logistics of chemical additives for fire fighting is economical.

LITERATURE CITED

1. Davis, J. B., Private Communication, United States Department of Agriculture, Forest Service, Division of Forest Fire Research. (March, 1961)
2. Aidun, A. R., "Additives to Improve the Fire Fighting Characteristics of Water", Quarterly Progress Report No. 9, Contract No. NBY 13027 (October, 1959).
3. Ibid., Quarterly Progress Report No. 11 (April, 1960).
4. Ibid., Quarterly Progress Report No. 12 (July, 1960).
5. Davis, J. B. and Phillips, C. B., "Fire Fighting Chemicals -- New Weapons for the Fire Suppression Crew", Pacific Southwest Forest and Range Experiment Station, Research Note No. (In press), 1961.
6. Davis, J. B., Private Communication, United States Department of Agriculture, Forest Service, Division of Forest Fire Research. (October, 1960).
7. Grove, C. S. Jr., "Methods to Improve the Fire Fighting Characteristics of Water", Proceedings of the Sixty Fourth Annual Meeting of the National Fire Protection Association, Page 38 (May 16-20, 1960).

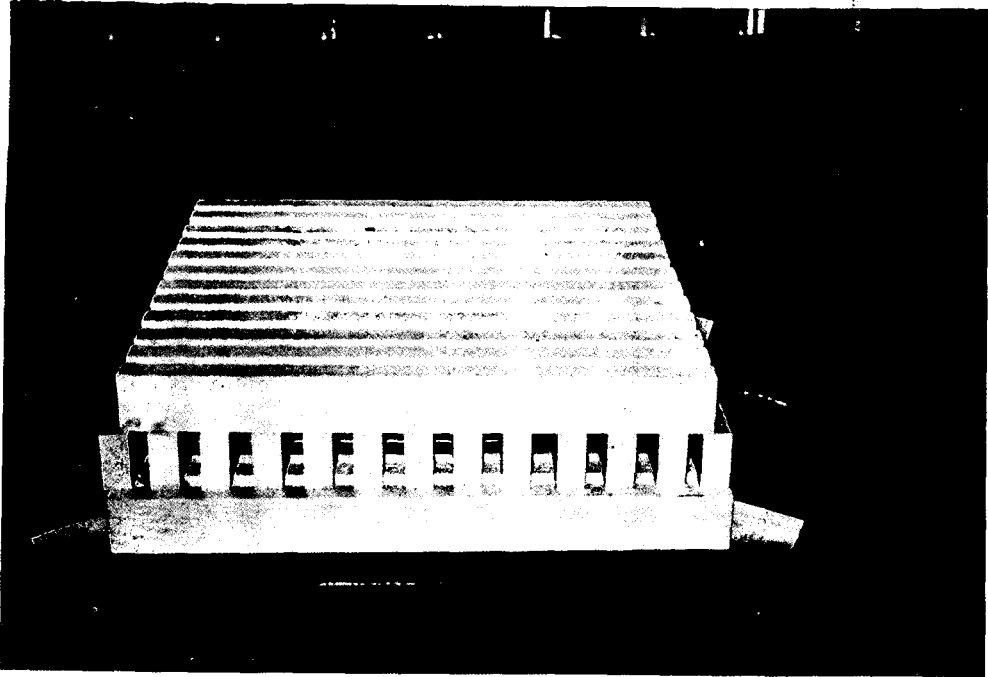


Figure 1

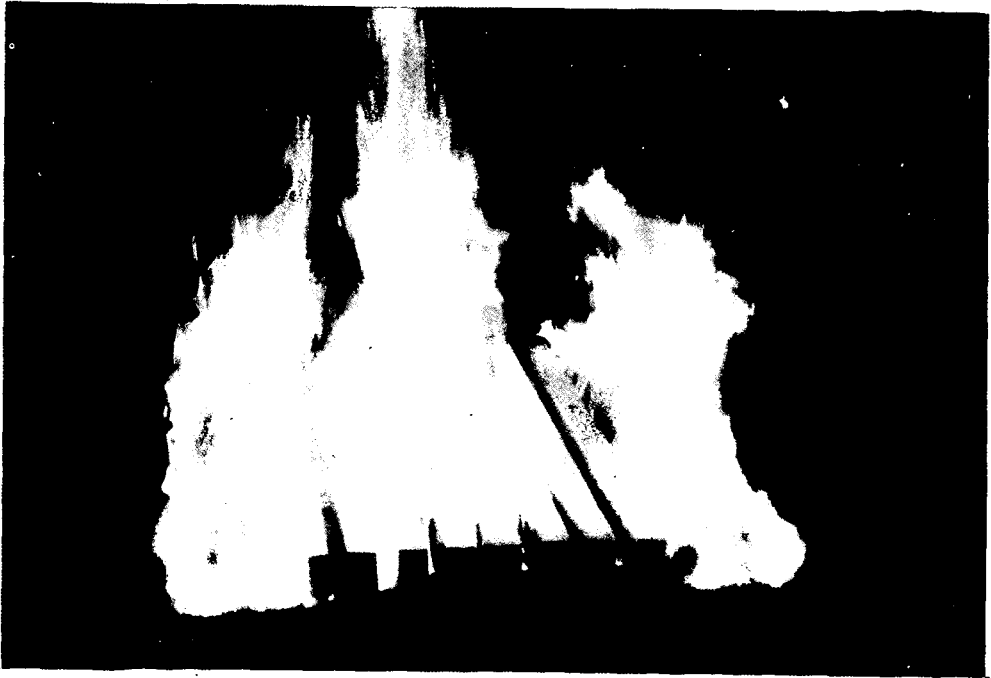


Figure 2

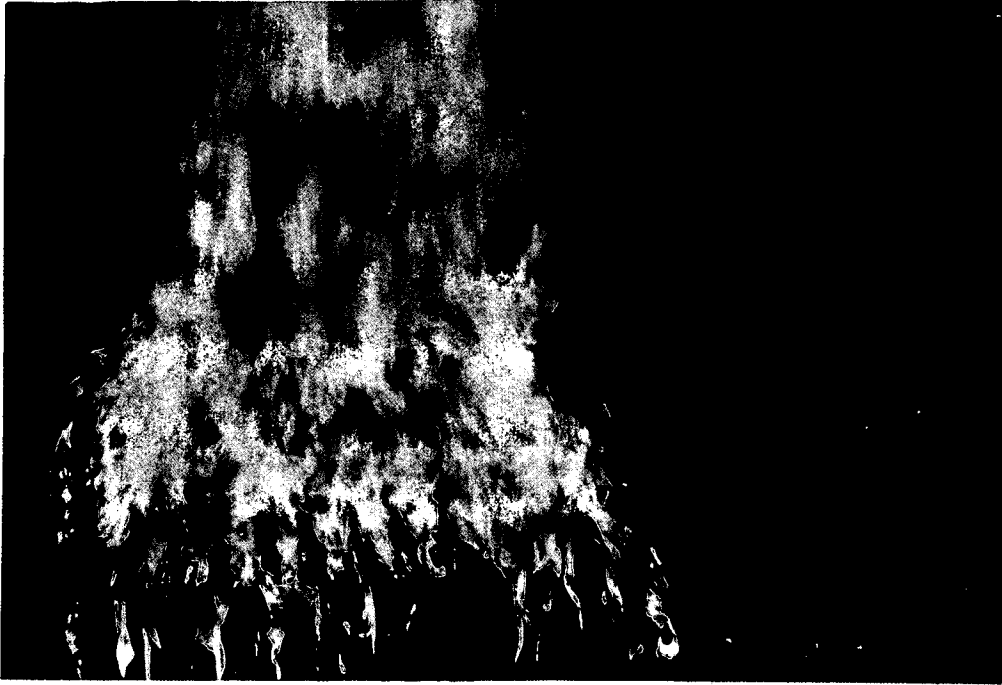


Figure 3

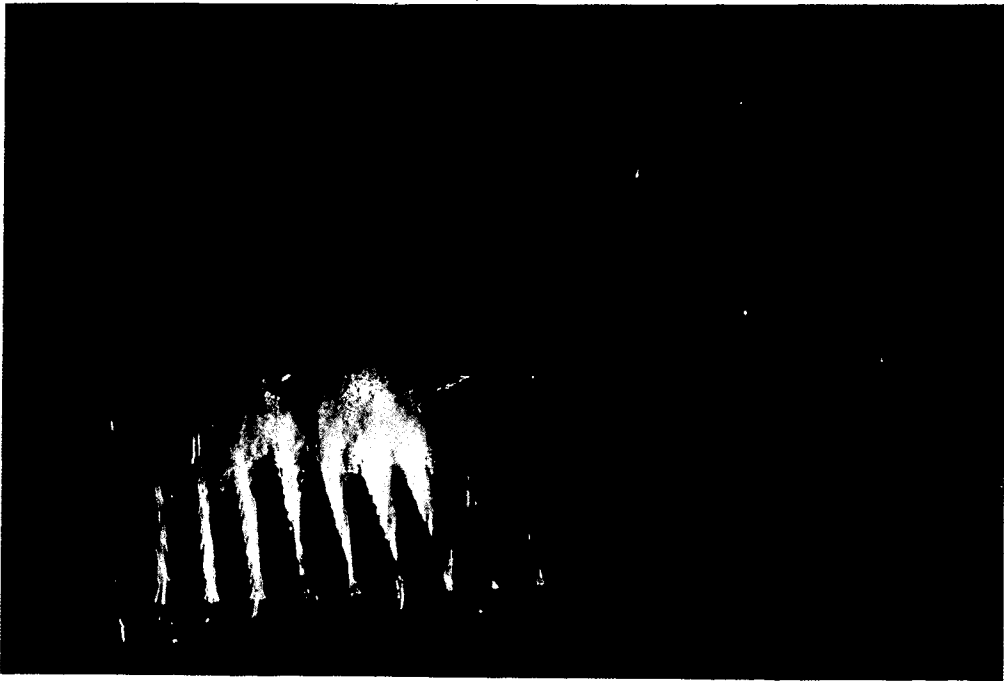
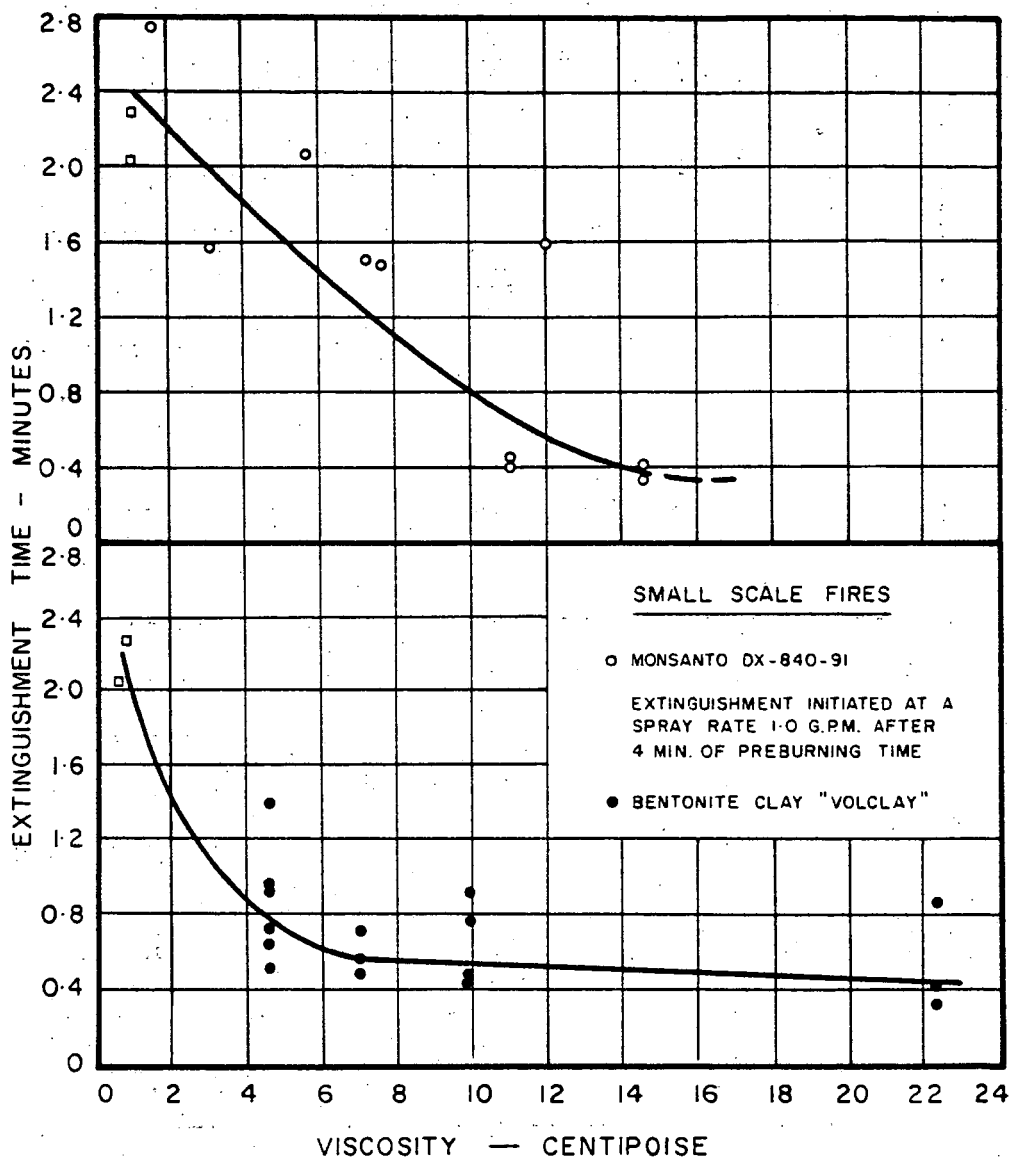
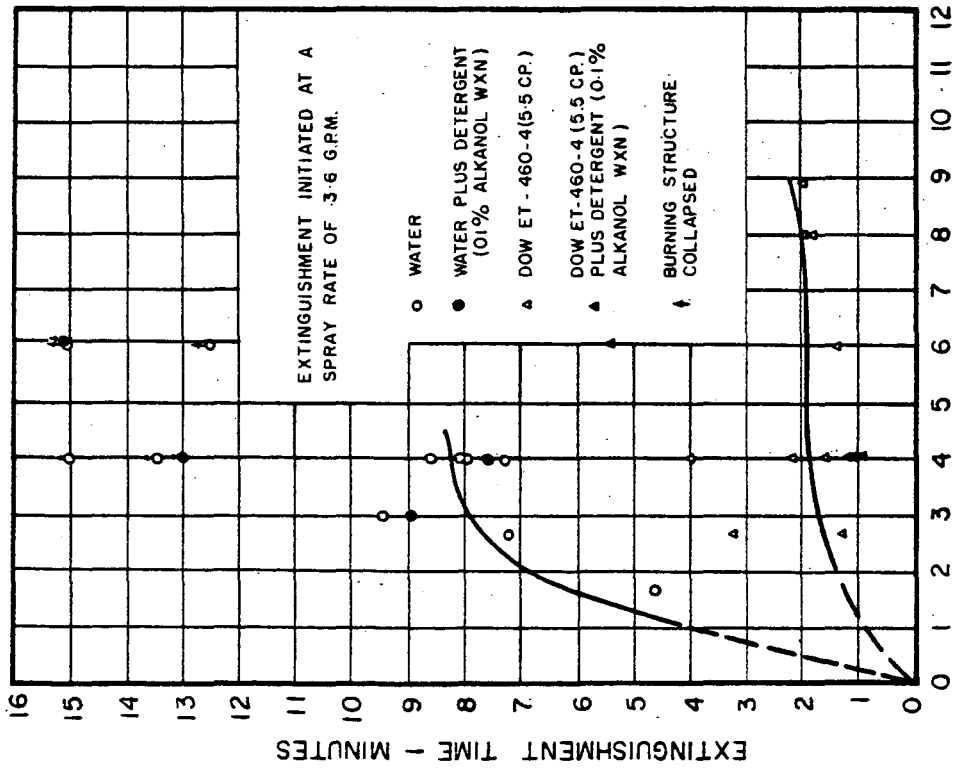


Figure 4



EXTINGUISHMENT TIME VS PREBURN TIME

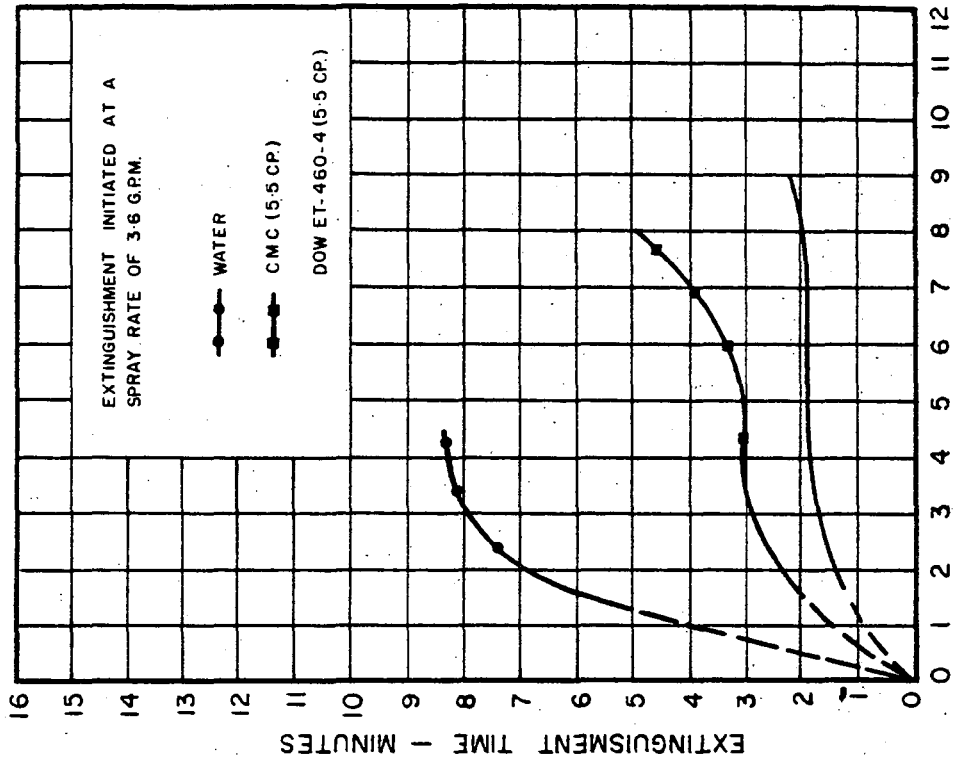
FIGURE 5



PREBURN TIME - MINUTES

EXTINGUISHMENT TIME VS PREBURN TIME

FIGURE 6



PREBURN TIME - MINUTES

EXTINGUISHMENT TIME VS PREBURN TIME

FIGURE 7

DIFFUSIVE BURNING OF LIQUID FUELS IN OPEN TRAYS

By David Burgess, Alexander Strasser, and Joseph Grumer

U. S. Department of the Interior, Bureau of Mines
Explosives Research Laboratory
Pittsburgh, Pennsylvania

INTRODUCTION

An assessment of the hazards of a new liquid fuel requires an estimate of its liquid burning rate (i.e., linear regression rate of the liquid surface) during spill fires in open air. The best-known work on this subject is that of Blinov and Khudiakov (1) who reported on flames of several hydrocarbon blends contained in shallow trays. Their findings, as reviewed and interpreted by Hottel (3), suggest that the burning rate above large pools is determined by the rate of radiative feedback of the flame's heat of combustion to the pool of liquid. The important implication of this rate-controlling process is that burning rate should increase asymptotically to a maximum value at very large pool diameter; this maximum rate should not be much greater than with pools of moderate dimension, i.e., 1-2 meter diameter.

Some support was given to the picture advanced by Blinov and Khudiakov and by Hottel in an earlier paper from this Laboratory (2). The present paper gives additional corroborative evidence based on data for methanol, liquefied natural gas, liquid hydrogen, and two amine fuels as well as four typical hydrocarbons. The paper also describes the effects of fuel temperature and of wind on burning rate, discusses the special problem of cryogenic fuels, and suggests that burning rate may be predicted with some confidence from the heats of vaporization and combustion of the fuel.

EXPERIMENTAL

Materials

The liquid hydrogen was preconverted parahydrogen, supplied by the contractor.* Unsymmetrical dimethyl hydrazine (UDMH) used was specification grade "Dimazine" supplied by the Chlor-Alkali Division of Food Machinery and Chemical Corporation; and diethylenetriamine (DETA) was obtained as a technical grade product from the Carbide and Carbon Chemicals Company. Liquefied natural gas (LNG) was prepared by total condensation of the local pipeline product, boiling at -150°C ., cf. methane, b.p. -161.5°C . Reagent grade hexane and xylene, purified absolute methanol, and technical grade benzene were used as received from the Fisher Scientific Company and c.p. butane as obtained from the Matheson Company, Inc.

Procedures

Our burning rate tests followed generally the experimental conditions of Blinov and Khudiakov (1, 3). The noncryogenic fuels were burned in trays of 7-240 cm. diameter and about 8 cm. depth, particular attention being given to flush-filling of the trays at the smallest diameters. Liquid hydrogen was burned in

*See Acknowledgment.

stainless steel dewars of 7-33 cm. diameter and LNG in insulated trays or within a diked area which had been precooled with liquid nitrogen. Almost all tests were conducted out-of-doors in winds of less than 1 f.p.s. average velocity.

Radiation from the flames was measured with one or more Eppley thermopiles (CaF₂ windows) spaced around the flames in a horizontal plane and far enough from the flames for the inverse square law to apply. Two typical records appear in Figure 1. The radiant power of a flame was calculated on the assumption that radiation is emitted with spherical symmetry from the center of the fuel tray. The total thermal power was computed on the assumption that combustion is complete, neglecting soot formation, with CO₂, N₂, and H₂O vapor as products.

Burning rates were calculated by assuming that the instantaneous radiation level is proportional to the burning rate at the same point in time and that the area under the radiation record is proportional to the total volume of fuel consumed. Alternative methods were used for specific purposes: (1) The liquid surface level was monitored with a thermocouple and burning rate computed from the required addition rate of fuel to maintain the level constant. (2) Measured volumes of water-insoluble fuels were poured onto water and burned completely; several depths of fuel, for example 1, 2, and 5 cm., were burned to comprise each burning rate determination. (3) Small trays of up to 38 cm. diameter were supported on a balance so that fuel consumption was established intermittently by weight loss. It was found that convection currents were sufficiently different around a small elevated tray that burning rates were generally higher than those obtained with the tray on a broad flat surface.

RESULTS AND OBSERVATIONS

Burning Rate as a Function of Time

Typical behavior on ignition is for the burning rate to accelerate through a short "burning-in" period. In the case of benzene, the burning rate was found to reach its steady value at about the time when bubbles appeared on the liquid surface. This induction period was observed at all tray diameters and is illustrated in Figure 2; methanol, UDMH, and the cryogenic fuels H₂ and LNG provided exceptions by the absence of an induction period.

Methanol and benzene flames at the same pool diameter (7.5 cm.) and the same initial vapor pressure (40 mm.Hg) were snuffed out after short intervals of burning as shown in Table 1; heat required for fuel vaporization, column 3, was estimated from the weight loss during burning; heat retained in the liquid, column 4, was estimated from the average temperature rise; total heat transfer from flame to liquid, column 5, is almost time-independent, and by chance circumstance of the tray diameter, almost equal for the two fuels. The induction period for benzene occurs during the first two minutes while much of the transferred heat is being stored in the liquid phase. Burning rate is constant after the "burn-in."

Burning Rate as Function of Fuel Temperature

Several fuels were burned in small brine-jacketed trays for an estimate of the temperature coefficient of burning rate. Results with ethyl ether, absolute methanol, and 95 percent ethanol are given in Figure 3. The correlating lines conform closely to our expectation that burning rate should vary inversely with the fuel's sensible heat of vaporization.

Burning Rate as Function of Pool Diameter and Wind Velocity

Steady burning rates in the near-absence of wind at various diameters of fuel tray are plotted in Figure 4. The curves represent the empirical expression

$$v = v_{\infty} (1 - e^{-Kd}) \quad (1)$$

wherein v is the linear burning rate and d the tray diameter. Two points for each fuel (solid circles) were used to evaluate the constants K and v_{∞} , which are listed in Table 2. Figure 5 presents data specifically for benzene, the points near the curve resulting from experiments under nearly wind-free conditions. The dashed line represents the extrapolated burning rate, v_{∞} , and the points near this line were obtained by burning benzene in various natural and artificial winds ranging up to 4 meters per second.

Values of v_{∞} for the nine fuels studied are given as ordinates in Figure 6. The correlating line has the form

$$v_{\infty} = 0.0076 \left(\frac{\text{net heat of combustion, } \Delta H_c}{\text{sensible heat of vaporization, } \Delta H_v} \right) \text{ cm./min.} \quad (2)$$

No correction was made for incompleteness of combustion which was particularly evident in the soot-forming benzene flames.

Radiation and Absorption Measurements

The radiative outputs of some gaseous diffusion flames are compared in Table 3 with the total heats of combustion involved. It was demonstrated at several burner diameters that the apparent percentage of heat radiated to the surroundings was independent of the flow rate of fuel supplied. The effect of wind was always to reduce the percentage of heat dissipated radiatively.

Radiative outputs at various diameters of liquid-supported flames are given in Table 4. The percentage of heat radiated in the largest scale test is combined with burning rate values to give the radiant output per unit area of the liquid surface shown in the final column of Table 2. Hazards arising from this radiation may be diminished somewhat through absorption of the flame radiations by atmospheric water. Some representative percentages of absorption at various lengths of optical path by water vapor, by fuel vapor, and by the liquid fuel are given in Table 5.

Special Behavior of Cryogenic Fuels

Unconverted liquid hydrogen was poured into a deep pyrex dewar (7.0 cm. diameter \times 45 cm. deep), the bottom 15 cm. of which was filled with paraffin at 25° C. The time-dependent vaporization rate is illustrated in Figure 7. The first 20 seconds represents the transfer period during which spattering occurred and the vaporization rate was somewhat uncertain. Thereafter, vaporization seemed to follow a curve given by

$$v \text{ (linear regression rate)} = Kt^{-1/2} \quad (3)$$

wherein K has a value consistent with the solution of the one-dimensional, time-dependent, heat transfer problem (5), and zero time represents the point at which the paraffin surface was apparently cooled to liquid hydrogen temperature. Similar results were obtained on spilling liquid nitrogen onto warm insulating materials within deep vessels. However, on spillage of the cryogenic liquids N_2 and LNG into shallow insulated trays the time-dependent "tail" corresponding to equation 3 could not be reproduced; as illustrated in Figure 8 the vaporization rate typically decays to a nearly time-independent value which is clearly affected by air currents across the tray.

The result of igniting a cryogenic fuel during the first seconds after spillage is shown in the upper curve (LNG) of Figure 1. Start of spilling is indicated by a pip on the radiation record labeled A. Ignition was accomplished 7 seconds later and the duration of the radiative flash was no more than 4 seconds. The shape

of the radiation record during the first 30 seconds was never found to resemble the vaporization rate curves of Figures 7 and 8. The lower curve of Figure 1 shows the comparable flash on igniting benzene followed by a typical "burning-in" period of 30-40 seconds encountered with liquid hydrocarbons at room temperature.

The burning rates reported here for liquid hydrogen are less reliable than for the conventional fuels since evaporative losses become very high when one attempts to flush-fill a container. The liquid was burned in stainless steel dewars of three diameters with fuel consumption as shown in Figure 9. Burning rates were obtained from the initial slopes of the curves in Figure 9 corrected for the heat losses of the dewars. The dashed line of the figure shows this heat loss to be about equal to the terminal burning rate as the liquid level approached the bottom of the dewar. Burning rates in such small diameter vessels, i.e., 7, 15, and 33 cm. diameter, are typically very much affected by such casual crosswinds as occurred during these particular tests.

Other Observations Relative to Rate Measurements

Figures 10 and 11 illustrate phenomena which were observed in large diameter flames and which could be simulated by benzene flames above small pyrex dishes. The underside views of Figure 10 show the distribution of soot through the vapor zone between flame and liquid surface. The density of soot is increased by increasing the radial draft with a chimney as in Figure 10b. Soot has also been observed under ethylene flames in open air (4). The shape of the flame in 10b is quite similar to that of a large flame in quiet air; the burning rate, plotted in Figure 5, is comparable to v_{∞} . Figure 10c shows the flame dislocated from the rim of the tray by an excessive draft. With rectangular trays this tearing of the flame occurred with winds of about 3-4 m./sec., although the critical velocity was sensitive to the configuration of the apparatus. The burning rate typically decreases at this point of incipient blowoff, but if premixing of fuel vapor and air occurs at a point of flame stabilization then a much hotter flame develops (note the bright zone in Figure 10c) and burning rates can exceed v_{∞} .

In Figure 10 the pyrex dish is set into the bench top so that the rim of the dish is 1/2-inch above the surrounding flat surface. The flame is then stabilized at the rim. In Figure 11 the rim of the dish is mounted flush with the surrounding surface and one observes the "creeping" of the flame as heavy fuel vapors diffuse outward along the surface against the radial inflow of air. This phenomenon was noted particularly with butane flames and brought about the discontinuance of measurements above 76 cm. diameter. Burning rates and radiation levels increased appreciably (>20 percent) during each period of this flame instability.

It was confirmed that linear burning rates increase at tray diameters below 5-10 cm., such rate values being omitted from Figure 4 to avoid confusion. Flames at very small diameter are simple laminar diffusion flames and heat transfer to the liquid is demonstrably an edge effect of no interest in large-scale experiments. For example, methanol burning in a 7.5 cm. diameter, water-jacketed brass tray was consumed at a rate of 3.8 cc./min.; when a concentric inner tray of 4.4 cm. diameter was added, this inner tray being left empty, there was no change in the consumption rate of fuel; when the inner tray had a diameter of 5.4 cm., the volumetric rate fell to 3.1 cc./min. Thus, the "edge" of interest in small methanol flames is an annulus of slightly greater width than 1 cm.

DISCUSSION

The Dominance of Radiative Heat Transfer

From their studies of hydrocarbon flames, Blinov and Khudiakov proposed that burning rates are controlled by heat flux from the hot zone to the liquid surface. This concept was put into semi-quantitative form by Hottel in his review of the Russian paper (3).

$$\frac{q}{\pi d^2/4} = k_1 \frac{T_F - T_B}{d} + k_2(T_F - T_B) + \sigma T_F^4 \cdot F(1 - e^{-kd}) \quad (4)$$

(Heat flux = conductive + convective + radiative components)

wherein T_F is the flame temperature, T_B the liquid surface temperature, presumably the boiling point, k_1 and k_2 are conductive and convective coefficients, respectively, d the pool diameter, σ the Stefan-Boltzman constant, F a flame shape factor for radiation to the liquid, and k an opacity coefficient. On dividing both sides of equation 4 by the volumetric heat of vaporization, $\rho\Delta H_v$, and neglecting conductive and convective terms, one obtains

$$v = \frac{\sigma T_F^4 F}{\rho\Delta H_v} (1 - e^{-kd}). \quad (5)$$

Conductive heat transfer becomes negligible at large diameters by virtue of being an edge effect. If one assumes that the Blinov and Khudiakov burning rates at small diameter are completely conduction-controlled, then by equation 4 the contribution of conduction is less than our experimental uncertainty at all diameters represented in Figure 4. It is not so easy to dispose of convective transfer, especially with the slower-burning flames. We have noted a steep temperature gradient at the interface between liquid and vapor phases in both methanol and benzene flames. The presence of soot particles above the benzene pool as shown in Figure 10 is also suggestive of convection. The strong absorption of flame radiation by methanol vapor; Table 5, dictates that the flame stand very close to the liquid surface which again favors convection as the heat transfer mode. On the other hand, we can rule out convection with the faster-burning butane and hydrogen flames since there was no sharp rise in temperature as a thermocouple emerged from the liquid phase into the vapor zone. Assuming for the sake of further discussion that heat transfer in large trays is exclusively radiative, equation 1 becomes the empirical equivalent of equation 5. On this basis, the empirical constant κ of equation 1 may be identified with Hottel's opacity coefficient k , and our extrapolated burning rate, v_∞ , is given by

$$v_\infty = \frac{\sigma T_F^4 \cdot F}{\rho\Delta H_v}. \quad (6)$$

No precise explanation is offered for the simple correlation of data given by equation 2 and Figure 6. Qualitatively, the relationship is easy to understand. The reciprocal of $(\Delta H_c/\Delta H_v)$ is the fraction of the flame's heat that must be fed back to the liquid to maintain a steady rate of vaporization. The smaller this fraction, the taller the flame must be to limit the efficiency of heat transfer; but the height of a diffusion flame, other things being equal, is determined by the rate of fuel feed, i.e., the burning rate. The linearity of the curve in Figure 6, and the small degree of scatter of data, were unexpected.

Since equation 2 is expected to have some practical significance in predicting the relative hazards of fuels, it is important to list its limitations. The data involved only single-component fuels (the LNG used was more than 90 percent methane) burning in unvitiated air, under unusually calm atmospheric conditions and at one atmosphere pressure. We know from experiments with methanol that the effect of atmospheric humidity must be minor. It is particularly important to note that no fuel studied was a monopropellant and that decomposition flames could hardly conform to the heat transfer picture described above.

The Effect of Wind on Burning Rate

The effect of minor winds (Figure 5) may be rationalized on the basis of the three variables T_F , F , and k in equation 5. If the effect of the wind is only to move the flame around, then T_F and F could reasonably remain unchanged; but as the flame's hot zone is ruffled the opacity is visibly increased and the result of Figure 5 could arise from such an increase of k , the opacity coefficient, that e^{-kd} becomes negligibly small. The effects of wind and of large pool diameter should therefore be identical.

Some caution is necessary in applying this concept to practical problems. In the case of an idealized spill in which the liquid surface is flush with the surrounding terrain and there are no velocity gradients in the moving air, one would expect v_{∞} to be the highest attainable burning rate. At higher wind velocities than those of Figure 5 the flame begins to blow off. However if the fuel is contained behind a bluff body (consider for example a half-empty fuel tank) one may no longer be dealing with a diffusion flame but with a turbulent premixed flame in which T_F is hundreds of degrees higher than in diffusion flames. We have observed burning rates equal to twice v_{∞} under some such circumstances and know of no upper limit.

Special Problems with Cryogenic Fuels

The data for liquid hydrogen and for liquefied natural gas were made consistent with other data in Figures 4 and 6 by either minimizing or correcting for any heat flow from the warm surroundings. However, in actual spills with ignition occurring at or shortly after spillage, heat conducted from the ground may be the dominant factor in the fuel's rate of vaporization. For example, when hydrogen was spilled onto warm paraffin, Figure 7, about 7 cm. of the liquid depth was vaporized in chilling the paraffin surface; thereafter, the liquid regression rate still remained faster for several minutes than the liquid burning rate obtained with insulated pools (Figure 9). With typical soils, the thermal diffusivity is higher than with paraffin and a liquid depth of 20 cm. can well be dissipated within the first minute after spillage (5).

We have no radiation records for the initial flash on spilling a large depth of liquid hydrogen into an ignition source. The data that we do have pertains to LNG and Figure 1 is representative. The area under the initial spike is never comparable to the radiation expected from fuel vaporization curves. We can only suppose that a large fraction of the fuel vapor escapes unignited.

CONCLUSIONS

Due to the dependence of burning rate on radiative heat transfer from flame to liquid, the burning rate approaches a constant value with increasing pool diameter. This constant burning rate is proportional to the ratio of the net heat of combustion to the sensible heat of vaporization. Winds raise the burning rates of unshielded fires to approach the large diameter value unless the flame is disrupted. The radiative flux to the environment is about 20-40 percent of the heat of combustion.

ACKNOWLEDGMENTS

This research was supported in part by the Department of the Air Force, Wright Air Development Center (Delivery Order (33-616)58-5: Research on the Hazards Associated with the Large Scale Production and Handling of Liquid Hydrogen); Department of the Navy (Office of Naval Research, Bureau of Ships, Bureau of Yards and Docks, and Bureau of Weapons)(Contract No. NAonr 8-61: Hazards of Vapor Explosions Associated with New Liquid Propellants); and Conch International Methane Limited and Continental Oil Company (Contract No. 14-09-0050-2155: The Flammability of Methane).

LITERATURE CITED

1. Blinov, V. I., and Khudiakov, G. N., Certain Laws Governing the Diffusive Burning of Liquids. Acad. Nauk, USSR, Doklady, vol. 113, 1957, pp. 1094-98.
2. Burgess, D. S., Grumer, J., and Wolfhard, H. G., Burning Rates of Liquid Fuels in Large and Small Open Trays. First International Symposium on Fire Research, November 1959, in print.
3. Hottel, H. C., Review of reference 1. Fire Research Abstracts and Reviews, vol. 1, 1958, pp. 41-44.
4. Singer, J. M., and Grumer, J., Unpublished data, this Laboratory.
5. Zabetakis, M. G., and Burgess, D. S., Research on the Hazards Associated with the Production and Handling of Liquid Hydrogen. Bureau of Mines Report of Investigations 5707, 1961.

Table 1.--Heat transferred to liquid phase during short periods of burning.

Minutes burned	Grams burned	ΔH_v , cal.	ΔH_f , cal.	ΔH_t , cal.
<u>Methanol, 5° C., initial</u>				
1	3.8	1100	250	1400
2	7.5	2300	500	2800
3	11.3	3400	700	4100
4	15.0	4500	900	5400
5	18.0	5400	1050	6500
<u>Benzene, 9° C., initial</u>				
1	4.0	500	750	1300
2	11	1400	1250	2700
3	21	2600	1550	4200
4	31	3800	1700	5500
5	41	5000	1800	6800

Table 2.--Summary of computed values bearing on radiative hazards of fires.

Fuel	K , cm. ⁻¹	v_m , cm./sec.	Thermal output per unit liquid surface, kcal./cm. ² sec.	
			Total	Radiated
Hexane	0.019	0.73	5.1	2.0
Butane	.027	.79	5.1	1.4
Benzene	.026	.60	5.1	1.8
Xylene	.012	.58	5.0	-
Methanol	.046	.17	.64	.11
UDMH	.025	.38	2.2	.60
Hydrogen	(0.07)	(1.4)	(2.8)	(0.7)
LNG	.030	.66	3.2	.74

Table 3.--Radiation by gaseous diffusion flames.

Fuel	Burner diameter, cm.	$100 \times \frac{\text{Radiative output}}{\text{Thermal output}}$
Hydrogen	0.51	9.5
	.91	9.1
	1.9	9.7
	4.1	11.1
	8.4	15.6
	20.3	15.4
Butane	40.6	16.9
	0.51	21.5
	.91	25.3
	1.9	28.6
	4.1	28.5
	8.4	29.1
Methane	20.3	28.0
	40.6	29.9
	0.51	10.3
	.91	11.6
	1.9	16.0
	4.1	16.1
Natural gas (95% CH ₄)	8.4	14.7
	20.3	19.2
	40.6	23.2

Table 4.--Radiation by liquid-supported diffusion flames.

Fuel	Vessel diameter, cm.	$100 \times \frac{\text{Radiative output}}{\text{Thermal output}}$
Hydrogen	33	25
Butane	30	20
	46	21
	76	27
LNG	38	21
	76	23
Methanol	2.5	12
	5	14
	15	17
	122	17
Benzene	5	38
	46	35
	76	35
	122	36

Table 5.--Percentage of absorption of flame radiations in cells with CaF_2 windows.

Fuel	Absorbing medium, path length, temperature		
	Liquid fuel,	Fuel vapor,	Steam,
	0.3 cm., 30° C.	8.9 cm., 100° C.	8.9 cm., 165° C.
Methanol	100	27*	13
Hydrogen	-	0	33
UDMH	> 98	43	18
Hexane	71	-	< 6
Benzene	62	11	-

*38 percent absorbed over 18.4 cm. path.

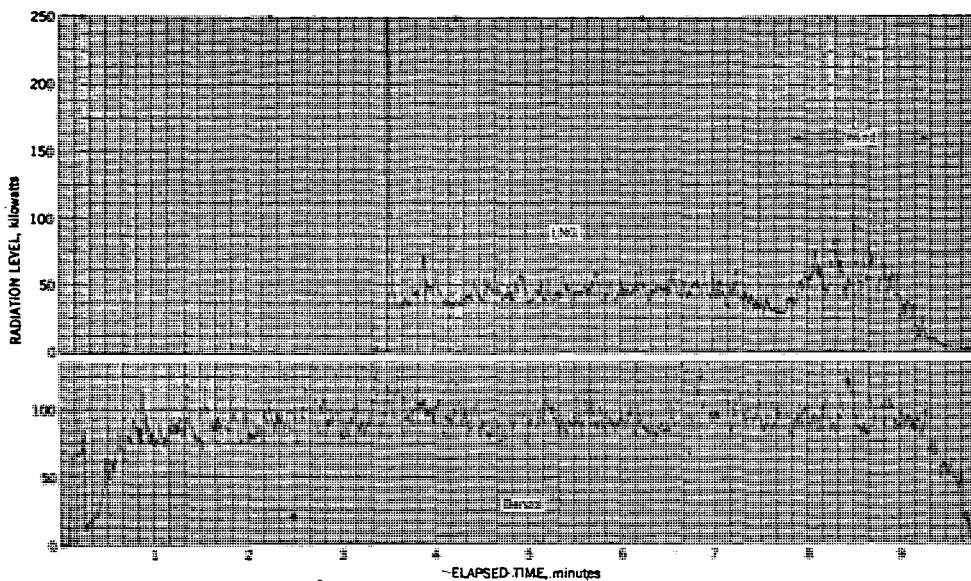


Figure 1.--Radiation Records on Burning about One Gallon (3640 cc.) of LNG and of Benzol in 15-inch Diameter Tray. LNG poured into warm tray at point A.

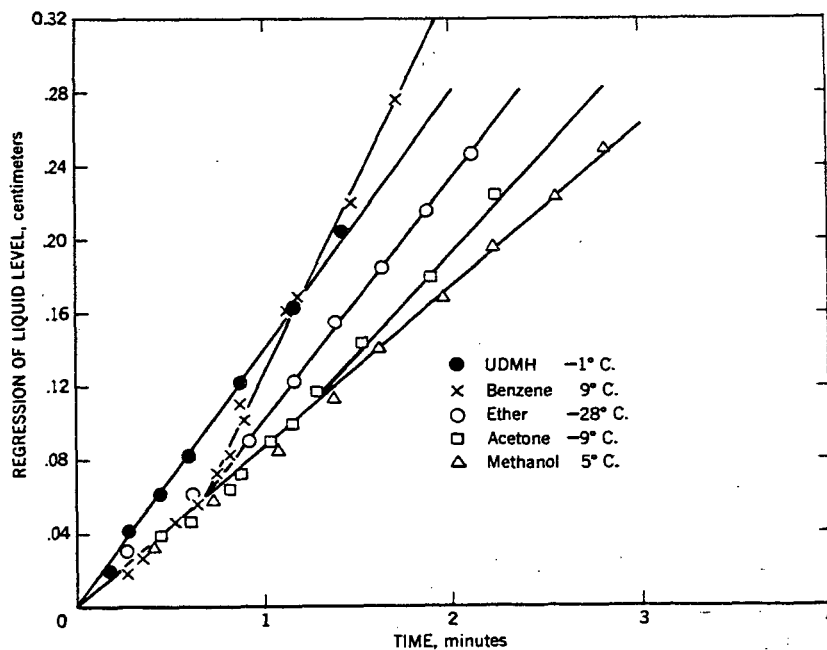


Figure 2.--Burning Rates of Five Liquid Fuels in a 3-inch Pyrex Vessel (3.5-inch for UDMH). Vapor Pressure 40 mm.Hg at Initial Liquid Temperature.

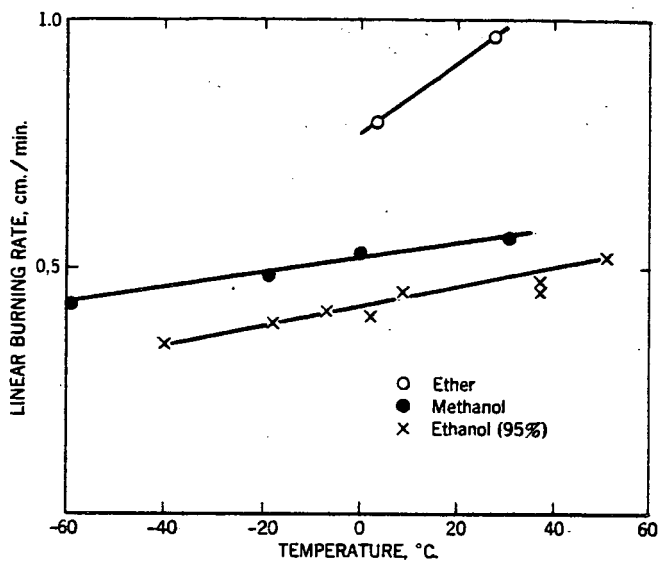


Figure 3.--Effect of Fuel Temperature on Steady Burning Rates in 7.5 cm. Diameter Brine-Jacketed Burner.

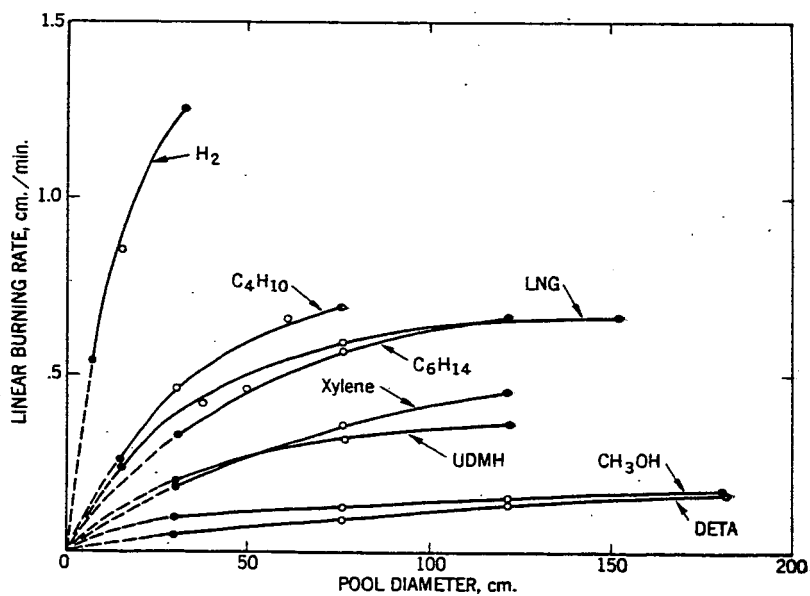


Figure 4.--Dependence of Liquid Burning Rate on Pool Diameter.

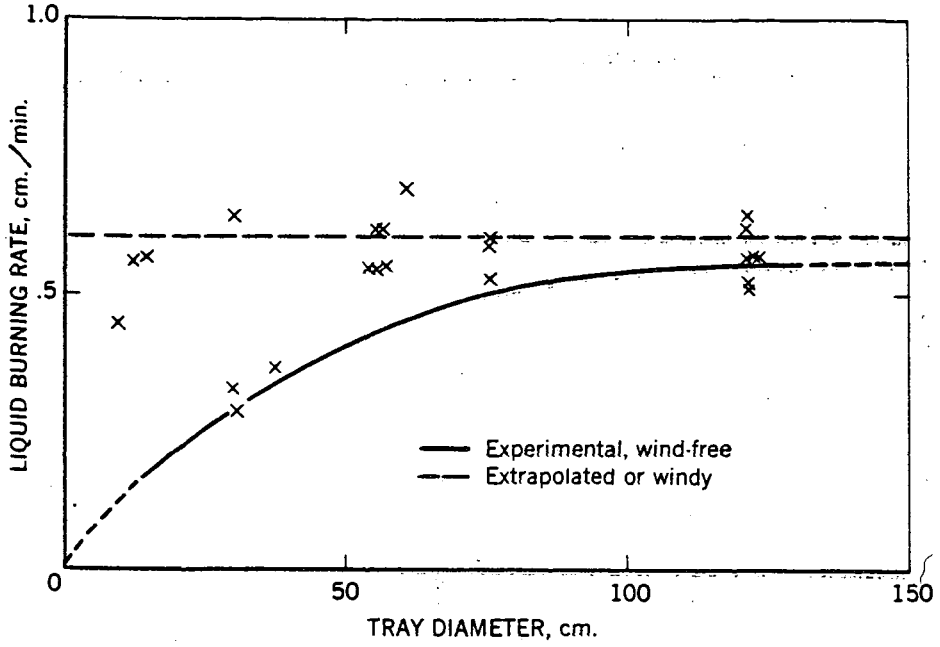


Figure 5.--Effect of Wind on Burning Rate of Benzene.

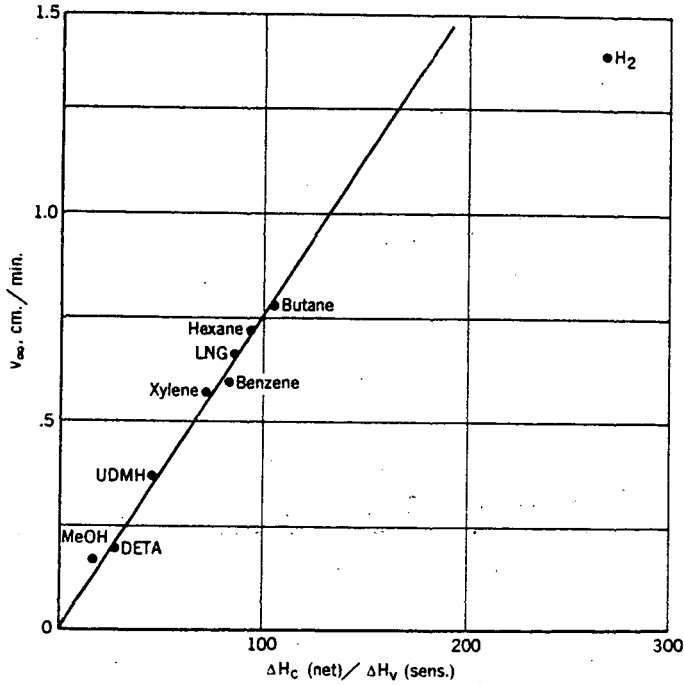


Figure 6.--Relation Between Liquid Burning Rates at Large Pool Diameter and Thermochemical Properties of the Fuels.

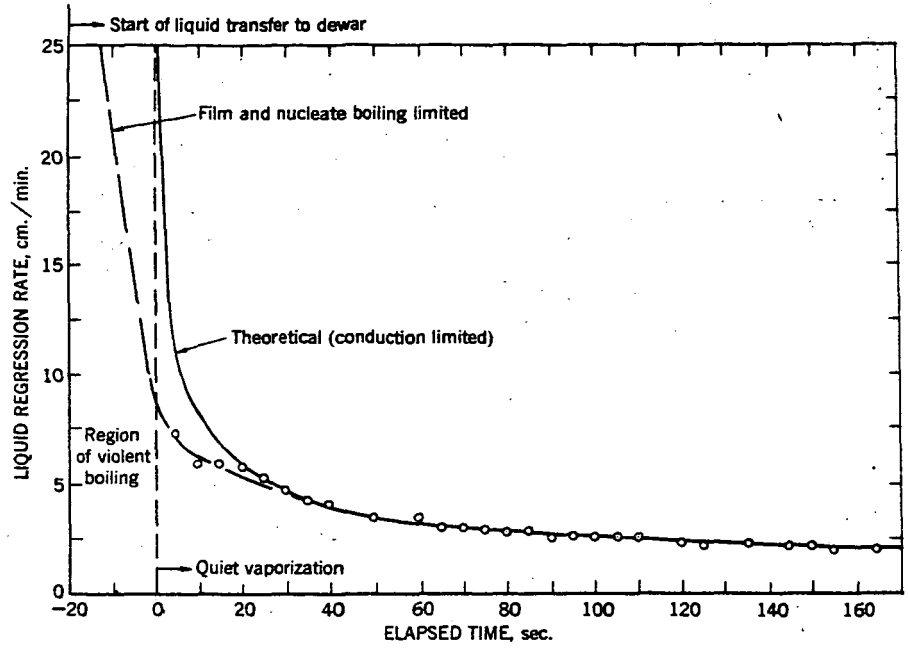


Figure 7.--Rate of Vaporization of Liquid Hydrogen from Paraffin in a 2.8-inch Dewar. Initial liquid depth 6.7 inches.

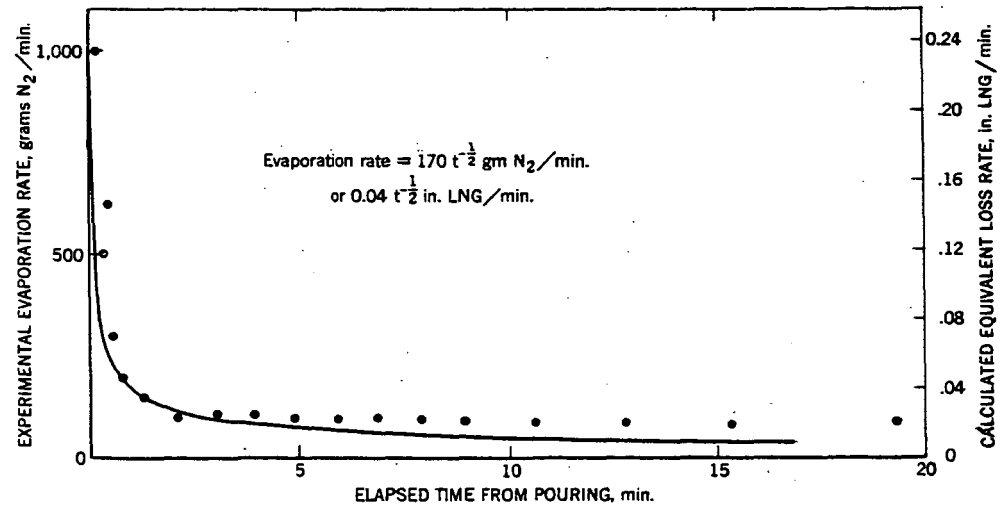


Figure 8.--Evaporation of Liquid Nitrogen after Spillage into a Warm 15-inch Diameter Tray.

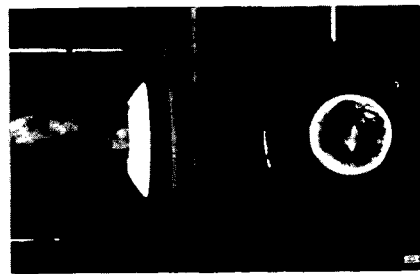
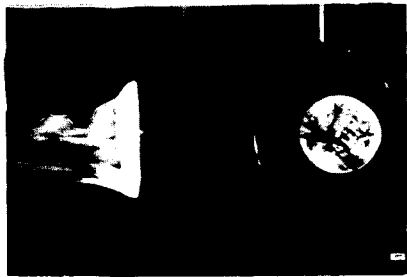


Figure 10.--Side Views and Under Views of Benzene Flames in 6-inch Diameter Dish.
 (a) Flame Undisturbed.
 (b) Radial Draft Induced by Chimney.
 (c) Flame Torn from Rim of Tray.

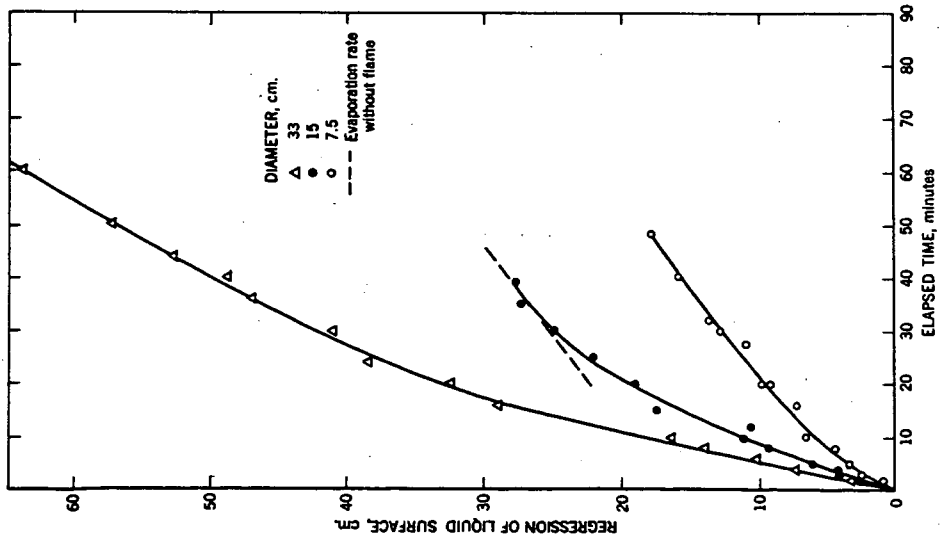


Figure 9.--Burning of Liquid Hydrogen in Stainless Steel Dewars of Three Diameters (reconstructed from flame radiation data, three thermopiles).



0 ————— 5
Scale, inches



Figure 11.--Creeping Flame on Lipless Dish (below)
Compared with Noncreeping Flame on
Dish with 1/2-inch Lip.

UNCONTROLLED DIFFUSIVE BURNING OF SOME NEW LIQUID PROPELLANTS.

By Joseph Grumer, Alexander Strasser,
Theodore A. Kubala, and David Burgess

U. S. Department of the Interior, Bureau of Mines
Explosives Research Laboratory
Pittsburgh, Pennsylvania

INTRODUCTION

The safe use of new liquid fuel-oxidizer combinations for rockets requires evaluation of the hazards that may result from accidental spillage and ignition. One such combination is based on hydrazoid and amine type fuels--consisting essentially of mixtures of unsymmetrical dimethyl hydrazine (UDMH) and diethylenetriamine (DETA); the mixtures are designated as MAF-1 and MAF-3; MAF-1 is (by weight) 41 percent UDMH, 9 percent CH_3CN , and 50 percent DETA; MAF-3 is 20 percent UDMH and 80 percent DETA. Materials of this type present special problems in fire fighting. They are water-soluble, possibly toxic, and more likely to be chemically reactive with their environment or fire extinguishing chemicals than common hydrocarbon fuels. Fires of these new fuels may be less readily extinguished by common extinguishing agents. Deep pools of blended fuels may boil over during burning, etc. Laboratory scale techniques for evaluating such hazards and defensive measures are obviously useful. This paper reports techniques (and results) which were developed and which should be extendable to other similar fuel-oxidant systems. These techniques were used to measure burning rates of large pools of fuels, radiation from flames, temperature profiles in flames and liquid beneath, composition of combustion products, and limits, in terms of water dilution, of fire points and of hypergolicity.

MEASUREMENTS AND DISCUSSION

Burning Rates in Large Pools

Single-Component Fuels

Judging by the work of Blinov and Khudiakov (1, 5) and our own more extensive work with other single-component fuels (2, 13), the burning rate of a fuel in shallow trays approaches constancy as the tray diameter increases (Fig. 1). Burning rates taken with trays about a meter or two in diameter can be extrapolated to yield burning rates in very large trays. This extrapolation for single-component fuels and the basis for it are discussed in references 2 and 13. As explained in these discussions, the burning rates of single-component liquid fuels in large pools, v_∞ , in centimeters per minute, is given by equation 1:

$$v_\infty = 0.0076 \frac{\Delta H_{\text{comb.}}}{\Delta H_{\text{vap.}} + \int_{T_a}^{T_b} C_p dt} \quad (1)$$

where $\Delta H_{\text{comb.}}$ is the "net" heat of combustion and $\Delta H_{\text{vap.}}$ is the heat of vaporization at the boiling point, T_b . The integrated heat capacity in the denominator determines the temperature dependence of burning rate, normally about 1/2-percent per degree

Centigrade variation of the initial liquid temperature, T_a . The dependence of burning rates of such fuels on thermochemical properties is shown by Table 1 (2, 13). Values for UDMH and DETA are included in Figure 1 and Table 1.

Blended Fuels

Fires of pools of blended fuels, especially those whose components differ widely in their volatility, do not burn with a uniform rate. In the beginning, the burning rate is characteristic of the more volatile component. During the middle portion of the burning, the less volatile component still must be brought to the boiling point of the blend. Finally as the fractionation proceeds the burning rate becomes characteristic of the higher boiling fraction. The burning rates of a blend are given by:

$$v_{\infty} = 0.0076 \frac{n_1 \Delta H_{\text{comb.}1} + n_2 \Delta H_{\text{comb.}2} + \dots}{n_1 \Delta H_{\text{vap.}1} + n_2 \Delta H_{\text{vap.}2} + \dots + m_1 \int_{T_a}^{T_b} C_{p1} dt + m_2 \int_{T_a}^{T_b} C_{p2} dt + \dots} \quad (2)$$

where n_1 and m_1 refer to mol fractional composition in the vapor and liquid phases, respectively. For such blends as gasoline whose specific heats of combustion and of vaporization of the components are comparable and $n_1 \approx m_1$, equation 2 leads to a simple mixture rule:

$$v_{\infty} = n_1 v_1 + n_2 v_2 + \dots \quad (3)$$

On burning an unleaded gasoline in a 122 cm. diameter tray we found a steady burning rate of 0.54 cm./min. From distillation data furnished by the supplier, the value given by equation 2 should be 0.57-0.60 cm./min. In the absence of distillation data covering compositions of liquid and vapor, equation 4 may be used for rough estimates of v_{∞} or v for medium sized trays. The average burning rate of a 2:1 benzene-xylene blend in a 76 cm. diameter tray was given by equation 4 using experimental values for the individual burning rates of benzene and xylene (0.47 cm./min. (exp.) versus 0.48 cm./min (calc.)). Even for blends with components of widely separated boiling points, equation 3 yields rough estimates, except during the first and last stages of the fire. For example, the major components of MAF-1 and MAF-3 differ very widely in their volatility--UDMH boils at 63° C. and DETA at 207° C. However, for the 76 cm. tray and the 122 cm. tray predicted values exceed observed averages for the middle half of the burning time by about 15 percent for MAF-1 and about 50 percent for MAF-3.

Figures 2 and 3 confirm our analysis that for blends with appreciable concentrations of components of widely differing volatility, the initial burning rate is about that of the most volatile component and the final burning rate, about that of the least volatile. The radiation records in Figure 3 show that the steady burning rate for DETA was approached at the end of the burning of MAF-1 and MAF-3 in a 122 cm. tray.

Flame Radiation and Absorption

Radiation from flames and absorption of radiation by fuel vapor and liquid affect the burning rate, as discussed in references 2 and 13. In addition, consideration of absorption of radiation by the liquid phase of the fuel or by water in the gaseous or liquid state is pertinent to attenuation of heat radiated to the liquid fuel or to the surroundings. About 24 and 28 percent of the heat of combustion was radiated to the surroundings by flames of UDMH, burning on the 76 and 122 cm. diameter tray, respectively (Table 2). Combination of photographic and radiation data gave

the magnitudes and variations shown in Table 3 in the specific radiation from such a flame.* The data in Table 2 can be used to compare the radiant flux from large UDMH and hexane flames of the same diameter; that is, ratio of linear burning rates \times ratio of liquid densities \times ratio of heats of combustion \times ratio of percentages radiated =

$$\left(\frac{7.0 \text{ mm./min.}}{3.5 \text{ mm./min.}}\right) \left(\frac{0.66 \text{ gm./cc.}}{0.78 \text{ gm./cc.}}\right) \left(\frac{11.5 \text{ kcal./gm.}}{7.9 \text{ kcal./gm.}}\right) \left(\frac{42\%}{26\%}\right) \approx 4.$$

A fourfold reduction in radiation level compared to hydrocarbon flames should be a significant factor in safety considerations.

Furthermore, data in Table 4 and Figure 4 show that UDMH and MAF flames resemble flames of methanol more nearly than those of benzene with regard to self-absorption of radiation from their respective flame. Liquid UDMH and the MAF are good self-absorbers since a depth of 0.3 cm. of liquid absorbs about all the radiation.

An additional factor to be considered is the absorption of flame radiation by atmospheric water vapor. When a flame is only weakly luminous, its emission spectrum may differ from that of a black body, a large proportion of the energy being emitted within the emission bands of water and carbon dioxide. This energy is susceptible to absorption by atmospheric water and carbon dioxide, and in the case of hydrogen fires or methanol fires, atmospheric absorption is a factor to be considered. In the case of UDMH and MAF fires (Table 4), absorption of radiation by water vapor roughly follows Lambert's law for the two shortest pathlengths of water vapor but not for the whole range up to 37 cm. This means that radiation from UDMH and MAF fires cannot be blanketed by long distances through moist air.

Temperature Profiles in Flames and Liquid; The Boilover Problem

Temperatures observed underneath a small UDMH diffusion flame and at its surface are given in Table 5. A flame burning on a 50 mm. diameter petri dish and standing about 23 cm. high was probed with a ceramic coated (NBS ceramic A-418) platinum-platinum-10 percent rhodium unshielded 10 mil thermocouple. It is apparent that high temperatures (about 600° C.) are obtained in the unburned gas about a centimeter or so above the liquid (liquid level was about a centimeter below the rim of the dish). Maximum temperatures at the flame front are about 1100° C. Similar temperatures have been observed in diffusion flames of hydrocarbons (10, 11, 12), and of alcohol, benzol, petrol, and kerosene (8). Calculations of adiabatic flame temperatures for premixed flames are given in Table 6 for comparison with values observed in the diffusion flame. The temperatures observed in the gas phase beneath the diffusion flame of UDMH are consistent with the radiation measurements showing self-absorption of flame radiation. The radiation absorption measurements also showed that the liquid absorbed strongly and so a steep temperature gradient is to be expected at the liquid surface of burning UDMH. Such steep gradients were observed at the liquid surfaces of fires of UDMH and DETA. Conceivably, such hot layers at the surface of a burning deep pool of MAF-1 or MAF-3 may cause violent bumping and splashing of burning fuel. Violent expulsion of fuel (called "boilover") may occur with oil tank fires, due generally to an immiscible layer of water below the oil, which is suddenly converted into steam (4, 9).

*Cycling of flame size may be due to partial self-smothering which causes the flame to lengthen. This lengthening of flame improves the diffusion and entrainment of air, causing the flame to shorten. Evidence for this explanation of fluctuating flame size comes from studies of smoke limits of flames in ethylene-air mixtures. Limit flames only emitted smoke when the flame was in the tallest stage (3).

Somewhat different circumstances than with oil fires may lead to boilovers with the MAF's--a mechanism involving instabilities of convection currents in the liquid. Consider that at room temperature the density difference between high and low boiling components is more extreme in UDMH-DETA blends than in most hydrocarbon blends, and that the viscosities of DETA and of UDMH-DETA blends are quite comparable to the viscosities of higher hydrocarbons. A hot, metastable layer may therefore form at the surface of a deep, burning pool of MAF and suddenly fall to the bottom, boiling out UDMH from cold bottom layers. For this to occur, a considerable mass of metastable hot liquid must gather at the surface. Otherwise such a layer would not contain much heat, and as it fell it would only accelerate the heat front downward; it could not produce a boilover. However, if the gravitational forces downward were almost counterbalanced by the viscous forces holding the layer in place, a large mass might accumulate at the surface. Secondly, boilover is possible only if the density of the hot liquid at the top is greater than the density of the initial liquid. Thirdly, the likelihood of boilover increases if the viscosity of the hot liquid is equal to or greater than that of the initial liquid. If the hot layer falls and the viscosity of the hot liquid is less than the viscosity of the initial liquid, viscous shear will tend to disperse the hot liquid and prevent the sudden transport of much heat to the bottom layer. The data in Table 7(A) indicate that there is no danger of boilover due to accumulation of boiling DETA at the surface. Table 7(B) indicates that boilover is potentially possible as long as the surface layers atop cold MAF-1 are colder than about 120° C., and those atop cold MAF-3 are colder than about 60° C. In Table 7(C), a comparison is based on 60° C., the approximate temperature at which MAF-1 and MAF-3 start to distil. Hot surface layers of DETA up to about 160° C. appear to be metastable compared to MAF-1 at 60°, and correspondingly up to about 100° C. for MAF-3. The temperature difference for MAF-1 (158-60°) is about two and one-half times that for MAF-3, about the same as for the comparison in Table 7(B). It appears, therefore, that if metastable layers form atop either MAF-1 or MAF-3, the heating potential in the MAF-1 case is more than double that in the MAF-3 instance. On the basis of these analyses, a boilover with MAF-3 is far less likely than with MAF-1.

Experiments were performed with MAF-1 and MAF-3 in which 38 kg. of MAF-1 and 47 kg. of MAF-3 were burned in an instrumented drum measuring 30 cm. in depth and 47 cm. inside diameter. Temperature profiles as a function of time are given in Figures 5 and 6. The history of selected isotherms is given in Figures 7 and 8. The temperature profiles were observed by means of thermocouples in the liquid (at about 0.6 radius from the wall). Temperature-sensitive paints on the sides of the container were also used. In general, thermocouples and paint showed about the same rate of heat travel. Figures 5 and 6 show that a temperature inversion at the bottom of the tank occurred with MAF-1 but not with MAF-3. Figure 7 shows that the heat front moving downward through MAF-1 accelerated during burning from about 0.2 cm./min. to about 0.8 cm./min. Figure 8 shows that the heat front moved steadily downward in MAF-3 at about 0.14 cm./min. The acceleration of the travel of heat front through MAF-1 started after about an hour of burning. After 1-1/2 hours of burning, the temperature paints showed that the bottom of the container was at least at 65° C. About the time this heat front reached the bottom of the tank, a vigorous foaming suddenly started and continued for approximately 10 minutes. No appreciable head of foam was apparent, nor was there any bumping of the liquid. Thereafter, as it did before, the liquid bubbled smoothly and quietly over its entire surface until burnout. As soon as the foaming stopped, a sample of fluid was withdrawn through a tap 5 cm. from the bottom and about 10 cm. from the top of the liquid. The specific gravity of this sample was 0.94 at 27° C., about equal to that of DETA. Therefore, following the foaming all of the UDMH was gone from the MAF-1. Temperatures were fairly uniform throughout the liquid, and were about 165° to 175° C. About 5 minutes before the foaming started, temperatures were above 140° C., except for the bottom 8 cm. of liquid which was around 65-70°C. Within these 5 minutes, temperatures in the bottom 8 cm. rose above 140°. These temperatures are in fairly good agreement with temperatures listed in Table 7 for MAF-1. MAF-3 burned smoothly. The only novel observation was the appearance after a

couple of hours of burning of very fragile brown clots. Although the observed foaming did not raise or throw liquid, its occurrence, the data in Figures 5 and 7, and Table 7 all indicate that boilovers or perhaps only foaming are possible with MAF-1. The weight of experimental and theoretical evidence indicates that boilovers are unlikely with MAF-3.

Composition of Combustion Products

As shown in Tables 8 and 9, samples drawn from UDMH diffusion and premixed flames contain hydrogen cyanide, methyl cyanide, and carbon monoxide. A few centimeters past the flame surface of diffusion flames, these toxic gases are absent. DETA produced as much as 1.5 percent of hydrogen cyanide on combustion. Therefore, fumes from incompletely burned UDMH, DETA, and the MAF fuels may be unusually toxic. Observed flame temperatures in Table 9 are in good agreement with calculated temperatures in Table 6.

Fire Points of Aqueous Solutions

Water is the least expensive and generally most readily available extinguishing agent for fires of MAF fuels. Foam has to be specially prepared and is rapidly disintegrated. Other extinguishing reagents are expensive or soluble or reactive. To evaluate water requirements for fighting fires of the MAF's, measurements were made of the water dilution necessary to render nonflammable aqueous solutions of UDMH, MAF-1, and MAF-3. About two volumes of water per volume of fuel suffice for this purpose. (For very deep pools, less water will be required if only the upper portion of the tank's contents has to become nonflammable.) The data are given in Table 10 along with dilutions needed for some alcohols and acetone. The ratios in the last column of Table 10 of heat of vaporization to heat of combustion indicate that the water requirements can be simply estimated, without recourse to measurement. At worst, the estimate provided a fivefold safety factor and for three of the seven tests provided good agreement with experiment. The estimate is based on the assumption that an aqueous solution of a fuel will not burn when the heat of combustion of the solution equals the heat of vaporization at the boiling point of the liquid, that all of the heat of combustion is transferred to the liquid and the compositions of vapor and liquid phases are identical. Errors due to the last two assumptions tend to neutralize each other with regard to the prediction of water concentration at the fire point. It is obviously difficult to compute the heat transfer from flame to liquid. It is also questionable whether vapor phase composition can be computed accurately enough using the liquid composition. Figure 9 shows that equilibrium between compositions of the liquid and the vapor burning above it may not be assumed near the fire point. Equilibrium curves were taken from the literature (6). Experimental points were obtained by adding an arbitrary mixture of methanol-water, e.g., 1:1 on a molar basis, to a burning methanol pool. The rate of addition was such as to maintain a constant weight of liquid. Eventually the composition of the liquid, as determined by specific gravity measurements, became constant. (There were no significant concentration gradients in the body of the liquid.) At this stage the composition of the mixture being distilled by the flame was identical to that of the mixture being added.

Hypergolicity of Aqueous Solutions

Since the MAF fuels would typically be used with such oxidants as inhibited red fuming nitric acid (IRFNA) there are special problems of preventing hypergolic ignition on simultaneous spillage of fuel and oxidant. It was observed that when the vapors above UDMH and above RFNA were permitted to interdiffuse in a particular closed apparatus at 23° C., there was no ignition. On raising the temperature to 38° C., ignition occurred. Vapors above either MAF-1 or MAF-3 ignited spontaneously with vapors from RFNA at 45° C. but not at 38° C. Impinging jets of the vapors at 60-100° C. in open air led to ignition despite precautions to eliminate liquid spray. Thus there is a need for newly obtained data on flammability limits and spontaneous ignition temperatures with air and inert gases as ignition-preventing diluents (7).

With regard to liquid phase interactions it was observed in preliminary spot-plate tests that ignition could be prevented by pre-diluting either the RFNA or the fuel (UDMH, MAF-1, or MAF-3) with 40 volume percent water and that DETA-RFNA were not hypergolic. These results were duplicated with 100 cc. quantities of propellant in dewars. To estimate the required water dilution for nonignition in large systems with no heat loss, the following conventional concept of hypergolicity was invoked:

- (a) There are fast neutralization reactions, independent of the degree of dilution, yielding about 10-20 percent of the overall heat of combustion;
- (b) The temperature of the system is thus raised sufficiently to permit slower reactions, such as oxidation or nitration, to lead on to ignition.

Accepting the neutralization step to be inevitable, one must dilute sufficiently with water so that the system never exceeds a critical temperature for initiation of second-stage reactions. Figure 10 shows the temperature rises obtained on adding water-diluted RFNA (50-50) incrementally to 200 cc. of water-diluted UDMH in a dewar, the diluted reactants having been precooled in each case to 25° C. Curves A, B, C, and D refer to 10, 20, 40, and 100 percent initial concentrations of UDMH and the dashed lines depict temperature rises from a hypothetical neutralization yielding 12 kcal./mole. In curves A and B the initial points are below predicted temperatures and heat evolution has virtually ceased when acid and UDMH are equimolar. However, in curve C, involving 50 percent acid and 40 percent UDMH, there is evidence of some additional reaction at the start and of heat evolution extending beyond the equimolar point. At about this dilution of reactants, and depending critically upon apparatus parameters, ignition was found to occur in the gas phase.

As best one can judge from the figure, the highest reaction temperature for safety in any conceivable environment would be about 50° C. From this, if the reactants are initially at 25° C., the minimum dilution should be about 8 grams of water per gram of UDMH-RFNA propellant. There is evidence that less water would be needed with the MAF fuels. For example, 100 cc. of (60-40) water-(MAF-1 or MAF-3) were mixed with 100 cc. (60-40) water-RFNA with a heat release that was judged to be 15 kcal./mole; 100 cc. of (50-50) water-MAF-3 were added to 100 cc. of RFNA, giving a heat release of 18 kcal./mole. In each case there was no ignition or evidence of delayed reaction.

CONCLUSIONS

The MAF fuels are similar in their gross burning characteristics to more conventional fuels. The hazards due to accidental fires of these materials appear to be manageable. As with hydrocarbons, radiative heat transfer is the dominant factor in the burning of large diameter pools. Burning rates are expressible as functions of the rates of the component fuels and are of the order of those of conventional fuels. Temperature profiles indicate that boilover during fires of deep pools is unlikely. About two volumes of water per volume of fuel results in a nonflammable solution. The products of incomplete combustion of the amines contain cyanides, a factor to be considered in fire fighting. Hypergolicity between the MAF fuels and red fuming nitric acid can be prevented by adding about two volumes water before mixing. The concepts used in this study should be applicable to other fuel-oxidant systems.

ACKNOWLEDGMENT

This research was supported in part by the Department of the Navy (NAONR 8-61)(Office of Naval Research, Bureau of Ships, Bureau of Yards and Docks, and Bureau of Weapons).

LITERATURE CITED

1. Blinov, V. I., and Khudiakov, G. N., Certain Laws Governing the Diffusive Burning of Liquids. Acad. Nauk, USSR, Doklady, vol. 113, 1957, pp. 1094-98.
2. Burgess, D., Strasser, A., and Grumer, J., Diffusive Burning of Liquid Fuels in Open Trays. This Symposium.
3. Grumer, J., and Harris, M. E., Smoke Limits of Bunsen Burner Ethylene-Air Flames. Ind. Eng. Chem., vol. 51, 1959, pp. 570-72.
4. Hall, H. H., Oil Tank Fire Boilovers. Mech. Eng., vol. 47, 1925, pp. 540-44.
5. Hottel, H. C., Review of ref. 1. Fire Research Abstracts and Reviews, vol. 1, 1958, pp. 41-44.
6. Hughes, H. E., and Maloney, J. O., The Application of Radioactive Tracers to Diffusional Operations. Chem. Eng. Prog., vol. 48, 1952, pp. 192-200.
7. Perlee, H. E., Imhof, A. C., and Zabetakis, M. G., Flammability Characteristics of Hydrazine and Related Compounds. This Symposium.
8. Rasbash, D. J., Rogowski, Z. W., and Stark, G. W. V., Properties of Fires of Liquids. Fuel, vol. 35, 1956, pp. 94-107.
9. Risinger, J. L., How Oil Acts When It Burns. Petroleum Refiner, vol. 36, 1957, pp. 114-6, 259-62.
10. Singer, J. M., and Grumer, J., Carbon Formation in Very Rich Hydrocarbon-Air Flames. I. Studies of Chemical Content, Temperature, Ionization, and Particulate Matter. Seventh Symposium (International) on Combustion, Butterworths Scientific Publications, London, 1959, pp. 559-69.
11. Singer, J. M., and Grumer, J., Unpublished data.
12. Smith, S. R., and Gordon, A. S., Studies of Diffusion Flames. I. The Methane Diffusion Flame. Jour. Phys. Chem., vol. 60, 1956, p. 759.
13. Zabetakis, M. G., and Burgess, D., Research on the Hazards Associated with the Production and Handling of Liquid Hydrogen. Bureau of Mines Rept. of Investigations 5707, 1961.

Table 1.--Relation of liquid burning rates to thermochemical properties of fuels.

Fuel	ΔH_c (net) kcal./mol.	ΔH_v (sens.)	$0.0076 \frac{\Delta H_c}{\Delta H_v}$	v_w , cm./min.
Hydrogen	58.2	0.22	2.02	1.6
Butane	623	5.95	.81	.79
Hexane	916	9.77	.72	.73
Benzene	751	9.20	.63	.60
Xylene	1038	14.72	.55	.58
UDMH	432	9.53	.35	.38
DETA	735	26.1	.22	.20
MeOH	150	9.18	.13	.17

Table 2.--Radiation by diffusion flames of liquid fuels.

Fuel	Burner diameter, cm.	$100 \times \frac{\text{Radiative output}}{\text{Thermal output}}$
DETA	76	35
DETA	122	28
MAF-1	76	26
MAF-3	76	42

Table 3.--Specific flame radiation from diffusion flame of UDMH. Pool diameter 76 cm.

Time, minutes	Specific flame radiation,* watts/cm. ²
1.0	6.75
1.5	9.15
2.0	9.90
2.5	7.90
3.0	6.50
3.5	8.40
4.0	7.25
4.5	12.9
5.0	9.6
5.5	12.4
6.0	13.2
6.5	6.1

* $\frac{\text{Radiation output}}{2 \times \text{vertical cross section of flame}}$

Table 4.--Transmission of flame radiation.

Flame of fuel	Cell length, cm.	Transmission, percent		
		Through water vapor at 165° C.	Fuel vapor at 100° C.	Fuel liquid
UDMH	0.3			1
MAF-1				1
MAF-3				0.3
UDMH	8.9	82	57	
MAF-1		89	61*	
MAF-3		81	65*	
DETA		--	--	
Methanol		87	73	
UDMH	18.4	72	49	
MAF-1		72		
MAF-3		76		
DETA		77		
UDMH	37	70		
MAF-1		69		
MAF-3		70		
DETA		69		

*Predominant vapor was UDMH.

Table 5.--Temperatures in a diffusion flame of unsymmetrical dimethyl hydrazine in air.

Tray diameter 50 mm., flame height about 230 mm.

Height above dish, mm.	Distance from axis, mm.					
	0	5	10	15	20	25
	Temperatures, ° C.					
0	600	600	600	650	730	1080*
5	600	620	640	700	1120*	480
10	660	700	750	1120*	1040	
15	820	840	930	1120*	810	
25	770	670	680	1000*	950	
50		1040	1080*	1050	1060	

*Approximate position of flame edge.

Table 6.--Adiabatic flame temperatures of diethylenetriamine and air mixtures and of unsymmetrical dimethyl hydrazine and air mixtures at one atmosphere initial pressure.*

DETA,** percent	UDMH,** percent	Flame temperature, °K. (Calc.)
3.0		2387
4.0		2288
5.0		2058
6.0		1766
7.0		1482
8.0		1276
9.0		1220
	11.5	1314
	17.5	1177
	31.6	974

*Calculations by E. B. Cook of this Laboratory.

**Initial temperatures of gaseous mixture:

DETA = 423° K., UDMH = 330° K.

Table 7.--(A) Comparison of densities and viscosities of MAF-1 and MAF-3 at 25° C. with those of DETA at its boiling point.
 (B) Comparison of temperatures of DETA at which its density or viscosity equals those of MAF-1 or MAF-3 at 25° C.
 (C) Comparison of temperatures of DETA at which its density or viscosity equals those of MAF-1 or MAF-3 at 60° C.

Fuel	A		B		C	
	Density, ρ , gm./cm. ³	Viscosity, η , centipoise	Temperatures, ° C.		Temperatures, ° C.	
			ρ	η	ρ	η
MAF-1*	0.869	1.22	120	80	158	138
MAF-3**	.916	3.5	60	40	98	> 100
DETA**	.785	.43				

*Correspondence: Reaction Motors Division, Denville, New Jersey.

**Ethylene Amines, Dow Chemical Company, Midland, Michigan, 1959.

Table 8.--Mass spectrometric analyses of combustion products of UDMH diffusion flames.

Sampling point, cm. above flames	Diffusion flames over tray					
	5.1 × 25.4 × 1.4 cm.			76 cm.		
	0	0	0	5	0	5
Analysis, percent:						
Carbon dioxide	4.3	2.9	4.0		3.2	0.3
Carbon monoxide	3.1	2.3	3.2		1.6	0
Methane	4.0	1.3	2.4			
Formaldehyde or ethane*	.3	.1	.1		1.6**	0
Ethylene	1.8	1.2	1.2			
Acetylene	.3	.1	.3			
Methyl cyanide	.2	.1	.1	0		0
Hydrogen cyanide***	1.5	1.1	1.8	0	.7	0
Water	1.6	1.2	1.0			
Hydrogen	3.6	1.8	3.0		1.4	0
Nitrogen + argon	75.6	77.2	76.3	Air	80.5	Air
Oxygen	3.7	10.7	6.6		11.0	

*Probably ethane, since Schiff's test for aldehydes was negative.

**Total of methane, ethane, ethylene, and acetylene.

***Presence or absence confirmed by Prussian blue test for cyanides.

Table 9.--Mass spectrometric analyses of combustion products along axis of UDMH-air flat flames.*

	UDMH, percent				
	11.5	17.5	17.5	17.5	31.6
Distance above blue flame, mm.	4	1	2	4	4
Observed flame temperature, ° K.	> 1340	1240	1250	1270	1030
Analysis, percent:					
Ethylene	2.2	3.4	3.4	3.4	5.5
Hydrogen cyanide	4.4	6.2	4.5	5.6	7.2
Ammonia	.7	1.6	1.5	1.3	4.0
Carbon dioxide	1.8	.2	.5	.7	.1
Oxygen	.2	2.0	1.6	.7	1.3
Nitrogen	63.8	53.2	56.6	55.2	46.2
Methane	1.1	6.3	3.8	3.4	11.6
Carbon monoxide	13.0	11.5	12.6	14.0	8.4
Hydrogen	11.6	14.9	14.8	14.3	14.6
Argon	.8	.7	.7	.7	.6

*Data obtained by J. M. Singer of this Laboratory.

Table 10.--Fire points of fuel-water solutions.

Fuel	Temperature, ° C.	Volume percent fuel	<u>Heat of vaporization</u> <u>Heat of combustion</u>
<u>Tray 15 × 76 × 1.6 cm. deep</u>			
Methyl alcohol	25	42	
	56	20	0.60
Acetone	25	15	
	60	10	.92
Isopropyl alcohol	25	40	
	66	8	1.09
Tertiary butyl alcohol	25	35	
	64	8	1.01
UDMH	33	50	
	60	34	.22
	63	34	
	Burnout*	28*	
MAF-1	34	64	
	60	39.5	.39**
	63	38	
MAF-3	25	63	
	60	53	.52**
	63	51	
<u>Tray 5.1 × 25.4 × 104 cm. deep</u>			
Methyl alcohol	25	49	
Acetone	25	21	
Isopropyl alcohol	25	42	

*A sufficiently concentrated solution was ignited and permitted to burn to self-extinction. Residual fuel concentration was determined by measurement of specific gravity.

**Assumed DETA in aqueous solution did not vaporize or burn.

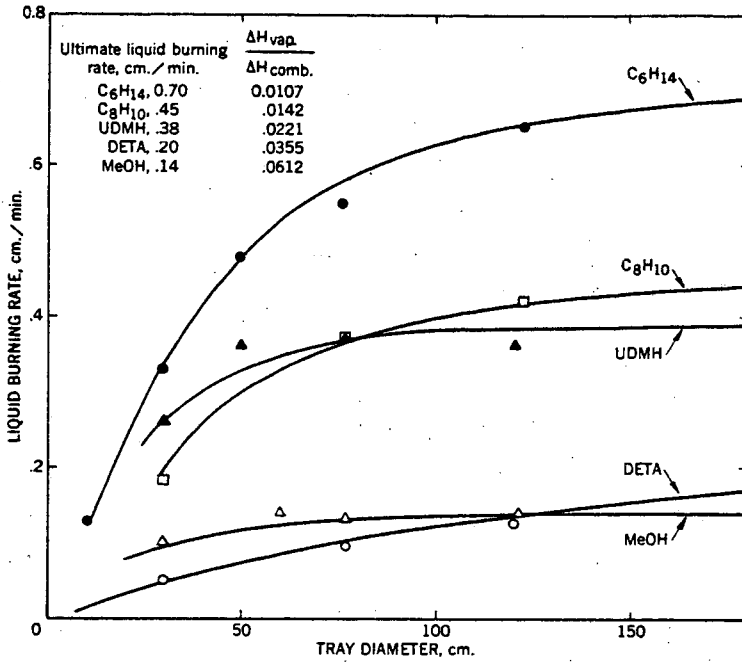


Figure 1.--Variation of Liquid Burning Rate with Tray Diameter.

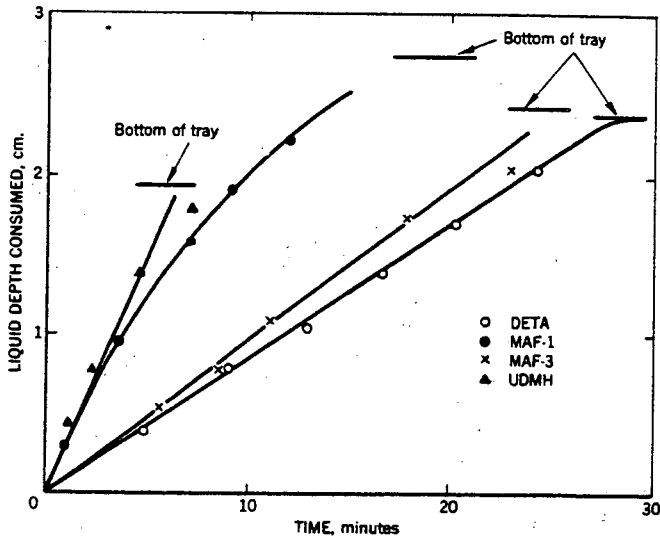


Figure 2.--Burning Time in 76 cm. i.d. Tray of UDMH, DETA, and the Blends MAF-1 and MAF-3.

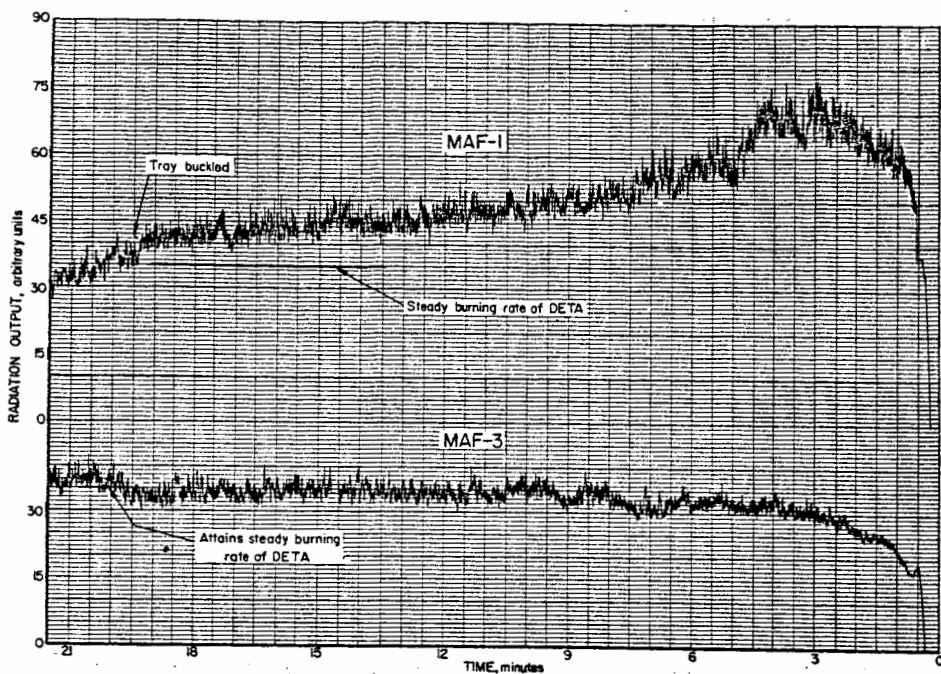


Figure 3.--Radiation Records of MAF-1 and MAF-3 Burning in 122 cm. i.d. Tray.

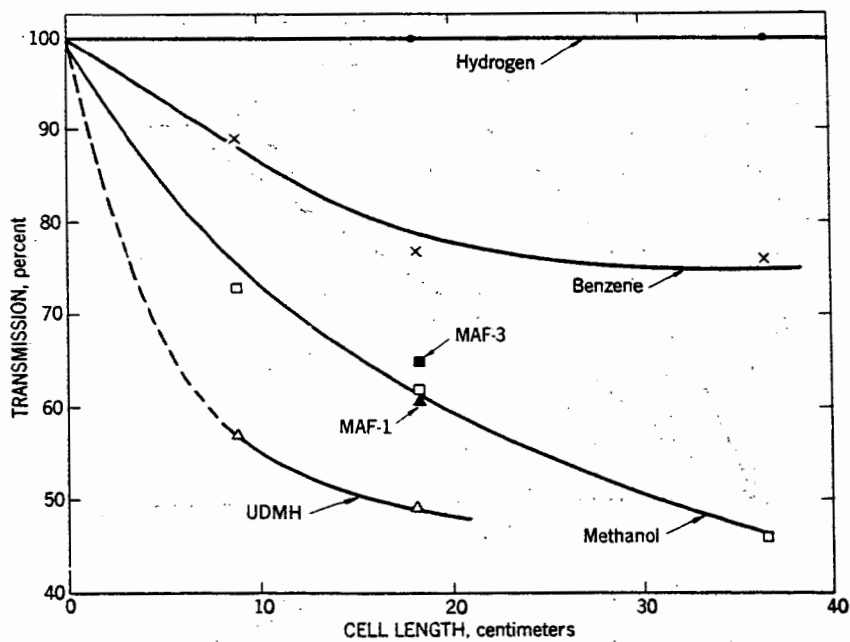


Figure 4.--Transmission of Flame Radiation Through Cells Filled with Vapor of Burning Fuel.

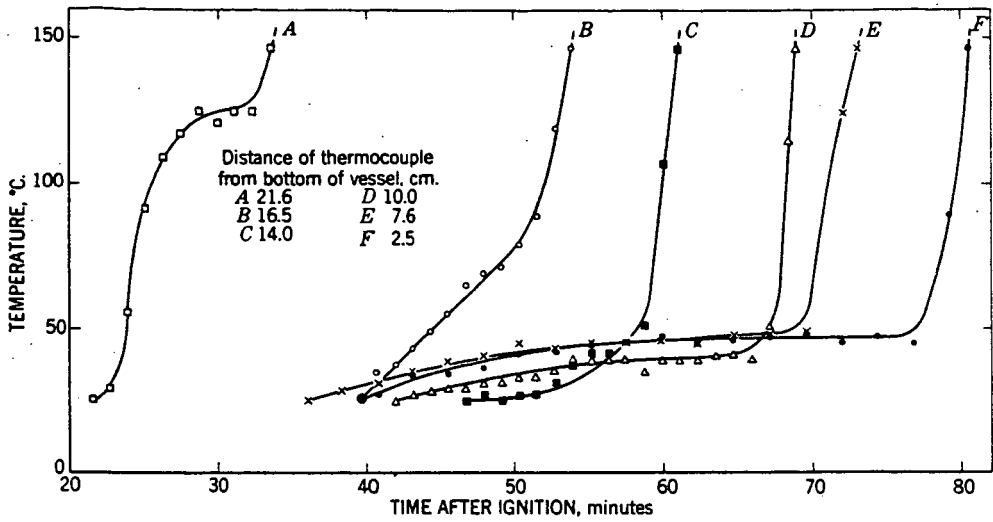


Figure 5.--Temperature Profiles near Liquid Surface of MAF-1, Burning in 47 cm. i.d. Vessel.

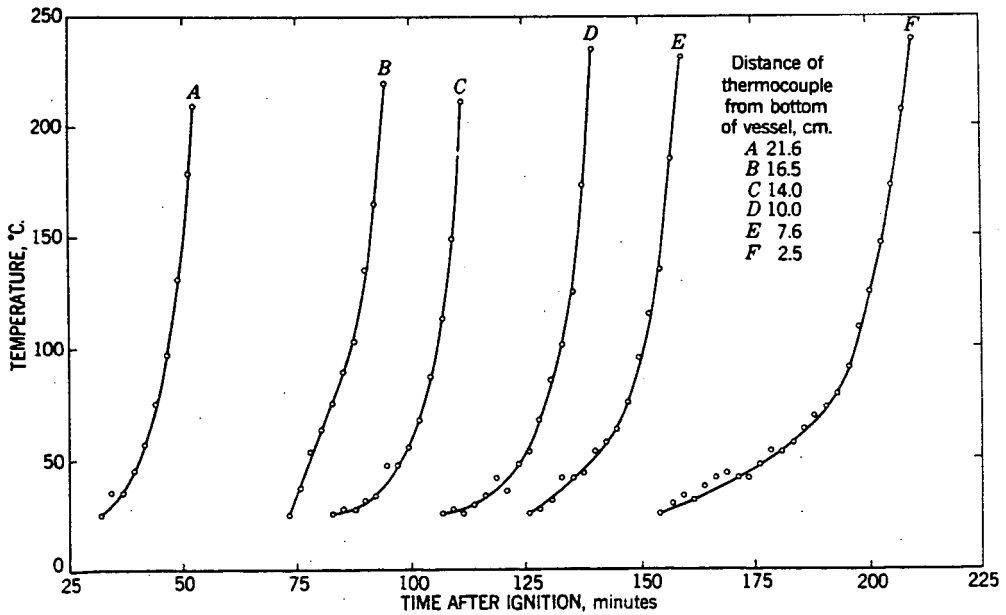


Figure 6.--Temperature Profiles near Liquid Surface of MAF-3 Burning in 47 cm. i.d. Vessel.

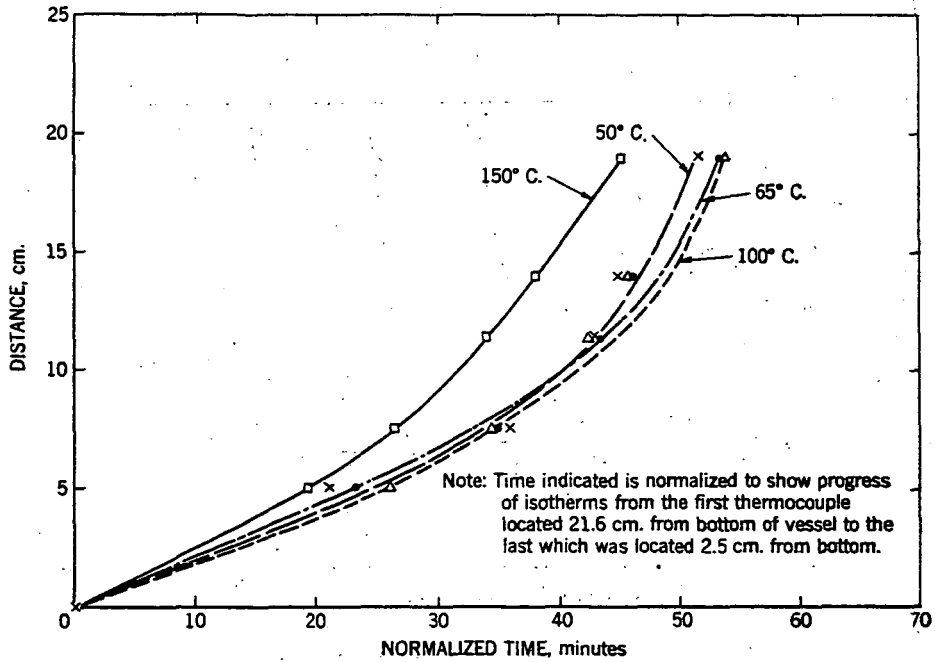


Figure 7:--Progress of Isotherms Through Burning MAF-1.

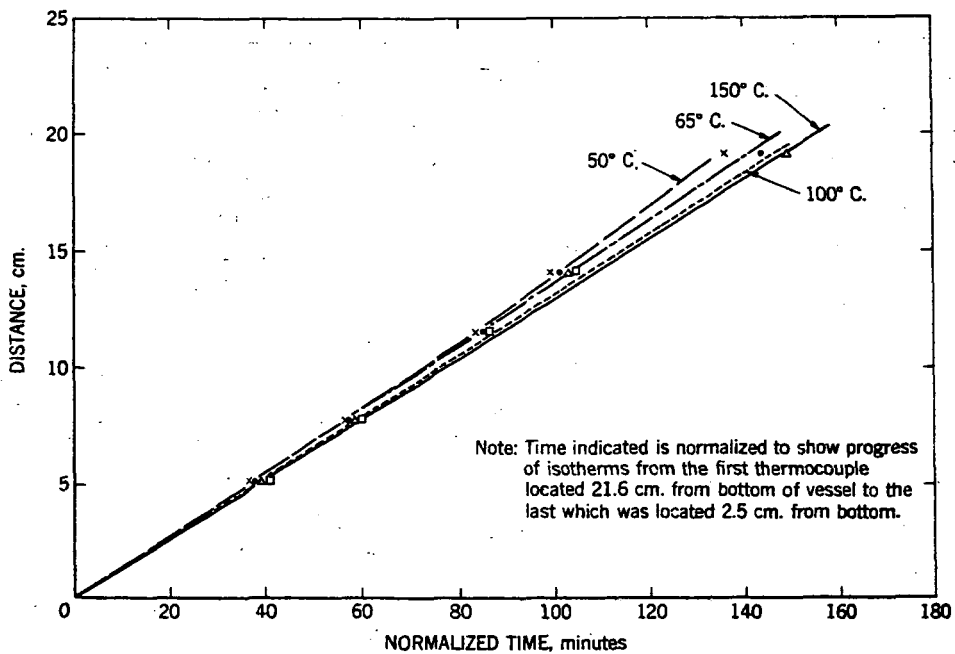


Figure 8:--Progress of Isotherms Through Burning MAF-3.

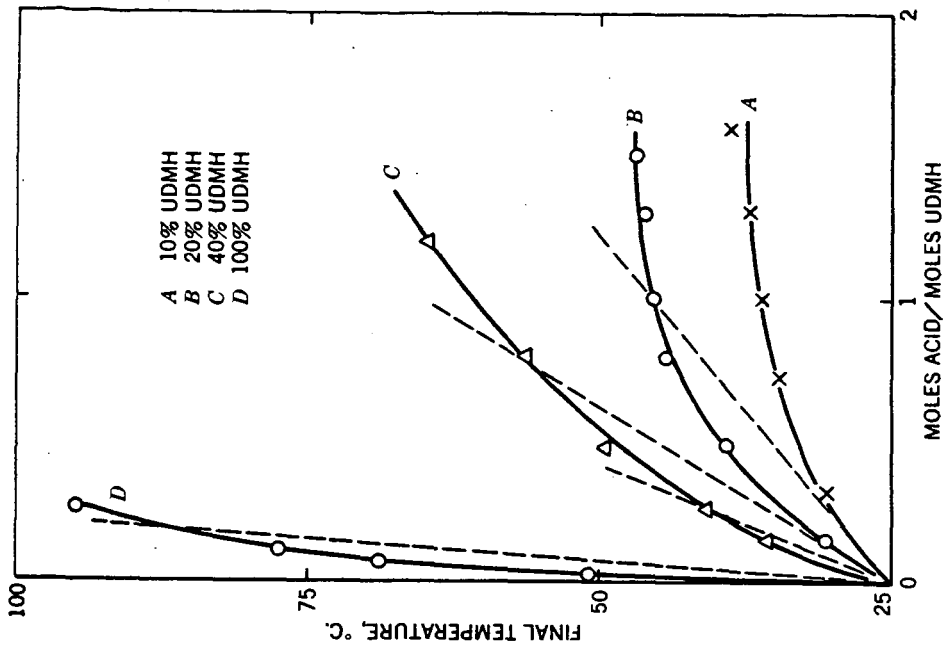


Figure 10.--Temperature Rise on Addition of Water-RFNA (50-50) to 200 cc. Water-UDMH.

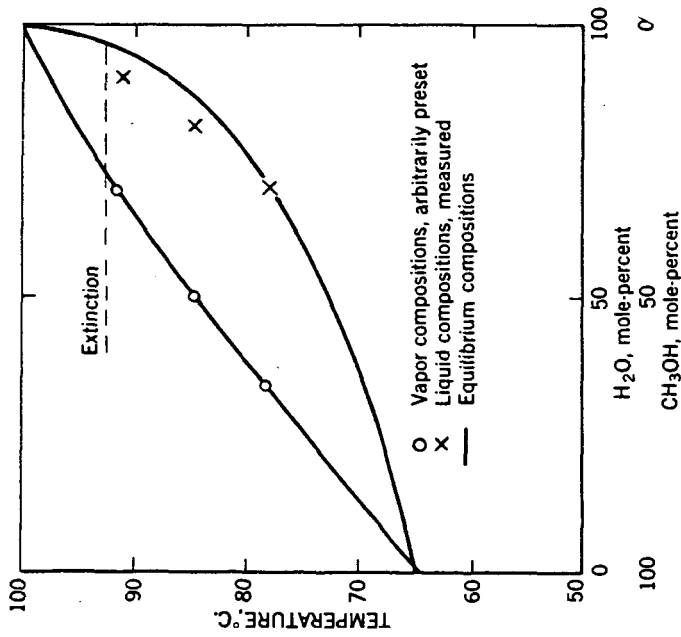


Figure 9.--Fractionation of Methanol-Water Burning in 30 cm. l.d. Tray.

**EXTINGUISHMENT STUDIES OF HYDRAZINE AND
UNSYMMETRICAL-DIMETHYLHYDRAZINE FIRES***

Wilburt Haggerty, Michael Markels, Jr., and Raymond Friedman

Atlantic Research Corporation, Alexandria, Virginia

I. INTRODUCTION

The employment of new high-performance liquid propellants has resulted in new problems of fire protection for personnel and facilities in the vicinity in which these chemicals are stored, handled, or used. By their very nature these propellants are reactive. Toxicity of the fuels or their combustion products may exist. Many of the fuel and oxidizer combinations are hypergolic, requiring no outside ignition source to start a fire. In other cases, these materials may burn as monopropellants without an outside oxidizer, making a particularly difficult extinguishment problem. The materials under discussion may be used in a wide variety of situations or geometries. This produces a wide variety of possible fire and explosion events. Yet, if these propellants are to be used, some form of fire protection must be provided.

This investigation was undertaken to determine the materials and techniques necessary for the extinguishment and control of fires involving two of these new propellants, hydrazine and unsymmetrical-dimethylhydrazine. Some properties of these fuels are shown:

Fuel	Formula	Boiling Point (°F)	Density (gms/cc)	Flash Point (closed cup) (°F)	Fire Point (°F)	Flammability Limits in Air	
						Lower (vol per cent)	Upper (vol per cent)
Hydrazine	N_2H_4	236	1.008	104	126	4.7	100
UDMH	$(CH_3)_2N_2H_2$	146	0.786	34 (?)	5	2.5	95

The program also included studies of the 50-50 mixture of these fuels, the fuel JP-X (a solution of UDMH in JP-4, a petroleum fuel), and fires involving all these fuels in contact with nitrogen tetroxide in either liquid or vapor form. This paper is limited to a summary of data for the hydrazine or UDMH and air combinations. Further details including results from the other combinations, are available from the progress reports (1).

While the primary objective of the investigation was to determine the requirements for fire protection systems capable of coping with fires involving these propellants, an important by-product was the development of basic knowledge in the use of small models for fire-extinguishment research. Since the application of the results of this investigation to fire-extinguishment practice depends, in part,

* This work was sponsored by the Flight Accessories Laboratory, Aeronautical Systems Division, Air Force Systems Command, under Contract 33(616)-6918.

upon being able to extrapolate laboratory results to very large fires, the appropriate scaling factors must be well known. This involves determination of the mechanisms by which various agents extinguish fires and the effects of agent-application parameters, fire geometries, and fire size on the extinguishing capabilities of the various agents.

The experimental approach involved three fire sizes. The smallest test, 6.54-sq in, were conducted in a laboratory hood; providing an extensive amount of data to screen candidate agents, determine the mechanisms of extinguishment, and the optimum methods and rates of application. The burner shown in Figure 1, was a square stainless-steel pan which could be heated to maintain the fuel at a temperature above its fire point. A 3/4-inch freeboard on the sides of the pan reduced splashing and fuel spillage. Any propellant spillage or excess extinguishing agent was caught in the stainless steel tray on the sides of the pan. This tray also served to reduce the updraft caused by the fire and to prevent these updrafts from cooling the sides of the burner.

To evaluate an extinguishing agent, 0.6 to 2.4 cubic inches of fuel (corresponding to about 0.1 to 0.4 inches depth) were placed in the burner, allowed to reach the desired temperature, and ignited by means of a hot wire. After a selected preburn time, usually 10 seconds, the agent was directed onto the fire. The length of time required for extinguishment, the amount of agent required, and the amount of propellant remaining unburned were determined as a function of agent, rate of application, application technique, and propellant.

The larger pans, 49- and 324-sq in, were identical in geometry to the smallest pans and were used to determine the scaling factors necessary for extrapolation of the results to still larger fires. They were located in the outdoor facility shown in Figure 2. After the photograph was taken, an eight-foot-high windbreak was built around the facility to minimize the effects of variable winds.

In spite of all precautions, a substantial variability in the results of consecutive tests was found. This seems to be characteristic of pan fire extinguishment tests. Hence a large number of tests were made, and averages of a series of identical tests were used to compute each datum point plotted on the curves which follow. A total of 994 test fires were burned to obtain the results discussed herein.

II. EXPERIMENTAL RESULTS

A. BURNING RATES OF HYDRAZINE AND UDMH

Burning rates of hydrazine and UDMH were found from burning time vs. fuel depth curves for a series of square pans:

<u>Fuel</u>	<u>Pan Area (sq in)</u>	<u>6.54</u>	<u>49</u>	<u>324</u>
Hydrazine		0.74 in/min	0.47 in/min	1.41 in/min
UDMH		0.088 in/min	0.046 in/min	0.195 in/min

Hydrazine is seen to burn an order of magnitude faster than UDMH. This is ascribed to the ability of hydrazine to burn like a monopropellant; a decomposition flame not requiring oxygen exists close to the liquid surface. The hydrogen produced by this flame then burns with air as a diffusion flame. Addition of water to the hydrazine reduces its burning rate substantially.

The slower-burning UDMH has a burning rate of the same magnitude as ethanol or gasoline, so a decomposition flame is evidently not present.

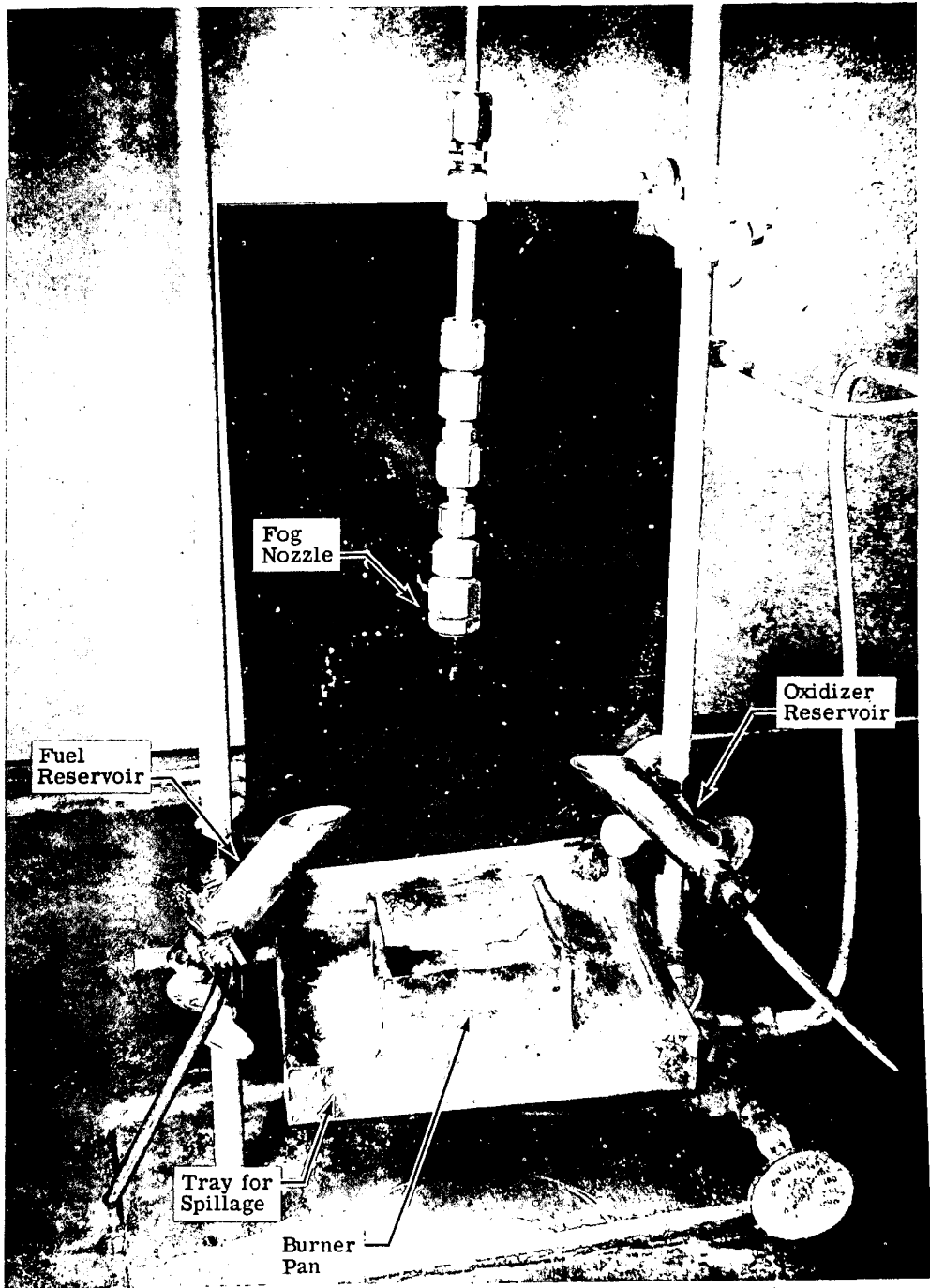


Figure 1. Burner Apparatus with Spray Nozzle.

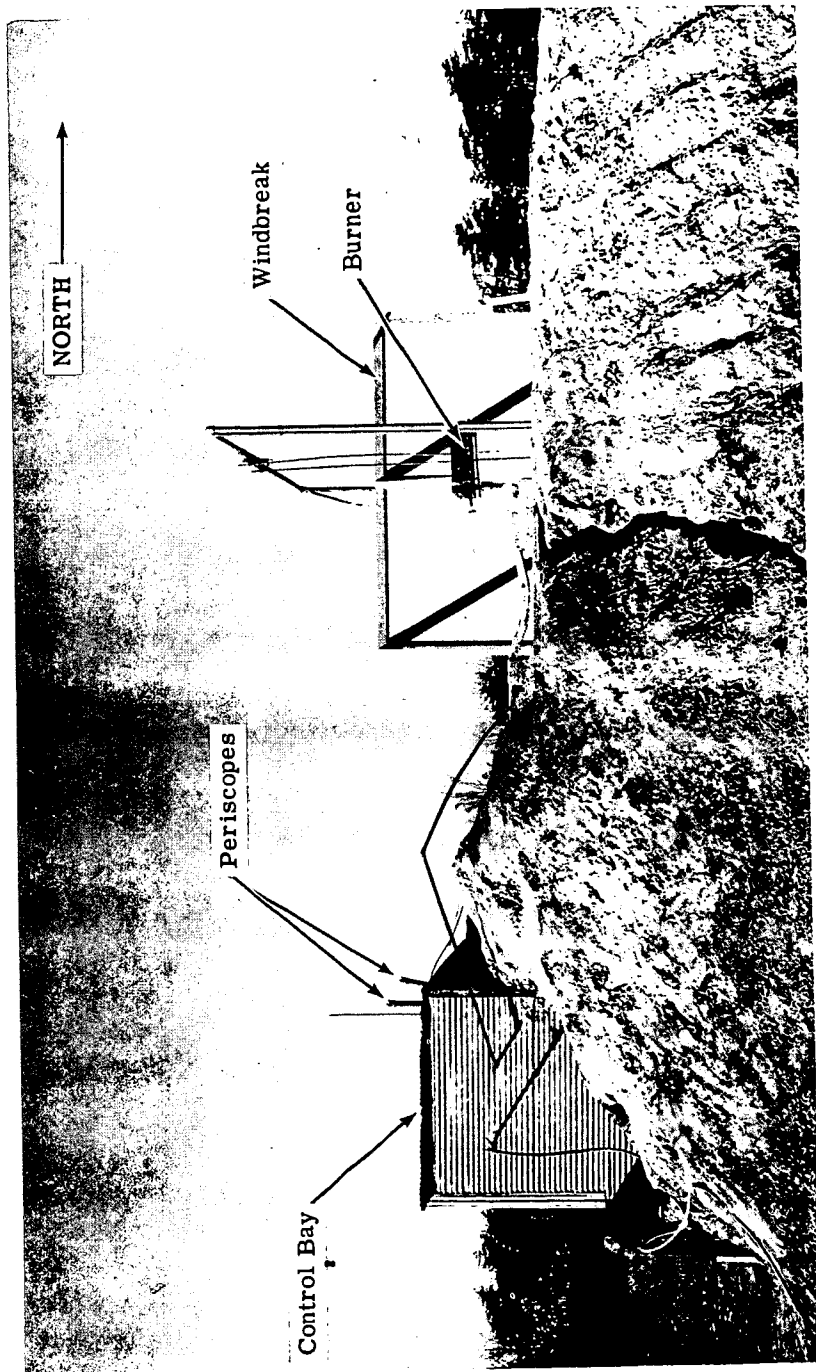


Figure 2. Side View of Outdoor Fire Extinguishment Facilities.

The variation with pan size for both fuels is explicable on a heat-transfer basis (2,3) and will not be discussed here.

B. EXTINGUISHMENT OF HYDRAZINE FIRES

1. Water Sprays

The mechanism by which water sprays extinguish hydrazine fires appears to be dilution of the hydrazine to a concentration which will not support combustion. As shown in Figure 3, when water was applied to 6.5-, 49-, and 324-sq in hydrazine fires at rates of 0.01 to 0.33 gal water/sec gal of fuel (0.2 to 1.2 gpm/ft²), the hydrazine concentration after extinguishment indicated a dilution to 40-70 weight per cent. The residue remaining after extinguishment of the larger fires was more dilute than those from the smaller fires. In the larger fires, more heat was radiated to the liquid and therefore the liquid temperature was higher. This meant that more dilute solutions supported combustion. The concentration of hydrazine in the residue remaining after extinguishment was found to decrease as the depth of the fuel was decreased. Decreasing depth is indicated by increasing normalized water spray rate in Figure 3. Since water and hydrazine have approximately the same densities concentration gradients are easily established. Mixing depends mostly on the force with which the water spray impinges on the surface and the depth of the pool. Both effects are responsible for the decrease in the concentration of hydrazine in the residue as the normalized spray rate was increased as shown in Figure 3.

Since the mechanism of extinguishment is primarily one of dilution, in an idealized case the time that spray must be applied to cause extinguishment should be directly proportional to the amount of fuel present and inversely proportional to the rate of application of spray. However, the simplicity of the dilution mechanism is complicated by the following factors:

- 1) As the fire progresses, some of the fuel is consumed, leaving only the remainder to be diluted.
- 2) Some of the water which does reach the burning liquid is later vaporized.
- 3) Some of the water is vaporized in the flame and never reaches the burning liquid.
- 4) Mixing rate of the water and fuel is not instantaneous.

Because of the above factors, the length of time that spray must be applied is not simply proportional to the volume of fuel or the inverse spray rate. However, as shown in Figure 4, the data may be correlated by plotting the logarithm of the extinguishment time versus the logarithm of a normalized rate of application of spray (gal water/sec gal of fuel). In view of the above complicating factors, the fact that even an empirical correlation can be obtained is indeed fortuitous. The slopes and intercepts of the curves would be expected to be complex functions of the properties of the fuel, pan size, and agent. The main conclusion from the curves is that larger fires require a longer application of spray before extinguishment occurs, for the same normalized spray rate, but that the increased time is slight when compared to the increased fire size.

The percentage of original fuel remaining after extinguishment, an expression of the efficiency, is presented in Figure 5 as a function of the rate of application of water. As can be seen, faster rates of application are more efficient on this basis than slower ones, and deeper pools of fuel are more efficiently extinguished than shallow ones.

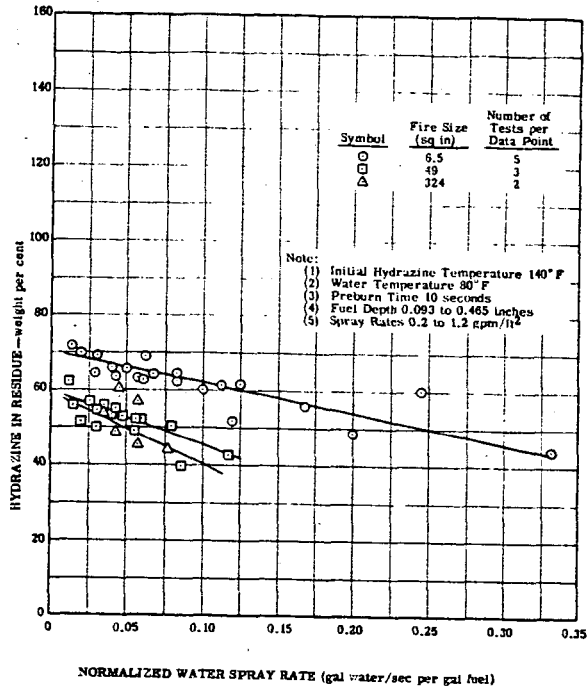


Figure 3. Concentration of Hydrazine in Residue Remaining after Extinguishment of Hydrazine Fires by Water Spray.

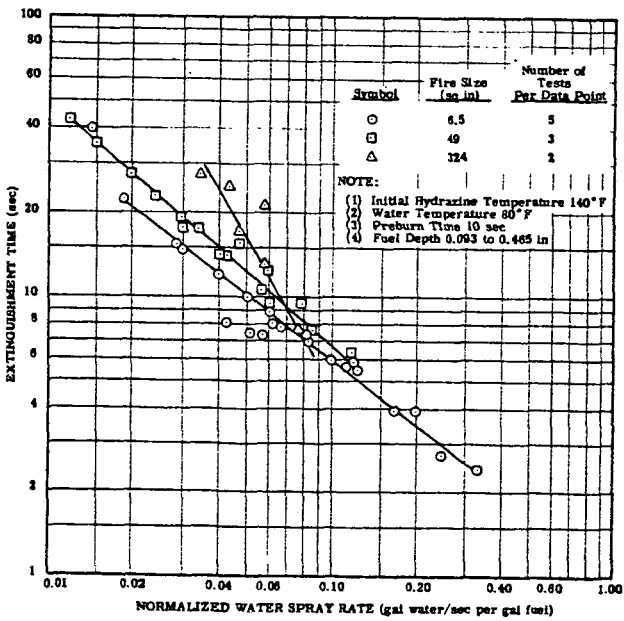


Figure 4. Effect of Normalized Spray Rate on Extinguishment Time of Hydrazine Fires.

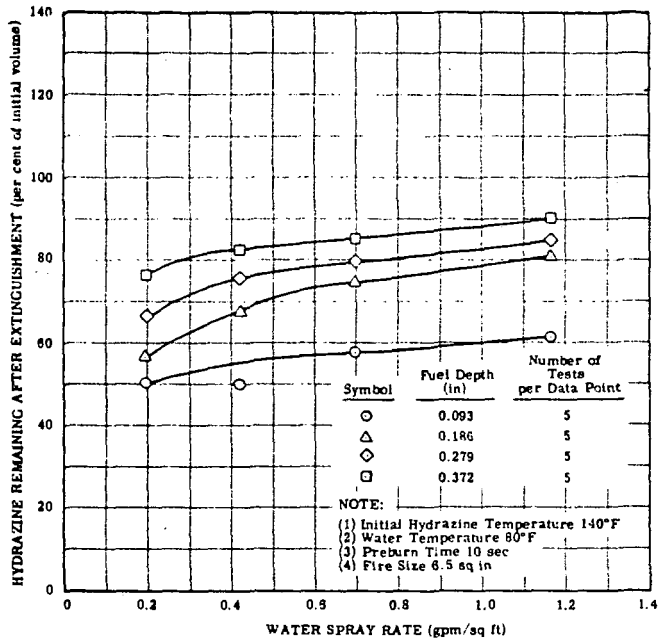


Figure 5. Effect of Water Spray Rate on Amount of Hydrazine Remaining after Extinguishment.

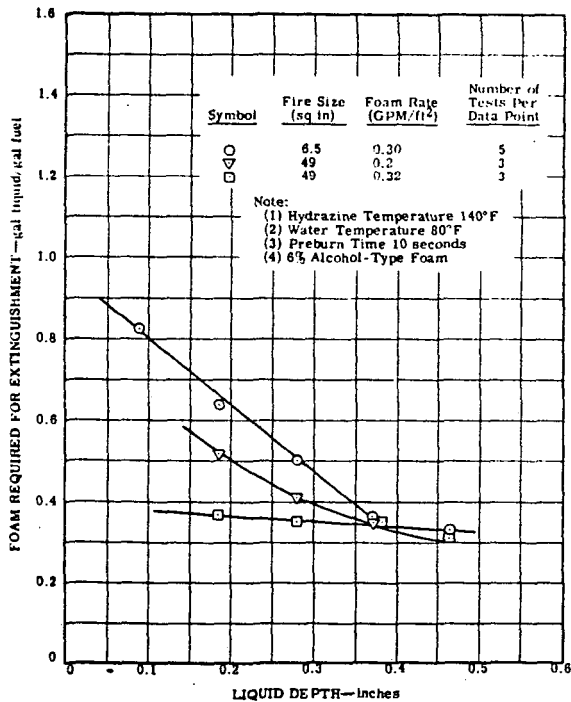


Figure 6. Effect of Liquid Depth on Amount of Foam Required for Extinguishment of Hydrazine Fires.

Because dilution is the mechanism by which water sprays extinguish hydrazine fires, the major scaling factor for extinguishment is a function of the amount of fuel present and is not a function of diameter, per se. However, spray rate, liquid depth, and fire diameter do influence scale-up slightly. Since dilution to 50 weight per cent concentration appears to be adequate, the amount of water required for extinguishment would be about one gallon per gallon of fuel. Any consumption of fuel or vertical concentration gradients would reduce the amount required. Conversely, any vaporization of water in the flame would increase the amount of water required.

The weight average particle size, \bar{D}_w , of the spray used on each fire size was:

Pan Size sq in	\bar{D}_w microns
6.5	160
49	245
324	290

2. Fog

Measurements with the 6.5-sq in burner indicated that water fog was less effective than coarse water sprays against hydrazine fires. Since the concentrations remaining after extinguishment were comparable, the lower efficiency was probably due to increased vaporization of the fine droplets in the flame. Fog was less effective against 49-sq in fires than against 6.5-sq in fires, again because of vaporization in the flame, preventing liquid dilution. The fact that as much as 1.5 gallons of water per gallon of fuel originally present were required for extinguishment, in comparison to 1.0 gal/gal for spray, indicates the magnitude of the vaporization, especially since most of the fuel originally present was consumed in the fire.

Fog is not a good extinguishing agent for hydrazine fires and would probably fail to extinguish very large fires.

3. Foam

The mechanism by which foam* extinguishes hydrazine fires appears to be dilution of the surface of the burning liquid below the concentration which supports combustion. Since the hydrazine causes the foam to break down rapidly, a surface layer of water is built up over the fuel. The foam on top of the water film is stable until it contacts fresh hydrazine further out on the burning pool. When the foam blankets the entire surface, the fire is extinguished.

As shown in Figure 6, the amount of foam required for extinguishment is a function of application rate, depth of liquid fuel, and size of the fire. Faster rates of application require less foam because the foam has less time to break down and is therefore able to blanket the fire more quickly. Figure 7 shows that times required to extinguish the 49-sq in fires were about 10 seconds longer with 0.2 gpm/ft² application than with 0.32 gpm/ft². The slower rate of travel across the hydrazine surface at the lower application rate permits more breakdown of the foam, and therefore more foam is required.

The decrease in the amount of foam required per gallon of fuel for deeper pools of hydrazine confirms the mechanism of surface dilution. Although the concentrations of hydrazine remaining after extinguishment shown in Figure 8 are decreased by the

*

A 6% alcohol-type foam was used at a 10 to 1 expansion ratio.

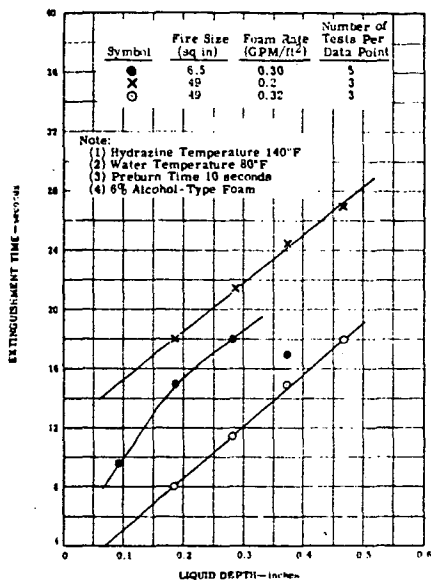


Figure 7: Effect of Liquid Depth on Time Required for Extinguishment of Hydrazine Fires by Foam.

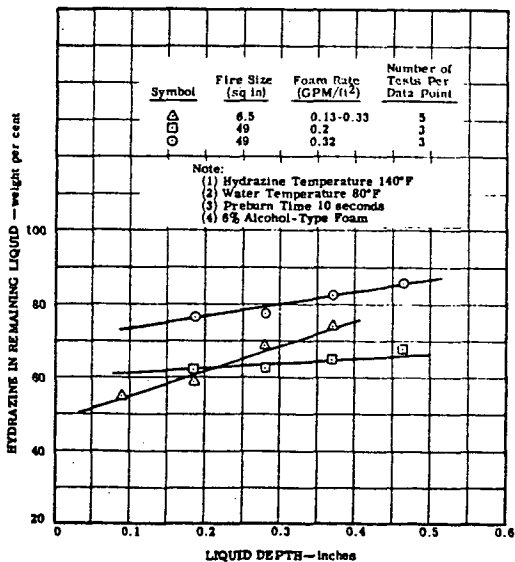


Figure 8: Effect of Liquid Depth on Concentration of Hydrazine Remaining after Extinguishment of Hydrazine Fires by Foam.

collapse of the foam blanket remaining after extinguishment, the fact that the final hydrazine concentration may be as high as 86 weight per cent shows that the concentration gradients are very steep.

The mechanism of surface dilution suggests that scaling factors are strongly dependent on surface area of the fire as well as liquid depth and stability of the foam. Any agitation of the fuel would disturb the concentration gradients and render the foam less effective. The foam should be distributed evenly over the surface and applied at as fast a rate as possible. Although foam is a more efficient extinguishing agent than water spray, the ease of application of water sprays and the required dilution below the fire point, which eliminates the reignition hazard, make water sprays more attractive than foam.

4. Dry Chemical

A modified sodium bicarbonate powder of 50 micron average particle size was very effective in extinguishing fires involving hydrazine and air. As seen in Figure 9, when as little as 0.016 lbs/sec/ft² was applied, the fires were extinguished in less than four seconds. The depth of burning liquid had no observable effect, but complete coverage of the burning surface was required before extinguishment occurred. This requirement is probably the cause of the apparently anomalous results in which more time was required for extinguishment at the faster rate. These results are similar to those obtained in the 6.5- and 324-sq in burners, in which 0.016 lbs/sec/ft² extinguished the fires in less than three seconds. After extinguishment the fires could be reignited by the hot wire igniter. In practice, therefore, some other agent such as water might have to be applied in addition to the dry chemical to prevent reignition after extinguishment had been achieved.

A solution of 8 per cent by weight sodium bicarbonate in water applied as a water spray at a rate of 0.6 gpm/ft² showed no improvement over water as an extinguishing agent in the 6.5-sq in burner. This is consistent with other work which has shown that extinguishment by dry chemical involves reactions in the flame.

A potassium bicarbonate powder of 25 micron diameter was as effective as the sodium bicarbonate. However, an ABC Type powder was ineffective against the hydrazine fires.

Scale-up in dry chemical extinguishment is a function of fire area. Good results with this agent are dependent on the ability of the extinguishing system to completely blanket the fire and thereby prevent flashover from reigniting the extinguished areas. Dry chemicals are attractive in that they can extinguish the fires in a comparatively short time with the minimum weight of agent.

5. Chlorobromomethane

Chlorobromomethane (CB) was sprayed on hydrazine fires at a rate of 0.11 gpm/ft² through the nozzles also used for water spray. The CB reacted with the hydrazine, increasing the intensity of the fire and producing dense white fumes. The fires continued to burn until the hydrazine was consumed. CB is ineffective as an extinguishing agent for hydrazine fires under these conditions.

6. Investigation of Other Agents

Several screening tests were made to determine if chemicals other than sodium bicarbonate could inhibit the combustion of hydrazine-type fuels. Since aniline is capable of trapping the NH₂· radical believed to be involved in the combustion process, this chemical was the first to be investigated. When 2 weight per cent aniline was added to hydrazine, the burning rate of the hydrazine was reduced by only 10 per cent. Since the alkali metal bicarbonates in powder form were so

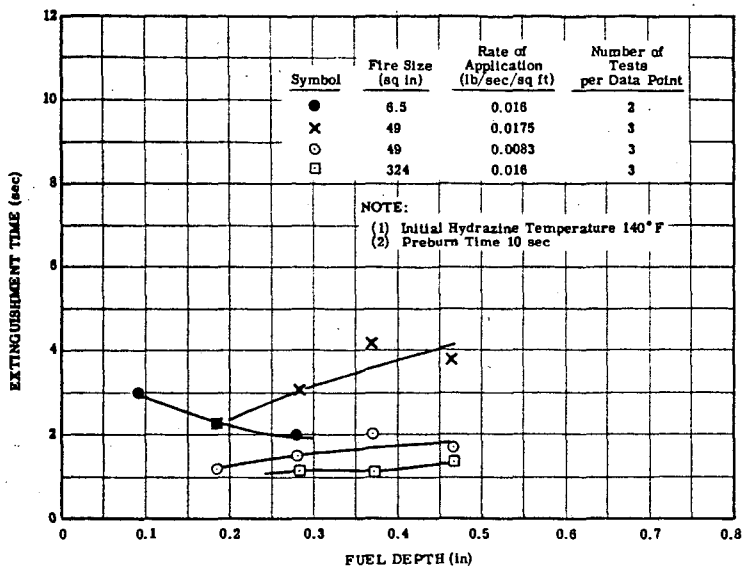


Figure 9. Effect of Fuel Depth on Extinguishment Time of Hydrazine Fires by Sodium Bicarbonate.

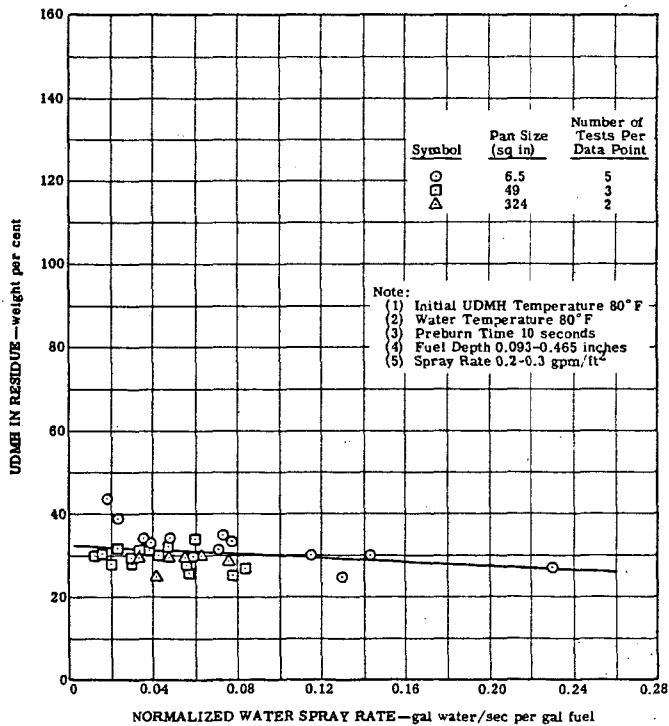


Figure 10. Concentration of UDMH in Residue Remaining After Extinguishment of UDMH Fires by Water Sprays.

effective against hydrazine fires, other methods of applying alkali metal salts were investigated. A solution containing 8 per cent by weight sodium bicarbonate showed no improvement over a plain water spray. Since potassium iodide is very soluble in hydrazine, a solution containing 20 grams of potassium iodide per 100 grams of hydrazine was burned. The combustion was slowed down considerably by the formation of a molten slag over the burning liquid, but all of the hydrazine was consumed. Addition of 10 weight per cent boric acid, (a constituent in some ABC powders) had a similar effect. It was thought that an inert liquid might blanket the surface of burning hydrazine and prevent combustion. However, a silicone oil added to burning hydrazine formed a film on the surface, but did not extinguish the flame.

C. EXTINGUISHMENT OF UDMH FIRES

1. Water Sprays

As was the case with hydrazine fires, the length of time that water sprays must be applied before extinguishment of UDMH fires occurs is a function of the amount of fuel present and the rate of application of the spray. This indicates that the mechanism of extinguishment of UDMH fires is also one of dilution of the burning liquid to a concentration which will not support combustion. The UDMH fires required a longer application of spray than did the hydrazine fires because more dilute solutions of UDMH will support combustion and the UDMH burns at a slower rate, thus consuming fuel more slowly. Figure 10 shows that the fires in the 6.5-, 49- and 324-sq in burners were extinguished when the UDMH concentration was reduced to approximately 30 weight per cent. This final concentration was the same for all spray rates, pan diameters, and liquid depths. Since water is more dense than UDMH, it is believed that good mixing occurred as the water settled through the UDMH.

As was the case with the hydrazine fires, the larger fires required a longer application of spray before they were extinguished, cf. Figure 11. Since the concentrations of UDMH remaining in the residue after extinguishment were comparable regardless of fire size, increased vaporization of the water droplets in the larger flames would appear to be the cause of the increased amount of water required for extinguishment.

The percentage of UDMH remaining after extinguishment as a function of spray rate is presented in Figure 12. As can be seen, faster spray rates are more effective for extinguishing UDMH fires than slower rates. There is little or no change in the percentage of fuel remaining after extinguishment as the depth of UDMH is increased. This indicates that a basic difference in extinguishment behavior arises from the more complete and rapid mixing of water with UDMH than with hydrazine.

2. Fog

Fog extinguished UDMH fires by the same mechanism as water sprays, i.e., dilution. Fog applied at a rate of 0.2 gpm/ft² against the 49-sq in fires required 2.13 gal/gal of UDMH as compared to 1.46 gal/gal of UDMH for water spray at the same rate. Fog does not seem as desirable as water spray against UDMH fires, since part of the fog evaporates and is unable to dilute the fuel.

3. Foam

Although UDMH caused the alcohol-type foam to break down, it nevertheless extinguished UDMH fires. As with hydrazine, the mechanism of extinguishment appears to be one of floating water on top of the burning liquid and diluting the surface below the concentration which will support combustion. Because this is a gentle application of water, concentration gradients are set up and the average concentrations of 35-55 weight per cent are well above the minimum concentrations which support combustion. Figure 13 illustrates this. As seen from Figure 14, the relative amount of liquid required for extinguishment decreases as the fuel depth is increased because

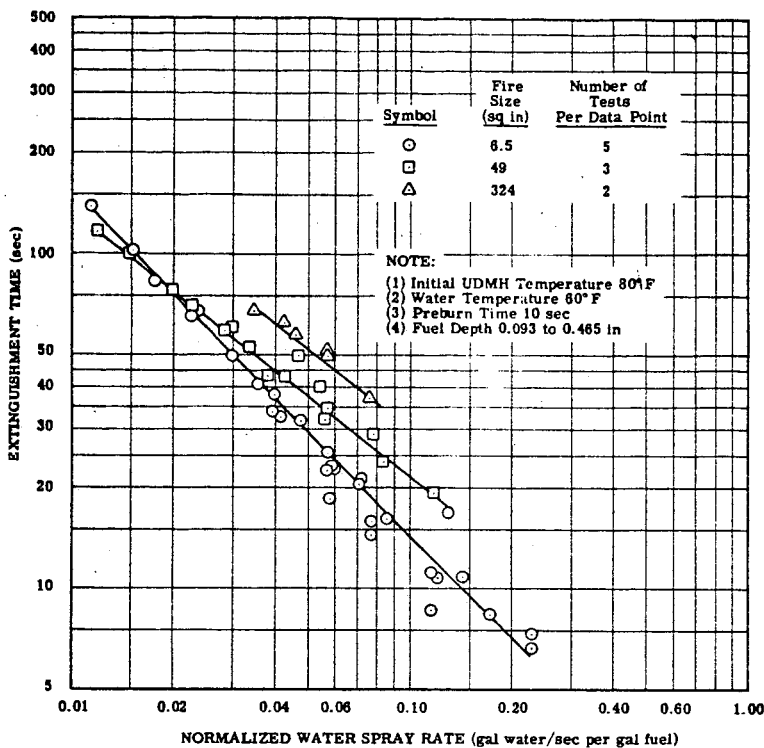


Figure 11. Effect of Normalized Water Spray Rate on Extinguishment Time of UDMH Fires.

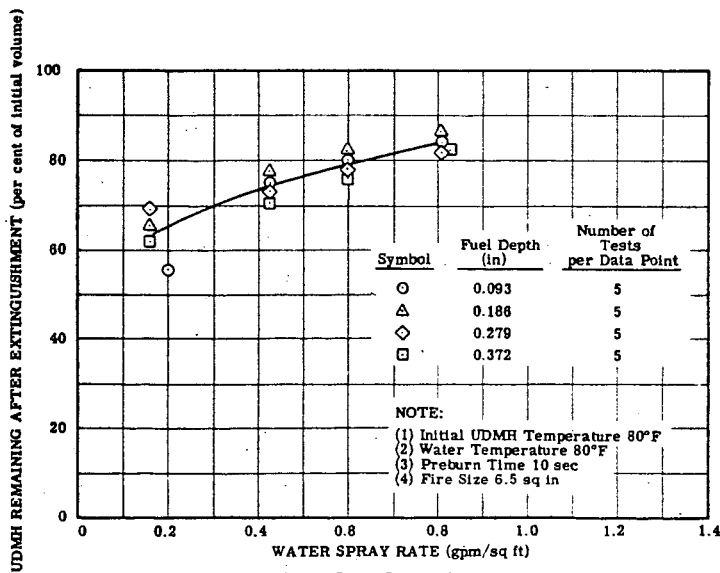


Figure 12. Effect of Water Spray Rate on Amount of UDMH Remaining after Extinguishment.

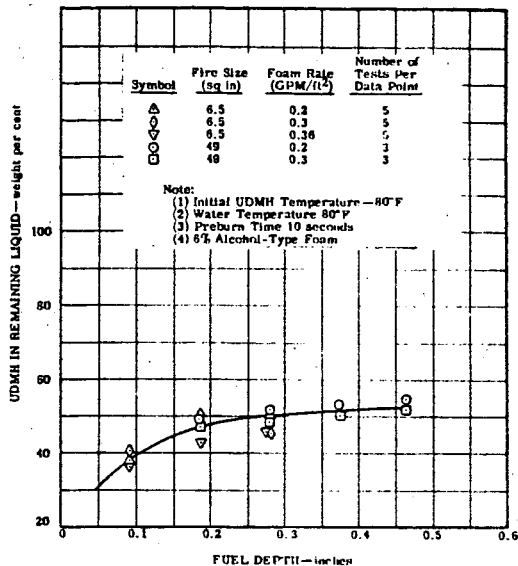


Figure 13. Effect of Fuel Depth on Concentration of UDMH Remaining after Extinguishment by Foam.

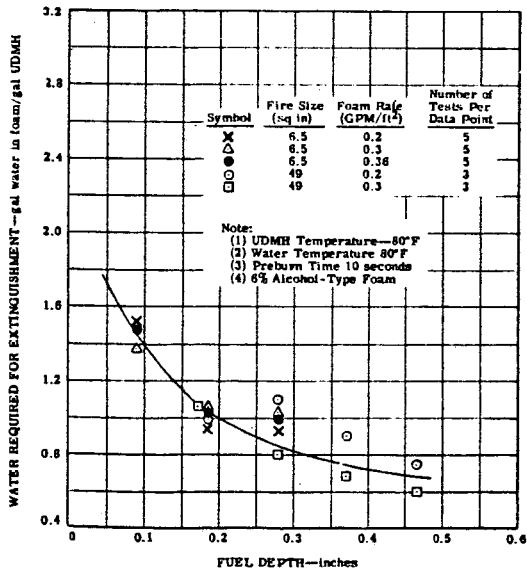


Figure 14. Effect of Fuel Depth on Amount of Liquid Required for Extinguishment of UDMH Fires by Foam.

of the concentration gradients mentioned above. The effectiveness of foam is increased by faster application rates. Increasing the pan diameter did not increase the amount of foam required per gallon of fuel at any given depth. The scaling factor would therefore be a function of volume of fuel, depth of fuel, and application rate.

As was the case with hydrazine fires, foam is a more efficient method of applying water to UDMH fires than is spray. However, if an adequate supply of water is available, the ease of application and the faster rates at which it can be applied make water spray more attractive.

4. Dry Chemical

Sodium bicarbonate powder rapidly extinguished UDMH fires. When the dry chemical was applied at rates of 0.0175 or 0.0083 lb/sec/ft² and when complete coverage of the surface was obtained, all fires were extinguished in less than 5.2 seconds. Fire size was varied from 6.5- to 324-sq in and depth of fuel from 0.093 to 0.47 inch. If complete coverage was not obtained, the fire flashed over the surface when the flow of agent was stopped. As was the case with hydrazine, the fire could be reignited by a hot wire. Dry chemical is particularly suitable when speed of extinguishment is important or when a minimum amount of agent must be applied.

5. Vaporizable Liquid Agents

As shown below, trichlorotrifluoroethane extinguished 6.54-sq in UDMH fires when applied at a rate of 0.5 gpm/ft². The fires could be reignited after extinguishment, but burned less intensely. Since trichlorotrifluoroethane has a boiling point of 115.7°F, and the fire point of UDMH is 34°F, cooling of the UDMH does not appear to be a mechanism of extinguishment. Although dense white fumes were given off when the trichlorotrifluoroethane contacted the burning UDMH, there was no increased intensity of the fire such as occurred when chlorobromomethane was added to hydrazine. Trichlorotrifluoroethane might be useful in locations where limited access to the fire is available. It appears to be somewhat more effective than water spray or foam.

Extinguishment of UDMH Fires by Trichlorotrifluoroethane:

Liquid Depth (inches)	Extinguishment Time (seconds)	Gallons of Agent per Gallon of UDMH
0.093	6.9	0.99
0.186	6.7	0.48
0.279	9.5	0.45
0.372	24.0	0.86

Notes:

1. Application rate: 0.5 gpm/ft²
2. UDMH temperature: 80°F
3. Preburn time: 10 seconds
4. Fire Size: 6.5 sq in

D. EXTINGUISHMENT OF FIRES INVOLVING A MIXTURE OF HYDRAZINE AND UDMH

Although an investigation of fires involving a mixture of 50 parts each by weight hydrazine and UDMH is incomplete, enough data have been obtained to indicate that this mixture behaves very much like pure UDMH in regard to burning rate and quantity of agents required for extinguishment. The reason is that the vapor pressure of UDMH is much greater than that of hydrazine, so that the vapors above the mixture are essentially UDMH.

In addition to the agents applied to UDMH fires, several other agents have been tested against small fires involving the mixture. These agents were bromotrifluoromethane and carbon dioxide.

Bromotrifluoromethane, when applied at a rate of 0.04 lb/sec/ft^2 (0.18 gpm/ft^2), failed to extinguish fires involving the 50-50 mixture in the 6.54-sq in burner. The agent was applied in gaseous form and directed on the fire both from above and from the side. It did not react with the burning fuel. Further tests are in progress, with other methods of application.

Carbon dioxide when applied at a rate of 0.17 lb/sec/ft^2 failed to extinguish fires involving the 50-50 mixture in the 6.54-sq in burner. The carbon dioxide was applied in the gaseous form and no attempt was made to direct "CO₂ snow" on the fire.

III. CONCLUSIONS

Based on results to date the following conclusions are drawn:

1. Hydrazine fires can be extinguished by water sprays, alcohol-type foams, or dry chemical powders containing primarily sodium bicarbonate. Water sprays are best suited for spill-type fires. At least one gallon of water per gallon of fuel must reach the surface of the burning liquid. Foams can be used for deep pools or in chases where the water supply is limited. Dry chemicals should be used in cases where rapid extinguishment is necessary or when the amount of agent available is limited, and where reignition is not a problem. Chlorobromomethane should not be used against hydrazine fires.

2. UDMH fires may be extinguished by water sprays, alcohol-type foams, dry chemical powders containing primarily sodium bicarbonate, or trichlorotrifluoroethane. Water sprays are best suited for spill-type or deep-pool fires. Dry chemicals are effective when rapid extinguishment is necessary or when the supply of agent is limited, and reignition is not a problem.

3. Fires involving the 50-50 mixture of hydrazine and UDMH behave essentially as UDMH fires. The same quantities of agents are required for fires involving the mixture as for fires consisting of pure UDMH. Neither bromotrifluoromethane nor carbon dioxide have extinguished fires involving the 50-50 mixture, in tests to date.

IV. ACKNOWLEDGEMENTS

The authors wish to acknowledge helpful discussion with F. W. Thompson, B. P. Botteri, and R. Cretcher of Aeronauticals Systems Division, Air Force Systems Command.

REFERENCES

159.

- (1) Markels, M. Jr., Friedman, R. and Haggerty, W., Quarterly Progress Reports, Contract AF 33(616)-6918, Aeronautical Systems Division, Wright-Patterson Air Force Base, Ohio, 1960-1961.
- (2) Blinov, V. I. and Khudiakov, G. N., Acad. Nauk, SSSR Doklady 113, 1094-1098 (1957) and discussion by H. C. Hottel, Fire Research Abstracts and Reviews, Vol. I, 1958, pp. 41-44.
- (3) U. S. Bureau of Mines Tech. Report 1290, "Burning Rates of Liquid Fuels in Large and Small Open Trays," December 1, 1959.

The Flammability of Methane-Air Mixtures in Water-Base Foams

by J.H. Burgoyne and A.J. Steel

Department of Chemical Engineering & Chemical Technology
Imperial College, London, S.W.7. England.

This investigation forms part of a programme of research into flame propagation phenomena in systems in which the gas phase is accompanied by a physically-distributed liquid phase (e.g. spray, foam or film) which plays some part, either as a fuel or as a suppressant, in the combustion process. In the present instance the object was to examine the extent to which the flammability range of a methane-air mixture is restricted by inclusion in water foams of defined properties. So far as we are aware this subject had not previously been studied, except for some preliminary experiments (as yet unpublished) carried out at the Safety in Mines Research Establishment at Buxton, England, through which the problem first came to our attention. The influence of water vapour upon the flammability range of methane in air has been studied by Coward & Gleadall⁽¹⁾ and by Yeaw & Shnidman⁽²⁾; and Billett⁽³⁾ has examined the effect of water spray on the flammability of butane in air.

The foam properties with which correlation of the flammability range was sought were "wetness" and bubble size. "Wetness" was defined by an inverse function, the "expansion ratio", which was taken to be the ratio of the volume of a certain quantity of foam to the volume of liquid therein. An object of the experimental method of foam generation was to attain uniform bubble-size throughout any particular foam and the size was defined by a mean diameter.

Apparatus and methods.

A continuous flow system was employed to prepare methane-air mixtures and to generate foams having these mixtures as the contained gas-phase. Air and methane from compressed gas cylinders were passed through drying towers, flow control valves and orifice flow meters before mixing. The mixture then passed through a water saturator and a capillary to damp out bubbling pulsations before entering the foam generator. In this, the gas mixture bubbled through a copper gauze submerged in detergent solution to a controlled depth. The bubbles escaping from the liquid surface gave rise to a foam of reasonably uniform bubble size which ascended a perspex drainage column of controllable

height before turning into the horizontal flammability testing tube. This consisted of a perspex tube $2\frac{3}{4}$ in. internal diameter and some 4 ft. long which was continuously rotated about its axis so as to minimise drainage from the foam travelling along it. Foam emerging from the end of the tube fell into an open waste receiver.

Inflammability of the foam in the tube could be tested at any time by applying a one-inch coal gas flame to the open end and seeing whether or not flame would propagate throughout the contents of the tube. The products of propagation, if any, were swept out by the oncoming foam in readiness for another test. The rate of flow of foam along the tube did not exceed 1 cm/sec. whereas the minimum rate of flame propagation was 12 cm/sec. The flow of foam did not, therefore, interfere with flammability testing.

The foam properties were measured on samples emerging from the end of the tube. Expansion ratio was measured by allowing a known volume of foam to fall into a measuring vessel containing a layer of hexanol as separable foam breaker, and measuring the volume of the aqueous liquid formed. Bubble size was measured by allowing the foam to fall into a flat-bottomed perspex receiver containing a thin layer of the detergent solution. The foam was photographed through the bottom of this receiver, which was inscribed with a cm. scale, and after suitable enlargement of the plate, the mean diameter of some 250 bubbles was found by measurement.

The detergent solution consisted of a 1% solution in distilled water of "Perlankrol" (Lankro Chemicals Ltd., Eccles, Manchester, England) and had a surface tension of 26.3 dynes/cm. at 20°C, as measured by the capillary rise method.

The expansion ratio of the foam could be controlled by the gas flow (bubbling) rate and also by varying the height of the foam drainage column. Bubble size was primarily controlled by the mesh of the copper gauze through which bubbling took place, but was also influenced by the gas flow rate. Approximate ranges of variation available for satisfactory use were: expansion ratio 20 to 1500; bubble diameter 1 to 4.5 mm.

The method of conducting an experiment was as follows. With a gauze appropriate to the bubble size required, the air flow was adjusted to give approximately the desired expansion ratio. Methane was then added to the gas stream and its flow rate adjusted to give a limit mixture in the foam, as judged by repeated flammability tests. Samples of foam were then taken for measurement of properties and these were recorded against the limit gas mixture composition as determined from the flow meter readings.

Results.

In the absence of foam, the flammability limits of the

methane in air in the horizontal tube were 5.41 and 15.94 vol.-%. In the presence of foam these were narrowed to varying degrees. The narrowing was in general increased with decreasing bubble size. The effect of varying expansion ratio (R) was however somewhat complex. It is illustrated by a few figures in the accompanying table, but may be summarised as follows:

- (1) For values of R between 1500 (the highest used) and about 300, the flammable range narrowed with decreasing R (increasing wetness), and at 300-250 reached a minimum, which for the smaller bubble sizes amounted to complete suppression.
- (2) For values of R between 300 and 70, the flammable range widened again, reaching a maximum at about the latter value.
- (3) For values of R below 70, the flammable range again contracted with increasing wetness and with R about 20, flame propagation ceased.

In regions (1) and (2) the flame front was almost flat and vertical. With the driest foams in region (1), a definite gap appeared between the flame-front and the collapsing foam ahead. In both regions spray arising from the collapsing foam could be seen in and near the flame-front.

In region (3), the passage of the flame did not result in complete destruction of the foam. Kernels of flame travelled independently of one another, leaving behind considerable amounts of unconsumed foam.

A convincing demonstration of the existence of regions (1) and (2) could be provided by allowing an initially non-flammable foam of expansion ratio about 300, mean bubble size 1.50 mm. containing a 9% methane-air mixture, to drain for about 20 sec. by stopping the rotation of the tube, prior to ignition. The upper and lower halves of the foam could then be ignited separately and would propagate flame independently leaving unconsumed a central layer some 2 cm. thick. Due to drainage, the upper and lower layers had moved respectively into Regions (1) (dry) and (2) (wet), leaving the central layer non-flammable between the two regions.

Discussion.

The fact that the limits of flammability in foams of fixed bubble size, but varying expansion ratio, are generally symmetrical about the stoichiometric methane-air mixture, and converge upon it when convergence occurs, suggests that the principal function of the foam is to absorb the available energy in the mixture. For flame propagation to continue, some of the energy released by mixture burning in one bubble must be used to rupture the walls of the bubble and so gain access to unburnt mixture in adjacent bubbles. The heat transferred from the existing flame front towards the unburnt mixture thus released will be shared by such

liquid water as is in the area to an extent dependent upon the state of division (i.e. surface area) of the water at the time.

In Region (1) the foam is dry and bubble walls are thin. The rupture of the walls by the advancing flame gives rise to water droplets which lower the flame temperature in the course of being volatilised. Thus mixtures just able to propagate flame in the absence of foam are no longer able to do so in its presence and the limits of flammability are narrowed. With decreasing expansion ratio, the bubble walls become thicker and hence the water droplets formed become larger. So long as the droplets remain small enough to be vaporised completely during their passage through the advancing flame, this increase in size will cause increasing suppression of the limits as is observed in Region (1).

In Region (2) it appears that with increasing wetness (decrease of R) the size of droplets formed is rapidly increasing and ultimately droplet formation associated with the foam rupture ceases to be recognisable. In these circumstances the cooling effect of the foam, which is primarily exerted through droplet formation, has become much decreased and the limits are widened.

Finally, in Region (3), the energy required to break through the bubble walls, which increases continually with decreasing expansion ratio, becomes great enough to take significant toll of the energy available from the burning mixture and the limits converge to final suppression. In this region the situation is complicated a little by the fact that flame propagation does not occur uniformly through the foam. It seems likely that the flame makes its way through slightly less wet parts of the foam with the result that the remaining parts become somewhat wetter, through the relegation of foam debris, and so remain unburnt.

Throughout regions (1) and (2) in which droplet formation, or the lack of it, is the controlling factor, an effect of bubble size (d) is superimposed upon the effect of expansion ratio (R). Thus with smaller bubble size (i.e. thinner bubble walls for a given expansion ratio) smaller droplets are formed and the suppression effect is greater. In fact, if limits are plotted upon a basis of R/d in these regions the curves superimpose fairly well for the range of bubble size examined.

References.

- (1) H.F. Coward and J.J. Gleadall, J.Chem. Soc. 1950, 243-8
Extinction of methane flames by water vapour.
- (2) J.S. Yeaw and L. Shnidman. Proc. Am. Gas Assoc. 1958, 20,
717-45.
Extinction of gas flames by steam.
- (3) H. Billett, vide B.P. Mullins & S.S. Penner. "Explosions,
Detonations, Flammability and Ignition".
Pergamon Press, 1959, pp. 247-9.

TABLE

Selected values of lower and upper flammability limits (vol.-%) methane in air in foam of varying expansion ratio, but approximately constant bubble diameter = 1.5 - 1.8 mm.

Expansion ratio	Lower limit	Expansion ratio	Upper limit
38.5	7.87	37.8	11.55
53.3	7.50	49.1	11.93
82.6	7.29	79.3	11.94
130	7.44	126	11.68
189	8.24	179	10.57
217	8.77	262	9.66
279	9.43	280	9.50
321	9.35	325	9.68
438	9.04	436	9.92
598	8.72	586	10.86
692	7.56	701	11.19
878	7.48		
∞ (dry)	5.41	∞ (dry)	13.94

THERMOGRAVIMETRIC AND DIFFERENTIAL THERMAL ANALYSIS
OF WOOD AND OF WOOD TREATED WITH INORGANIC SALTS
DURING PYROLYSIS¹

A Progress Report

by Frederick L. Browne, chemist
and Walter K. Tang, chemical engineer

Forest Products Laboratory, Forest Service, U.S. Department of Agriculture²

Burning of wood is preceded by pyrolysis to form gases and vapors and a solid residue of charcoal; some of the gases and vapors can burn in flames when mixed with air, and the charcoal can burn in air by glowing without flame. Empirically it has long been known that flaming combustion can be retarded by impregnating wood with suitable materials, such as certain inorganic salts. Although a number of theories of flame-retardant action have been proposed (6),³ the mechanism of wood's combustion and the effect of chemical treatment on it remain uncertain. It appears most likely that the best flame retardants act by altering favorably the preliminary step of wood pyrolysis.

The present research was undertaken to study the mechanism of wood pyrolysis and the effect of chemicals on it by the methods of thermogravimetric and of differential thermal analysis. Results so far indicate that the methods are promising but that much further work will be needed before their significance can be fully established.

In dynamic thermogravimetric analysis, wood samples were weighed and the weight recorded continuously and automatically as a function of the temperature attained by the sample while it was being heated in a stream of nitrogen with the temperature rising steadily at a linear rate. Such graphs disclosed the threshold temperature for active pyrolysis, the range of temperature within which most of the pyrolysis occurred, and the yield of char (or extent of volatilization) when pyrolysis was practically completed.

In static thermogravimetric analysis, the sample weight was recorded as a function of time at constant temperature at each of a series of temperatures from about the threshold for active pyrolysis to a temperature at which pyrolysis became inconveniently

¹The work here reported was financed in part by a grant from the National Science Foundation and in cooperation with the Koppers Company, Pittsburgh, Pa.

²Maintained at Madison, Wisconsin, in cooperation with the University of Wisconsin.

³Numbers in parentheses refer to literature cited at the end of this report.

rapid. Such graphs served as a basis for calculating reaction rate constants and activation energies for an early stage of pyrolysis. In differential thermal analysis the difference in temperature between wood or treated wood and a reference material was recorded continuously as a function of the sample temperature while both sample and reference material were being heated with the furnace temperature rising steadily at a linear rate. Such graphs revealed the occurrence of endothermic or exothermic reactions at the various levels of temperature and a rough estimate of the relative extent of evolution or absorption of heat.

Apparatus

A thermogravimetric balance made by the American Instrument Company was used (2). The sample to be pyrolyzed was suspended from a calibrated spring, all within a glass enclosure that could either be evacuated or supplied with a gas flowing at a controlled rate. The lower portion of the glass enclosure, the reaction chamber, could be quickly encompassed by an electric furnace that was either preheated to a desired constant temperature or else was programmed to rise in temperature at a predetermined linear rate. Movement of the balance spring was picked up by a transducer and demodulator and the impulse transmitted to the y-axis of an x-y recorder. The x-axis could be set to record the temperature attained by the sample as measured by a thermocouple located about 5 millimeters below the sample in the reaction chamber; or, by the flick of a switch, the x-axis could be set to record time instead of temperature. When the x-axis was set to record temperature, there was provision also for a discontinuous record of time in the form of pips scribed in the curve at intervals of 1, 5, or 20 minutes.

By a simple modification, the thermogravimetric balance was adapted for differential thermal analysis. A switch was provided to disconnect the impulse from the transducer and demodulator of the weighing system and to substitute for it the input from a differential thermocouple with one junction in the sample and the other junction in a reference material. Sample and reference material were contained each in its own glass tube with stopper carrying a thermocouple well and inlet and outlet tubes through which either vacuum or a stream of nitrogen could be applied. The nitrogen entered the tube through a glass sleeve at a point slightly above the level of the sample or reference material and discharged, together with any volatile products, from the top of the tube. Sample tube and reference tube slipped into wells drilled in a metal cylinder, which in turn fitted into the cylindrical chamber of the electric furnace of the thermogravimetric balance, now become a differential thermal balance.

Preparation of Samples

The size and shape of wood samples may affect the rate of pyrolysis and the yield of products because the diffusion of heat into the interior of the sample and the escape of volatile products from the interior enter into the overall process. Within thick samples the temperature at any instant varies more than in thin samples; the yield of char is greater for thick than for thin samples because volatile products formed at first undergo secondary pyrolysis, yielding tar coke to add to the wood charcoal if the volatile

products cannot escape fast enough. When delayed escape of volatile products is significant, pyrolysis in vacuum proceeds faster and yields less char than pyrolysis at atmospheric pressure.

Since the present purpose was to study as nearly the initial stage in pyrolysis as possible, it was necessary to minimize the effects of diffusion of heat and volatile products. Use of veneer (shavings) 0.16 millimeter thick, cut from green or re-soaked wood with a tool designed especially for the purpose, accomplished the objective remarkably well. This is demonstrated in figure 1, in which the curve for dynamic thermogravimetric analysis in nitrogen at atmospheric pressure nearly coincided with a curve for pyrolysis in a vacuum. Similar experiments with samples in the form of dowels about 1 centimeter in diameter showed that in nitrogen the pyrolysis proceeded much less rapidly and the yield of char at the end of active pyrolysis was much greater than in vacuum.

Ponderosa pine sapwood samples 0.16 by 46 by 47 mm. have been used for most of the tests so far. Samples were conditioned at 27° C. and 30 percent relative humidity. Those to be impregnated with a salt were immersed in aqueous solution of suitable concentration to provide the desired degree of treatment, evacuated for 30 minutes, left immersed at atmospheric pressure for approximately 2 hours, removed, wiped to remove excess solution, dried, and conditioned at 27° C. and 30 percent relative humidity. The quantity of salt retained by the wood was calculated as the difference between the equilibrium weights before and after treatment corrected for a loss of approximately 1.5 percent of water-soluble components of the wood to the treating solution, as determined by similarly impregnating matched wood specimens with distilled water and reconditioning them.

For differential thermal analysis, ponderosa pine sapwood was ground to particles less than 0.25 mm. in diameter. Samples to be treated were placed on a glass filter, repeatedly washed with aqueous solution with the aid of suction, drained with suction for about 30 minutes, dried, and conditioned at 27° C. and 30 percent relative humidity.

Inorganic Salts Tested

Tests have been made so far with the inorganic salts listed in table I, together with the residual weight left at 200°, 250°, and 400° C., respectively, when a sample of the salt was subjected to dynamic thermogravimetric analysis under the conditions described farther on for examination of wood treated with the salt.

Data in handbooks state that those of the salts that contain water of crystallization lose it before the temperature reaches 200° C. The ammonium phosphates and ammonium chloride begin to decompose before they reach a melting point. Ammonium sulfamate melts at 132.9° C. and begins to decompose to ammonia and sulfamic acid at 160° C. Ammonium sulfamate and ammonium chloride are distinctly volatile and sublime completely at temperatures well below 400° C. Ammonium chloride changes from the α to the β form with a heat effect at 184° C. The four remaining salts do not melt, decompose, or sublime before reaching temperatures at which active pyrolysis of wood has been completed.

sapwood veneer 0.16 mm. thick. The lignin was sulfuric acid lignin from aspen in the form of fine powder. The α -cellulose was from southern yellow pine in the form of a thin felted mass. The differences in origin and form of the samples do not impair qualitative comparison of the three materials in view of the great differences in the course of their pyrolyses.

The loss in weight of 5 percent for cellulose and of 6 percent for wood and lignin recorded at 200° C. in figure 2 had actually been attained already at 100° C. and represented moisture in the samples initially. Further loss in weight attributable to pyrolysis began near 220° C. for both wood and lignin, but not until 275° C. for cellulose. On the other hand, pyrolysis of cellulose proceeded very rapidly as temperature rose still further, whereas the pyrolysis of lignin accelerated very slowly. Cellulose pyrolysis was essentially complete at 400° C. with a yield of char of only 15 percent, which decreased to 9 percent at 800° C. Lignin at 400° C. still was 70 percent unvaporized and, at 800° C., was 45 percent unvaporized.

The relatively sudden collapse of cellulose within a narrow range of temperature and the slower disintegration of lignin over a broad band of temperature perhaps are explicable from the nature of their macromolecules. Cellulose, as a repeating polymer of a single monomer of moderate size, may well follow a shorter and less involved path to complete pyrolysis than the more intricate macromolecule of lignin with its more varied constitution of aromatic nuclei connected by straight-chain links. The indication that the threshold temperature of pyrolysis is lower for lignin than for cellulose seems at first to conflict with much of the literature (6), which holds that the hemicellulose in wood pyrolyzes most readily, the cellulose less so, and the lignin least readily; but the apparent conflict is easily reconciled, because only a small fraction of the lignin has been lost at temperatures at which the cellulose is already completely pyrolyzed.

Figures 3 and 4 present similar thermogravimetric curves for ponderosa pine treated with all the salts listed in table 1 except monobasic ammonium phosphate, which is omitted from the figures because its performance was almost identical with that of dibasic ammonium phosphate. When the salts contained water of crystallization, the initial loss in weight before 200° C. was increased correspondingly. If the curves were adjusted to start from the anhydrous weight as 100 percent, the curves for wood treated with sodium borate and sodium phosphate would as nearly coincide with the curve for untreated wood up to 300° to 350° C. as the curve for treatment with sodium chloride actually does. On the other hand, the curves for the three ammonium salts and for potassium carbonate reveal distinctly faster pyrolysis than that of untreated wood in a region between approximately 200° and 300° C.

Beyond about 350° C. the weight of char from wood treated with any one of the salts exceeded the weight of char from untreated wood. The char from some but not all of the treated samples still contained the injected salt or products of its decomposition. To learn the yield of wood charcoal on completion of active pyrolysis of the treated samples, correction must be made for any inorganic residue in the char. Such residue at any temperature up to 400° C. was estimated by thermogravimetric analysis of each salt by itself. The procedure involves the assumption that the salt loses weight at the same rate and to the same extent in the presence as in the absence of actively pyrolyzing wood, an assumption that may require more careful examination at a later stage in the research.

Hunt, Truax, and Harrison (8), on the basis of laboratory tests by the fire-tube method, described the salts marked I in the last column of table 1 as "chemicals that have a considerable effect in retarding flame in light absorptions and a marked effect in heavy absorptions." They did not test ammonium sulfamate, but subsequent tests at the Forest Products Laboratory place it in group I. Salts of group II were described as "chemicals that have a very minor effect in retarding flame in light absorptions but a marked effect in heavier absorptions," salts of group III as "chemicals that have a moderate effect in retarding flame when present in wood in large quantities" and salts of group IV as "chemicals that have a noticeable but not important effect in retarding flame even when present in wood in large amounts."

Experimental Procedure

For thermogravimetric analysis, a sample of 0.16-mm. veneer weighing between 0.25 and 0.5 gram was suspended from the balance spring in a central position in the pyrolysis chamber. The y-axis of the recorder was so calibrated that the full weight of the sample just spanned 100 divisions of the graph paper and the x-axis was set to span the range in sample temperature to be studied. The system was evacuated and then flushed with nitrogen three times to remove air with its oxygen from the sample and the pyrolysis chamber.

For dynamic thermogravimetry the furnace, still unheated, was raised into position enclosing the pyrolysis chamber, heating was started at the programmed linear rate (usually 6° C. a minute), flow of nitrogen through the system was established at the desired rate (usually 2 liters a minute), and the recording mechanism was set in motion. The recorder scribed the decrease in sample weight in percent of its initial weight against the temperature attained by the sample and also indicated the lapse of time by pips scribed at 5-minute intervals.

For static thermogravimetry the furnace was brought to a constant temperature selected in advance and was then raised to enclose the pyrolysis chamber. The recorder was set in motion when the furnace reached its position with the x-axis of the recorder charting sample temperature together with 1-minute pips until the constant furnace temperature was nearly reached (usually in 13 to 15 minutes), after which the x-axis was switched to record time instead of temperature.

For differential thermal analysis the sample tube was packed with about 5 g. of ground wood and the reference tube was packed to an equal depth with aluminum oxide. Alternatively, for certain tests the sample tube contained chemically treated wood and the reference tube untreated but otherwise similar wood. With tubes in position, the furnace was set to rise in temperature at the rate of 12° C. a minute until it reached 600° C. The recorder charted the difference in temperature between sample and reference material against the temperature attained by the sample.

Results by Dynamic Thermogravimetry

Figure 2 records the portion of the dynamic thermogravimetric curves between 130° and 400° C. obtained for wood, lignin, and α -cellulose. The wood was ponderosa pine

From the yield of char as indicated by the curve in figure 3 or 4, corrected for the content of salt or its decomposition product, and from the content of dry wood easily calculable from the weight at 150° C., the extent of volatilization of the dry wood substance originally present in the sample was calculated for sample temperatures of 250° and 400° C. and is recorded in table 2, together with the temperature at which active pyrolysis began, the content of anhydrous salt in the sample before pyrolyzing, and the practical classification of the salt for flame retardance.

Untreated wood began to pyrolyze actively at 220° C., was volatilized at 250° C. to the extent of 4 percent only, but at 400° C. volatilization attained 76 percent. Wood treated with one of the ammonium salts began to pyrolyze at much lower temperatures, 150° or 180° C., was much more extensively volatilized than untreated wood at 250° C., but was much less extensively volatilized than untreated wood when active pyrolysis was essentially completed at 400° C. Treatment with potassium carbonate advanced the onset of wood pyrolysis slightly (to 210° C.), increased volatilization of wood at 250° C. significantly, but somewhat less than the ammonium salts, but did not diminish the volatilization of wood at 400° C. so much as the ammonium salts did. The three sodium salts failed to alter the temperature at which wood pyrolysis began and increased the volatilization of wood at 250° C. little if at all. At 400° C., however, sodium tetraborate restricted volatilization of wood about as much as the ammonium salts did, whereas sodium phosphate and sodium chloride permitted nearly as much volatilization of wood as occurred with untreated wood.

Apparently, the extent to which a salt might lower the temperature at which pyrolysis began depended on the nature of the salt but not, within wide limits, on the quantity of salt in the wood. On the other hand, those salts that increased volatilization of wood at 250° C. seemed to effect greater increase the greater the concentration of the salt. The salts that are highly effective flame retardants seemed to decrease the volatilization of wood at 400° C. to a greater extent the higher the concentration in the wood before heating, even though some of them, such as ammonium sulfamate and ammonium chloride, had been driven off completely before the temperature reached 400° C.

Sodium tetraborate differed from the other salts of group I for flame retardance in that it failed to lower the temperature at which pyrolysis began or to increase the volatilization of wood at 250° C. Sodium borate did, however, decrease the volatilization of wood significantly at 400° C.

Results by Static Thermogravimetry

The effort to study the kinetics of wood pyrolysis by static thermogravimetry presented problems that have not yet been solved satisfactorily.

The pyrolysis of wood usually has been considered amenable to treatment as a pseudo first-order reaction (1, 3, 5, 11, 17). The rate of loss in weight was therefore recorded at each of a succession of temperatures not too far above the threshold temperature for active pyrolysis, and the logarithm of the as yet unvolatilized fraction of the wood ultimately volatilized at the given temperature was plotted against the time since heating began. The weight loss of as much as 35 percent during the period of some 15 minutes required for the sample to attain the constant furnace temperature had to be ignored. Beyond this point, the charts took the form of straight lines from the slopes

of which velocity constant for each temperature was calculated. The slope of plots of the logarithm of the velocity constants against the reciprocal of the absolute temperature, which proved linear, yielded the activation energies given in table 3.

Results by Differential Thermal Analysis

Curves for differential thermal analysis of wood, α -cellulose, and lignin made with aluminum oxide for reference, are given in figure 5. All three substances presented endothermic nadirs at 130° C. that came chiefly from dehydration. Near 250° C. the curves entered the exothermic region. Lignin then showed a marked exothermic peak at 415° C. whereas cellulose, after reaching a very feeble exothermic peak at 310° C., fell rapidly to a sharp endothermic nadir at 350° C. succeeded by a strong exothermic peak at 470° C. Schwenker (16) observed a weak exothermic peak at 328° C. and a strong endothermic nadir at 372° C. for cotton fabric (alkali-scoured) but no appreciable temperature differential between 400° and 500° C. Both Schwenker (16) and Keylwerth and Christoph (9) found that the weak exothermic peak at 310° C. became strongly exothermic when the pyrolysis took place in air.

The curve for wood revealed the influence of both lignin and cellulose in that the sharp nadir in cellulose at 350° C., which was completely lacking in lignin, in wood became a valley between exothermic peaks at 340° and 440° C. Kollmann (10) and Tang (18) observed this valley in experiments in which the rate of rise in temperature at the center of a "thick" piece of wood was observed while the piece was being heated in a furnace at constant temperature. Keylwerth and Christoph gave the designations β_1 and β_2 to the peaks at 340° and 440° C., respectively.

Comparison of the thermogravimetric with the differential thermal data shows that, with lignin, loss in weight due to active pyrolysis began when the reaction became exothermic and proceeded fastest in the most strongly exothermic region. Weight loss of cellulose began in the feebly exothermic region about 310° C., but most of the weight loss occurred in the endothermic region, with its nadir at 350° C. With wood, nearly all of the loss in weight took place in the exothermic region preceding the valley between the β_1 and β_2 peaks; beyond the valley there was little further weight loss, despite a more strongly exothermic condition, until the peak at 440° C. was passed.

Figure 6 presents differential thermal analyses of wood treated with salts against untreated wood as the reference material in order to reveal the effect of the salts on the absorption or evolution of heat in the various regions of temperature. Figures 7 and 8 present the differential thermal analyses for untreated wood and for wood treated with the salts when the reference material is inert aluminum oxide, together with the corresponding thermogravimetric analyses.

Salts that contained water of crystallization caused an endothermic nadir at about 150° C. (fig. 6). (The small nadir at 150° C. for sodium chloride may be due to a slight increase in moisture in the treated wood, as can be observed in figure 4.) The three ammonium salts showed a common nadir near 220° C. that possibly was due to dissociation of ammonia and its possible reaction with wood. Decomposition of the ammonium phosphate to the pyro- and metaphosphates and decomposition and sublimation of ammonium sulfamate and ammonium chloride may account for most of the heat

effects between 220° and 450° C. Presumably ammonium sulfamate and ammonium chloride are volatilized completely before 400° C. The sodium and potassium salts, after their water of crystallization is lost, are believed to remain undecomposed and nonvolatile up to temperatures well beyond the present interest. All of the salts, however, exhibited an exothermic peak somewhere between 325° and 385° C.

Comparison of figures 6 and 8 shows that the three ammonium salts exerted a predominantly endothermic effect in the zone of temperature within which nearly all of the volatilization of wood took place. They also suppressed the exothermic peak β_1 of untreated wood or, in the case of ammonium phosphate, perhaps shifted it from 340° to 285° C. and shifted the β_2 peak from 440° to about 400° C. One is tempted to attribute the effectiveness of the three ammonium salts to these characteristics, which were not shared by such ineffective salts as sodium phosphate and sodium chloride. It must be recognized, however, that the characteristics in question were not exhibited by the effective flame retardant, sodium borate, or the somewhat effective retardant, potassium carbonate. All of the sodium and potassium salts exerted a predominantly exothermic effect in the region of chief volatilization of wood, made the β_1 peak more strikingly exothermic, and left the β_2 peak relatively unaltered.

Conclusions

The methods of dynamic thermogravimetric analysis and differential thermal analysis offer promise of contributing significantly to study of the mechanism of wood pyrolysis and the action of chemical treatments on it. The possible use of static thermogravimetric analysis to study the kinetics of the reactions seems to present greater difficulty.

The threshold temperature for active pyrolysis of lignin and of wood was found near 220° C., whereas that of α -cellulose was near 275° C. In each case the threshold temperature occurred soon after an endothermic region of the pyrolysis yielded to a definite exothermic trend. Once started, however, the collapse of cellulose was rapid, was essentially complete before 400° C., left little char, and was associated with a marked endothermic nadir. Lignin, on the other hand, lost weight slowly, losing only one-fourth its weight by the time 400° C. was reached and only half at 800° C., and the pyrolysis appeared to be steadily exothermic. Wood exhibited the effects of its two chief constituents; the pyrolysis showed exothermic peaks at 340° and 440° C., with a valley between them that was due to the endothermic region of the cellulose.

The inorganic salts tested so far fall into three groups according to the effects they exhibited.

(1) Two ammonium phosphates, ammonium sulfamate, and ammonium chloride lowered the threshold temperature for active pyrolysis, markedly accelerated loss in weight between the threshold temperature and 250° C., exerted a markedly endothermic effect through the region of temperature in which most of the loss in weight of wood occurred, and kept to a minimum the amount of wood volatilized when pyrolysis was essentially complete at 400° C. These ammonium salts are recognized as highly effective flame retardants.

(2) Two salts of limited or negligible effectiveness as flame retardants, trisodium phosphate and sodium chloride, failed to lower the threshold temperature for active pyrolysis or to increase the volatilization of wood up to 250° C. very much, exerted a predominantly exothermic effect in the region of temperature in which most weight loss occurred, and allowed nearly as much wood to volatilize when pyrolysis was complete as was the case with untreated wood.

(3) The highly effective flame retardant, sodium tetraborate, behaved like the ineffective salts of the second group in the region of temperature up to 250° C. It resembled the effective salts of the first group, however, in holding down the extent of volatilization of wood when pyrolysis was complete at 400° C. Potassium carbonate, which is considered a moderately effective flame retardant, proved less effective than sodium tetraborate in reducing the extent of volatilization at 400° C. but showed a slight ability to stimulate volatilization of wood below 250° C. and to advance the threshold temperature of active pyrolysis.

A more extensive study of chemical treatments is needed before decisions can be reached but it may be mentioned that the salts of the first group are formed between a weak base and a strong acid, those of the second group between a strong base and a strong acid, and those of the third group between a strong base and a weak acid. It has been suggested repeatedly (4, 12, 13) that good flame retardants are likely to be substances that readily decompose to form a strong acid or to form a strong base. No doubt the mechanism of action may differ according as the effective reagent is an acid or a base (7, 14, 15).

References

1. Akita, Kazuo, Report of Fire Research Institute of Japan, vol. 9, no. 1-2, (1959).
2. American Instrument Company, Aminco Laboratory News, 16(3):5, 6 (1960).
3. Bamford, C. H., Crank, J., and Malan, D. H., Proc. Cambridge Phil. Soc. 42:166-82 (1946).
4. Bergström, Hilding, Jernkontorets Annaler 107:37-45, 309-50 (1923); 109:90-2 (1925).
5. Bowes, P. C., Fire Research Note No. 266, Department of Scientific and Industrial Research and Fire Offices' Commission, Joint Fire Research Organization (Great Britain) (1956).
6. Browne, F. L., Forest Products Laboratory Report No. 2136 (Dec. 1958).
7. Gottlieb, Irvin M., Textile Research Journal 26:156-68 (1956).
8. Hunt, G. M., Truax, T. R., and Harrison, C. A., Amer. Wood Preservers' Assoc. Proc. 28:71-93 (1932).
9. Keylwerth, R., and Christoph, N., Deut. Verband Materialprüfung, Materialprüf 2(8):281-328 (1960).

10. Kollmann, Franz, Holz als Roh- und Werkstoff 18(6):193-200 (1960).
11. Martin, S., Research and Development Technical Report, USNR DL-TR-102-NS081-001 (1956).
12. Metz, Ludwig, VDI-Verlag G.M.B.H., Berlin (1942).
13. Serebrennikov, P. P., Tzentralny Naouchno-Izslidovatel'ski Institut Lessnogo Khoziaistva Bulletin 2:43-66 (1934).
14. Schuyten, H. A., Weaver, J. W., and Reid, J. D., Advances in Chemistry Series No. 9, "Fire Retardant Paints" (1954); Ind. Eng. Chem. 47:1433-9 (1955).
15. Schwenker, R. F., Jr., and Pacsu, E., Ind. Eng. Chem. 50:91-6 (1958).
16. Schwenker, R. F., Jr., Paper No. 42, Division of Cellulose Chemistry, 138th National Meeting of the American Chemical Society, New York (Sept. 1960).
17. Stamm, A. J., Ind. Eng. Chem. 48:413-17 (1956).
18. Tang, Walter K., "Study of the Effect of Chemical Treatment on the Thermal Decomposition of Wood," Forest Products Laboratory Report (Aug. 1960).

Table 1. --Salts used to treat wood samples

Salt	Residual weight on dynamic thermogravimetric analysis			Classification for relative flame retardance
	at 200° C.	at 250° C.	at 400° C.	
	percent	percent	percent	
Dibasic ammonium phosphate, $(\text{NH}_4)_2\text{HPO}_4$	97	88	71	I
Monobasic ammonium phosphate, $(\text{NH}_4)\text{H}_2\text{PO}_4$	--	--	--	I
Ammonium sulfamate, $\text{NH}_4 \cdot \text{SO}_3 \cdot \text{NH}_2$	94	91.5	0	I
Ammonium chloride, NH_4Cl	99	95	0	I
Sodium tetraborate, $\text{Na}_2\text{B}_4\text{O}_7 \cdot 10\text{H}_2\text{O}$	52.8	52.8	52.8	I
Tribasic sodium phosphate, $\text{Na}_3\text{PO}_4 \cdot 12\text{H}_2\text{O}$	43.1	43.1	43.1	III
Potassium carbonate, $\text{K}_2\text{CO}_3 \cdot 1.5\text{H}_2\text{O}$	83.6	83.6	83.6	III
Sodium chloride, NaCl	100	100	100	IV

Table 2. --Dynamic thermogravimetric analysis of untreated wood and of wood treated with inorganic salts

Salt present in the wood	Content of anhydrous salt in sample	Temperature of onset of active pyrolysis	Extent of volatilization of wood in sample	Classification of salt for flame retardance
	percent	° C.	percent at 250° C. : percent at 400° C.	
None (untreated wood)	0	220	4 : 76	---
Dibasic ammonium phosphate	40.5	180	35 : 48	I
.....Do.....	11.1	180	21 : 50	I
.....Do.....	2.4	180	11 : 57	I
Ammonium sulfamate	23.4	180	45 : 42	I
.....Do.....	16.6	180	44 : 50	I
Ammonium chloride	29.8	150	52 : 54	I
.....Do.....	18.6	150	34 : 57	I
.....Do.....	9.0	150	22 : 60	I
Sodium tetraborate decahydrate	11.0	220	4 : 53	I
.....Do.....	1.0	220	2 : 57	I
Tribasic sodium phosphate dodecahydrate	37.6	220	15 : 73	III
.....Do.....	3.2	220	9 : 64	III
Potassium carbonate sesquihydrate	29.2	210	36 : 65	III
.....Do.....	18.6	210	29 : 60	III
.....Do.....	6.7	210	18 : 60	III
Sodium chloride	31.1	220	6 : 69	IV
.....Do.....	13.5	220	6 : 70	IV

Table 3. --Activation energies computed from static thermogravimetric analysis of untreated and treated wood

Salt present in wood	Content of anhydrous salt in sample	Activation energy
	percent	kilocalories/mole
None (untreated wood)	0	35.8
Dibasic ammonium phosphate	10.8	31.9
Monobasic ammonium phosphate	15.1	33.1
Ammonium sulfamate	15.7	34.0
Ammonium chloride ¹	17.7	8.1 (1st step) 34.8 (2nd step)
Sodium tetraborate decahydrate	17.4	24.7
Tribasic sodium phosphate dodecahydrate	18.0	29.3
Potassium carbonate sesquihydrate	20.0	25.4
Sodium chloride	12.0	33.0

¹Figure 4 shows that pyrolysis in the presence of ammonium chloride occurs in two steps, for each of which the activation energy was computed.

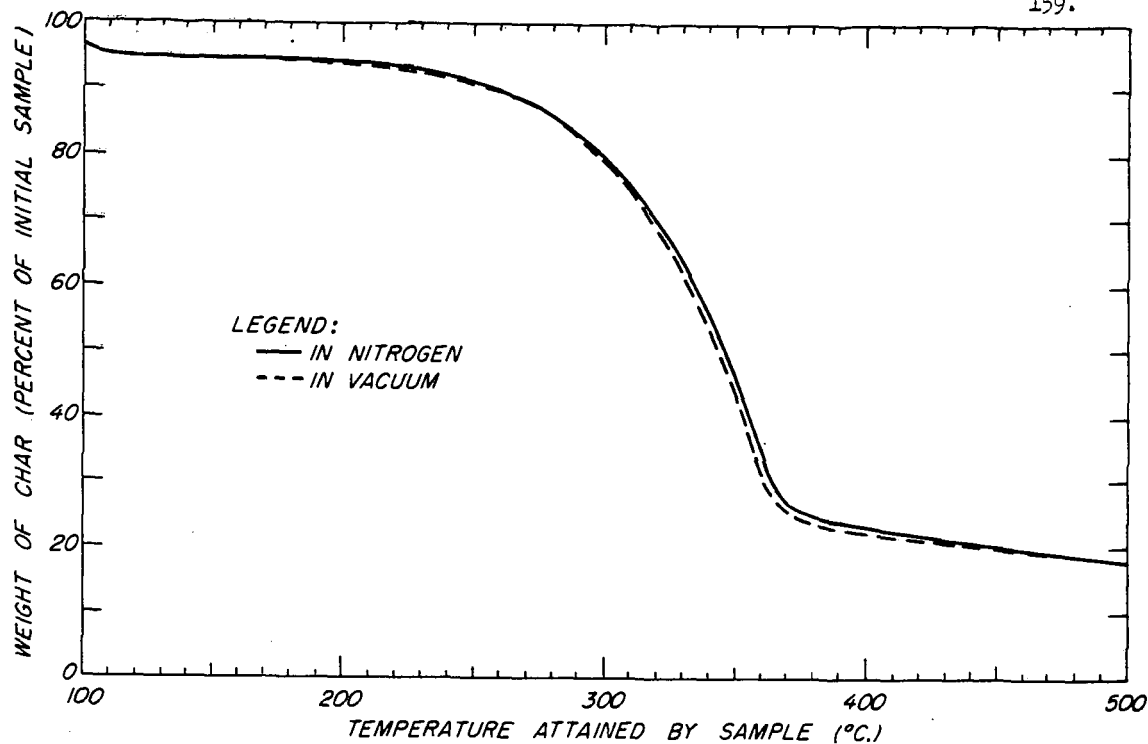


Figure 1.--Close agreement between curves for dynamic thermogravimetric analysis of thin veneer (0.16 mm thick) in nitrogen flowing at 2 liters a minute at atmospheric pressure and in vacuum of 10 Hg absolute.

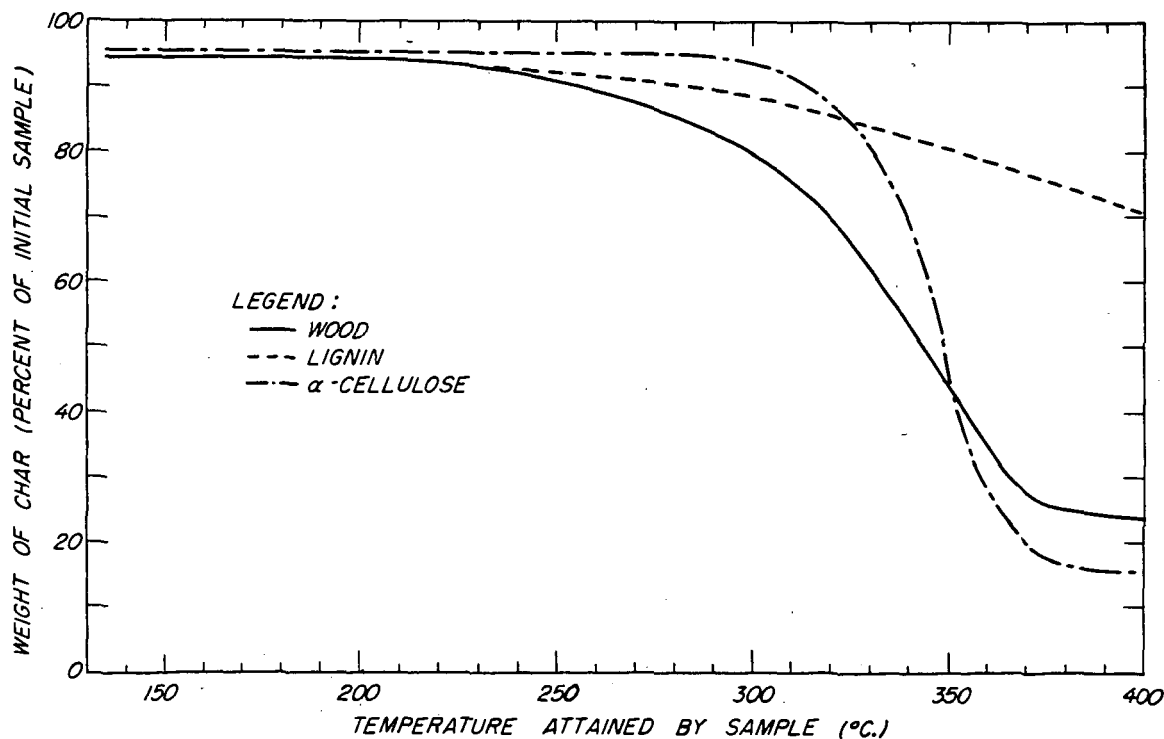


Figure 2.--Portion of dynamic thermogravimetric curves between 130° and 400° C., with temperature rising 6° a minute, for wood, lignin, and α -cellulose.

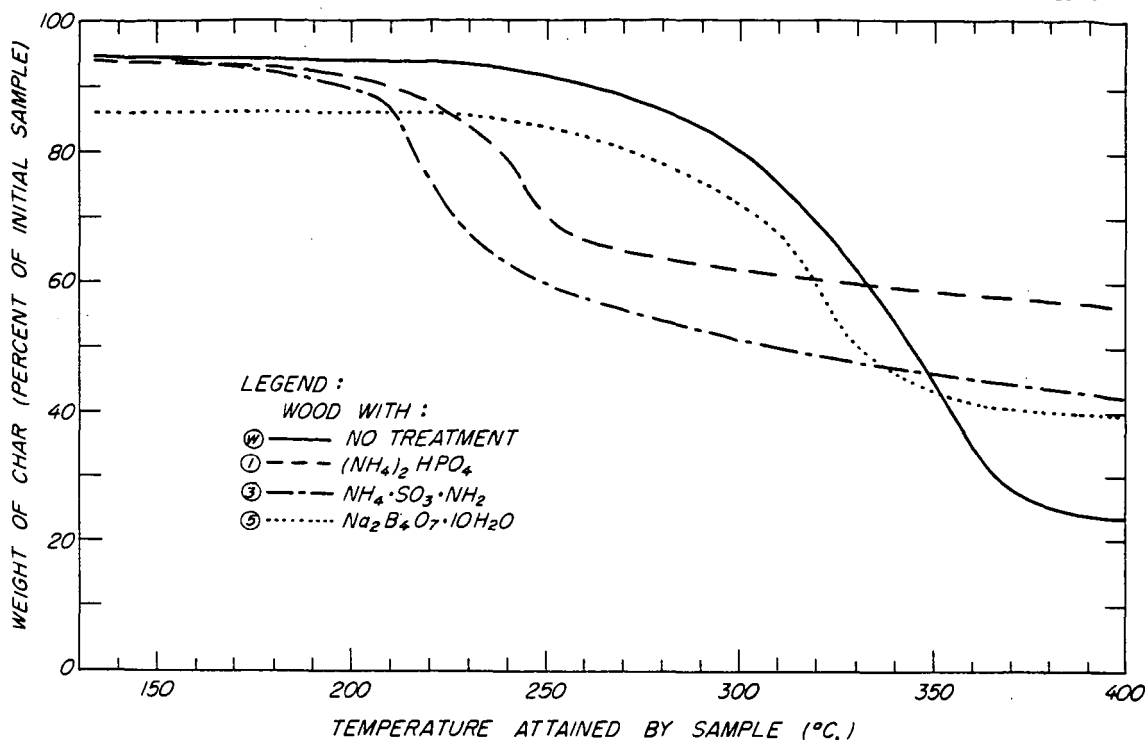


Figure 3. --Portion of dynamic thermogravimetric curves between 130° and 400° C., with temperature rising 6° a minute, for untreated wood and for wood treated with dibasic ammonium phosphate, ammonium sulfamate, or sodium tetraborate, respectively, at the maximum retention of salt indicated in table 2.

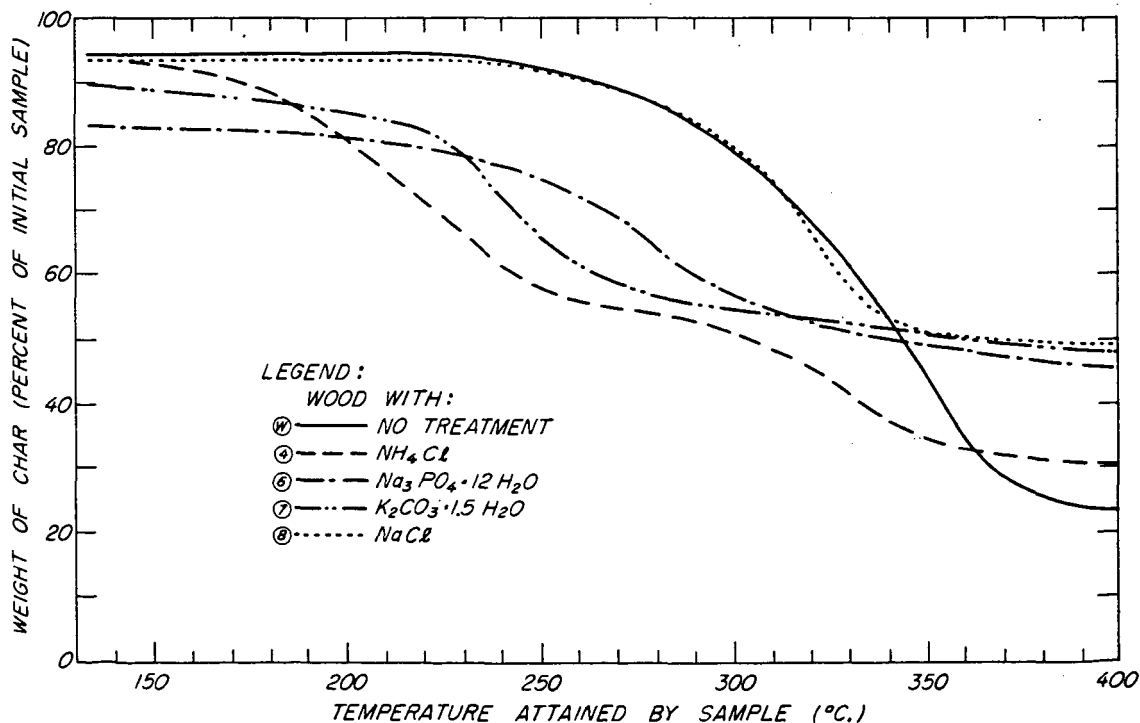


Figure 4. --Portion of dynamic thermogravimetric curves between 130° and 400° C., with temperature rising 6° a minute, for untreated wood and for wood treated with ammonium chloride, tribasic sodium phosphate dodecahydrate, potassium carbonate sesquihydrate, or sodium chloride, respectively, at the maximum retention of salt indicated in table 2.

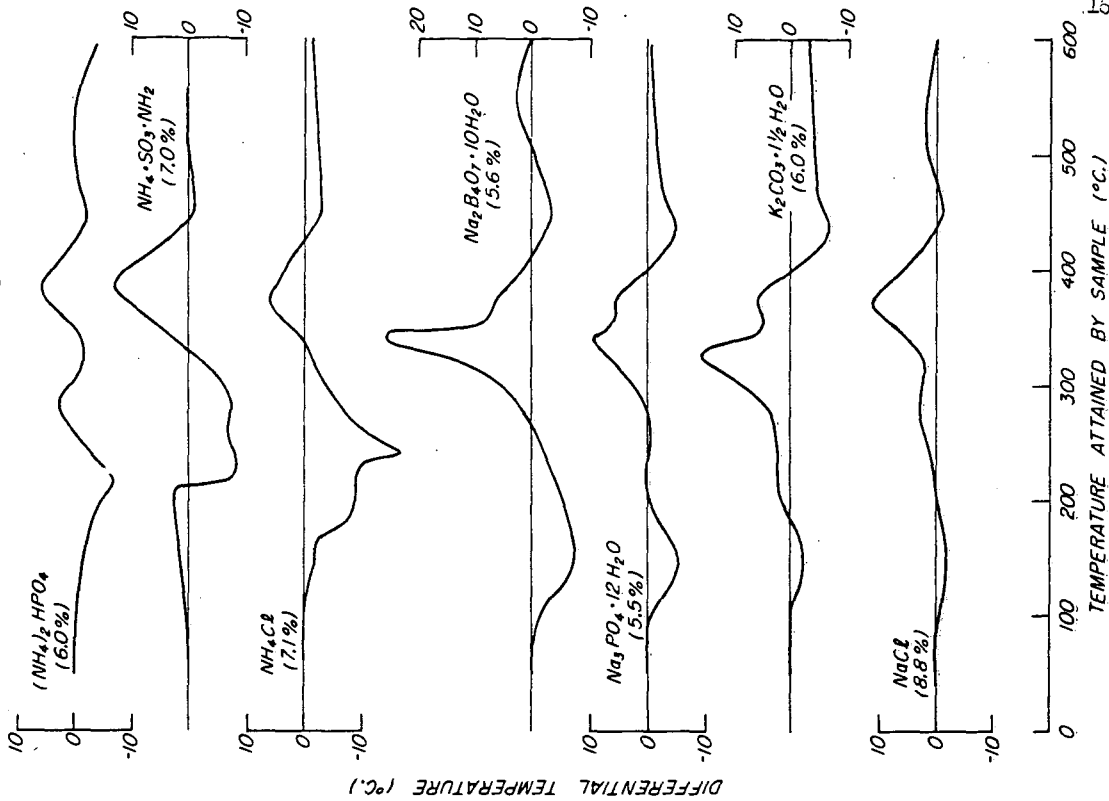


Figure 6. -- Differential thermal analyses of wood containing salts (at the concentration indicated within parentheses) with untreated wood used as the reference material.

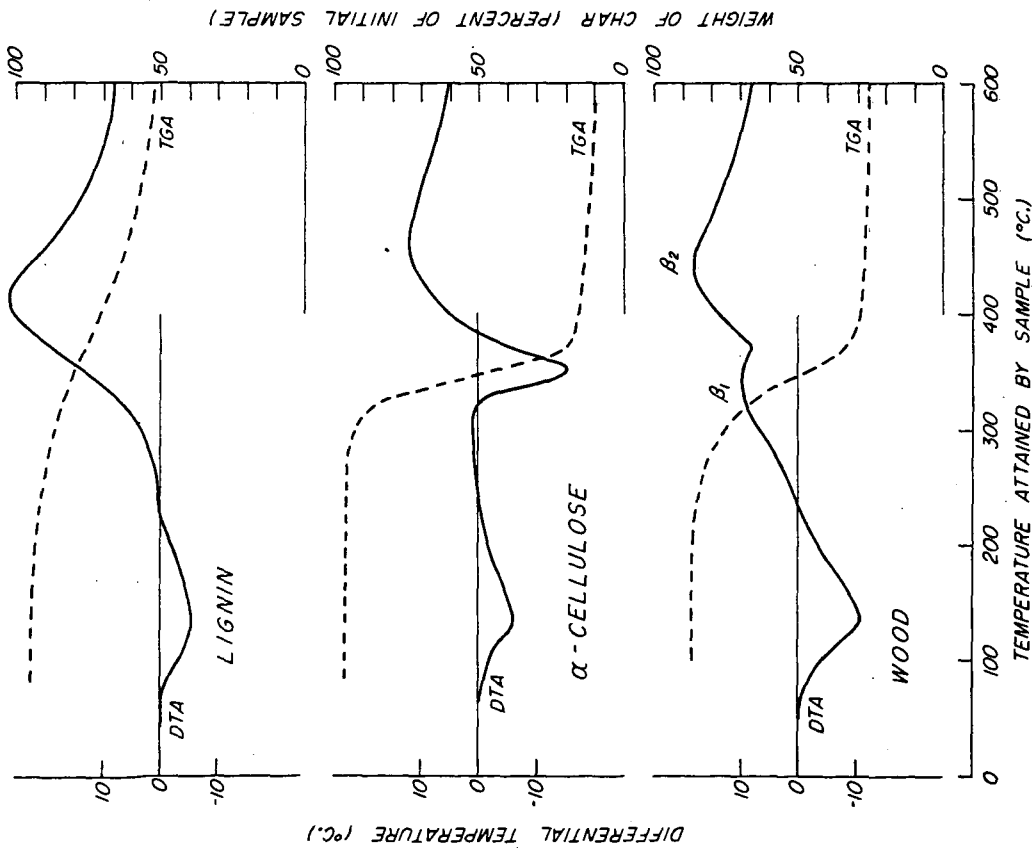


Figure 5. -- Curves for differential thermal analysis (DTA) of lignin, α -cellulose, and wood (solid lines, scales at left, reference material aluminum oxide) with the curves for dynamic thermogravimetric analysis (broken lines, scales at right) superimposed.

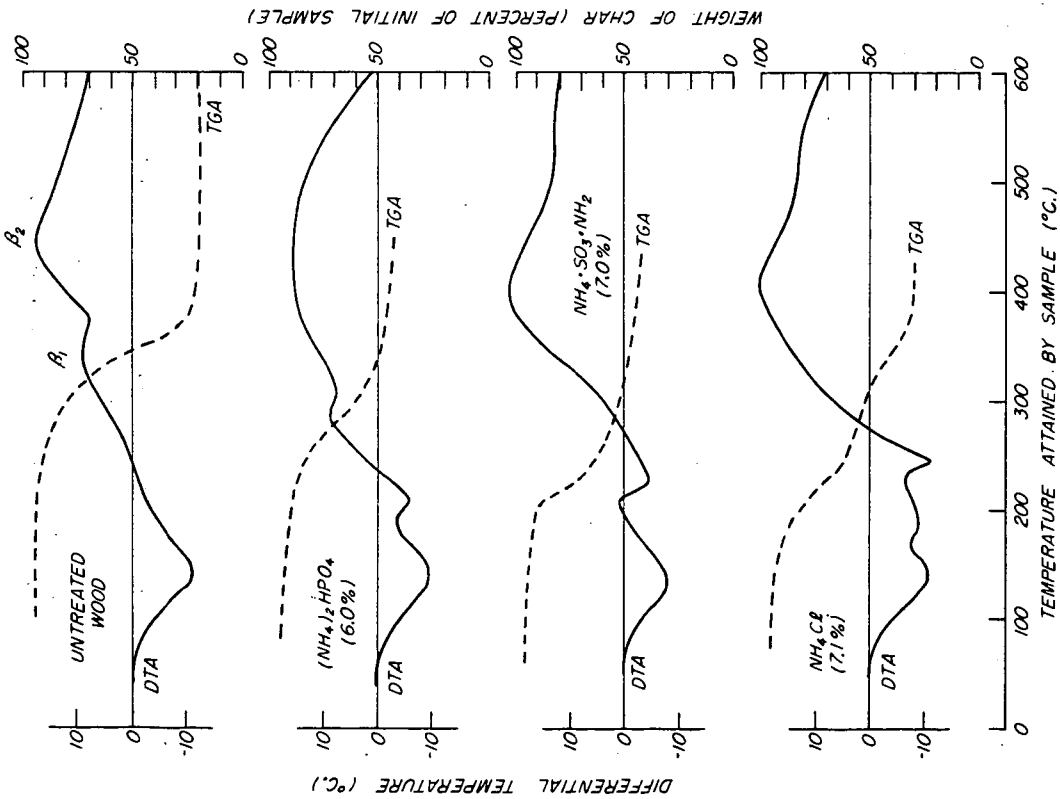


Figure 7. --Curves for differential thermal analysis (DTA) of untreated wood and of wood treated with salts that decompose thermally below 400° C. (solid lines, scales at left, reference material aluminum oxide) with curves for dynamic thermogravimetric analysis (TGA) superimposed (broken lines, scales at right).

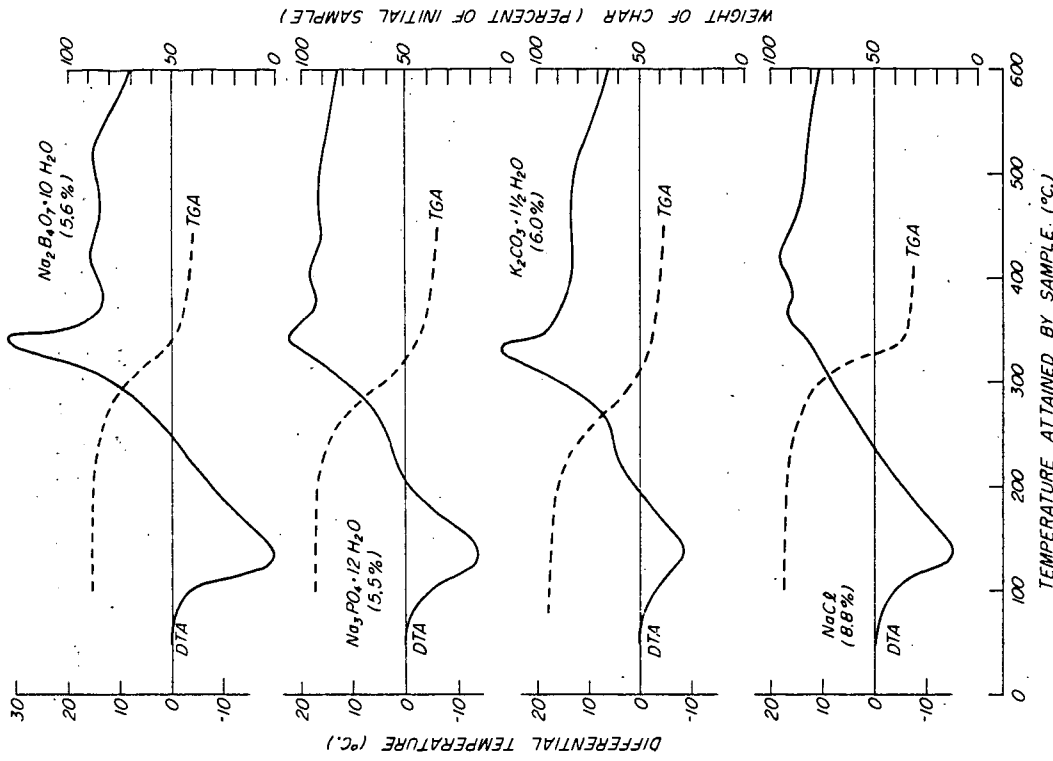


Figure 8. --Curves for differential thermal analysis (DTA) of wood treated with salts that, except for loss of water of crystallization, do not decompose below 400° C. (solid lines, scales at left, reference material aluminum oxide) with curves for dynamic thermogravimetric analysis (TGA) superimposed (broken lines, scales at right).

Effect of Potassium Bicarbonate on
the Ignition of Cellulose by Radiation

A. Broido

Forest Service—U. S. Department of Agriculture
Pacific Southwest Forest and Range Experiment Station
Berkeley 1, California

S. Martin

U. S. Naval Radiological Defense Laboratory
San Francisco 24, California

Introduction

Most combustion reactions of interest in the field of fire control involve cellulosic materials. For such materials the fire reactions may be considered as proceeding in essentially two steps—first, a pyrolysis of the solid phase which yields, among other things, combustible gaseous products and, second, a highly exothermic gas-phase oxidation reaction. Since most of the energy in the fire is produced in the gas-phase reactions (and incidentally, since simple gas-phase reactions lend themselves more readily to study), most research programs on fire extinguishment have considered primarily the gas-phase flame reactions.

Investigations into the action of flame extinguishing agents have established that, besides the obvious physical effects (cooling, smothering, etc.), a chemical effect, attributed to a chain-breaking reaction, also occurs in the gas phase. On the other hand, the possible chemical effect of the extinguishing agent on the pyrolysis reactions of the solid has frequently been overlooked in the fire extinguishing field (although such an effect forms the basis of the chemical theories of flame-proofing of wood and fabrics). However, fire extinguishment procedures generally attempt to bring the extinguishing agents in intimate contact with the solid fuel. Here the agents can affect pyrolysis to give gaseous products differing in kinds, amounts, proportions, or temperatures, and thus, so to speak, affect the gas-phase flame reactions before they occur. This possibility is strikingly illustrated by the observation that many of the highly recommended fire extinguishing materials, including potassium bicarbonate, can "catalyze" the combustion of carbohydrates (for example, make sugar cubes burn) (2).

The present report describes some of the results obtained in a series of experiments undertaken at the United States Naval Radiological Defense Laboratory (NRDL) to determine how impregnation of cellulose with small amounts of potassium bicarbonate alters the combustion characteristics of the material and the gaseous products evolved in the pyrolysis. Purified alpha-cellulose, in the form of specially prepared papers, had been in use for a number of years in studies of the thermal decomposition and ignition of cellulosic materials by thermal radiation (4, 6, 7), an important phase of the Laboratory's program investigating the effects of thermal radiation from nuclear detonations. Such papers had been selected for study in an attempt to insure reproducible results which could be of direct value in interpreting the behavior of heterogeneous, highly variable, natural fuels. The present experiments were undertaken when it became evident that the low ash content of these papers might give results which differed markedly from results obtained

with impure natural fuels and that indiscriminate application of fire-extinguishing and fire-proofing materials might lead to undesirable consequences.

Apparatus and Procedures

Test Materials

In 1953, the Forest Products Laboratory, Madison, Wisconsin, prepared, from a single batch of wood pulp, a series of alpha-cellulose papers (5) for use in the program of the Thermal Radiation Branch, Naval Radiological Defense Laboratory. These papers were made up in varying thicknesses and densities, and carbon black was added to some to provide a gradation in optical properties. The paper (No. 4095) chosen for the present experiments was made with 2.5% (dry weight basis) carbon black added to the pulp. The density of the dry paper was 0.67 g/cm^3 , its thickness was 0.54 mm, and its radiant absorptance for the spectral distribution of the radiant energy source was > 0.9 , as measured with a General Electric Model 8 PVI reflectometer.

Chemical analysis of this paper indicated an ash content of 0.15%, consisting largely of Ca, Mg, Na, Fe, and Si. As a result, it was decided that the minimum addition of KHCO_3 it would be profitable to investigate was 0.15%—doubling the ash content of the sample. To investigate the influence of more drastic changes in composition, a 10-fold increase—to 1.5%—was selected. Finally a few experiments were conducted with 15% KHCO_3 added to a limited number of samples.

Initial attempts were made to distribute the KHCO_3 throughout the cellulose by adding it in aqueous solutions. Because of the tendency of the paper to warp and swell when wet, this approach was abandoned in favor of one in which the KHCO_3 is produced within the cellulose by the neutralization of alcoholic KOH with moist CO_2 . With such a procedure no noticeable change in the appearance of the paper could be detected.

For the treatment, three solutions of KOH in anhydrous methanol were prepared—with concentrations 0.02 M, 0.2 M, and 2 M. The paper samples, $1\frac{1}{2}$ by $1\frac{3}{4}$ inches in size, weighed $0.63 \pm .02\text{g}$, so the treatment consisted of adding to each sample 0.5 ml of the appropriate solution from a repeating pipette and placing the samples immediately on racks in an atmosphere of CO_2 saturated with water vapor. The atmosphere was maintained by bubbling tank CO_2 through water and removing excess water from the stream by passing it through a cellulose filter. After an overnight exposure to the moist CO_2 atmosphere, the samples were mounted in standard holders and left exposed to the normal atmosphere until they were used.

In appearance, the treated samples were indistinguishable from the untreated samples, and no change in absorptance was detected with the reflectometer. Evidence that the treatment did indeed convert the KOH to KHCO_3 was obtained in two ways: (1) a number of samples were weighed before and after treatment, the weight changes being in accord with the stoichiometry, (2) the same samples were leached with a small amount of distilled water, and the pH of the resulting solution was compared with that of an aqueous KHCO_3 solution of the expected concentration. As a final check on the method of sample preparation, the effects of exposure to radiant energy were compared for a limited number of the samples treated with aqueous KHCO_3 solution and those treated with alcoholic KOH. The results showed only negligible differences between the two groups of samples.

Radiant Energy Source

For these experiments, samples were exposed to an intense beam of thermal radiation produced by means of a high current carbon arc and a relay-condenser optical system. This source (1) can provide a maximum irradiance level of 30 calories per square centimeter per second, uniform over a circular area of three square

centimeters. The spectral distribution of the thermal output from the source, as operated, approximates that of a 5,500° K black body emitter. Attenuation of the whole beam to the desired irradiance level was accomplished using Libby-Owens-Ford "color-clear" plate glass, ground to produce a diffusing surface of appropriate attenuation. Exposures were made by means of a high speed square-wave shutter capable of providing exposures as short as 0.1 seconds reproducible to 0.01 seconds. The samples of test materials were individually mounted for exposure in brass shim-stock holders through which an accurately centered 3/4-inch diameter hole had been punched. A water-cooled aperture with a slotted guide received the holders and automatically aligned them into the focal spot.

Phenomena Observed

The effect observed when a particular cellulose sample is exposed to radiant energy depends upon both the irradiance and the time of exposure. At sufficiently high irradiance, the first ignition phenomenon observed is transient flaming—a flaming which terminates promptly at the end of the exposure. For somewhat longer exposures at a particular irradiance level in this range, sustained flaming occurs—the flaming extends beyond termination of the exposure and results in the nearly complete combustion of the sample. At somewhat lower irradiance levels, transient flaming never occurs; whenever the exposure is sufficiently long to permit initiation of flaming, it is always sustained. At still lower irradiance levels a sufficiently long exposure produces glowing ignition, and the sample may be consumed without the appearance of flame.

Analytical Procedures

The principal evidence concerning the influence of KHCO_3 on the combustion characteristics of cellulose was obtained from visual observation of the effects on exposed samples. However, to gain some insight into possible explanations for the observed results, a few comparative measurements were made of the quantities of the principal volatile pyrolysis products generated by treated and untreated samples exposed to the same thermal input.

At two irradiance levels and exposure times chosen on the basis of the ignition effects in air, first an untreated sample and then a sample impregnated with KHCO_3 were exposed in a helium atmosphere. The volatile products were swept by the helium carrier into a two-stage gas chromatography system (8). As a means of confirming the identity of the components, the effluent stream from the liquid-partition stage of the two-stage system was monitored by a Bendix time-of-flight mass spectrometer. A combination of the chromatographic retention time and the mass spectrum gives ample proof, in general, of the identity of each component.

Results and Discussion

Method of Quantification

The result observed when a single test sample is exposed to one specified pulse of thermal radiation is a "go - no go" phenomenon. That is, for a given irradiance, if the critical exposure time (threshold for a particular effect) is exceeded, the effect will occur (a success); if the critical time is not exceeded, no effect, or a different, lesser effect will be observed (a failure). To obtain an estimate of the critical value, then, a series of samples must be exposed to different values of the variate. From the results, an estimate of the critical value, usually defined as that value for which just half of all samples would exhibit the effect, that is, the LD_{50} in biological experimentation, may be obtained.

For a given sample population, the value of the estimate depends upon such factors as the variability in sensitivity of the samples in the population and the variability of the population as a whole with external factors—temperature, humidity, etc. For experiments with the present exposure apparatus, additional variability is

introduced as a result of uncertainties in the delivered dose. The source is not equipped for continuous monitoring. It is calibrated by mounting a calorimeter in the position at which samples will subsequently be exposed. However, the irradiance is not invariate with time. It has short time fluctuations (1-2% in seconds as the carbons rotate) and long time fluctuations (5-10% over several minutes as the carbons feed in and out or as voltage drifts). Thus, the method of estimating a critical value must take into account all such variations.

The procedure that has been adopted in determining the critical value for a single material is the so-called "up-and-down" method (3). In this method, fixed increments of the variate, in this case exposure time, are selected. The result of each exposure then determines the next time setting. If a "success" is obtained, the time is set down one increment; if a "failure", the time is increased. Neglecting a long series of steps in one direction as the critical value is first approached, the final estimate is obtained by simply averaging all subsequent exposure times.

For comparing two materials whose critical values differ only slightly, a modified up-and-down procedure was adopted and will be described in a future report. Samples of the two materials are exposed alternately in quick succession, the time setting being adjusted only if the same effect is observed for both samples. Such procedures permit the use of one material as a control to minimize the effect of any long time fluctuations.

Critical Values

The regions of occurrence of the various ignition phenomena for the pure No. 4095 paper are delineated by the curves in Fig. 1. These curves represent the composite results of a large number of experiments on this paper and extrapolations from results obtained with the similar papers of different density and thickness. As may be seen, there is a critical irradiance for the material—a level below which ignition will not occur no matter how long the exposure. For sustained ignition at the high irradiance levels, so-called reciprocity is approached, the effect occurring at approximately the same total exposure regardless of the irradiance level. More obvious from a logarithmic plot than from Fig. 1 is the fact that for pure alpha-cellulose papers of the type used in these experiments, the occurrence of transient flaming may be expressed by a constant product of the irradiance and the radiant exposure. The value of the constant is a function of the thermal conductivity, the density, and the heat capacity of the material. For the pure No. 4095 paper the relationship is given by

$$HQ = H^2 t = 59 \quad (1)$$

where H is the irradiance in $\text{cal cm}^{-2} \text{sec}^{-1}$

Q is the radiant exposure in cal cm^{-2}

t is the exposure time in sec

For determination of the influence of KHCO_3 impregnation, four irradiance levels were chosen: 11 and 18 $\text{cal cm}^{-2} \text{sec}^{-1}$, where both transient and sustained flaming are observed for the untreated material; 4.2 $\text{cal cm}^{-2} \text{sec}^{-1}$, where only sustained flaming is observed; and 1.4 $\text{cal cm}^{-2} \text{sec}^{-1}$, where only glowing ignition is observed. At each irradiance level, parallel "up-and-down" sequences were obtained by alternating untreated and treated papers. The average irradiance to be used for the treated material was estimated on the basis of the average exposure time for the untreated samples. The results are presented as the points in Fig. 1. For those points at which the effects observed differed from those observed at the same irradiance level for the untreated material, the actual effect observed for the treated material is also indicated in the figure.

Several interesting observations may be noted in Fig. 1. First, if only 0.15% KHCO_3 is added, the effects are the same as for the untreated materials at

all irradiance levels used. At the highest irradiance level, little difference in sensitivity is found between the treated and untreated materials. At the intermediate irradiance levels slightly more energy is necessary to produce a given effect in the treated material. However, at the low irradiance level the treated material is appreciably more sensitive.

Second, under no conditions attainable with this source was it possible to induce a sustained flaming in material treated with 1.5% KHCO_3 . Transient flaming did occur, at exposure times slightly longer than for the untreated material, but all sustained ignitions were of the glowing variety and all occurred at times appreciably less than those necessary to produce sustained ignition in the untreated material.

Third, only at the highest irradiance level was it possible to obtain a transient flame from the material impregnated with 15% KHCO_3 , except that a brief transient flaming, presumably as the gaseous products of pyrolysis were ignited by the radiant beam, could be produced at the $12 \text{ cal cm}^{-2} \text{ sec}^{-1}$ level at an exposure well beyond that necessary to produce the first glowing ignition. On the other hand, the times to produce a sustained ignition were always much lower for the treated material than for the untreated material, and the minimum irradiance level necessary to produce ignition was much less.

One final point should be made. The highest irradiance levels measured on conventional fires are always less than $2\text{-}3 \text{ cal cm}^{-2} \text{ sec}^{-1}$. Thus, the largest differences in sensitivity between treated and untreated materials occur in the region of greatest interest from the point of view of fire spread, with the treated material always the more sensitive.

Analysis of Volatile Pyrolysis Products

Summary of the gas chromatography-mass spectrometry results is given in Tables I and II. In addition to the weight loss during exposure in a helium atmosphere for an untreated 100 mg α -cellulose sample and for an equivalent sample impregnated with 2 mg KHCO_3 , each table gives the measured weights of various pyrolysis products and their relative ratios (the ratio of weights of the specific constituent divided by the ratio of total weight change). Table I gives results obtained after exposure to an irradiance of $4.2 \text{ cal cm}^{-2} \text{ sec}^{-1}$ for 2.5 sec (a time intermediate between those necessary to produce sustained ignition in air for the two materials). Table II gives similar results after exposure to an irradiance of $11 \text{ cal cm}^{-2} \text{ sec}^{-1}$ for 1.4 sec (a time somewhat more than the minimum necessary to produce sustained ignition in air for both materials).

Under conditions of these experiments, pyrolysis of cellulose gives a large number of products ranging from the low molecular weight gases to high molecular weight tarry materials. As may be seen from the tables, the volatile fraction (boiling point less than about 150°C) includes only about 25% of the weight loss from the untreated samples but about 50% of the weight loss from the treated samples. As might be expected, the increased sensitivity of the treated material to radiant exposure results in a more complete pyrolysis (that is, to a larger fraction of low molecular weight materials) for the same exposure conditions.

The volatile materials may be broken into two categories: gases (boiling points less than 0°C) and vapors (boiling point $0\text{-}150^\circ \text{C}$). For the untreated material, CO_2 and CO constitute $>98\%$ of the gas fraction. For the treated material, the CO_2 and CO components are still quite large, but the other, combustible, gases show a marked increase. Since the treated samples do not exhibit sustained flaming, while the untreated samples do, this result is more than mildly surprising.

The principal constituent of the vapors is H_2O , which for both treated and untreated samples makes up about 80% of the vapor fraction. About 90% of the

materials in the "Other Vapors" category in the tables have been identified. They include acetaldehyde, acrolein, acetone, biacetyl, crotonaldehyde, furan, methanol, and propionaldehyde. Here, too, some of the results are rather surprising. Although KHCO_3 treatment does not change the relative ratio of most of the vapors, several constituents, notably acetone and biacetyl are increased by an order of magnitude, or more.

The apparent contradiction between the ignition behavior of the treated and untreated materials in air and the pyrolysis results in helium, gave impetus to a detailed study of the temperature behavior of the samples during exposure. Such experiments have now begun. Although no conclusive results are yet available, it appears that under ignition conditions in air a treated sample will attain a lower temperature than will an untreated sample during an identical exposure, but that in helium the treated samples attain a somewhat higher temperature than the untreated samples.

Summary

As part of a program investigating the mechanisms of action of fire extinguishing agents, a study has been started on the influence of potassium bicarbonate additives on the ignition behavior of cellulosic materials. Pure α -cellulose papers and others to which varying amounts of KHCO_3 had been added were exposed in air to the intense radiation flux of a refocused carbon arc beam, and the ignition thresholds were determined at several irradiances. Several samples were then similarly exposed in a helium atmosphere, and the gases and vapors generated were passed through a gas chromatography-mass spectrometry analytical system.

From the results of this experimental work it is concluded that adding potassium bicarbonate to α -cellulose papers prior to radiant heating reduces the sensitivity to transient flaming and, furthermore, that sustained flaming may be prevented without adding more than 1.5% by weight. Such an observation is in complete accord with the fact that the effectiveness of KHCO_3 as a fire extinguishing agent has been repeatedly demonstrated over the years and is beyond question. Not in accord with its proven value in firefighting is the fact that the addition of KHCO_3 increases the rate and degree of pyrolysis of cellulose to volatile substances, and, as an apparent consequence, greatly increases the sensitivity to glowing ignition. Further, KHCO_3 treatment markedly enhances the production of gases such as hydrogen, methane, ethane, and ethylene as well as organic liquids (at room temperature) such as acetone and biacetyl. These seemingly contradictory results may be resolved by careful temperature measurements during pyrolysis, and such measurements have now begun.

ACKNOWLEDGMENT

The authors are grateful for the extensive assistance of Robert W. Ramstad in the conduct of these experiments.

Literature Cited

- (1) Broida, T. R., U. S. Naval Radiological Defense Lab. USNRDL-417, 42 (1953).
- (2) Broido, A., Effect of fire extinguishing agents on the combustion of sucrose, Science, 113(3465): 1701-1702 (1961).
- (3) Brownlee, K. A., Hodges, J. L., Rosenblatt, M., J. Am. Stat. Assoc. 48: 262-277 (1953).
- (4) Butler, C. P., Martin, S. B., Lai, W., U. S. Naval Radiological Defense Lab. USNRDL-TR-135, 84 (1956).
- (5) Forest Products Laboratory, U. S. Forest Serv. Madison, Wis., Experimental papers made for the San Francisco naval shipyard under work authorization dated Oct. 2, 1953. Job No. 1306, Proj. No. D2-7-034.
- (6) Martin, S. B., Lai, W., U. S. Naval Radiological Defense Lab. USNRDL-TR-252, 41 (1958).
- (7) Martin, S., Lincoln, K. A., Ramstad, R. W., U. S. Naval Radiological Defense Lab. USNRDL-TR-295, 29 (1958).
- (8) Martin, S. B., Ramstad, R. W., U. S. Naval Radiological Defense Lab. USNRDL-TR-467, 18 (1960), (also J. Anal. Chem., in press).

Table I—Pyrolysis products of untreated α -cellulose and α -cellulose impregnated with 2% KHCO_3 , both exposed under helium to $4.2 \text{ cal cm}^{-2} \text{ sec}^{-1}$ for 2.5 sec.

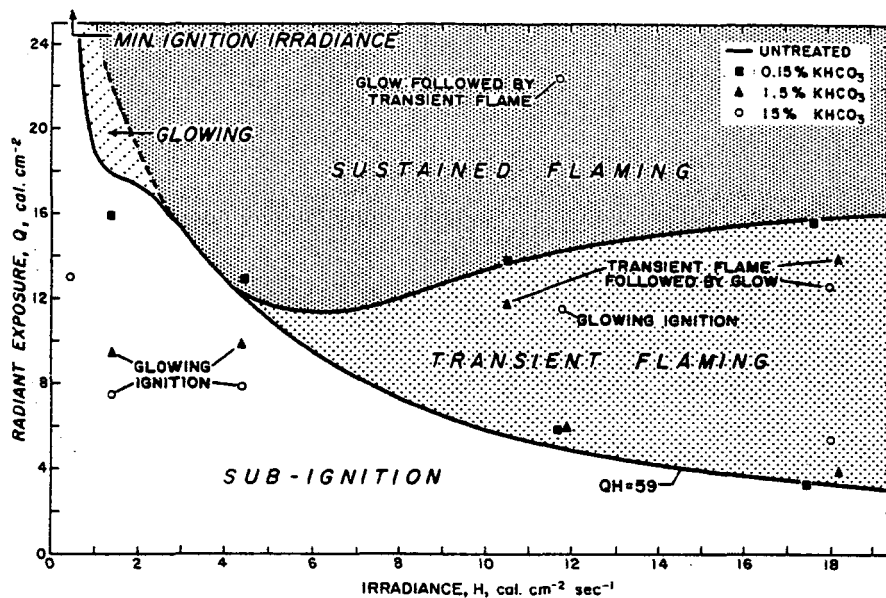
Product	Weight produced from—		Relative ratio
	Untreated sample	Treated sample	
	(mg.)	(mg.)	
Weight loss ^a	22.7	53.7	1
Total volatiles (B. P. <150° C)	6.2	26.9	1.8
Total gases (B. P. <0° C)	1.75	7.8	1.9
CO ₂	1.22	4.7	1.6
CO	0.53	3.0	2.4
H ₂	0.003	0.014	2
CH ₄	0.002	0.030	6
C ₂ H ₄	<0.001	0.026	> 10
C ₂ H ₆	<0.001	0.046	> 20
Water	4.0	16.5	1.8
Other vapors (B. P. 0-150° C)	0.48	2.6	2.3

^aOriginal sample weight = 100 mg.

Table II—Pyrolysis products of untreated α -cellulose and α -cellulose impregnated with 2% KHCO_3 , both exposed under helium to $11 \text{ cal cm}^{-2} \text{ sec}^{-1}$ for 1.4 sec.

Product	Weight produced from—		Relative ratio
	Untreated sample	Treated sample	
	(mg.)	(mg.)	
Weight loss ^a	68.1	79.3	1
Total volatiles (B. P. <150° C)	15.6	38.7	2.1
Total gases (B. P. <0° C)	4.3	13.0	2.6
CO ₂	2.54	6.3	2.1
CO	1.65	5.1	2.6
H ₂	0.015	0.3	17
CH ₄	0.020	0.66	28
C ₂ H ₄	0.034	0.51	13
C ₂ H ₆	0.007	0.19	23
Water	9.5	19.6	1.8
Other vapors	1.8	6.0	2.8

^aOriginal sample weight = 100 mg.



Ignition behavior of No. 4095 α -cellulose paper.
Points indicate effect of KHC0₃ impregnation.

Figure 1

Surface Flammability of Fire-Retardant
and
Conventional Paint Assemblies

Daniel Gross and Joseph J. Loftus

National Bureau of Standards, Washington, D. C.

Introduction

The results of a previous study [1] have shown that paints and other thin coverings applied to a flammable base material can provide a new surface of substantially lower flammability than that of the untreated base. Although with coatings of more than 50 mils (0.050-inch) thickness the particular base material used did not appreciably affect the flame spread index of the assembly, it appeared that with thinner finish coatings the base material had an important bearing on the flame spread results obtained. In cases where the coating is intended to be applied to a specified substrate, the surface flammability of the prescribed assembly is required. However, in cases where a particular substrate is not specified and a comparative evaluation of coatings only is desired, a suitable standard substrate material is required.

In choosing a standard substrate for paints, the use of an incombustible material such as asbestos cement board would obviously restrict the range of the flame spread index values and therefore the evaluation of the effectiveness of the paint film in reducing surface flammability. A study was therefore undertaken for measuring the surface flammability of a number of conventional paints and fire-retardant coatings as applied to common combustible building finish materials. The primary objects of the investigation were:

- (1) to evaluate the effectiveness of typical fire-retardant and conventional coatings applied to several combustible substrates at various spreading rates,
- (2) to evaluate those characteristics of the substrate material which were important in surface flammability measurements on painted assemblies, and
- (3) to select, if possible, one substrate as a standard for paint flammability measurements.

Material and Preparation

Five fire-retardant and three conventional interior paint finishes were applied to each of four substrates: paper wallboard, plywood, fiberboard and tempered hardboard. The coatings were applied to the smooth finished side of each substrate. Table 1 lists and briefly describes the substrates and Table 2 gives the schedule employed in the preparation of these test assemblies. With the exception of coating systems 7, 7a, and 7b, the effective spreading rate employed in the preparation of the assemblies was 125 ft²/gal (two coats at 250 ft²/gal). This rate, unusually heavy for conventional paints, was fairly representative of the spreading rates commonly used and recommended for fire-retardant coatings. The paints consisted of two alkyd flat paints (Nos. 3 and 8), one latex water emulsion paint (No. 6), four fire-retardant paints (Nos. 1, 2, 4, and 5), and one coating system consisting of an intumescent fire-retardant main coat plus a supplemental top coat (No. 7). The fire-retardant paints selected were typical proprietary materials.

Table 1

Substrate Materials

Symbol	Substrate	Thickness in.	Density lb/cu ft
A	Paper Wallboard-Factory Finished One side	3/16	35.0
B	Plywood-Douglas Fir, exterior grade	1/4	39.0
C	Fiberboard-Interior Insulating Board, Class D (factory- finished)	1/2	19.4
D	Hardboard- Tempered	1/4	67.6
E	Hardboard- Tempered	1/4	55.1

The first step in preparing the test assemblies was to coat the substrate boards, at a spreading rate of 450 ft²/gal, with a white pigmented primer-sealer conforming to Federal Specification TT-P-56. After 72 hours the primed substrates, with the exception of those reserved for coatings 7, 7a and 7b, received two coats of the paint under test at 250 ft²/gal per coat, allowing 72 hours between coats. Sample 7 consisted of a flat fire-retardant main coat at 250 ft²/gal plus a supplemental gloss fire-retardant top coat at 250 ft²/gal. Sample 7a received only one main coat at 350 ft²/gal. Sample 7b was coated in the same manner as sample 7 but with spreading rates of 350 ft²/gal and 500 ft²/gal for the main and top coats, respectively. The coatings on samples 7, 7a and 7b were purposely varied to study the effect on flame spread behavior of different rates of spreading of the same paints.

Table 2. Coating Schedule

Coating System	Main Paint Coating			Supplemental Top Coat			Description	
	Density lb/gal	Color	No. of Coats	Spreading Rate ft ² /gal	Density lb/gal	No. of Coats		Spreading Rate ft ² /gal
1	11.9	Aqua	2	250	-	-	-	Fire-Retardant Paint
2	12.8	White	2	250	-	-	-	" "
3	12.2	"	2	250	-	-	-	Flat Alkyd Paint
4	10.6	"	2	250	-	-	-	Fire-Retardant Paint
5	13.6	"	2	250	-	-	-	" "
6	11.5	"	2	250	-	-	-	Styrene-Butadine (Latex) Water Emulsion
7	12.3	"	1	250	11.95	1	250	Main Coat-intumescent, resin-base, flat, fire- retardant coating. Top Coat-interior gloss fire-retardant paint.
7a	12.3	"	1	350	-	-	-	Same as 7 Main Coat
7b	12.3	"	1	350	11.95	1	500	Same as 7
8	12.1	"	2	250	-	-	-	Flat Alkyd Paint

Note: A primer-sealer (10.8 lb/gal density) was applied to all substrates, at a rate of 450 ft²/gal, before coating

In another study of the effect of spreading rate, one flat alkyd (No. 3) and one latex water emulsion type (No. 6) were applied to a tempered hardboard substrate (E). The rates and film thicknesses are given in Table 3. These paints were applied directly (without primer-sealer) to the smooth substrate surface in a sufficient number of coats to obtain the desired effective spreading rate, allowing 24 hours between coats.

Table 3. Spreading Rates and Film Thicknesses for Two Conventional Paints Applied to Tempered Hardboard Substrate (E)

Number of Coats	Effective Spreading Rate ft ² /gal	Paint Film Thickness	
		Computed*	Measured**
		mils	mils
1	900	0.6	0.3
1	500	1.1	1.2
1	250	2.1	1.6
2	125	4.2	4.4
3	60	8.8	8.5
6	30	18.	21.

* 530 divided by effective spreading rate; based upon one-third nonvolatiles by volume.

** Average for paints 3 and 6, based upon microscope measurements across smooth-sanded edge surface.

After the application of the finish materials, the assemblies were dried for not less than 72 hours and then cut to produce five specimens, each 6 by 18 inches. The specimens were then dried in an oven at 160°F for 24 hours and again conditioned, in a room maintained at 73°F and 50 per cent relative humidity, for not less than one week prior to testing. An alternate drying procedure, 24 hours at 140°F, was used for half of the test specimens prepared for the spreading rate study. However, no appreciable difference in the test results could be attributed to the effect of the slightly different drying procedure.

Test Procedure

The apparatus used for the tests is shown in Figure 1, and has been described in detail [2, 3]. It consists of a radiant panel, a frame for support of the test specimen, and associated measuring equipment.

The radiant panel consists of a cast iron frame enclosing a 12- by 18-inch porous refractory material. The panel is mounted in a vertical plane, and a premixed gas-air mixture supplied from the rear is burned in intimate contact with the refractory surface to provide a radiant heat source. The energy output of the panel, which is maintained by regulating the gas flow according to the indication of a radiation pyrometer, is that which would be obtained from a black body of the same dimensions operating at a temperature of 670°C. A stack placed under the hood above the test specimen receives the hot products of combustion and smoke.

For test, the 6- by 18-inch specimen was placed in a metal holder and backed with a 1/2-inch sheet of asbestos millboard of 60 pound per cubic foot density. At time zero, the specimen was placed in position on the supporting frame facing the radiant panel and inclined 30 degrees to it. A pilot igniter fed by an air-acetylene mixture served both to initiate flaming at the upper edge of the test specimen and to ignite combustible gases rising from the specimen. Observations were then made of the progress of the flame front, the occurrence of flashes, and so forth. An electrical timer calibrated in minutes and decimal fractions to hundredths was used for recording the time of occurrence of events during the tests. The test duration was 15 minutes, or until sustained flaming had traversed the entire 18-inch length of the specimen, whichever time was less.

The flame-spread index, I_s was computed as the product of the flame spread factor, F_s , and the heat evolution Q , thus

$$I_s = F_s Q$$

where:

$$F_s = 1 + \frac{1}{t_3} + \frac{1}{t_6 - t_3} + \frac{1}{t_9 - t_6} + \frac{1}{t_{12} - t_9} + \frac{1}{t_{15} - t_{12}}$$

The symbols t_3 . . . t_{15} correspond to the times in minutes from specimen exposure until arrival of the flame front at a position 3 . . . 15 inches, respectively, along the length of the specimen. $Q = 0.1 \Delta\theta / \beta$, where 0.1 is an arbitrary constant, $\Delta\theta$ is the observed maximum stack thermocouple temperature rise, in degrees F, at any stage of combustion of the specimen minus the maximum temperature rise observed with an asbestos-cement board substituted for the specimen, and β is the slope of the line obtained by plotting the maximum stack thermocouple temperature rise as a function of the corresponding measured heat input rate, in Btu per minute, as supplied by a diffusion-type gas burner placed near the top of an asbestos-cement board specimen during normal operation of the radiant panel.

Results and Discussion

A minimum of four replicate tests were run on each test assembly. The mean flame spread indices and the coefficients of variation are listed in Tables 4 and 5. The weight of the smoke deposit listed is the mean for replicate tests. Although not directly related to surface flammability, the smoke deposit is considered to be an indication of possible parallel hazards, such as toxicity and the interference to be expected in evacuation and fire-fighting procedures. The smoke deposit values represent the contribution of both the coating and substrate materials as evidenced by the somewhat higher mean smoke deposits for coatings on hardboard (D) than on the other substrates. The fire-retardant coatings tested did not produce significantly greater smoke deposits than the conventional paints.

Intumescence was exhibited by paints 1, 7a, and 7b. Paints 2, 4, 6, and 7 blistered, whereas the alkyd paints 3 and 8 did not blister or intumesce. Paint 5 flaked off from the substrate during test. Blister and intumescent formations were responsible for a wide variation in flame spread indices for the paints which exhibited these properties.

Of the four substrates used, the plywood and the hardboard showed the widest range in flame spread index values, affording good opportunity for discrimination between coatings. The hardboard values, however, had lower coefficients of variation than the plywood values, and much lower than those obtained with the other two substrates. Considering the results obtained with the hardboard, the conventional paints 3, 6, and 8 appeared to be comparable to the fire-retardant paints 1, 4, and 5, when applied to this substrate at the same effective spreading rate of 125 ft²/gal. The intumescent fire-retardant coating, 7a, showed both the lowest flame spread index and the lowest smoke deposit value of any of the coatings.

At effective spreading rates of 250 ft²/gal or greater, the flame spread index was found to be strongly affected by the spreading rate as shown in Figure 2. One coat of a flat alkyd paint applied at a rate of 250 ft²/gal reduced the flame spread index of a tempered hardboard substrate by a factor of almost 5. Similarly, a coat of a latex paint effected a more than three-fold reduction. For film thicknesses greater than those corresponding to 250 ft²/gal, the additional improvement in flame spread index was quite small. The effect of very thick films, such as might be encountered on surfaces frequently repainted, was not investigated. It is possible, however, that a higher flame spread index might result from the formation and disintegration of blisters, from cracking, peeling or other separation from the flammable substrate, or by the direct involvement of the thick paint layer.

The effect of paint thickness upon surface flammability properties refers only to typical combustible cellulose-base substrates in contrast to non-combustible substrates such as plaster, concrete or metal.

Table 4. Mean Flame Spread Index and Mean Smoke Deposit of Coated Assemblies Based on Four Replicate Tests

Coating System	SUBSTRATE											
	A Paper Wallboard			B Plywood			C Fiberboard			D Hardboard		
	Mean I _s	Coef. of Var. ^a	Mean Smoke mg	Mean I _s	Coef. of Var.	Mean Smoke mg	Mean I _s	Coef. of Var.	Mean Smoke mg	Mean I _s	Coef. of Var.	Mean Smoke mg
Uncoated Substrate	126	11	-	167	7	0.3	83	16	0.2	150	9	2.6
1	44	48	2.5	21	85	3.1	35	115	3.1	29	39	4.1
2	48	37	1.5	75	25	1.7	17	96	1.0	75	21	4.5
3	20	56	1.1	27	6	1.4	7	62	0.7	28	15	5.0
4	34	62	2.6	34	21	2.2	18	71	1.9	37	5	3.6
5	9	55	1.6	14	42	2.6	6	70	1.6	33	7	4.9
6	60	39	2.2	46	60	2.8	15	101	2.5	42	25	5.1
7	8	64	2.1	9	69	2.7	9	103	1.4	40	54	3.2
7a	1.2	86	1.3	2	71	1.8	1.2	151	1.5	1.5	73	1.2
7b	9	183	1.6	7	94	1.5	9	96	1.9	6	54	1.9
8	46	30	1.0	42	76	1.4	13	54	0.9	28	15	3.9

^aDefined as the ratio of the standard deviation to the average, expressed as a percentage

Table 5. Mean Flame Spread Index of Two Conventional Paints at Varying Spreading Rates Applied to Tempered Hardboard

Paint	Effective Spreading Rate ft ² /gal	Number of Tests	Mean Flame Spread Index	Coeff. of Variation per cent	Mean Smoke Deposit mg
Uncoated Substrate	-	4	116	8	2.1
Alkyd Flat No. 3	900	4	58	13	2.4
	500	4	52	11	2.4
	250	4	24	13	2.7
	125	4	20	4	2.4
	60	4	13	8	2.4
	30	5	27	72	1.7
Latex No. 6	900	4	94	2	2.6
	500	5	30	25	2.0
	250	4	35	9	1.8
	125	4	42	24	2.0
	60	5	37	10	2.7
	30	5	32	91	3.4

In another study, in which non-flammable substrates were used, it was found that the flame spread index increased with increasing thickness of a paint coating applied on steel sheet. For example, the flame spread index of a No. 18 gage, red lead primed steel sheet had values of 1, 7, 69, and 110 for oil-base paint coatings of 5, 10, 15, and 20 mils, respectively. An assembly of a 10 mil coating of the same paint applied to 1/8-inch thick asbestos-cement board had a flame spread index of 2. Thus it appears evident that the flame spread behavior of coatings applied to either flammable or non-flammable substrates depends not only on the type and thickness of the paint film but also on the characteristics of the substrate.

For a conventional paint, such as flat alkyd (No. 3) applied at an effective spreading rate of 125 ft²/gal, the ratio of the flame spread index of the painted assembly to that of the substrate was found to be related to the density of the substrate material. The effect at other spreading rates was not explored. As shown in Figure 3, this paint was most effective on the low density fiberboard substrate. A majority of the other paints tested were also most effective on the low density substrate. However, for critical evaluation of a paint for fire-retardancy, the burden of effective performance should be placed upon the paint without ascribing to the paint undue advantage resulting from the properties of the substrate. For this reason, tempered hardboard is considered a more suitable substrate.

An analysis of the data was made to provide a statistical measure of variability. Particular attention was directed toward evaluation of the substrate materials both from the standpoint of (a) selection of a standard material for paints and other liquid coatings and (b) interpretation of previous and subsequent flame spread data on coated assemblies employing a variety of substrates.

The analysis showed that although the wallboard and fiberboard substrates gave a more consistent behavior of dispersion about the mean than the plywood and hardboard substrates, the coated hardboard assemblies did exhibit:

- a. A substantial range of flame spread index values for the coating materials, and
- b. The lowest coefficients of variation.

It should be noted that considerable variation was observed in the rankings of the coatings on the four substrates. In addition, the coefficients of variation were considerably higher than those obtained in an earlier investigation of conventional paints on the same or similar substrates [1]. This is not unreasonable when consideration is given to the special types of coatings and rates of application employed here. Inasmuch as the hardboard did result in the lowest coefficient of variation and provided a substantial range of flame spread index values for the coating materials tested, its choice as a standard substrate is indicated.

Conclusions

On the basis of the work reported, the following conclusions seem justified:

1. Tempered hardboard may be considered a suitable choice as a standard substrate for evaluating the fire-retardant effectiveness of paints and other thin surface coatings. Of the substrates studied, it gave results with the lowest coefficient of variation, provided a substantial range in flame spread index values for the coating materials tested, and placed the burden of effective performance upon the paint under test.
2. The fire-retardant effectiveness of paints and other coatings is highly dependent upon the effective spreading rate of the paint and on the type and density of the substrate material, as well as on the coating composition and the undercoat-overcoat combination employed. Coatings of latex and flat alkyd paints applied to a tempered hardboard substrate at an effective spreading rate of 250 ft²/gal reduced the flame spread index of the uncoated substrate by factors of 3 and 5, respectively.

3. In general, conventional paints of the flat alkyd and latex emulsion types tested, when applied at the heavy rate common for fire-retardant coatings, appear to have flame spread indices comparable to those of the fire-retardant coatings. However, one intumescent fire-retardant coating showed a flame spread index significantly lower than that of any other tested.

Acknowledgements

Mr. Neil B. Garlock of the National Paint, Varnish and Lacquer Association, Inc., took a strong interest in the work and kindly provided all the paint coating systems. Mr. Harry Ku of the Statistical Engineering Section, National Bureau of Standards, made the statistical analysis.

References

- (1) Gross, D., Loftus, J. J., Flame Spread Properties of Building Finish Materials, Am. Soc. Testing Mats., Bul. No. 230, 56-60, May 1958.
- (2) Interim Federal Standard No. 00136 (Comm-NBS) July 31, 1959.
- (3) Robertson, A. F., Gross, D., Loftus, J. J., A Method for Measuring Surface Flammability of Materials Using a Radiant Energy Source, Proceedings, Am. Soc. Testing Mats., 56, (1956).

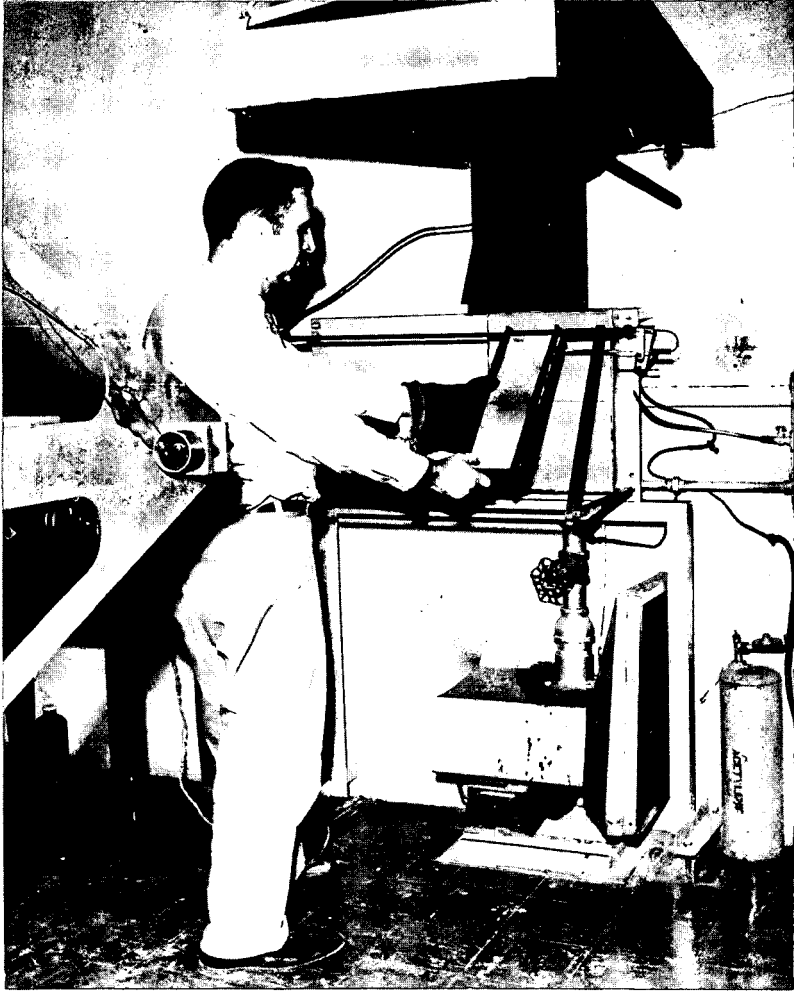


FIG. I - RADIANT PANEL TEST APPARATUS

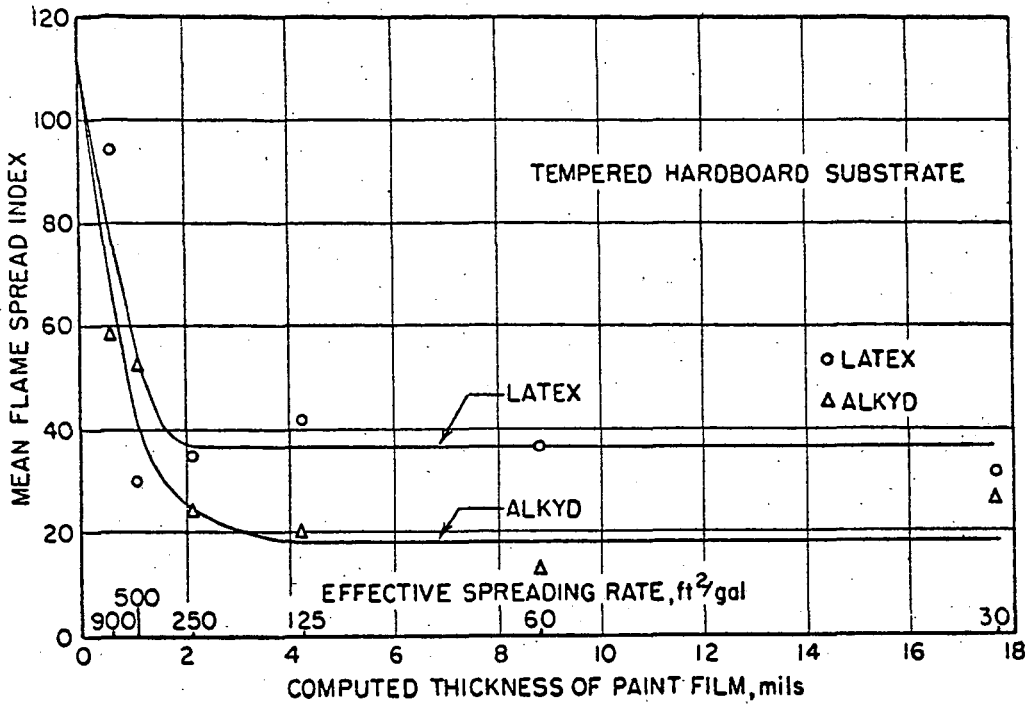


FIG. 2- EFFECT OF PAINT FILM THICKNESS ON MEAN FLAME SPREAD INDEX FOR TWO CONVENTIONAL PAINTS

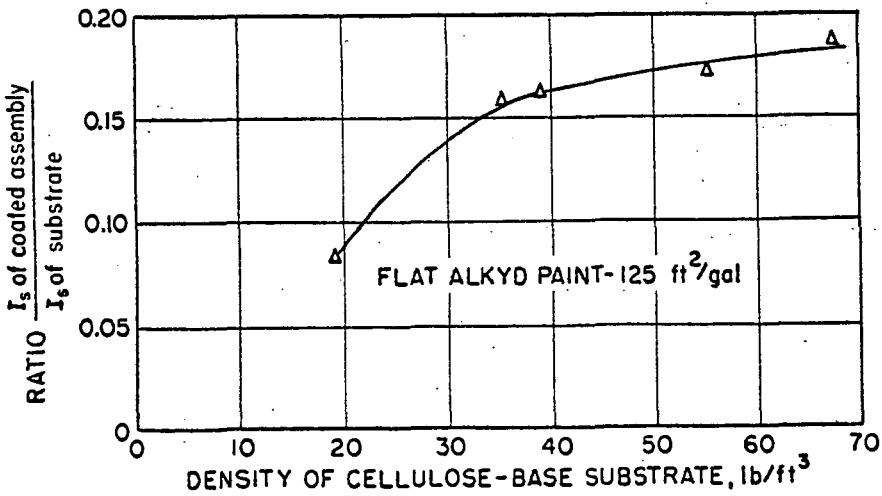


FIG. 3- EFFECT OF SUBSTRATE DENSITY UPON FLAME SPREAD INDEX RATIO

by Thomas F. Seamans and Hans G. Wolfhard

Thiokol Chemical Corporation
Reaction Motors Division
Denville, New Jersey

INTRODUCTION

Gaseous detonations have been studied extensively and our basic knowledge of pressures in the detonation wave, its velocity and detailed structure is extensive. However, there is no way of predicting under what conditions a detonation rather than a deflagration will be established. This is no particular concern in fuel-oxygen mixtures as a detonation usually forms from a deflagration after a very short time period and distance from the ignition source. Fuel-air mixtures in contrast have seldom been observed to detonate although one would expect that given large and long enough vessels eventually detonation will occur. This has, in fact, been observed in natural gas and air mixture, where a detonation developed even at 0.4 atm initial pressure in tubes of 61 cm diameter and 93 meter length (ref. 1).

Detonations and the resulting high pressure peaks are a danger in many industrial applications. This experimental investigation was undertaken to assess the dangers of detonations or very high pressure peaks in large volumes containing fuel-air mixtures. Of special interest was the possibility of arresting detonations or deflagration by spraying into the tube large amounts of water. It was the original intention to conduct all experiments in a tube of 54.6 cm diameter and 9.45 m length that was designed to withstand high pressure. However, after initial experiments that lead to extremely high pressure peaks, it was decided to use this large tube for experiments at one atmosphere initial pressure only and to conduct detonation experiments at initial pressure higher than one atmosphere in a tube of smaller diameter but the same length as the large tube.

The experiments fall roughly into four categories.

- A. Pressure dependence of fuel-air detonations.
- B. Comparison of the onset of detonation in the large and small diameter tube.
- C. The occurrence of autoignition in the large tube.

D. The influence of water curtains on explosions and detonations.

In A it was our intention to see whether fuel-air mixtures detonate at high pressure in systems where detonations do not occur at one atmosphere. Initial pressures were therefore raised up to 40 atm.

In B a comparison between the large and small diameter tube was made. As fuel-air mixtures did not detonate at one atmosphere initial pressure in either tube oxygen enrichment was used to induce detonation and the oxygen index was taken as measure for the ease with which a mixture would detonate.

In C a study was made of the very high pressure peaks that occur in regions where detonation is marginal. These peaks will be seen to be due either to pressure piling or autoignitions induced by forward or reflected shock waves.

In D the effectiveness of water curtains was investigated. These experiments were done in the large tube with oxygen enrichment. The sprays covered the whole cross section of the tube and the amount of injected water was extensive.

The instrumentation was restricted to high-speed pressure measurements. This allowed a full analysis of the pressure history in the tube but gave only indirect evidence of the position of the flame front. Surface thermocouples were tried to get this additional information but were not too successful, no doubt due to the fact that the flame front during the deflagration stage was highly turbulent and clear signals were not received, except when a detonation had been established.

EXPERIMENTAL APPARATUS

Two closed tubes of approximately the same length were employed in this investigation. A large tube, 54.6 cm in diameter, was used for the bulk of the tests at initial pressures of one atmosphere and for all tests in which water was injected into the path of a deflagration or detonation. A small tube, 38 mm in diameter, was used principally for tests at elevated initial pressures. Both tubes were equipped to accept piezoelectric pressure gages at various positions along the walls of the tubes. The locations of these stations and of the water injection ports are given in Table I and diagrammatically in Figure 1. Free stream pressures were measured with as many as eight Kistler SLM PZ 6 miniature pickups whose signals were displayed on oscilloscopes and recorded photographically. PC 6R Piezo-Calibrators were used with four of the pickups; PT 6R Amplifier-Calibrators were used with the other four. With the Amplifier-Calibrators, the response of the pickups is 150,000 cps; with the Piezo-Calibrators, the response is somewhat less. For tests in the smaller tube, adapters were necessary to extend the range of the gages to the much higher pressures produced by detonations at elevated initial pressures. These adapters reduce the response of the more sensitive gages to approximately 50,000 cps but have little effect on the response of the others.

Two four-beam oscilloscopes displayed the pressure signals and two high speed (1.53 meters/sec) streak cameras recorded them. A drum camera (12.7 meters/sec) was used for a very few tests but, though it provided more accurate wave velocity determinations, it was not possible to use the faster camera generally. The reason is that a history of the reflected waves was sought as well as of the incident wave and this would have resulted in double exposure of at least a part of the film. Consequently the Fairchild cameras were used in almost all of the runs. One millisecond timing blips were superimposed on the pressure traces, providing a time scale. A coil around a lead to one spark plug (see below) gave a signal, displayed on the oscilloscopes, indicating the capacitor discharge and therefore the start of a run on the film.

Considerable difficulty was encountered in attempting to load to one atmosphere the 2,130 liter

volume of the large tube with a known uniform mixture of explosive gases. The first method was based on loading the previously evacuated tube by partial pressures and then mixing the gases with a blower in an external recirculation line. This method was found to be unsatisfactory due to the time required to achieve even a semblance of adequate mixing and due to air leakage into the system at the blower shaft during the long mixing times.

A revised system proved satisfactory and all tests discussed herein employed this system. In essence, the method was based on filling the vessel with the component gases premixed externally in the desired proportions in the flow system.

The large tube was evacuated to approximately 5 cm Hg absolute with an air ejector. The desired flowrates of air, oxygen (if required for the particular run), and fuel (methane, ethylene, or hydrogen) were established using calibrated orifices in which the flow was maintained critical. The three streams joined in a "mixer" from which one stream emerged at a pressure only slightly above ambient. This stream was vented to the atmosphere while the flows were being established; it then was allowed to flow into the large tube while the air ejector remained in operation. After a purge at low pressure for several minutes, the tube was permitted to fill to one atmosphere with the premixed gases. Samples of the final mixture in the tube and also of the emerging stream from the mixer were taken and subsequently analyzed by Orsat.

Ignition of the mixture at one end of the large closed tube was ensured by the use of three surface gap spark plugs, each with an independent capacitor circuit. The energy to which each capacitor was charged in all runs was 18 joules.

Loading of the 38 mm tube for initial pressures of up to 40 atmospheres was achieved in the following manner. A large tank was loaded with the desired gas mixture to one atmosphere in the same manner as the 54.6 cm tube (discussed above). The mixture in the large tank was then forced by water into the 38 mm tube. By this method, the tube was prepared for tests at initial pressures of from one to 40 atmospheres.

Ignition of the gas mixture in this tube was accomplished by the discharge of a capacitor (18 joules) across a surface gap spark plug similar to those used in the 54.6 cm tube.

Water injection into the 54.6 cm tube was through three poppets located on a spiral on the tube circumference. The distances between the spark plugs and the three spring loaded water injectors, which produce fine sprays, are given in Table I. For the runs with water injection, a 100 gallon tank was filled prior to the run. With a suitable delay mechanism, high pressure nitrogen was admitted to the water tank, forcing the water through the three poppets in the tube just prior to the spark. The delay period between water flow initiation and the capacitor discharge could be varied as desired.

RESULTS

High Pressure Data

In a closed steel tube 38 mm in diameter and 9.15 meters in length, a number of tests were made with fuel-air mixtures at initial pressures of 1 to 40 atmospheres absolute. The principal fuels employed were hydrogen, ethylene, and methane. For these tests, only mixtures of approximately stoichiometric proportions were used.

In no case was a detonation observed in any methane-air run. Even at the highest initial pressure tested, 40 atm, the wavelike pressure fluctuations within the tube were rounded. The maximum pressures recorded at any station for these methane-air runs were only two to three times the initial pressure.

Quite different results were obtained with the hydrogen-air and ethylene-air mixtures. For these mixtures, pressure ratios of about 15 for the former mixture and more than 20 for the latter mixture were recorded in some runs (Table II). These pressure ratios were caused by detonations. Pressure, however, could not be the sole criterion on which to base the description of the type of combustion. Average velocities of the pressure pulses between various stations along the tube-axis provide a better basis. The average velocities are plotted in Figures 2 and 3 for the hydrogen-air mixtures and the ethylene-air mixtures respectively. These velocities were computed from the measured time interval for passage of the pressure pulse between two successive stations at which the piezoelectric gauges were located. The average velocities so computed are plotted against distance from spark to the mid-point between the two appropriate stations as abscissa.

Two distinct regimes are evident in Figures 2 and 3; the lower corresponding to deflagrations or pressure pulses resulting from deflagrations, the upper to detonations. Clearly, detonations form in hydrogen-air mixtures at 6 atm initial pressure or above. For the ethylene-air case, 20 atmospheres appears to be the marginal initial pressure at which a detonation generally forms. Below 20 atm, detonations were not observed within the tube length.

The occurrence of a detonation is readily evident from Figures 2 and 3. However, they are misleading with regard to the location of the onset of detonation. The pressure-time records show that in those runs in which a detonation occurred, it was formed between stations 1 and 2 in every case. The pressures due to the incident wave passing station 2 are at least 10 times the initial pressure in all "detonation" runs as opposed to a maximum factor of 3 for the hydrogen-air "deflagration" runs and 7 for the C_2H_4 -air "deflagration" runs (Table II). Additional evidence indicating detonation onset was between stations 1 and 2 is the fact that the records show the rate of pressure rise at station 2 was essentially infinite, as at succeeding stations, in detonation runs. In deflagration runs, on the other hand, the pressurization rates throughout were finite except at the far end of the tube where discontinuities of low amplitude were recorded. In hydrogen-air detonation runs, furthermore, no precompression of the unburned gas was observed at station 2 or at stations 6, 7, and 8 prior to the arrival of the pressure discontinuity. For the ethylene-air detonation mixtures, slight precompression at station 2 (from 20 atm initial pressure to about 28 atm) was recorded.

It should be mentioned that the average velocities for the intervals between stations 6 and 7 and also 7 and 8 lack precision mainly for two reasons. These intervals are 0.5 meters in length. For the highest velocities, therefore, the time differentials for traversal of the intervals by the flame front are of the order of 10^{-4} seconds or, for the camera employed, tenths of a millimeter of film. In addition, very high frequency oscillations were recorded at stations 6, 7, and 8 in many of the runs, particularly those in which detonations occurred. The amplitude of the oscillations prior to arrival of the detonation wave was generally very small; nevertheless, the precise instant of wave arrival was sometimes difficult to determine at stations 7 and 8. For these reasons, the average velocities between stations 6 and 7 and also 7 and 8 are subject to an error of up to 40% in runs in which detonations occurred. However, for the station 2 to station 6 interval, a distance of 4.5 meters, the average velocities are subject to an error of only about 5%.

The oscillations at 6, 7, and 8 referred to above made pressure determinations at these stations highly

questionable in many cases. No values, therefore, are given for these locations in a number of runs. In some cases, a value is given preceded by the symbol "~" to denote lack of precision due to the presence of the oscillations.

In several runs, one or more pressure traces went off the film. In these cases, the symbol ">" has been used in the tables before the number which corresponds to the maximum pressure able to be recorded at that station in the particular run. The true pressure may have been only slightly greater, or considerably greater, than the value reported.

Comparison of Detonation Runs in the Two Tubes

A series of tests were made at one atmosphere initial pressure in each of two closed tubes of approximately the same length. The large tube is 54.6 cm in diameter, the small tube 38 mm in diameter. The tests used fuel-air mixtures enriched with oxygen in approximately stoichiometric proportions. To describe the degree of air enrichment with oxygen, the parameter oxygen index is employed. Oxygen index is the ratio of moles of oxygen to moles of oxygen plus nitrogen. For air, O.I. = 0.21.

The results of the runs show that detonations are formed at lower oxygen indexes in the smaller (38 mm) tube. Table III presents the minimum oxygen indexes of approximately stoichiometric mixtures supporting detonations in each tube. The next lower oxygen indexes tested are also included. The significance of "autoignitions" reported in the table for some runs in the larger tube will be discussed in the next section.

Tables IV and V present pressure and velocity data of the incident waves for runs in the 38 mm tube and 54.6 cm tube respectively. Only runs in which detonations were formed are included for in these runs only could the location of the flame front at any instant be determined from the signals of the piezoelectric gauges. Runs in which water was injected into the path of a detonation wave are not given due to the interactions of the water curtain with the wave.

A comparison of the tables leads to some interesting observations. Practically without exception, the pressure due to the incident waves are higher in the larger tube. For the cases of hydrogen and methane, one

might say this fact is due to the higher oxygen indexes in the larger tube. Surely, this is one consequence of a greater oxygen concentration necessary to induce detonation. However, the ethylene runs in each tube include similar oxygen indexes; and here also are found the higher pressures in the larger tube, regardless of which stations in each tube are compared.

The two tables also indicate that at least some degree of precompression occurred at some stations in the large tube prior to arrival of a detonation wave. No such pressure rises were recorded for the runs in the smaller tube. This, however, cannot preclude entirely the non-existence of precompression because of the reduced sensitivity (up to 1/5th) of the gauges in the smaller tube, necessitated by the fuel-air tests at higher initial pressures.

In addition to the pressure data, Tables IV and V give the average velocity of the flame front as it passes between various pairs of stations. From Table I, Locations of Stations, the distances between the spark and station 9, stations 9 and 10, and stations 10 and 11 in the larger tube are comparable respectively, to the distances between the spark and station 6, stations 6 and 7, and stations 7 and 8 of the smaller tube. The average velocities in these regions are plotted in Figures 4, 5, and 6 for the hydrogen, ethylene and methane runs respectively. It is evident from these plots that the average velocity of the flame front as it traverses the first 80% of the tube length is greater in the smaller tube for similar runs with the same oxygen index. For example, the average flame velocity in an ethylene run with an oxygen index of 0.37 was 722 meters/sec between the spark and station 6 in the smaller tube and just 380 meters/sec in the comparable distance in the larger tube. This trend is to be expected, however, as it leads to the previously stated fact that detonations are formed more readily in the smaller tube.

Further examination of Figures 4-6 indicates that the average velocity of the detonation wave in the subsequent 0.5 meter of the tube length is greater in the larger tube than in the smaller tube. Referring again to the ethylene runs with an oxygen index of 0.37, the average velocity between stations 6 and 7 in the small tube was 1670 meters/sec as opposed to 2270 meters/sec in the comparable region in the larger tube.

The data indicates, then, that for similar mixtures supporting detonations in each tube the average velocity of the flame front is greater in the smaller tube over the first 8 meters and then lower in the subsequent 0.5 meter distance. This is to be expected because the induction distance was found qualitatively to be shorter in the smaller tube than in the larger tube for the same test mixture. Consequently a stable detonation velocity would be approached earlier in the smaller tube; whereas, in the same region of the larger tube, the detonation velocity would still be significantly in the overdriven mode.

Occurrence of Autoignitions under Marginal Conditions

In addition to the deflagration and detonation processes on which the present work was based, a third phenomenon, termed autoignition, was observed in some runs in the 54.6 cm tube only. Invariably, the process occurred in the downstream end of the closed tube in the region of the conical frustum (Figure 1). In general, the phenomenon was observed in runs in which the oxygen index was between those supporting deflagrations and those forming detonations. Pressure disturbances from the accelerating flame front in such runs are comparatively strong. In fact, shocks were recorded in all "autoignition" runs just prior to the occurrence of the phenomenon.

The events leading to the autoignitions in all twelve such runs with the three different fuels can be classed as one of three types:

1. Double shocks of low strength which pass down the tube, are reflected, pass up the tube, are again reflected, merge into one shock, and pass down the tube for the second time. A second reflection at the downstream end of the tube, i.e. the region of the conical frustum, may or may not occur just prior to the large pressure "kick" of the autoignition. This mechanism was observed clearly in two ethylene runs and one methane run. All three runs had the lowest oxygen indexes for a particular oxygen-fuel ratio of any runs in which autoignition occurred. Table VI shows that the two ethylene runs of the type under discussion had compositions of O.I. = 0.29 with O/F = 2.3 and O.I. = 0.37 with O/F = 4.6. The methane run was for O.I. = 0.39 with O/F = 2.1. All runs with these fuels under conditions of similar oxygen-fuel ratios and lower

oxygen indexes resulted in deflagrations only.

2. Double shocks whose strengths are somewhat greater than those discussed above (i.e. pressure ratios of ~ 2.5 vs. ~ 1.8). In this case, the first shock of the pair is reflected at the downstream end of the tube and is then met near station 12 by the second shock traveling downstream. This mechanism was observed in four runs as indicated in Table VI.

3. A single shock of greater strength (pressure ratio ~ 3.5). Here, no reflected wave was recorded at station 12 prior to the sudden large pressure kick of the autoignition. Five runs exhibited this behavior.

Table VI indicates that the last two mechanisms occurred indiscriminately at oxygen indexes above those of (1) above.

The fact that the first large pressure "kick" appeared at station 12 in all runs is significant. Furthermore, the station 12 pressure-time trace recorded one or more small shocks, as described above, just prior to the sudden, large pressure rise. Consequently, the autoignitions occurred between station 12 and the end-flange in all cases. In a few cases, the phenomenon occurred practically at station 12. Here, the sudden pressure rise was not in the form of a discontinuity in the trace; rather, the trace showed a continuously increasing slope from essentially zero to infinity. This rounded nature of the trace corresponds to the period of rapid but finite build-up from ignition to nearly instantaneous explosion of the compressed mixture.

In the majority of runs, however, even the first large pressure kick, which was always recorded at station 12, was in the form of a discontinuity. In these runs, then, ignition occurred sufficiently downstream of station 12 to allow the resultant detonation wave, traveling upstream to overtake the pressure disturbances of the building-up process. The trace at station 12, therefore, recorded a discontinuity due to the resultant overdriven detonation wave. Although precise determinations were limited by the time resolution of the streak camera, an approximate average velocity of the overdriven detonation wave between stations 12 and 9 was 3000 meters/sec. The computation

does not reflect the possibility that the overdriven detonation wave, traveling upstream, might enter before reaching station 9, the burned gas region behind the flame front propagating downstream from the spark ignition source.

The most striking effect of the autoignitions is the very high pressures generated from initial pressures of one atmosphere. These pressure peaks are greater by a factor of 2 or 3 than the pressures recorded in detonation runs due to the incident detonation wave traveling downstream. Pressure peaks of approximately 80 atmospheres were recorded in two methane runs due to autoignitions (Table VI).

Water Injection Tests

Several tests were made in the 54.6 cm tube with water injected into the path of a deflagration or detonation. Three poppets were used as injectors, producing a fine spray. The distances between the spark and the three water injection ports are given in Table I. The ports are located 120° apart on a spiral on the tube circumference. Each spring-loaded water injector has spray shields suitably oriented such that the major axis of the resulting elliptical hollow spray is normal to the tube axis. Since the angle of upstream penetration is approximately 20° , an atomized water curtain was produced whose thickness was more than 36 cm. Generally, the total water flowrate in each run was 51 kg/sec.

The presence of the water curtain had two principal effects. It either prevented ignition of the combustible mixture by the spark, or it slowed propagation of the flame front.

In nearly half of the runs made with water injection, no pressure rises were recorded and no audible evidence of an explosion was heard. Nevertheless, the capacitor discharge signal was recorded indicating that a spark did occur. It is believed that although a spark occurred, the mixture failed to ignite due to the presence of much water vapor and/or droplets in the immediate vicinity of the spark plugs. Qualitatively, the amount of water, for constant inlet flowrate, in the form of vapor and/or droplets in the immediate vicinity of the spark plugs may be expressed by the time delay between initiation of water flow and the discharge of the capacitors. This delay period was necessary due partly to the velocity of a flame and partly to the fact that up to 0.10 second elapsed between the beginning of flow through the poppets and attainment of steady state

flow. The delay period, Δt , is included where known for the appropriate runs in Table VII. In general, the longer the delay period, the more likely ignition will not occur. However, runs 120, 130, and 133 (Table VII) are exceptions. It should be emphasized that the records indicate the combustible mixtures failed to ignite in such runs. There was no indication that combustion occurred in the tube section between the spark and the water curtain. The pressure records of station 2, which is located in this section, showed no pressure rises. In a few of these runs a surface thermocouple, whose response is equal to that of the pressure gauges, was located at station 1. The thermocouple, too, gave no indication of combustion in the tube between the spark and the water curtain. It must be inferred, then, that the injected water in no case extinguished a flame already established; rather, the water prevented ignition in such runs.

The second principal effect of the water curtain was to delay the propagation of a deflagration or detonation. Figures 7, 8, and 9 illustrate this fact graphically. High frequency oscillations which were generally recorded at each station after passage of a detonation wave have been omitted from the figures for purposes of clarity. These oscillations were usually of relatively low amplitude though occasionally they obscured, to some degree at least, subsequent pressure pulses. The reflected waves (see below) at station 12 of Figure 7 and at station 9 of all three figures were so affected and consequently their representations are less precise.

As indicated in Table I, the three water injection ports are located between stations 2 and 3. From Figures 7 and 8 especially, it is evident that the water curtain attenuated the shock recorded at station 2. If it is assumed that the first pressure disturbance recorded at station 3 (Fig. 7) is due to the shock at station 2, then the average velocity of the wave between the two stations is about 200 m/sec. Clearly, the water curtain not only attenuated the shock but also caused the wave to travel at an apparently subsonic velocity. The pressure traces at stations 4 and 9 give evidence that a flame emerged from the water curtain and subsequently accelerated to form a detonation between the two stations. The second

peak at station 9 is due to the wave traveling upstream after being reflected off the closed downstream end of the tube. The reflected wave is seen at a later time at station 4, than at 3 and finally at 2. Between stations 3 and 2, the reflected wave was again attenuated as it passed through the water curtain.

Because a detonation was formed between stations 4 and 9 in this run, the double peaks, recorded on the station 4 trace between the incident and reflected waves, are believed to be due to a retonation wave. This wave has been partially overtaken by the reflected wave at station 3 and hence the latter wave was strengthened to the point of going off the film (indicated by the dotted lines). It is believed that the double peaks recorded on the station 4 trace are due to the three dimensional characteristics of the combustion in such a large volume. Inside a tube of 54.6 cm diameter, a deflagration wave traveling through a combustible mixture is not a plane surface but rather it advances as tongues of flame leap forward at various acute angles with the tube axis. Consequently, the pressure disturbances which result from these tongues of flame and which are propagated in all directions reach various points on a given circumference of the tube at different times. The waves are then reflected from the tube walls, interact, etc. In consequence of this behavior, a pressure transducer, which occupies but a small point on the large circumference of the tube, can be expected to receive multiple pressure disturbances as it is passed by deflagration or retonation waves. A detonation wave, because of its velocity, is more likely to be planar and therefore less apt to cause multiple pressure peaks as it passes a transducer.

DISCUSSION

Systematic studies of detonations in fuel-air flames have so far not been reported in the literature. However Bollinger, Fong and Edse (Ref. 2) found that hydrogen-oxygen flames, slightly diluted with nitrogen have a shorter induction distance from the spark to the onset of detonation at 5 atm initial pressure than at ambient conditions. Thus detonations seem to be induced more easily at high pressures than at 1 atm. It has now been established that hydrogen and ethylene-air mixtures will detonate given high enough initial pressure in tubes as short as approximately 10 meters. The reason for this fact is not entirely clear. A trivial explanation would be that at lower pressures the tube diameter (38 mm) is below the critical diameter necessary for detonation. This however overlooks the fact, as discussed below, that a small diameter tube may induce detonations more readily than a tube of large diameter. More significant is the fact that even at low pressure, deflagration or pressure pulses reach very high velocities that are normally the precursor of detonation. It is felt that the greater ease with which detonations are established at higher pressure is due to the slower dissipation of heat due to the higher density of the burnt gas. The way a deflagration forms a detonation can be described in general terms as follows: A laminar flame close to the spark is driven forward by the expansion of the burnt gases and gradually becomes highly turbulent. Very high velocities up to 1000 meters/sec are recorded during this stage. Shock waves are formed and partially overtake the flame front. These shock waves form a detonation rather suddenly, creating strong pressure pulses that are also transmitted through the walls of the steel tube and record on the pressure transducers. These pressure pulses in some instances allow to determine the accurate location of the onset of detonation. The burnt gases also will suffer heat losses due to conduction to the wall. It seems that a critical condition is reached at an early stage before the turbulent flame reaches high velocities. If the burnt gases cool fast enough at low pressure then the forward thrust of the flame front will not reach the value necessary to create the turbulent flame that in turn reaches the very high velocities. The creation of the fast turbulent flame will therefore depend on pressure that controls the dissipation of heat of the

burnt gases, and on the fundamental burning velocity which controls (together with the forward movement of the gas) the flame speed. This explains the greater ease with which hydrogen-air forms the fast turbulent flames than ethylene-air. In methane-air the very fast flames were never observed.

A second critical condition not yet fully understood is the ease with which a detonation forms from shock waves. This condition may be related to spontaneous ignition with short induction period. In general terms the formation of a detonation thus would depend on two conditions; one relates to the formation of very fast turbulent flames that will create shock waves, the second concerns ignition from shock waves.

Methane-air flames have a smaller burning velocity than ethylene-air flames, but the reduction is rather minor when one considers the differences between hydrogen and ethylene. It is therefore a surprise that methane-air flames do not give rise to detonations at 40 atm; in fact the deflagration is so mild that pressure ratios are very small and much less than theoretical. At one atmosphere the rate of heat dissipation is comparable to the formation of heat in the flame front, thus a fast flame never materializes in a tube of small diameter. At high pressure it has been found that the fundamental burning velocity of methane-air is greatly reduced (Ref. 3), and is only about 6 cm/sec at 40 atm. Thus again no fast turbulent flame will form. Methane-air flames seem to be unique in that increased pressure does not promote detonation. In general, it is felt that increased pressure has an influence on the first conditions (fast turbulent flame) for detonation rather than on the second (formation of detonation from shock waves) as shock waves of a given pressure ratio will lead to nearly identical temperature increases independent of initial pressure.

It is also interesting to note that detonations always occurred between stages 1 and 2; thus either detonation sets in relatively early or not at all. It is therefore questionable whether hydrogen-air would detonate in a tube of 100 meters length and 38 mm diameter at a lower pressure than in the 10 meter long tube.

In making a comparison between the data on the large and small tube it has to be realized that practically all data were taken in a region where

detonation is marginal. Thus no stable detonation velocities are established as yet, detonations may be overdriven and overpressures may be present. This region is of little interest theoretically but of great interest practically as all fuel-air detonations are marginal.

Originally the comparison between small and large tube was made to ascertain that the high pressure data discussed above are meaningful, i.e. may be applicable to the large tube. The oxygen index was thus chosen for a comparison. It was quite unexpected to find that detonations need a higher oxygen index in the large tube than in the small one.

The course of events from spark to detonation as sketched before helps to understand the phenomenon. The early slow flame and its burnt gases will expand into three dimensions rather than only into one direction as in the small tube. Thus accelerations are smaller and a fast turbulent flame will form later or not at all within the given geometry. This qualitatively explains the slower original velocities and the higher oxygen indices necessary for detonation in the large tube. Shock waves formed in the turbulent flame will not only move forward but undergo multiple reflections on the walls and be more subject to attenuation before they can cause a detonation.

Overpressures and overdriven detonations have been observed before but have not been extensively studied. They are of great importance if one considers the safety of containers where explosions or detonations may occur. The present data allows a closer analysis of these phenomena. Little evidence of overpressures is found in the small tube, whereas truly astonishing pressure ratios are found in the large tube. It seems that two phenomena contribute to the large pressures observed and both can only occur in marginal detonations. In the first case a detonation develops so late in the tube that the unburnt gas was already precompressed before the detonation reaches the end of the tube. Evidence of this precompression has been found; it has, however, to be pointed out that events under conditions of marginal detonation are not very reproducible. Also the pressure transducers had to be calibrated to read up to 100 atm thus a precompression of one or two atmospheres is difficult to detect on the records. As detonations

developed in the small tube always very early, the detonation could overtake the precompression wave and no overpressures are possible.

A second cause of overpressures is due to the reflection of shock waves at the end of the tube with possible contributions from the adiabatic compression in the tapered end section of the large tube. Ignitions have been observed due to incident, reflected and double shock waves. In each case the ignition occurs in precompressed gas, thus leading to overpressures. The largest pressure ratio observed being 80.

It was hoped that powerful water curtains would cause deflagrations or detonations to die out or at least to moderate appreciably the pressure peaks in the vessel. This was not found to be the case. Details of the events in the water curtains are fully discussed in the previous paragraph.

Finally it may be mentioned that the very high pressure peaks could be fully substantiated by strain gage measurements on the outside wall of the large vessel.

Acknowledgments

The authors wish to thank Messrs. A. H. Clark and R. H. Tromans for conducting the experiments and Mr. J. Macatician for many valuable discussions. This work was supported by the U. S. Navy under contract NOas 60-6047c.

REFERENCES

1. Gerstein, M., Carlson, E. R., and Hill, F. U., Ind. Eng. Chem., 46, 2558-62, (1954).
2. Bollinger, L. E., Fong, M. C., and Edse, R., WADC Technical Report 58-591, August, 1959 (ASTIA Document AD 239 677).
3. Wolfhard, H. G., The Burning Velocity of Methane Flames at High Pressures, Trans. Farad. Soc., 52, 1, 1956.
4. Bone and Townend, Flame and Combustion in Gases, Longmans, Green and Co., London (1927).

TABLE I. LOCATIONS OF STATIONS AND WATER INJECTION PORTS

<u>STATION</u>	<u>DISTANCE FROM SPARK, meters</u>	
	<u>54.6 cm TUBE</u>	<u>38 mm TUBE</u>
1	1.00	0.80
1a		1.53
2	1.48	3.30
3	2.49	5.31
4	3.50	6.30
5	4.00	7.30
6	5.01	7.80
7	6.01	8.30
8	7.01	8.80
9	8.01	
10	8.51	
11	9.01	
12	9.51	
End-Flange	9.85	9.15
<u>WATER INJECTION PORT</u>		
1	1.79	
2	1.97	
3	2.15	

TABLE III

MINIMUM OXYGEN INDEXES OF MIXTURES AT ONE ATMOSPHERE SUPPORTING DETONATIONS
IN EACH TUBE (ALSO NEXT LOWER O.I.'S. TESTED)

54.6 cm TUBE				38 mm TUBE				
FUEL	O.I.	O/F	ONSET (DISTANCE FROM SPARK) Meters	RUN NO. 10B-1-X-	O.I.	O/F	ONSET (DISTANCE FROM SPARK) Meters	RUN NO. 10B-1-X-
H ₂	0.30	9.53	3.5 - 8.0	113	0.23	0.56	3.3 - 7.8	149
	.25	.55	Deflagration	53	.21	.49	Deflagration	156
C ₂ H ₄	0.37	3.4	1.5 - 4.0	97	0.30	3.5	0.8 - 3.3	148
	.34	3.3	3.5 - 8.0	133*	.21	3.2	Deflagration	177
	.33	3.1	Autoignition	96				
	.30	3.6	Deflagration	95				
CH ₄	0.52	1.8	1.5 - 4.0	85	0.32	2.2	3.3 - 7.8	142
	.48	2.5	Autoignition	90	.29	2.3	Deflagration	150
	.47	2.1	Autoignition	124				
	.45	1.8	Deflagration	84				

* Water injection occurred in this run.

TABLE IV

INCIDENT WAVE DATA FOR MIXTURES AT ONE ATMOSPHERE IN 38 mm TUBE (a)

O.I.	O/F	RUN NO. 10B-1-X-	PRESS. AT STATION (b)				AV. VELOCITY BETWEEN STATIONS				CHARACTER OF REACTION
			2	6	7	8	0-6	6-7	7-8	0-2	
			Atmospheres absolute				Meters per second				
H₂											
0.23	0.56	149	9.5	17.1	~15	354	1670	166	2040	Detonation 2-6	
.26	.57	139	8.5			~500		250	~1900	Detonation 2-6	
C₂H₄											
0.30	3.5	148	14.3	19.7	14.5	406	1670	192	2250	Detonation 1-2	
.32	3.4	145	21.6	18.8	15.0	600	1670	311	1875	Detonation 1-2	
.37	3.5	146	17.3	16.4	13.8	722	1670	384	2040	Detonation 1-2	
.45	3.5	147	20.5	17.0	14.8	1040	2000	590	2370	Detonation 1-2	
CH₄											
0.32	2.2	142	7.7		13.1	291	1000	150	938	Detonation 2-6	
.36	2.4	143	7.8		12.1	481	1000	270	1140	Detonation 2-6	
.42	2.4	144	9.9		~12	~620	~1670	344	~1550	Detonation 1-2	

(a) Only runs in which detonations were formed are given. Data for flame front of deflagration runs cannot be obtained from the pressure transducers alone.

(b) Pressure changes due to incident wave at station 1 were negligible or so slight that error is disproportionate. (Any rises were very gradual).

No precompression was observed prior to arrival of wave at any station in any run.

TABLE V

INCIDENT WAVE DATA FOR MIXTURES AT ONE ATMOSPHERE IN 54.6 cm TUBE (a)

O.I.	O/F	RUN NO. 10B-1-X-	PRESSURE AT STATION			RECOMPRESSION AT STATION			AV. VELOCITY BETWEEN STATIONS			DETONATION ONSET BETWEEN STATION			
			5	9	11	5	9	11	0-9	9-10	10-11		10-11		
			Atmospheres Absolute			Atmospheres Absolute			Meters per Second						
<u>H₂</u>															
0.30	0.53	113		~28		3.8	3.3	3.6	294	2270	1610	4 - 9			
.31	.57	54		22		3.6	3.1	4.5	307	3120	2380	8 - 9			
.33	.56	55	1.6	19	17.4	1.4	1	1	504	2170	1720	2 - 5			
.40	.57	56	19	16	12	1.6	1	1	611	2270	1670	2 - 5			
.40	.58	111	2.1	21	13.4	1	1	1	585	2270		2 - 3			
<u>C₂H₄</u>															
0.37	3.4	97		28.6	24.7	24.8	26.5	1.6	1	1	1	380	2270	1610	2 - 5
.38	3.6	109		>34.7	35	35	5.6	5.1	3.0			276	3120	1850	3 - 9
.43	3.5	98		26.8	28	28	22.9	1	1	1	1	581	2380	2380	2 - 5
<u>CH₄</u>															
0.52	1.8	85	2.1	33.3	28.8	24.9	24.9	1.6	1	1	1	469	1850	2080	2 - 5
.56	2.5	91	1.9	~26.5	~21	~18.4	~18.4	1.4	1	1	1	413	2000	1785	2 - 5

(a) Only runs in which detonations formed are given. Data for flame front in deflagration runs cannot be obtained from the pressure transducers alone. Same is true for runs in which autoignition occurred.

TABLE VI

AUTOIGNITION RUNS IN 54.6 cm TUBE

FUEL	O.I.	O/F	RUN NO. 10B-1-X-	PRESS. DUE TO LAST SMALL SHOCK @ 12 ATM. ABS.	IDEAL TEMP. DUE TO LAST SMALL SHOCK @ 12, CALC. °C	PRESS. DUE TO AUTOIGN. PULSE @ 12 ATM. ABS.	DOUBLE SHOCKS, TWO PASSES	MECHANISM
								DOUBLE SHOCK SINGLE PASS. SINGLE SHOCK SINGLE PASS. SINGLE SHOCK SINGLE PASS.
H ₂	0.32	0.34	80	6	117	~60		x
C ₂ H ₄	0.29	2.3	101	~14		>30	x	
	.33	3.1	96	13.7	332	>57		x
	.38	3.3	108*	7		>57		x
	.37	4.6	105	~12		>56	x	
CH ₄	0.39	2.1	72	~17		~80		x
	.45	2.3	118*	7.2		>53		x
	.47	2.1	124	~23		~66		x
	.47	2.2	114*	8		>52		x
	.48	2.2	120*	6		>57		x
	.48	2.5	90	11.5	307	>61		x
	.56	2.7	86	6		~77		x

* Water injection occurred in these runs.

TABLE VII

SUMMARY OF WATER INJECTION RUNS AND SIMILAR RUNS WITHOUT WATER INJECTION

FUEL	O.I.	O/F	RUN NO. 10B-1-X	H ₂ O FLOW RATE Kg/Sec	Δt - TIME BETWEEN H ₂ O INITIATION AND SPARK Signal, Sec.	CHARACTER OF REACTION
H ₂	0.21	0.52	126	51	0.86	Apparently no Combustion
	.21	.53	135	51	—	Apparently no Combustion
	.21	.54	52	a		Deflagration
	.21	.63	136	a		Deflagration
	.21	.67	137	51	.25	Deflagration
	.29	.51	131	51	~.8	Apparently no Combustion
	.29	.53	130	51	~.8	Detonation 4 - 9
	.30	.54	112	51	—	Detonation 4 - 9
	.30	.53	113	a		Detonation 4 - 9
	.33	.56	55	a		Detonation 2 - 5
	.37	.59	110	51	.21	Detonation 0 - 2
	.40	.57	56	a		Detonation 2 - 5
	C ₂ H ₄	0.21	3.1	134	51	—
.21		3.3	127	51	.86	Apparently no Combustion
.23		3.1	93	a		Deflagration
.33		3.1	96	a		Autoignition
.34		3.3	133	51	~.8	Detonation 4 - 9
.37		3.4	97	a		Detonation 2 - 5
.38		3.3	107	48.5	.13	Autoignition
.38		3.6	109	a		Detonation 3 - 9
.39		3.3	108	51	.17	Autoignition
CH ₄	0.32	2.1	71	a		Deflagration
	.32	2.3	132	51	—	Apparently no Combustion
	.35	2.8	89	a		Deflagration
	.36	2.3	115	51	.20	Deflagration
	.37	1.8	83	a		Deflagration
	.39	2.1	73	48.5	—	Apparently no Combustion
	.39	2.1	72	a		Autoignition
	.39	2.2	116	a		Deflagration
	.45	1.8	84	a		Deflagration
	.45	2.2	117	51	.25	Apparently no Combustion
	.45	2.3	118	51	.28	Autoignition
	.47	2.1	124	a		Autoignition
	.47	2.2	114	51	.19	Autoignition
	.48	2.2	120	51	~.8	Autoignition
	.48	2.5	90	a		Autoignition
.49	2.1	119	51	.37	Detonation 4 - 9	
.56	2.5	91	a		Detonation 2 - 5	
.57	2.1	51	36	—	Detonation 0 - 2	

a - No water injected in these runs.

FIGURE 2. EFFECT OF PRESSURE ON HYDROGEN-AIR MIXTURES (38 mm TUBE)

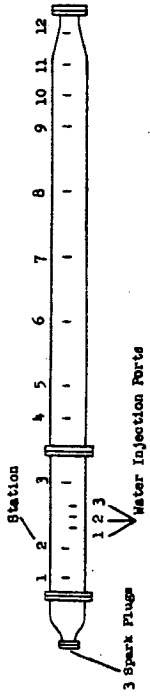


Figure 1(a). Diagram of 54.6 cm Tube



Figure 1(b). Diagram of 38 mm Tube

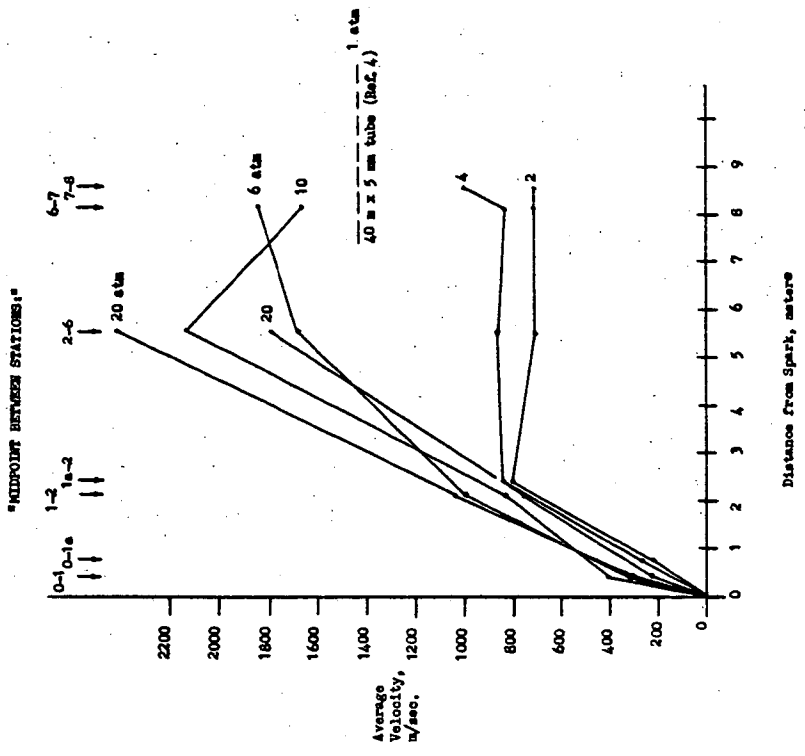


FIGURE 3. EFFECT OF PRESSURE ON ETHYLENE-AIR MIXTURES (38 mm TUBE)

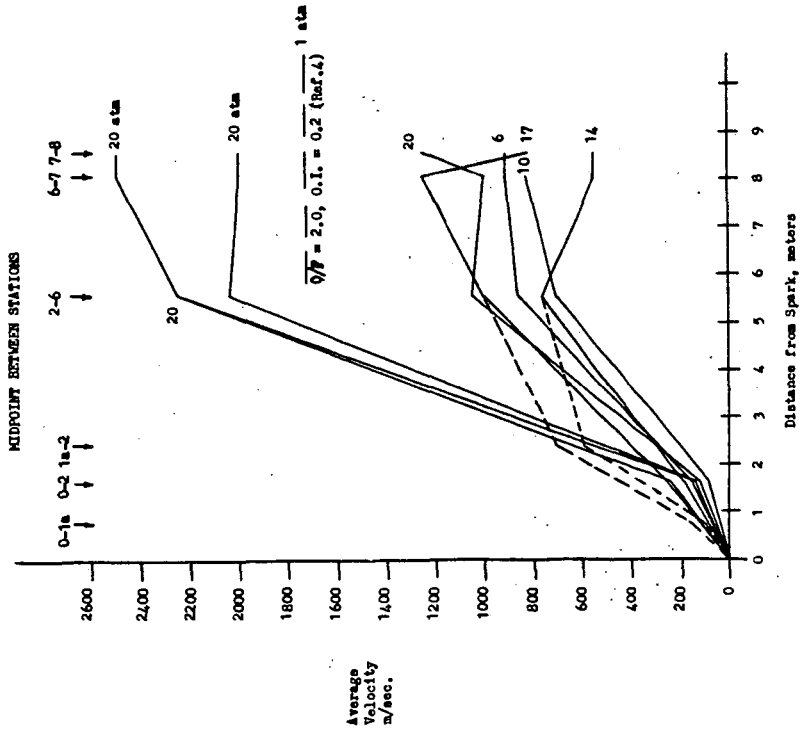


FIGURE 4. HYDROGEN-ENRICHED AIR RUNS IN BOTH TUBES AT ONE ATMOSPHERE

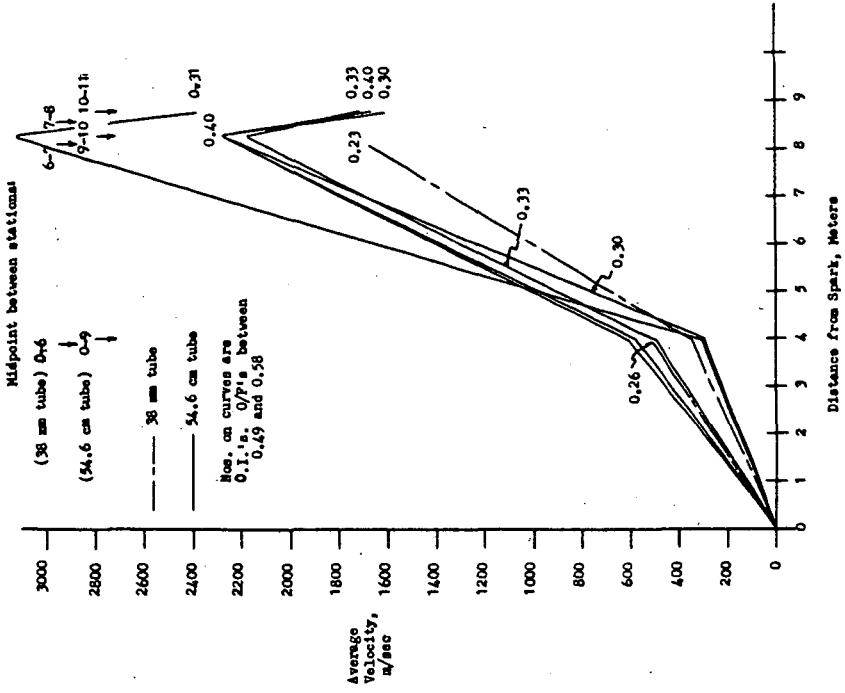


FIGURE 5. ETHYLENE-ENRICHED AIR RUNS IN BOTH TUBES AT ONE ATMOSPHERE

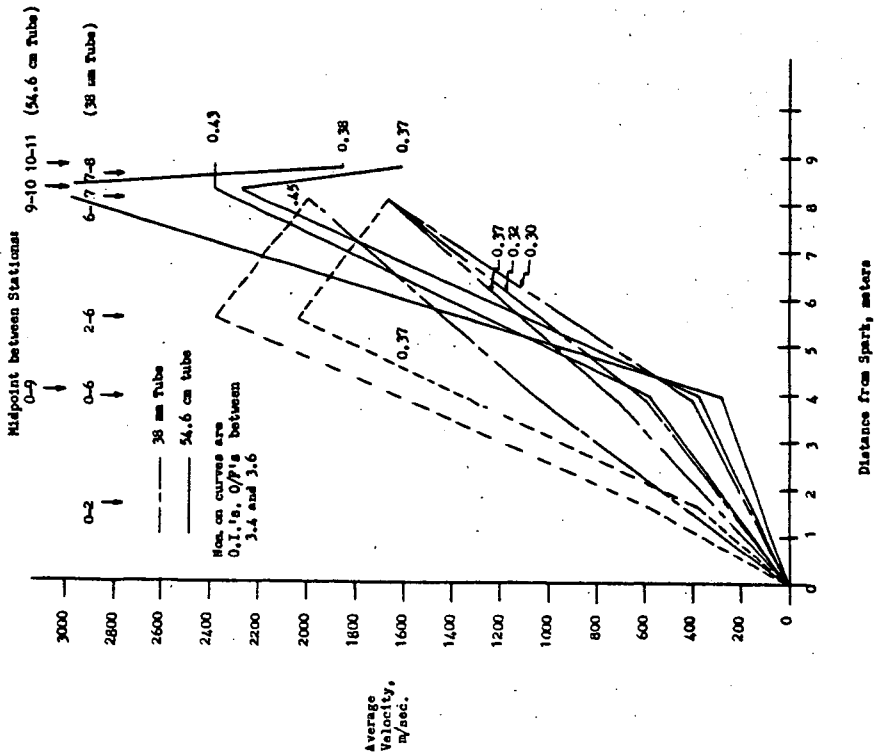
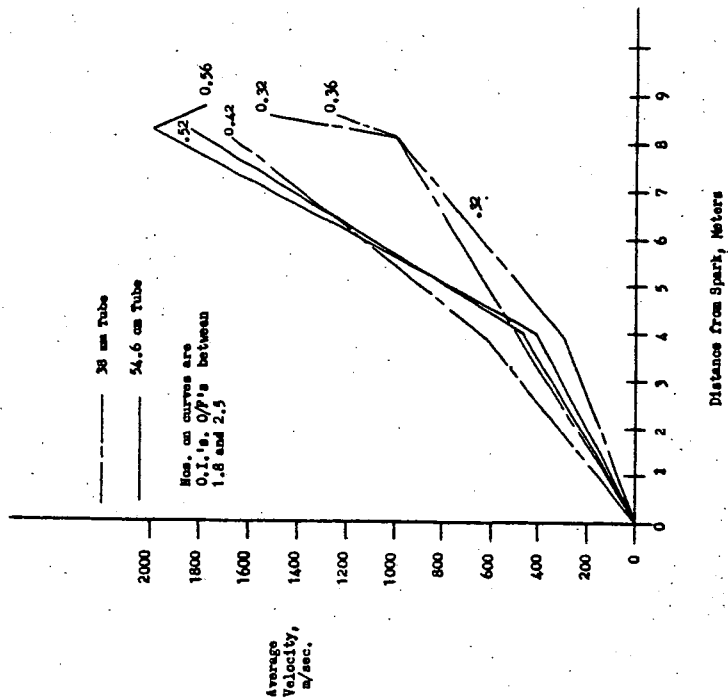


FIGURE 6. METHANE-ENRICHED AIR RUNS IN BOTH TUBES AT ONE ATMOSPHERE



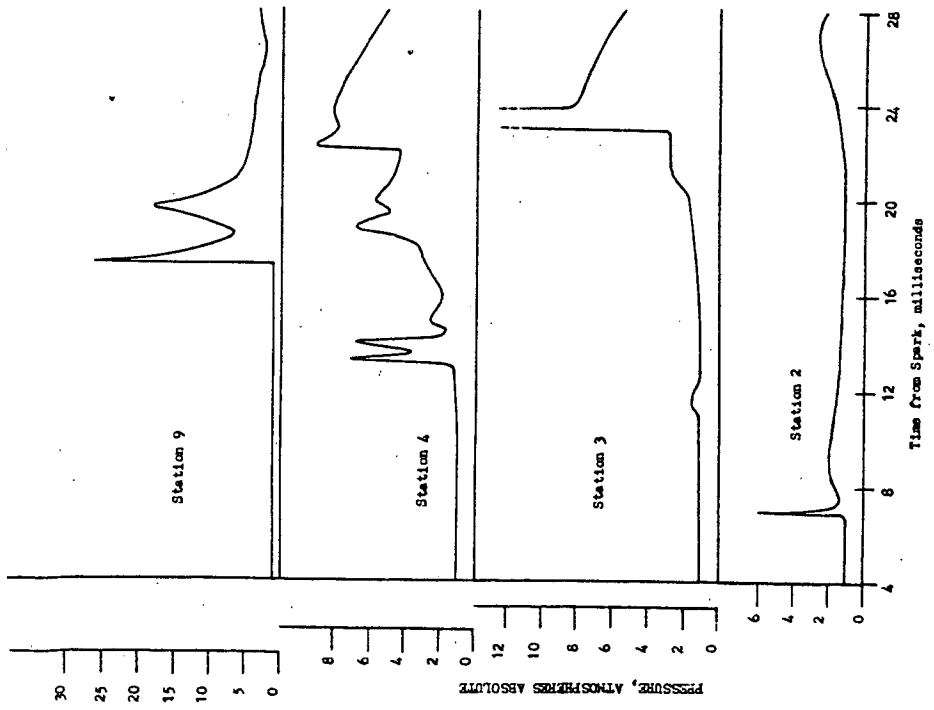


FIGURE 7. PRESSURE-TIME TRACES OF H₂-O₂-H₂ RUN (#112) WITH WATER INJECTION

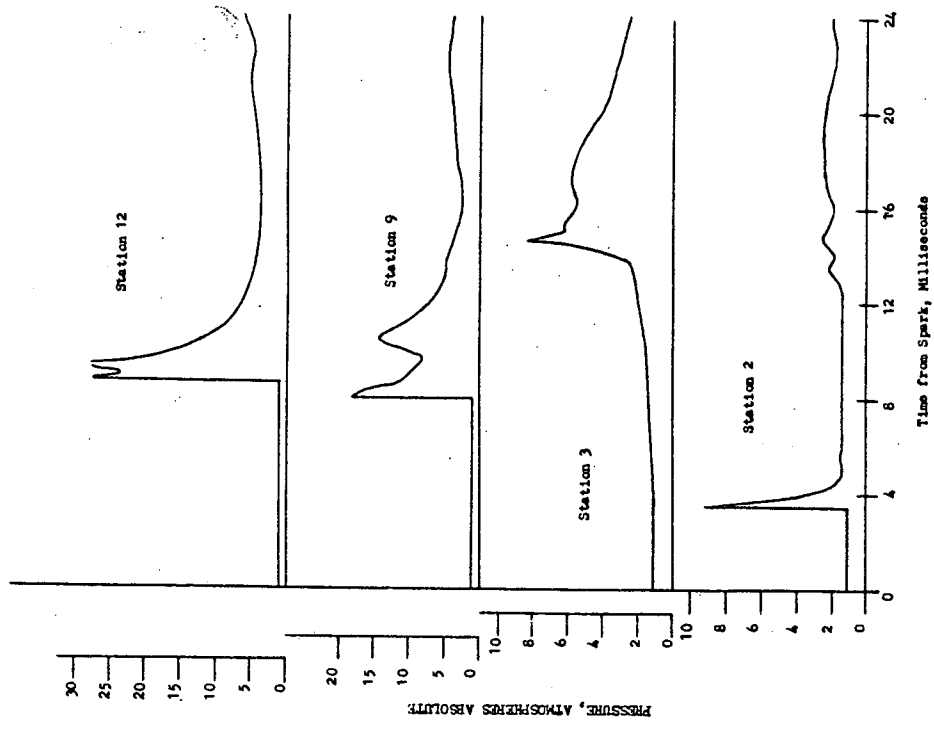


FIGURE 8. PRESSURE-TIME TRACES OF H₂-O₂-H₂ RUN (#110) WITH WATER INJECTION

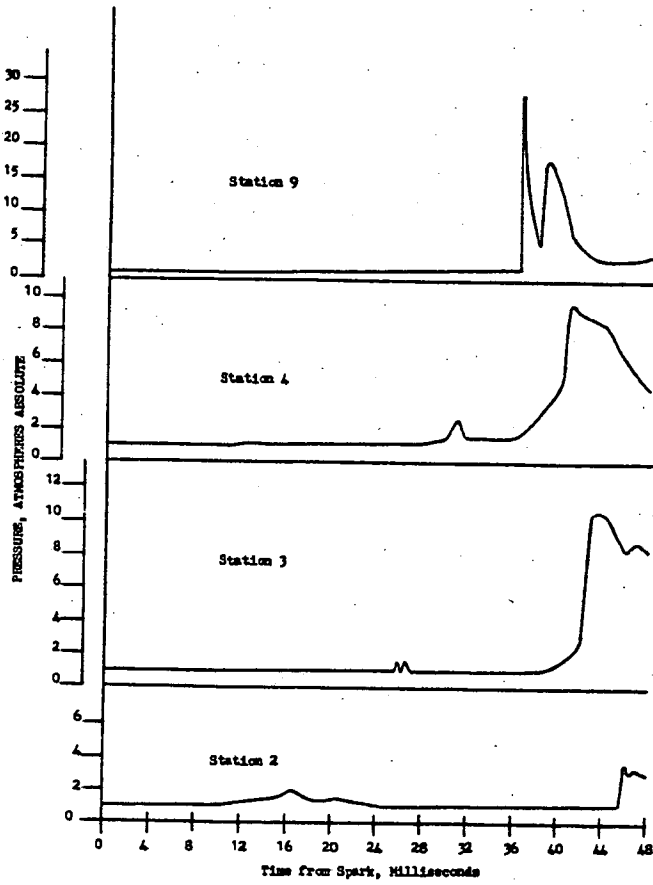


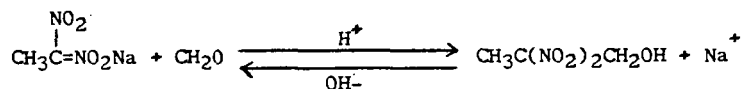
FIGURE 9. PRESSURE-TIME TRACES OF $\text{CH}_4\text{-O}_2\text{-H}_2$ RDE (#119) WITH WATER INJECTION

SYNTHESIS OF 2,2-DINITROPROPANOL.
STUDIES ON CONTINUOUS PREPARATION

Edward E. Hamel, John S. Dehn, Joseph A. Love
Joseph J. Scigliano, and Arden H. Swift

Aerojet-General Corporation, Sacramento, California

A program was undertaken to investigate various methods of preparing the 2,2-dinitropropanol (I), with the ultimate objective of developing a process suitable for large scale production. With the exception of one synthetic route, which will be discussed later, the key step in the synthesis of I is the preparation of 1,1-dinitroethane (II) or its nitronate salt. The conversion of II to I is straightforward using the method of Henry¹ in which an aqueous suspension of the dinitroparaffin is treated with formaldehyde in the presence of a basic catalyst. In practice, it is usually more convenient to start with the nitronate salt of the dinitroparaffin and add one equivalent of acid to the solution:



The product is isolated by extraction with a solvent followed by removal of the solvent in vacuo to leave I in the form of a waxy white solid. The material prepared in this manner is of satisfactory purity for use as an intermediate in most reactions without further purification. Analytically pure I can be prepared by repeated sublimation in vacuo; it is quite hygroscopic when pure and its melting point (92-94°) is extremely susceptible to depression by small amounts of impurities.

At the outset of this work, two routes to II were known which appeared sufficiently attractive for investigation as potential production processes.

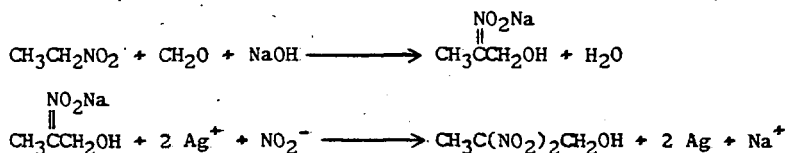
OXIDATIVE-NITRATION REACTION

The most convenient method for preparing gem-dinitro compounds involves the reaction discovered by Kaplan and Shechter² in which treatment of the nitronate salt of a primary or secondary mononitroparaffin with silver nitrate and an inorganic nitrite in aqueous media gives the corresponding gem-dinitro compound and metallic silver:

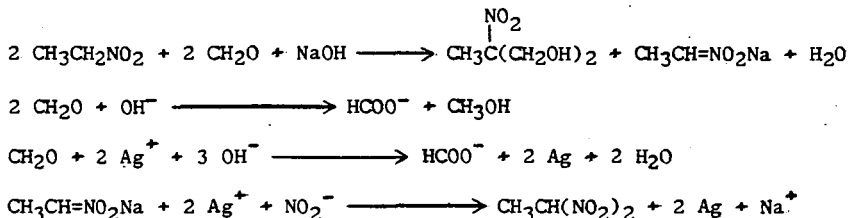


The reaction, which has been termed an oxidative-nitration process, has been used to prepare a variety of primary, secondary, and functionally substituted dinitroparaffins. The silver produced in the reaction may be separated and converted to aqueous silver nitrate by treatment with concentrated nitric acid; after pH adjustment of the resulting solution to 5-6, it is ready for re-use.

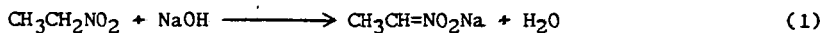
The preparation of I by this procedure was initially carried out in these laboratories via the intermediate sodium 1-hydroxy-2-propanenitronate, which in turn was prepared by treatment of a suspension of nitroethane in aqueous formaldehyde with sodium hydroxide:



Overall yields of 65-70% (corrected for the purity of commercial grade nitroethane) were obtained. Principal drawbacks to this procedure were side reactions which could be suppressed, but not eliminated, by careful control of reaction variables:



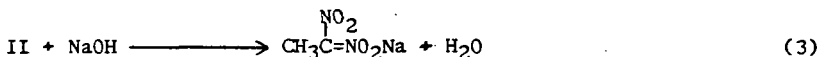
To circumvent these side reactions, a modified procedure was developed in which the oxidative-nitration was carried out before the methylation step:



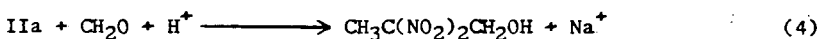
III



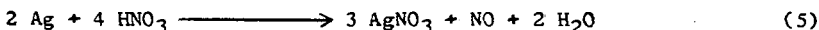
II



IIa



I



Under the conditions described below, laboratory yields in reactions 1-4 were approximately 98, 90, 98, and 97% respectively. With a 95% extraction recovery of I from the aqueous layer, this gives an overall yield of 80% based on nitroethane. A typical analysis of material produced by this method is given in Table 1. Reaction 5 is essentially quantitative and losses in this step are primarily mechanical; silver losses will be discussed later in this section. Reaction 1 was carried out at 0-10° in most instances, although temperatures up to 20° could be used without noticeable change in results; at temperatures above ambient, side reactions leading to trimethylisoxazoles become appreciable.³ Using a 5-10% excess of sodium hydroxide, added with vigorous agitation to the nitroethane-water suspension, the reaction was complete within 10 minutes after completion of addition of the base. At this point, sodium nitrite was added and the resulting solution (at 0-10°) was added rapidly to a vigorously stirred solution of the silver nitrate maintained at -5 to

0°. As reaction 2 proceeded, a solid (presumably an intermediate complex²) separated and the mixture became extremely thick, then progressively less viscous as metallic silver separated; the reaction is accompanied by an exotherm, and external cooling was applied as required to keep the temperature below 20°. When the exotherm was over, 50% sodium hydroxide was added over a 15-minute period at 15-20° to convert II to its water soluble sodium salt (reaction 3) and to precipitate excess silver ion as silver oxide. After filtration and water washing of the silver, the pH of the combined filtrates was reduced to 9-10 with acetic acid; a 10% excess of 37% formaldehyde was then added and the acidification was continued until a pH of 5.0-5.5 was reached (reaction 4). The aqueous solution, containing 7-9% of I was then extracted with ethylene chloride either batchwise or in a countercurrent column. Extraction efficiencies of 94-96% were attained. The ethylene chloride solution of I was then concentrated in vacuo to the desired strength prior to use as an intermediate in subsequent reactions. The metallic silver recovered from the oxidative-nitration step was converted to silver nitrate by slurrying in water and treatment with a slight excess of 67% nitric acid at 30-40°. The pH of the resulting solution was then adjusted to 5-6 with sodium hydroxide; some silver oxide was formed in this step, but did not interfere with use of the solution in a subsequent oxidative-nitration, since the oxide is also converted to silver in the reaction.

The procedure was adapted to batch pilot plant operation using 0.5 lb mole of nitroethane, and was eventually increased to a 2.0 lb mole scale. Although the overall yields on the pilot plant scale averaged about 5% lower than those obtained in laboratory preparations, the process presented no major scale-up problems. In initial pilot plant studies, silver was recovered by centrifuging the slurry after the neutralization step in which II was converted to its soluble sodium salt. In order to reduce silver losses due to handling, internal stainless steel filters were subsequently installed in the oxidative-nitration reactor and the slurry was pressure filtered rather than centrifuged. Using this procedure, the silver was not removed from the kettle from run to run; after filtration and washing, the silver was slurried with water and nitric acid was added to regenerate silver nitrate. Handling losses were reduced considerably and would have been reduced further had it not been for the occasional formation of very finely divided silver in the reaction. When this occurred, filtration was extremely slow and it was necessary to allow the slurry to settle, after which the supernatant liquid could be removed by siphoning. Subsequent washing of the silver was difficult and inefficient, and silver losses occurred despite filtration of the siphoned material. The cause of fine silver formation was not determined but appeared to be associated with the buildup of small quantities of organic material in the silver. Thus, once finely divided silver had formed, the problem was greatly magnified since it was difficult to wash the silver adequately, and the buildup of organic material in the silver cake increased rapidly in subsequent runs. It has been our experience that the best way to avoid this difficulty is to maintain a uniform dispersion of silver in the mixture by providing excellent agitation during the oxidative-nitration, neutralization, and silver washing steps.

Several hundred thousand pounds of I were produced by the oxidative-nitration method at this facility. Under normal operating conditions, silver losses averaged about 1%. Over short periods of time, losses ran as low as 0.5% and as high as 2%. The 1% loss can be tolerated for the preparation of development quantities of I but becomes a serious drawback for larger scale production. Other economic disadvantages to the process are the required use of expensive low-chloride grade sodium hydroxide (to avoid formation of silver chloride) and the relatively large quantities of nitric acid required to regenerate silver nitrate from recovered silver. A study of an alternate procedure, not requiring the use of silver nitrate, was therefore undertaken. It should be mentioned that a modification of the oxidative-nitration has been described recently⁴ in which the reaction is carried out in an electrolytic cell, with silver ion being regenerated as it is consumed. While this procedure

shows promise of overcoming the problem of silver losses, a considerable amount of development work remains to be done before its ultimate potential for large scale production is known.

TER MEER REACTION

An alternate method for preparing salts of terminal gem-dinitro compounds that has been known for many years is the ter Meer reaction,⁵ and involves treatment of 1-halo-1-nitroparaffins with nitrite ion in basic media to give the anion of the terminal gem-dinitro compound and chloride ion. In the case of 1-chloro-1-nitroethane the reaction is:



In practice it is desirable (by suitable choice of reaction solvent and/or metal cation) to force separation of the nitronate anion from the reaction mixture as a sparingly soluble salt as it is formed. In this manner, side reactions are suppressed and the reaction is driven to completion. Potassium ion is the cation of choice since potassium 1-nitro-1-ethanenitronate is sparingly soluble in water and essentially insoluble in most organic solvents; the sodium salt may be employed satisfactorily in nonaqueous systems but gives poor results in aqueous media, presumably due to its high solubility. The most commonly used solvents for the reaction are water, alcohol, or water-alcohol mixtures. The choice of base in the reaction is important. Strong bases, such as alkali metal hydroxides, give only fair results since they readily attack the 1-halo-1-nitroparaffin to give not only the nitronate salt but side reaction products resulting from cleavage of both C-NO₂ and C-Cl bonds. Extremely weak bases result in slow rates and incomplete reaction. Best results have been obtained using carbonates or, specifically, potassium carbonate. Reaction temperatures of 0-25° and times of 30-120 minutes are generally used; good agitation is essential to high conversions since the reaction system is heterogeneous regardless of the solvent employed. The product, potassium 1-nitro-1-ethanenitronate, is usually purified by filtration and washing with methanol to remove organic impurities which are adsorbed on the salt. This operation is undesirable inasmuch as the potassium salt, when dry, is quite sensitive to detonation by shock. It has a 50% fire point of less than 5 cm using a 2 kg weight in the Bureau of Mines impact tester (about the same as nitroglycerin). The material may be handled safely, provided it is kept wet with water or an organic solvent. The degree of improvement in impact stability depends upon the amount and nature of the solvent; water or aqueous alcohol is quite effective in amounts in excess of 30% based on the weight of the dry salt. The salt is easily converted to the dinitro-alcohol, I, by treatment with aqueous formaldehyde and acid as described in the previous section.

The ter Meer route to I was investigated at these facilities several years ago, both on a laboratory and small pilot plant scale. The best grade of 1-chloro-1-nitroethane available at the time in the quantities required was material of 80% purity. It also contained nitroethane (9.0%), 2-nitropropane (1.2%), 2-chloro-2-nitropropane (3.7%), and 1,1-dichloro-1-nitroethane (6.1%). In the laboratory, overall yields of I ranging from 57-62% (corrected for purity of the starting material) were obtained; the purity of I was acceptable (95-98%) provided the potassium salt of dinitroethane was filtered and washed thoroughly with methanol before proceeding with the methylolation reaction. However, procedures designed to avoid isolation of the hazardous salt on a pilot plant scale gave product of inferior quality. Thus, when the crude product slurry of the potassium salt was treated directly with formaldehyde and sulfuric acid, and the resulting product isolated by solvent extraction and vacuum stripping, product purity was only 85%;

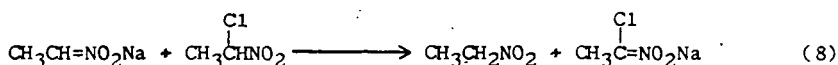
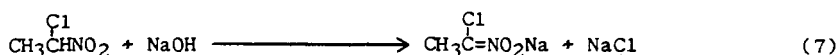
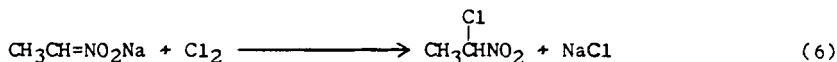
the bulk of the impurities were those present in the original 1-chloro-1-nitroethane. When the aqueous product solution of I was extracted with n-hexane to remove impurities before the ethylene chloride extraction, an improvement in quality to a maximum of about 93% was obtained. In view of these results, and taking into account the cost of 1-chloro-1-nitroethane at the time (\$1.50/lb, available in development quantities only), work on this route to I was discontinued in favor of the oxidative-nitration process. Recently, however, it was shown by other workers⁶ that the method commonly used to prepare 1-chloro-1-nitroethane, namely, the reaction of aqueous sodium ethanenitronate with chlorine, gave a product of considerably improved purity

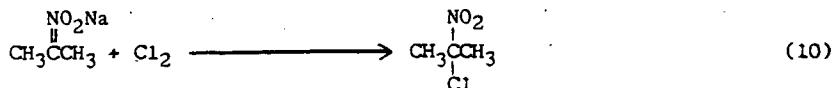
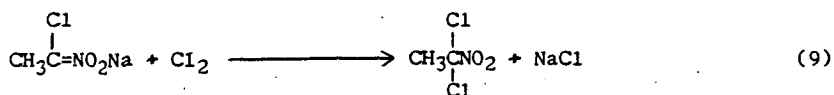


under certain reaction conditions. These results were confirmed and led to a detailed study of the chlorination reaction, as well as to a re-examination of the ter Meer route to I. Emphasis was placed on the development of continuous processes; batch runs were used primarily to outline the most promising conditions for continuous operation.

Preparation of 1-Chloro-1-Nitroethane. The first step in the synthesis, the conversion of the weak acid, nitroethane, to its sodium salt, presents little difficulty by either batch or continuous methods. Nitroethane is simply treated with aqueous sodium hydroxide at 0-10° in a well agitated vessel; in our work it was advantageous to employ concentrations which gave a solution containing approximately 23% of the salt. In batch runs, a sodium hydroxide addition time of 15 minutes and a post addition stirring period of 15 minutes gave excellent results. In continuous runs using the two stage reaction system shown in Fig. 1, a residence time of 45 minutes gave essentially complete conversion. Much shorter reaction times can be employed satisfactorily using extremely vigorous agitation, provided the heat of reaction (approximately 14 kcal/g mole) can be removed from the system. Aqueous sodium ethanenitronate is stable for a minimum of 24 hours at 0-10°; prolonged storage times and/or higher temperatures result in gradual degradation of the salt. The samples of commercial grade nitroethane used throughout these studies had a purity range of 92.8-93.3%; the balance was composed of nitromethane (0.5-1.5%), 2-nitropropane (4-6%) and traces of 1-nitropropane and nitrobutanes. It was found possible to effect a partial purification during sodium salt formation by using an amount of sodium hydroxide exactly equivalent to the nitroethane content of the commercial material. When this was done, a small amount of oil remained on top of the aqueous layer (pH 11.0) after the salt formation reaction was complete. Separation and chromatographic analysis of the oil showed it to contain 90.6% 2-nitropropane, 9.3% nitroethane, and 0.1% nitromethane. The reason for this selectivity of reaction with sodium hydroxide was not investigated but may be due to difference in solubility of 2-nitropropane and nitroethane in water (1.7 and 4.5 ml per 100 ml of water, respectively).

The conversion of the aqueous sodium salt to the chloro derivative was found to proceed extremely fast even at 0°; crude product separated from the reaction mixture as it was formed. The most important reactions occurring in the system are:





Reactions 7, 8, and 9 lead to formation of the byproduct 1,1-dichloro-1-nitroethane. Reaction 7 can be all but eliminated by close pH control of the sodium ethanenitronate feed solution. Reaction 8 can be minimized in batch reactions by using a non-agitated system to reduce contact between the aqueous salt solution and the organic product solution and by removing the product as it is formed; in a continuous system a slight excess of chlorine can be employed. Little can be done to suppress reaction 9, but if conditions are chosen as described above to minimize 7 and 8, there is little sodium 1-chloro-1-ethanenitronate present to undergo chlorination. The extent to which 10 proceeds is dependent, of course, upon the amount of 2-nitropropane in the starting material and upon the efficiency of layer separation after salt formation, as already described.

Throughout this work, vapor chromatography was used to determine composition of the chlorination products. Using a 5-meter column packed with GE-SF-96 silicone on 35/80 Chromosorb, nitromethane, nitroethane, 2-nitropropane, and 1-chloro-1-nitroethane were separated quite satisfactorily; 1,1-dichloro-1-nitroethane and 2-chloro-2-nitropropane eluted at the same time under these conditions and were therefore recorded as a single value. Since the amount of 2-nitropropane in the starting material (nitroethane) remained almost constant, it was assumed that the amount of 2-chloro-2-nitropropane in the product remained constant at 1.5% and that any increase in the combined value for the chloronitropropane and the dichloro-nitroethane above 1.5% was due to formation of the latter material. Thus, a product giving combined value of 4.0% was assumed to contain 2.5% of the dichloro compound.

Initial chlorinations were carried out on a batch basis at 0-10° in a jacketed vessel equipped with a thermocouple well, fritted tube for chlorine inlet and a bottom takeoff for product removal. Although the initial pH of the salt solution was maintained at 11.0 and no agitation was used some dichloro compound was formed. The highest quality product obtained in this system contained 92.4% 1-chloro-1-nitroethane, 0.02% nitromethane, 1.6% nitroethane, 0.38% 2-nitropropane, and 5.60% 2-chloro-2-nitropropane plus 1,1-dichloro-1-nitroethane (4.1% of the latter based on the assumption above). Apparently, under these conditions there was enough contact between the organic and aqueous phase to permit reaction 8 to occur to some extent.

Most of the chlorination studies were conducted in continuous systems. Coiled tube and straight tube reactors gave about the same results. A straight tube chlorination system is shown in Fig. 1a. Aqueous sodium ethanenitronate was metered by a proportioning pump to a pre-cooler maintained at -10 to -15°; the salt solution then entered the chlorination tube which was cooled by a brine system maintained at the desired temperature. Chlorine was fed directly to the tube through a rotameter. Effluent from the chlorinator passed to a decanter constructed to permit continuous overflow of spent aqueous layer at the top and product removal at the bottom. The pH of the spent aqueous layer was measured either directly in the decanter or in a line connected to the overflow system. When the pH of this layer was maintained at 5.5-6.5, essentially complete conversion was assured. Early in this work, no provision was made to measure the inside temperature of the chlorinator; it was assumed that it would be within 5-10° of the temperature of the circulating coolant. It was subsequently found that this was not the case and that temperatures in the reaction

zone were 30-90° higher than that of the coolant, depending on the system flow rates, chlorinator diameter, and coolant temperature. A typical profile of reaction zone temperatures as a function of residence time is shown in Fig. 2. The higher temperatures were not deleterious, provided the residence time at the higher temperature was kept to a minimum. Thus, as shown in Table 2, the purity of the chloronitroethane remained relatively constant (94.3-95.7%) over a wide range of flow rates and maximum temperatures in those cases where the residence time above 40° was less than one minute. As the time above 40° was increased to five minutes, product quality decreased rapidly to approximately 78%.

The necessity for maintaining the pH of the sodium ethanenitronate feed solution within a narrow range has been mentioned briefly. This was found to be the most critical variable in the system. As shown in Fig. 3, best results (i.e., high purity product and high conversions) were obtained in the pH range 11.0-11.15. Below this range, the conversion of nitroethane to its sodium salt is incomplete and low conversions to the chloronitroethane result. At higher pH ranges (11.3 and above) an excess of base is present, which results in conversion of 1-chloro-1-nitroethane to its sodium salt (reaction 7) and chlorination of the salt to give the dichloro compound (reaction 9). The experiments shown in Fig. 3 were carried out with slightly less (3-5%) than the theoretical amount of chlorine in the system. In subsequent work in which a slight excess of chlorine was used, total conversions above 95% and yields approaching 92% were obtained (Table 3).

Inasmuch as the chlorination reaction is quite exothermic (approximately 45 kcal/g mole), rapid heat removal in a production scale tubular reactor could not be accomplished without utilization of a complex and expensive system. This consideration led to evaluation of an agitated reaction system in order to provide rapid heat removal in a practical manner. It was feared that in an agitated system with intimate contact between organic and aqueous phases reaction 8 (salt interchange between reactant and product) would occur leading to formation of large amounts of the dichloro compound. However, when the system was investigated using a slight excess of chlorine at temperatures of 0-10°, product purity was at least as high as that produced in tubular reactors and yields were about the same. A comparison of results obtained in the two reaction systems is given in Table 3; a sketch of the agitated system is shown in Fig. 4. Apparently, the chlorination of sodium ethanenitronate proceeds at a much faster rate than salt interchange. To verify this qualitatively, a solution of 2.0 moles of 94.9% 1-chloro-1-nitroethane containing 0.17 mole of dissolved chlorine was stirred with 0.16 mole of aqueous sodium ethanenitronate for one hour at 0-10°. From the mixture, 2.13 moles of 94.8% 1-chloro-1-nitroethane were obtained, indicating the predominance of reaction 6 over 8. In a similar experiment in which the chlorine was omitted, 1.98 moles of 93.8% chloronitroethane were recovered which showed an increase of 1% in nitroethane content, indicating that reaction 8 does take place, but at a relatively slow rate.

Conversion of 1-Chloro-1-Nitroethane to 2,2-Dinitropropanol. The conversion of the chloro derivative to the alcohol was studied initially in batch runs to set conditions for a continuous process. In all work, the overall yield for the two step process was measured, since it was of interest to study the effect of variables during the ter Meer reaction on the final purity of the alcohol, as well as on yield. Conditions during the second step, the methylation reaction, were kept constant from run to run. In batch runs, 1-chloro-1-nitroethane and an aqueous solution containing sodium nitrite and potassium carbonate were fed simultaneously to a jacketed vessel containing a heel of water; the temperature was maintained in the desired range by circulation of coolant through the jacket. It was shown early in this work that an addition time of one hour and a post addition stirring period of 30-60 minutes gave the best results in batch systems. These conditions were adopted as standard procedure for the evaluation of other variables.

It has been mentioned that isolation and solvent washing of the potassium salt of 1,1-dinitroethane, the product of the ter Meer reaction, was undesirable as a purification procedure due to the impact sensitivity of the dry material. A number of alternate purification methods were investigated, as shown in Table 4. The best method found involved addition of a sufficient quantity of water to completely dissolve the salt after completion of the ter Meer reaction and removal of organic impurities by extraction of the resulting solution with ethylene chloride. The extraction was then followed by the methylation step. The yield and purity of I prepared by this method were almost identical to those obtained by the salt isolation procedure.

The effects of temperature and reactant ratios on yield were also investigated in batch runs. Temperatures of 15-20° gave best results, as shown in Fig. 5; at higher or lower temperatures, yields fell off slightly. A molar ratio of potassium carbonate/1-chloro-1-nitroethane of 1.0 gave best yields over the range studied (0.6 to 1.2), as shown in Fig. 6. An excess of nitrite ion favored high yields, as shown in Fig. 7; above a 20% excess, however, the increase in yield was slight. Thus, with molar ratios of sodium nitrite/1-chloro-1-nitroethane of 1.0, 1.2, and 1.6, overall yields of 63.7, 68.8, and 69.4% were obtained.

A continuous reaction system was constructed to operate under conditions indicated by the batch runs. The apparatus, shown in Fig. 7, was designed to carry out four steps on a continuous, integrated basis: 1) conversion of 1-chloro-1-nitroethane to the potassium salt of 1,1-dinitroethane; 2) dissolution of the salt in water; 3) extraction of the salt solution with ethylene chloride, and 4) conversion of the extracted salt solution to a solution of 2,2-dinitropropanol. The ter Meer reaction system consisted of three jacketed, cascade-type reactors connected in series so that the overflow was fed by gravity to the next reactor. Each vessel was stirred by a 2-1/4 in. diameter "Impellator" high shear stirrer at 870 rpm. The two feed streams, 1-chloro-1-nitroethane and an aqueous solution of sodium nitrite and potassium carbonate, were metered to the bottom of the first reactor (R-1) by proportioning pumps. Coolant was circulated through the reactor jackets to maintain the desired reaction temperature. The reaction product mixture overflowed the third reactor into a stirred dissolving vessel (V-1) to which water was metered to dissolve the potassium salt of dinitroethane; warm water was circulated through the jacket to maintain a temperature of 30-35°. The bottom outlet of V-1 was connected to a proportioning pump which metered this stream to the base of a modified Scheibel countercurrent extraction column. Another pump metered ethylene chloride to the top of the column to extract any unreacted 1-chloro-1-nitroethane and organic side reaction products. The column was operated so that the aqueous phase was continuous. The organic-free potassium salt solution overflowed the top of the extraction column and was mixed with a slight excess of 37% formaldehyde before entering the first stage of the methylation reactor, V-2. This vessel was equipped with a jacket, stirrer, thermometer, bottom outlet, and a dropping funnel filled with 20% sulfuric acid. Coolant was circulated intermittently as needed to maintain a temperature of 25-30°. The delivery rate of the 20% sulfuric acid was adjusted to maintain the pH at 6.8-7.0. The combined streams left this vessel by gravity flow and passed to an open-top vessel equipped with a stirrer and a side outlet near the top. Additional sulfuric acid was added to maintain the pH at 4.0 to 4.5 in this vessel. The aqueous solution of I overflowed the side outlet and was collected for isolation of product by extraction with ethylene chloride.

A series of runs was made in this system in which reactant ratios were kept essentially constant, while temperature and residence time were varied. Results, shown in Fig. 8, closely paralleled those obtained in batch studies. In the temperature range 3-25° with residence times of 0.5-2.0 hours in the ter Meer reaction, the best yield (71%) was obtained at 17° with a residence time of 1.3 hours. Data from this run are shown in Table 5. Samples were collected over 2-hour periods

beginning at 4.5 hours after system start-up. Steady state was attained in about 8 hours as judged by leveling off of product yield. The system was run for a total of 24.5 hours and gave reasonably consistent results during the period 8.5-24.5 hours. The system operated smoothly and presented no foreseeable major obstacles from the standpoint of scale-up. A number of other runs, carried out for periods of 12-26 hours, also proceeded smoothly.

COMPARISON OF METHODS

Under the best conditions for both systems, the oxidative-nitration route to 2,2-dinitropropanol gives about a 15% higher overall yield (80% vs. 65% based on nitroethane) than does the ter Meer route. Chemical costs, however, for the ter Meer process are about one-half those for the oxidative-nitration process due to silver losses, the necessity of using an expensive grade of sodium hydroxide, and the use of large quantities of nitric acid to regenerate silver nitrate. Based on these considerations, and on cost estimates for manpower and facility requirements, it appears that the oxidative-nitration process is the superior method for preparing small or intermediate quantities of 2,2-dinitropropanol, whereas the ter Meer route becomes the more economical at higher production levels.

EXPERIMENTAL

Materials. Sodium hydroxide - U.S.P., maximum chloride content 0.005%. Nitroethane - commercial grade, used as received from Commercial Solvents Corp.; the various samples used in this work averaged 93% nitroethane as determined by vapor chromatography. Potassium carbonate - commercial grade, calcinated, 99.0%. Sodium nitrite - U.S.P., granular, 99.4%. Chlorine - commercial grade obtained from The Matheson Co., 99.5%. Silver nitrate - C.P. crystals, 99.98%. Formaldehyde - commercial grade 37% aqueous solution containing 7-8% methanol. Sulfuric acid - technical grade, 98%. Nitric acid - commercial grade, 67%. Acetic acid - glacial, 99.5%. Ethylene chloride - technical grade. Methanol - commercial grade. Potassium hydroxide - technical grade, 85%. Ethyl ether - analytical reagent grade.

Analysis of nitroethane and 1-chloro-1-nitroethane. Analysis by vapor chromatography was investigated using a number of columns under several sets of conditions. Best results were obtained using a Perkin-Elmer Model 154-D Vapor Fractometer equipped with a 0.1 mv Leeds and Northrup recorder and a Perkin-Elmer Model 194 integrator. The instrument was operated at 90° with 5 meters of column packed with GE-SF-96 silicone on 35/80 Chromosorb (Wilkins Instrument and Research Co., Walnut Creek, California). A helium flow rate of 45 cc/min at 10 psig was maintained using 5 micro-liters of sample. Each major (>0.01%) component was trapped by repeatedly running samples of the crude material through the fractometer until enough material was obtained for infrared examination and for recycle to the column at a known concentration. In this manner, nitromethane (peak 3, V_r^0 496.8), nitroethane (peak 4, V_r^0 715.2), 2-nitropropane (peak 5, V_r^0 876.5), 1-chloro-1-nitroethane (peak 6, V_r^0 1235.4), 1,1-dichloro-1-nitroethane (peak 7, V_r^0 1498.8), and 2-chloro-2-nitropropane (peak 7, V_r^0 1498.8) were measured. The latter two components eluted at the same time and were calculated as a single value. Peaks 1 and 2 were present to the extent of <0.01% and were not identified.

Analysis of 2,2-dinitropropanol. A 10-g sample was weighed into a tared Erlenmeyer flask and dissolved in 50 ml of anhydrous methanol. The solution was maintained at -5 to 0°C while 50 ml of a solution containing 6.5 g of 85% potassium hydroxide in methanol was added gradually with stirring. After addition, the thick yellow slurry of potassium 1-nitro-1-ethanenitronate was stirred for an additional 2-3 minutes at -5 to 0°. The mixture was suction filtered on a sintered funnel and washed 3 times with cold anhydrous ethyl ether. When dry, the potassium salt is extremely shock sensitive (impact sensitivity of less than 5 cm using a 2-kg

weight in the Bureau of Mines apparatus) and should be kept damp with solvent during handling operations. After the last ether wash, the salt was transferred (behind a safety shield) to a tared Petri dish and spread as thin as possible. The dish was placed on a balance and solvent allowed to evaporate until constant weight was reached. The sample was safely disposed of by quenching with water before removal from the balance.

Preparation of 2,2-dinitropropanol by the oxidative-nitration method. A suspension of nitroethane (150 g, 93% purity, 1.86 moles) and water (400 ml) was stirred vigorously while a solution of 50% sodium hydroxide (168 g, 2.1 moles) was added over a 25-min period while keeping the temperature at 0-10°. After addition was complete, sodium nitrite (144 g, 2.1 moles) was added and the mixture was stirred an additional 5-10 min. The mixture was added, over a 2-min period, to a vigorously agitated solution of silver nitrate (644 g, 3.8 moles) in 2400 ml of water which had been precooled to 0°. Two minutes after addition, the temperature had risen to 12° and the pH was 5.0. After stirring an additional 30 min at 10-15°, the mixture was treated with 50% sodium hydroxide, added over a 25-min period at 10-20°, until a pH of 12-13 was reached. The mixture was filtered and the silver washed three times with 400-ml portions of water. The pH of the combined filtrates was adjusted to 8.5-9.5 with acetic acid, and 37% formaldehyde (170 g, 2.1 moles) was added all at once. The pH was then adjusted to 5.0 with acetic acid at 20-25° over a 30-min period. After stirring an additional 30 minutes, the solution was extracted eight times with 400-ml portions of ethylene chloride. Removal of the solvent in vacuo left 230 g of 97% 2,2-dinitropropanol; overall yield, 79.9% based on the nitroethane content of the starting material.

Conversion of recovered silver to silver nitrate. Recovered silver (454 g) was slurried with 350 ml of water in a reaction vessel equipped with a caustic scrubbing system to remove oxides of nitrogen. With good stirring, 67% nitric acid (640 g) was added over a 4-hr period at 30-40°. Stirring was continued after addition for 1 hr at 40° and the pH of the solution was then adjusted to 5.0-5.5 by gradual addition of 50% sodium hydroxide.

Preparation of sodium ethanenitronate for chlorination studies. (a) Batch procedure. To a precooled and vigorously stirred mixture of 92.6% commercial nitroethane (900 g, 11.08 moles) and 1800 ml of water, 35.85% sodium hydroxide (1275 g, 11.11 moles) was added at 5-10° in 15 min. The mixture was stirred an additional 15 min, diluted to 4 liters, and transferred to a separatory funnel where the unreacted organic layer (the majority being 2-nitropropane) was separated. The lower aqueous layer was stored at 5° prior to use. The final solution contained 23.45% sodium ethanenitronate and had a pH of 10.6-11.0. (b) Continuous procedure. Continuous reactions were carried out in a two stage cascade reaction system (Fig. 1) equipped with paddle agitators and jackets through which coolant was circulated. Equimolar streams of 15% sodium hydroxide and nitroethane were fed to the first 400-ml reactor by proportioning pumps. The stage heights were arranged to permit gravity overflow from the first stage to the bottom of a second identical reactor. The product overflowing the second reactor was fed to a decanter for separation of unreacted 2-nitropropane from the aqueous product solution.

Conversion of sodium ethanenitronate to 1-chloro-1-nitroethane. (a) Tube chlorinator. A sketch of the tube chlorination system is shown in Fig. 1a; the reactor was a jacketed tube 1 cm I.D. x 72 cm long and was equipped with a thermocouple well which extended the length of the tube. Precooled aqueous sodium ethanenitronate and chlorine were fed to the tube inlet through a proportioning pump and a rotameter, respectively. Coolant, at the desired temperature, was circulated through the tube jacket. Effluent from the tube flowed to a decanter where the pH of the spent aqueous layer was measured. (b) Stirred chlorinator. The stirred chlorination system is shown in Fig. 4. The reactor (2.54 cm I.D. x

28 cm height) was equipped with a jacket for coolant circulation, thermocouple well, and paddle stirrer. Precooled aqueous sodium ethanenitronate was fed to the top of the reactor by a proportioning pump; chlorine was fed to a bottom inlet through a rotameter. The product mixture flowed by gravity to a decanter where the spent aqueous and organic layers were separated continuously. The pH of the aqueous layer was measured in the decanter. After separation of the crude product, it was dried with sodium sulfate (3 g per 100 g of crude product) and filtered before analysis. Yields were based on the amount of dried, filtered material recovered. When an excess of chlorine was used, a stream of air was blown through the crude material to remove dissolved chlorine before the drying step.

Batch conversion of 1-chloro-1-nitroethane to 2,2-dinitropropanol. Typical run. A solution of potassium carbonate (138 g, 1.0 mole) and sodium nitrite (82.8 g, 1.2 mole) in 500 ml of water was added simultaneously with 95% 1-chloro-1-nitroethane (109.5 g, 0.95 mole) over a 1-hr period to a vigorously stirred 100 ml heel of water at 12-18°. After the addition, the slurry of precipitated yellow potassium salt of 1,1-dinitroethane was stirred 30 min at 12-18°. The salt was dissolved at 25° by addition of 1400-1700 ml of water, and the resulting solution extracted twice with 300-ml portions of ethylene chloride. The aqueous layer was treated with 37% formaldehyde (60.4 g, 0.745 mole) and the solution acidified, over a 30-min period, to pH 4.0-4.5 with 400-500 g of 20% sulfuric acid. The solution was allowed to stir another 30 min and was then extracted with 12 aliquots of 150 ml of ethylene chloride. The combined organic extracts were stripped in vacuo to leave 100.6 g of 99.0% 2,2-dinitropropanol; overall yield, 69.9% based on the 1-chloro-1-nitroethane content of the starting material.

Continuous conversion of 1-chloro-1-nitroethane to 2,2-dinitropropanol. The apparatus employed in these studies is shown in Fig. 8. 1-Chloro-1-nitroethane (94-96% purity) and aqueous feed (1.2 moles of sodium nitrite and 1.0 mole of potassium carbonate per 600 ml of water) were metered separately to the first stage reactor of the ter Meer reaction system by proportioning pumps. Rates were adjusted to maintain a molar feed ratio of $\text{CH}_3\text{CHClNO}_2/\text{NaNO}_2/\text{K}_2\text{CO}_3=0.95/1.2/1.0$ and a total residence time of 0.5-2.0 hr in the three stage reaction system. The "Impellator" stirrers in each reactor were adjusted to a rate of 870 rpm. Temperature was controlled in the desired range by circulation of coolant through the reactor jackets; maximum temperature spread through the three stages was 3°. The potassium salt product slurry overflowed the third stage to a dissolving vessel to which water (2000 ml/mole of 1-chloro-1-nitroethane fed) was pumped; temperature was maintained at 30-35° by circulation of water through the jacket. The resulting potassium salt solution was pumped to the base of a modified Scheibel column. Ethylene chloride (1000 ml/hr in all runs) was pumped to the top of the column. The extracted aqueous effluent from the column was allowed to flow by gravity to a jacketed reaction vessel to which 37% formaldehyde (0.85 mole/mole of 1-chloro-1-nitroethane fed) and 20% sulfuric acid were added; pH in this reactor was maintained at 7.0-7.5 and the temperature at 25-30°. Effluent from this reactor was allowed to flow to a second vessel in which the pH was maintained at 4.0-4.5 by further addition of 20% sulfuric acid. Effluent from this reactor, containing about 3% 2,2-dinitropropanol, was collected as product. A complete weight balance was conducted for each sample. Aliquots (4 liters) of each sample were extracted twelve times with 300-ml portions of ethylene chloride; solvent was then removed in vacuo in a rotary evaporator with final heating of the residue at 45°/0.1 mm for 1 hr. Phase distribution studies showed that the extraction procedure described above gave a 96% recovery of product from the aqueous layer. Continuous extractions in the modified Scheibel column gave a 94% average recovery.

TABLE 1

TYPICAL ANALYSIS OF 2,2-DINITROPROPANOL PREPARED VIA THE
OXIDATIVE-NITRATION REACTION

2,2-Dinitropropanol	97.0
Mononitro Compounds*	2.0
1,1-Dinitroethane	0.5
Formaldehyde	0.1
Silver	0.05
Water	0.1
Acetone Insolubles	0.1

*Includes nitroethane, 2-nitro-1-propanol and
2-nitro-2-methyl-1,3-propanediol

TABLE 2

EFFECT OF RESIDENCE TIME ABOVE 40°C ON THE PURITY OF
1-CHLORO-1-NITROETHANE

Run No.	Residence Time in Chlorinator, min.		Maximum Temp., °C	Mole % in Product	
	Total	Above 40°C		1-Chloro-1- Nitroethane	2-Chloro-2-Nitropropane 1,1-Dichloro-1-Nitroethane
1	1.35	0.31	68	95.7	1.50
2	1.72	0.30	58	94.8	2.34
3	3.70	0.52	58	95.6	1.86
4	4.88	0.00	39	95.7	1.87
5	6.90	0.73	50	95.5	2.50
6	10.40	0.55	50	94.3	2.39
7	17.50	1.23	50	92.5	3.70
8	9.90	5.57	76	78.5	8.65 ^a
9	5.22	5.22	70	77.3	10.90 ^b

^aAlso contained 11.9% nitroethane.

^bAlso contained 10.6% nitroethane.

TABLE 3

RESULTS IN TUBE AND STIRRED CHLORINATORS

Run	pH of Sodium Ethanimtro- nate Feed	Residence Time, min. Total	Above 40°C	Type Reactor	% Yield	Product Analysis, Mole %				
						Nitro- methane	Nitro- ethane	2-Nitro- propane	1-Chloro-1- Nitroethane	1,1-Dichloro-1- Nitroethane + 2-Chloro-2- Nitropropane
1	11.0	3.70	0.520	Straight Tube	84.0 ¹	.130	1.16	1.07	95.62	1.86
1	10.7	6.90	0.740	"	87.0	.070	1.30	0.46	95.63	2.44
2	10.8	1.13	0.395	"	90.7	.075	1.65	1.25	95.06	1.97
3	11.0	9.45	02	Stirred	91.6	.28	2.15	0.54	95.22	1.72
4	11.1	9.7	02	"	90.5	.23	0.86	1.09	95.81	1.74
5	11.0	17.8	02	"	89.5	.09	0.94	1.00	95.54	2.30
6	10.9	40.6	02	"	87.3	.06	1.57	0.77	95.51	2.04

¹pH of aqueous effluent maintained at 7.4-7.7; in all other runs the pH was maintained at 5.5-6.5. ²Temperature maintained at 0-10°.

TABLE 4

PURIFICATION PROCEDURES FOR 2,2-DINITROPROPANOL PREPARED BY THE TER MEER REACTION

Run	Procedure	2,2-Dinitropropanol % Yield	% Purity
1	Potassium salt of 1,1-dinitroethane filtered and washed with methanol before methylation step.	69.4	99.2
2	Aqueous 2,2-dinitropropanol product solution extracted with <i>n</i> -hexane before isolation of product by ethylene chloride extraction.	67.7	93.4
3	Same as Run 2 except for substitution of cyclohexane for <i>n</i> -hexane.	71.3	95.8
4	Same as Run 2 except for substitution of toluene for <i>n</i> -hexane.	63.7	98.2
5	Dissolved potassium salt of 1,1-dinitroethane in water and extracted with methylene chloride before methylation step.	58.3	98.0
6	Same as Run 5 except for substitution of ethylene chloride for methylene chloride.	68.8	99.6

TABLE 5

DATA ON CONTINUOUS CONVERSION OF 1-CHLORO-1-NITROETHANE TO 2,2-DINITROPROPANOL

Run & Sample	Sample Period, Hr.	Molar Feed Ratio $\text{CH}_3\text{CHClNO}_2/\text{NaNO}_2/\text{K}_2\text{CO}_3$	Ter Meer Residence Time, Hr.	Ter Meer Reaction Temperature, °C			Total wt. Balance, %	$\text{CH}_3\text{C}(\text{NO}_2)_2\text{CH}_2\text{OH}$ Assay, %	Yield %
				R-1	R-2	R-3			
15-A*	4.5-6.5	0.938/1.2/1.0	1.30	17.0	15.0	14.3	100.9	98.7	68.4
15-B*	6.5-8.5	0.938/1.2/1.0	1.305	17.0	15.0	14.3	99.8	98.5	68.5
15-C	8.5-10.5	0.953/1.2/1.0	1.305	17.2	15.1	14.6	94.8	99.4	70.8
15-D	10.5-12.5	0.960/1.2/1.0	1.31	17.1	15.1	14.5	101.2	98.2	69.7
15-E	12.5-14.5	0.968/1.2/1.0	1.305	17.1	15.1	14.5	95.3	98.8	70.0
15-F	14.5-16.5	0.953/1.2/1.0	1.30	17.1	15.1	14.5	98.4	99.2	69.4
15-G	16.5-18.5	0.938/1.2/1.0	1.295	17.0	15.0	14.6	99.0	98.8	71.6
15-H	18.5-20.5	0.930/1.2/1.0	1.30	17.0	15.0	14.6	99.4	99.3	74.0
15-I	20.5-22.5	0.938/1.2/1.0	1.305	17.0	15.0	14.6	99.4	98.8	72.8
15-J	22.5-24.5	0.938/1.2/1.0	1.31	17.0	15.0	14.6	96.3	99.1	69.9
Average							98.4	98.9	71.0

* Not steady state (not included in average).

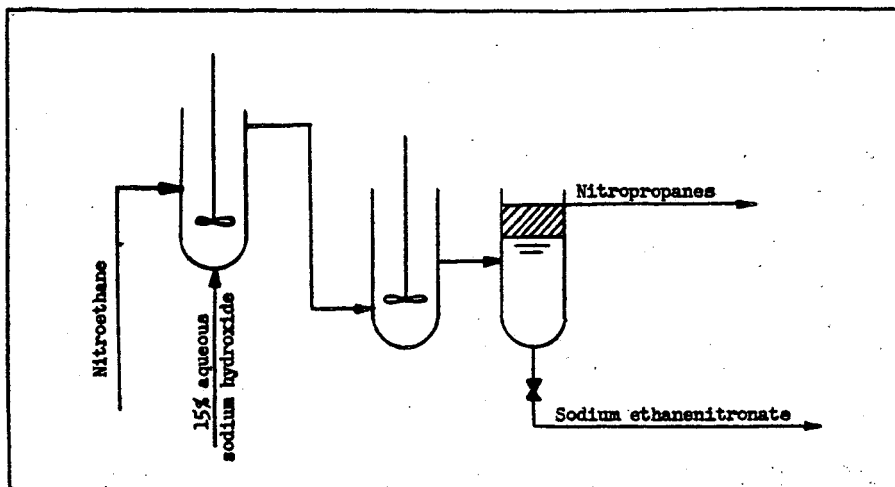


Figure 1. Reaction system for the continuous preparation of sodium ethanenitronate from nitroethane.

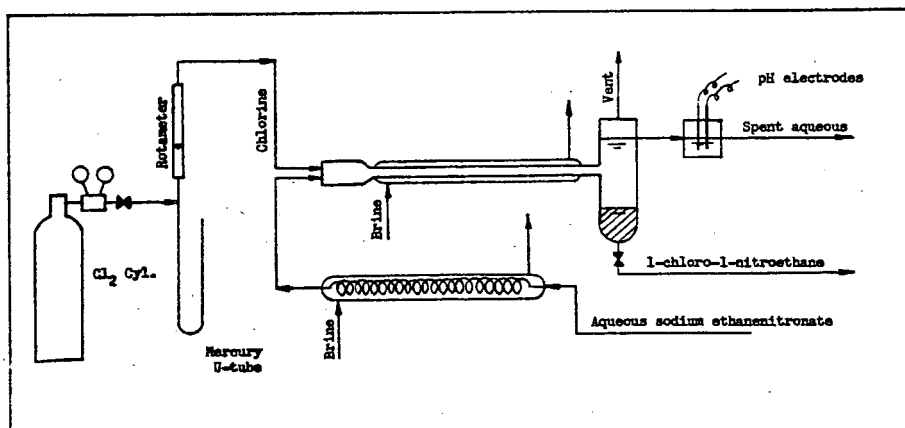


Figure 1a. Straight tube reactor system for the continuous conversion of sodium ethanenitronate to 1-chloro-1-nitroethane.

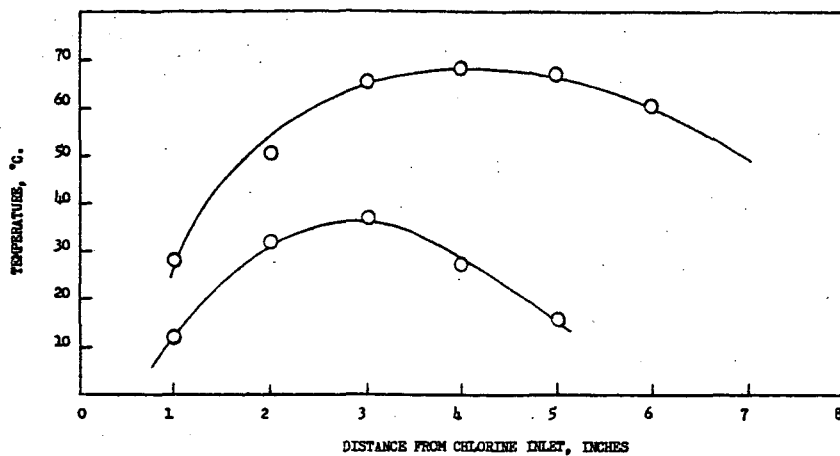


Figure 2. Reaction temperature profiles in straight tube chlorinator. Reactor length 28.4 inches. Sodium ethanesulfonate concentration 2.76 m/l. Total residence time: A = 4.05 min., B = 1.35 min.

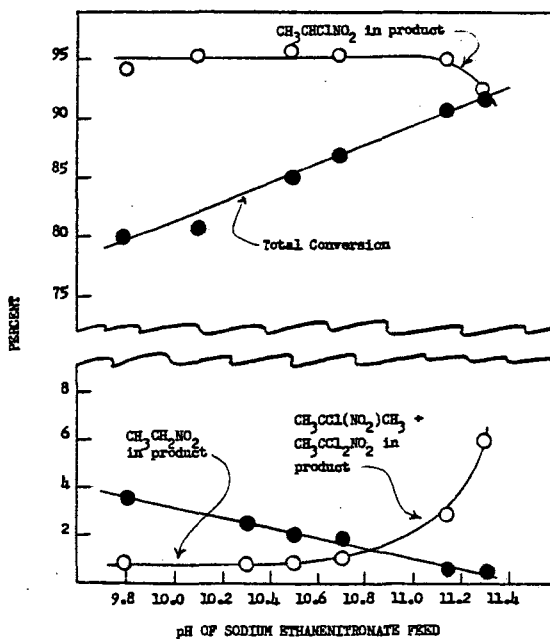


Figure 3. Effect of pH on conversion and product purity in continuous coiled tube reactor. Residence time 7 minutes.

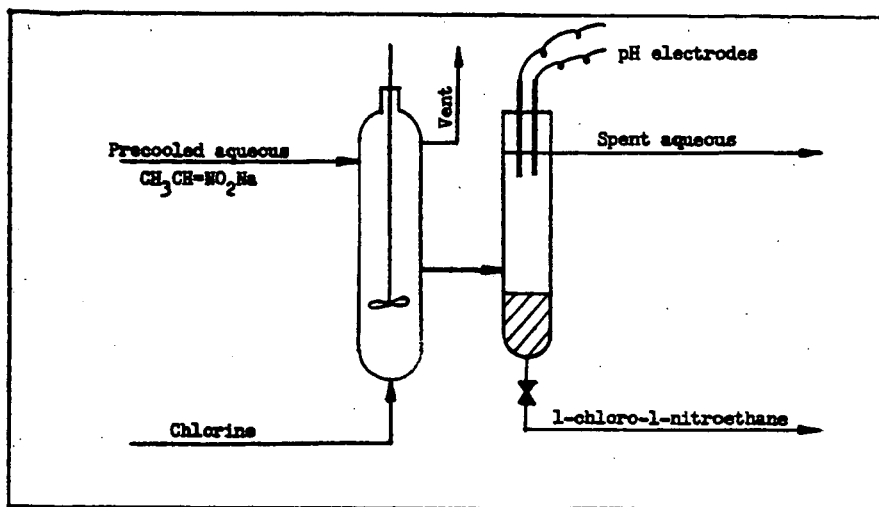


Figure 4. Agitated reaction system for the chlorination of sodium ethanenitronate.

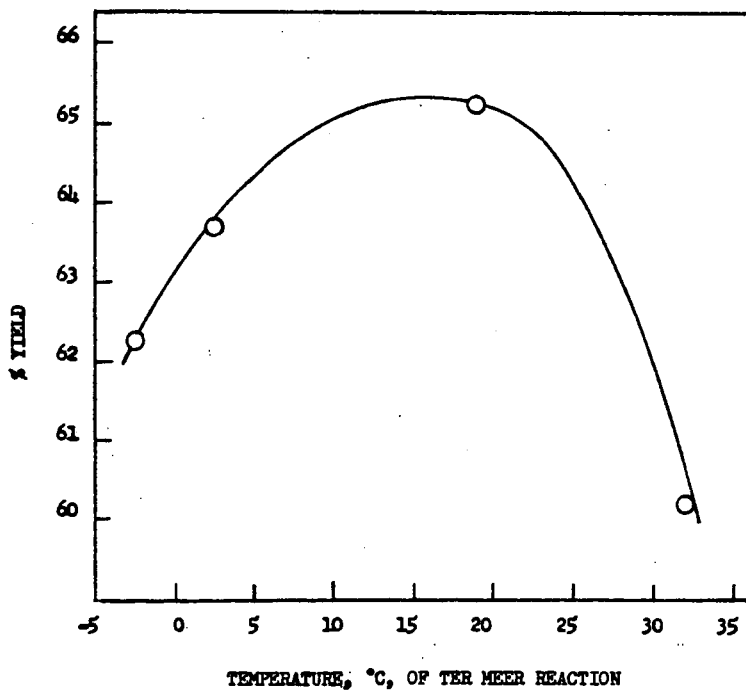


Figure 5. Effect of temperature during ter Meer reaction on 2,2-dinitropropanol yield in batch reactor. $\text{NaNO}_2/\text{K}_2\text{CO}_3/\text{CH}_3\text{CHClNO}_2$ molar ratio = 1.0/1.0/1.0.

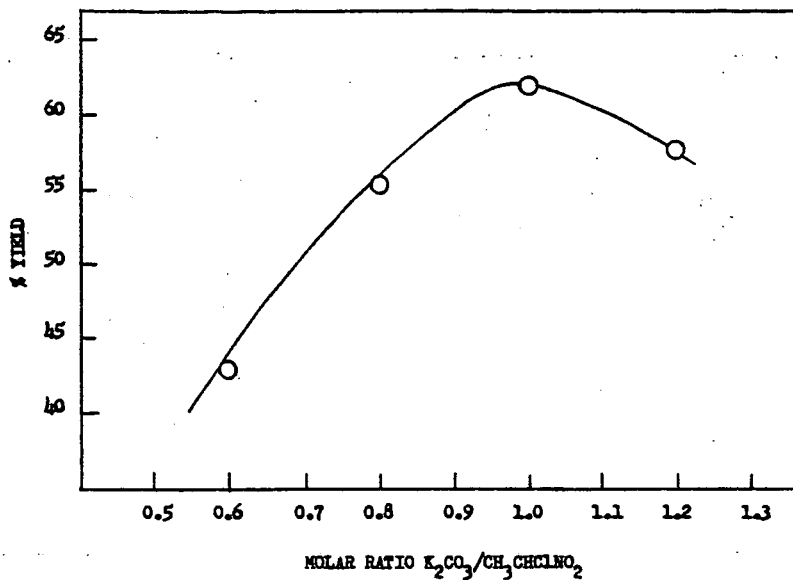


Figure 6. Effect of reactant ratios on 2,2-dinitropropanol yield in ter Meer reaction at 0 - 10°C in batch reactor. Molar ratio $NaNO_2/CH_3CHClNO_2 = 1.0$.

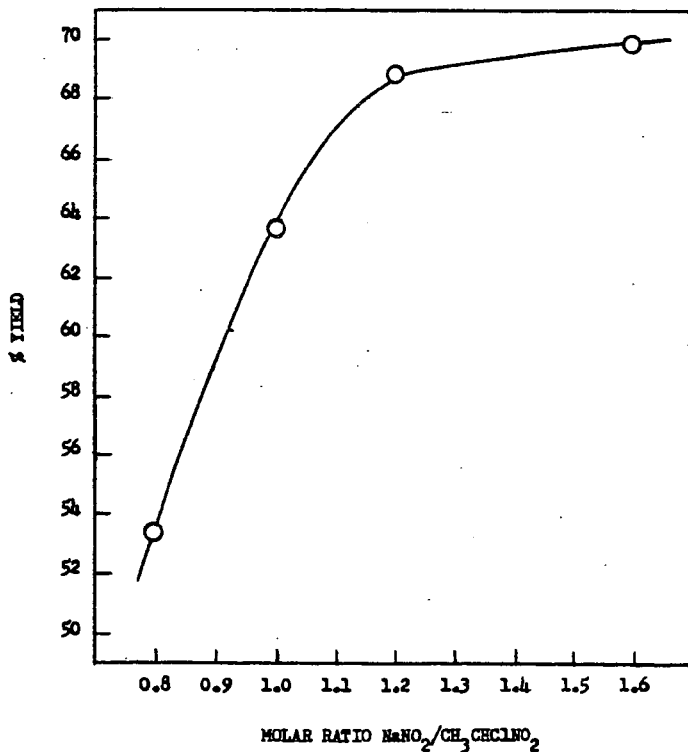


Figure 7. Effect of reactant ratios on 2,2-dinitropropanol yield in ter Meer reaction at 0 - 10°C in batch reactor. Molar ratio $K_2CO_3/CH_3CHClNO_2 = 1.0$.

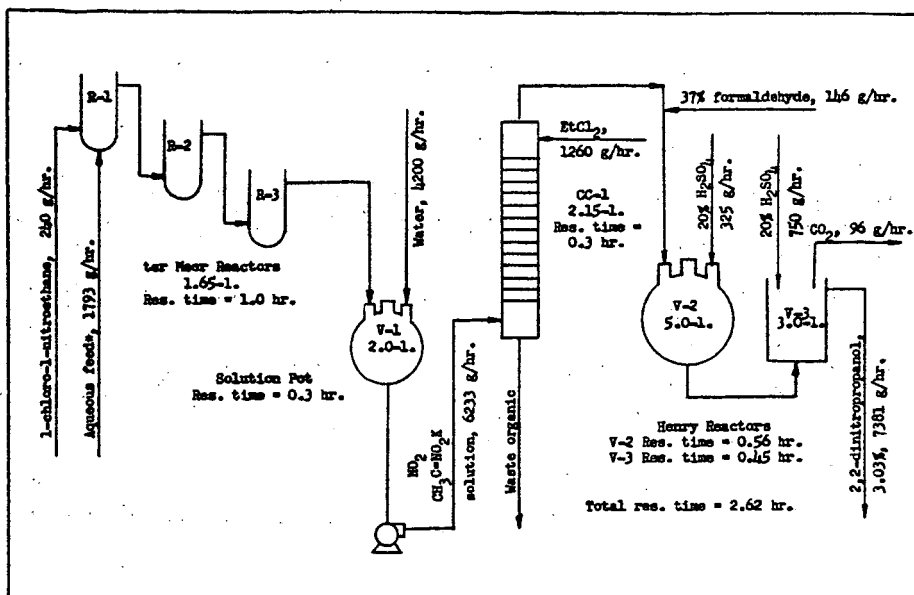


Figure 8. Reaction system for continuous preparation of 2,2-dinitropropanol from 1-chloro-1-nitroethane. Aqueous feed was prepared by dissolving 83 g. HNO_2 (1.2 mol.) and 138 g. K_2CO_3 (1.0 mol.) per 600ml. water.

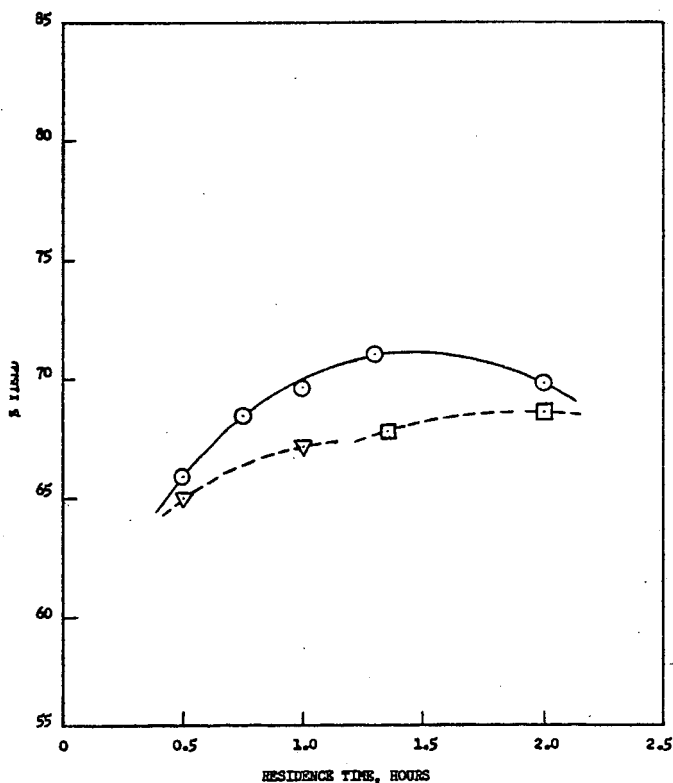


Figure 9. Effect of residence time on the yield of 2,2-dinitropropanol from 1-chloro-1-nitroethane via the ter Meer Reaction. Reaction temperature: □ = 3°C, ○ = 17°C, and ▽ = 25°C.

REFERENCES

- (1) L. Henry, *Compt. rend.*, 120, 1265 (1895)
- (2) R.B. Kaplan and H.O. Shechter, "A New General Reaction for Preparing gem-Dinitro Compounds." Paper No. 1, Symposium on Nitro Aliphatic Chemistry, Purdue University, May 25-26, 1961.
- (3) S.B. Lippincott, *J. Am. Chem. Soc.*, 62, 2604 (1940); U.S. Patent 2,260,256, Oct. 21, 1941.
- (4) C.M. Wright and D.R. Levering, "Electrolytic Preparation of gem-Dinitro-paraffins." Paper No. 2, Symposium on Nitro Aliphatic Chemistry, Purdue University, May 25-26, 1961.
- (5) E. ter Meer, *Ann.* 181, 1 (1876)
- (6) L.G. Maury and D.R. Levering, Hercules Powder Co., Private Communication.

A Method for Studying Precombustion Reactions of Liquid Propellants

Henry Ph. Heubusch

Bell Aerosystems Company
Buffalo 5, New York

Introduction

Since their inception, rocket engine development programs have been plagued with sporadic explosions. Some of these have occurred on start, others during a run, and still others on shutdown. Ordinarily, design changes are relied upon to correct such situations. A more fundamental approach was considered at Bell which consisted of looking at the chemistry of the system.

All work done along this line was based on the hypothesis that liquid phase reactions occur between rocket propellants and exert an influence on subsequent combustion reactions. In the case of nitric acid-hydrocarbon engines, e.g., liquid phase oxidation and/or nitration reactions appear possible. Depending on which reaction occurs or predominates, one can anticipate smooth or troublesome combustion.

Testing this hypothesis began with a literature survey which yielded little conclusive evidence. This led to a step-by-step experimental approach to rocket operating conditions of temperature, pressure and reaction time, and produced a useful method for studying precombustion reactions of liquid propellants.

Summary

The heart of the method was an apparatus designed to bring propellants separately to conditions of temperature and pressure equivalent to those encountered on injection into an operating rocket engine. The propellants were next flowed into the arms of a "Y" Tube, allowed to react in the stem, then subjected to a chemical stop. Reaction time was controlled by flow-rate and stem dimensions. In its final form this apparatus brought together propellants preheated to 300°F at 575 psig, allowed them to react for 15 milliseconds, and delivered the products in solutions suitable for conventional analyses. These analyses, largely spectrophotometric, showed to what extent particular reactions had occurred. Reaction mechanism was elucidated by analyses of products from parallel mixing experiments carried out under less drastic conditions and allowed to go to completion. The following is an account of the evolution of this apparatus and its role in the overall method.

Technical Approach

Experimental work began by mixing small quantities of typical propellants, WFNA (White Fuming Nitric Acid) and JP-4, in various proportions in the hope that at certain mixture ratios solutions would form which could be analyzed for oxidation products or explosives. Since little direction was afforded by the literature, initial mixing was done in open beakers without impressed heating. Exothermic reactions took place without incident in every case but no solutions resulted. Mixture ratio variation was achieved by dropwise addition of JP-4 in increments up to 15g. to 15g. of WFNA and vice versa.

To preserve all reaction products for analysis, the experiments were repeated using a two-neck flask fitted with a reflux condenser and thermometer. The set-up was contained in a water bath sitting on a magnetic stirrer capable of mixing the water and propellants. In these experiments heating was continued until reaction had ceased as evidenced by the cessation of nitrogen dioxide evolution. Temperature-time profiles were taken and the resulting mixtures were set aside for observation and analyses. Some showed a distinct third liquid phase assumed to be a collection of reaction products or the beginnings of solution formation.

At this point, mixing conditions were made more drastic in the hope of forcing solution formation. A three-neck flask was adopted and a high speed stirrer (1400 rpm) introduced. The flask was stationed on a hot plate. By this time analytical work had shown that the most interesting results were occurring at mixture ratios of O/F = 0.3, 1.0, 2.0, 4.0 and 5.0 so all future work was centered about these values. The procedure was much as before except that mixing time was varied within definite limits maintained by transferring the flask to an ice bath at the appropriate time. An extension of this work involved a series of high speed mixing studies carried out under the influence of intense light and/or sound. For these experiments the mixing flask was mounted in a box fitted with a lens which directed ultraviolet radiation of rocket engine intensity on the propellants. This reaction was from a filtered carbon arc. Rocket engine sound was simulated by directing a recording of a rocket engine run at an intensity of 122 decibels at the flask. Again no solutions formed but analyses of the individual phases from these and earlier experiments pointed to the direction for future work.

Careful observation disclosed that at least two liquid phases existed even during high speed mixing at reflux temperature. In many cases a third liquid phase was present and in some instances solid phases appeared. The liquid phases were easily distinguished in that they formed layers, the top being pale yellow and the bottom orange. Where a third phase appeared it was seen as a yellow band of liquid between the other two layers. One type of solid phase appeared in the middle layer, another in the lower layer. Using conventional techniques the liquid and solid phases were isolated and submitted for analyses.

It quickly became apparent that the top layers were largely unreacted fuel, the bottom unreacted oxidizer, and the middle reaction products. The crystals in the middle layers were identified as a p-nitrobenzoic acid and those in the bottom layers were oxalic acid. Attempts at further characterization by organic analytical techniques proved futile primarily because of the number of constituents in JP-4. Accordingly, it was decided to rely on experiments with pure hydrocarbons to elucidate the nitration and oxidation reaction sequences obviously in operation. At the same time data from spectrophotometric analyses focused attention on the need for studies under more vigorous conditions and at shorter reaction times.

The spectral approach was to dilute samples of each phase as required with an appropriate solvent, e.g., 2-propanol and measure absorbance as a function of wavelength in the ultraviolet region of the spectrum. A persistent peak occurred at 260 m μ in a curve remarkably similar to ones for nitroaromatics. As indicated earlier, this was quite obvious for mixtures prepared at O/F = 0.3. A plot of all the data at this wavelength for this mixture ratio gave three curves of absorbance vs time corresponding to the top, middle and bottom layers respectively. Extrapolation of these curves back to "0" time showed that significant reaction must have taken place in less than a minute. Extrapolation to "0" time was possible by assigning the absorbance of JP-4 to the upper phase, the absorbance of WFNA to the lower phase, and a value of zero for the middle phase. The fact that absorbances for the middle and lower phases were on the wane beyond the earliest measured time of approximately one minute showed reactions had occurred prior to this point. Subsequent studies explained the decreases in absorbance with time on the basis of interference from products produced by competing oxidation reactions.

The first attempt to reduce reaction time from minutes to milliseconds was made with a crude, manually operated "Y" Tube apparatus. The principle behind such an apparatus is relatively simple. One propellant is flowed at a controlled rate into one arm of the "Y", the other propellant into the second arm. Depending on the flow-rates chosen the propellants mix at a certain mixture ratio and react in the stem. Reaction time is then a function of total flow-rate, cross sectional stem area and effective stem length, i.e., the distance over which reaction is allowed to proceed. The apparatus built to reduce this principle to practice is described as follows.

Two steel tanks fitted with provisions for pressurization were connected to the arms of a metal "Y" Tube having an I.D. of 0.4 cm. In the oxidizer arm was installed an orifice of 1mm and in the fuel arm an orifice of 2mm. Upstream of each orifice was a quick-opening hand valve. Propellants loaded into the tanks and flowed out under 15 psig on the oxidizer side and 20 psig on the fuel side mixed in the stem at an O/F ratio of 0.3 and ejected from the stem at an overall flow-rate of 44 cc/sec. These values were established by flowing methylene chloride (in place of acid) and JP-4 through the system separately to establish mixture ratio and collectively to establish total flow-rate. Methylene chloride has the same density as WFNA and was used during calibrations for safety considerations. The next item has to do with control over effective stem length.

Originally, it was planned to use a "Y" Tube with a transparent stem and monitor reactions by direct spectral analyses at various stations down the stem to provide a record of reaction vs time. Unfortunately, absorbance was too high so a chemical stop was adopted. This consisted of a rapidly stirred, cold solution of equal parts of methylene chloride and n-heptane. Preliminary experiments indicated that such a solution not only quenched reaction but gave the products in form suitable for spectral analysis at a convenient time and location. This approach compounded design problems, though, in demanding a method for isolating a relatively small, representative sample.

This problem was solved by putting a cover with a hole in it on the beaker of quench solution. To the cover was welded a tube with holes overlapping the one in the cover. Into this tube was fitted a second, similarly perforated tube connected to a hydraulic actuator. Steady movement of this tube brought all holes in line momentarily and allowed a definite amount of material to enter the quench solution. Travel was adjusted during runs with methylene chloride and JP-4 to trap 1ucc. The balance of the propellant was discarded.

Runs were made with live propellant after the effective stem length was adjusted to 15cm. This is the distance from the intersection of the "Y" to the surface of the quench solution. Under these conditions, reaction time was limited to 43 milliseconds. Following the run, the quench solution was diluted to a given volume and examined spectrophotometrically. Absorbance about 260 μ was compared with a blank and with that obtained from a composite curve for a corresponding high speed mixing reaction which had been allowed to go to completion. These data showed that about 1/3 as much nitroaromatic forms in 43 milliseconds as in 30 minutes.

Having demonstrated a point, attention was next turned to refining the apparatus for work at higher temperatures and pressures. For safety sake, operation was made remote by replacing the hand valves with a solenoid operated, bi-propellant valve. To increase flexibility, the welded "Y" was replaced with a block drilled to form the channels for the "Y" and tapped to allow insertion of stems of various lengths via standard fittings. To provide better control over flow-rate, vane-type flowmeters were installed. The flowmeters were checked out by flowing a mixture of trichloroethylene and acetone through the system, collecting fractions in given lengths of time and measuring their refractive indices. Mixture ratio was established from a calibration curve and on comparison with flowmeter data showed excellent agreement. To provide better sampling, a shutter-type sampler was built.

The new sampler consisted on a piston-driven shutter programmed to momentarily expose a hole in a perforated, beaker cover. Programming was effected by loading the piston spring to 40 psig with nitrogen gas, then adjusting a bleed valve until 10cc portions of trichloroethylene/acetone mixtures were trapped.

Use of this equipment with two different stem lengths corresponding to 40 and 20 milliseconds of reaction time respectively gave data proving that quench was instantaneous and significant reaction was taking place within 20 milliseconds.

The same results were obtained after installing a back pressure orifice in the stem of the "Y" Tube. This was done in preparation for tests at elevated temperatures. By use of back pressure, reaction in the stem would be restricted to the liquid phase even if the propellants rose above their normal boiling points. Glas-Col heaters were attached to the tanks to allow prerun warm-up.

Satisfactory runs were made in this configuration over the temperature range 75 to 150°F. As anticipated, nitration reactions increased with temperature as shown by an increase in absorbance in the 260 m μ region of the spectrum. Attempts run at temperatures above 150°F were thwarted by a number of problems.

Corrosion of the steel tank by hot acid contaminated the oxidizer with salts and drastically reduced the concentration of the acid. The corrosion problem was solved by using WFNA modified with a corrosion inhibitor. The inhibited acid, called IWFNA, contained approximately 0.5 wgt% hydrofluoric acid.

Uncertainties in temperature due to heat loss in the flow system were solved by installing thermocouples in the arms of the "Y" Tube. The output from the fuel arm was fed to a temperature recorder. The output from the oxidizer arm was fed to an electronic device wired to activate the sampler on attainment of a predetermined temperature.

Reruns over the temperature range 75 to 150°F gave data equivalent to that obtained with WFNA. No corrosion was encountered above 150°F but thermal decomposition reduced the concentration of the oxidizer. An analysis of the situation showed it took approximately two (2) hours to reach 150°F and during this time water content increased from <2% to >7% at the expense of nitric acid concentration. Decomposition was reduced by strapping Calrod heaters to the tanks and covering them with insulation. This reduced heating time from hours to minutes. In addition, the tanks were pre-pressurized above the anticipated vapor pressure of the propellant on cessation of heating. With these modifications, a temperature of 200°F was reached with an attendant increase in nitration.

Above 200°F, the flowmeters bound and gave erratic data. The trouble was traced to the Kel-F shaft bearings. Reliability was re-established by replacing the flowmeters with differential pressure gages. These were strain-gage pressure pick-ups installed on either side of the line orifices. Calibration was accomplished by running the differential pressure gages in series with the vane-flowmeters to approximately 200°F.

Attempts to run above 200°F were still unsuccessful though, because of increasing temperature differentials between the tanks and "Y" Tube, and a tendency for the propellants to flash-off on leaving the "Y" Tube. The temperature differential problem was solved by installing the tanks and flow system in an insulated chamber attached to a Chromolox heater. By admitting hot nitrogen to the chamber during the propellant heating cycle and monitoring the operation with a network of strategically placed thermocouples, propellants and hardware were brought to the desired temperature.

The propellant flash-off problem was solved by adding an extension, dubbed a Jet Mixer, to the "Y" Tube stem. This extension, which brought the propellants

outside the insulated chamber, was so designed as to take a stream of cold quench solution from an independent cooling and circulating system and inject it into the issuing propellant stream. The flow-rate of quench solution was determined by prior calibration and the sampler was modified slightly to handle a larger volume of liquid.

In this final form the apparatus was used for runs to 300°F with propellants pressurized up to 575 psig, conditions simulating those of injection into an operating rocket engine. Although there were minor variations, mixture ratio was approximately 0.3 O/F for these runs and reaction time was approximately 20 milliseconds. Again nitration reactions increased with temperature over the entire range studied.

Figure 1 is a schematic for the "Y" Tube apparatus. Figure 2 shows the increase in reaction absorption with increase in temperature over the range 75 to 300°F.

Parallel with this work, high speed mixing studies were conducted with pure hydrocarbons of the principal types found in JP-4, viz., paraffins, olefins and aromatics. The compounds chosen were: n-heptane, n-heptene-2 and toluene, all of which contain seven (7) carbons. Through systematic separations, qualitative organic and ultraviolet spectrophotometric analyses, sufficient products were identified to allow postulation of probable reaction sequences. Among the products were acetic acid, oxalic acid, nitroheptene-2, 2-4 dinitrotoluene and p-nitrobenzoic acid.

With heptane, virtually no reaction takes place. (Hence the validity of its use in the quench solution). With heptene, the first reaction is replacement of an olefinic hydrogen with a nitrate group. This is followed by a sequence of oxidation and nitration reactions leading to oxalic acid. Nitration also appears to be the initial reaction with toluene. This occurs in the ring and is followed by oxidation of the chain and further nitration of the ring.

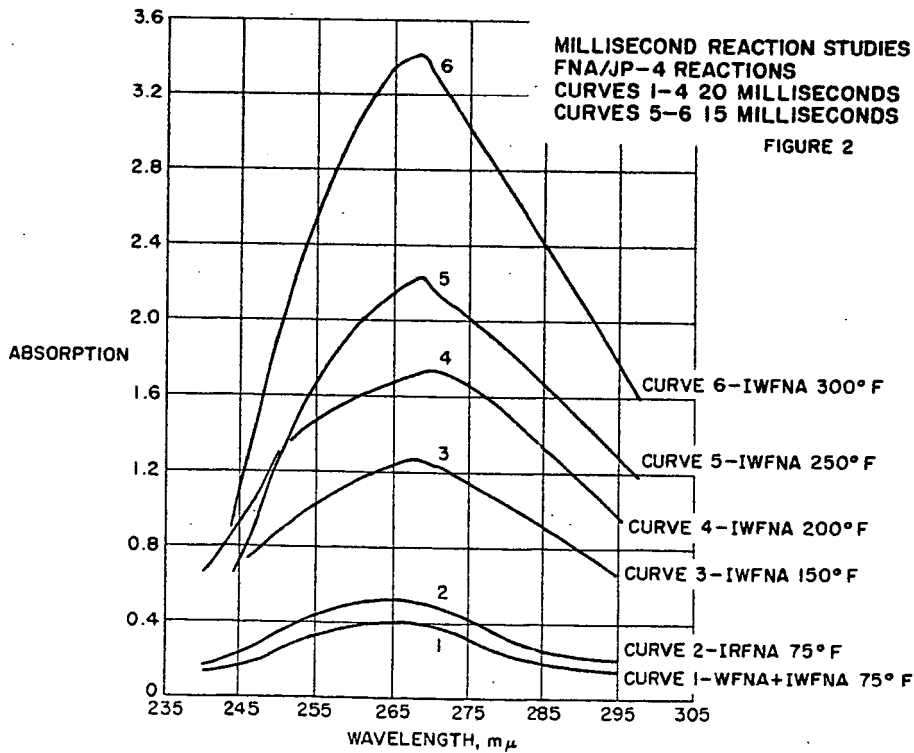
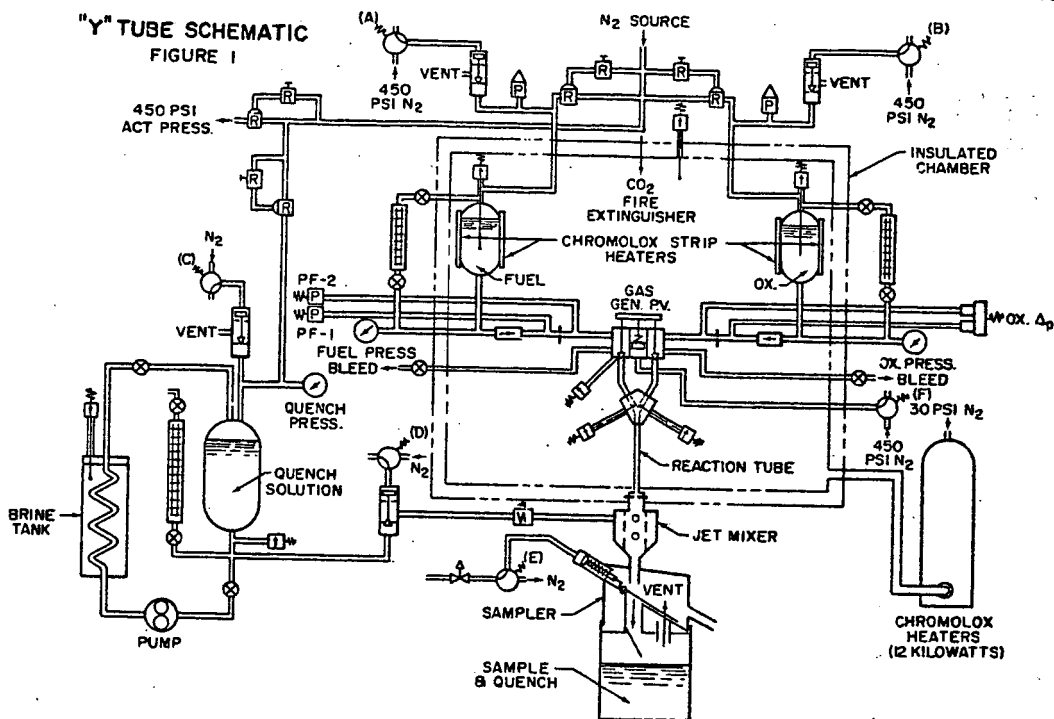
Conclusion

Thus we have shown that liquid phase reactions can occur under rocket engine operating conditions. Further we showed a mechanism for these reactions and indicated how nitration could well get out of hand and lead to combustion instability.

More important we showed the evolution of an apparatus which in its final form is suited for kinetic studies of reactive materials under extreme conditions of temperature and pressure.

But most of all we have demonstrated an approach to a problem which features interaction of the various branches of chemistry and engineering to reach a common goal.

"Y" TUBE SCHEMATIC
FIGURE 1



FLAMMABILITY CHARACTERISTICS OF HYDRAZINE FUELS
IN NITROGEN TETROXIDE ATMOSPHERES

By Henry E. Perlee, Agnes C. Imhof, and Michael G. Zabetakis

U. S. Department of the Interior, Bureau of Mines
Explosives Research Laboratory, Pittsburgh, Pa.

I. INTRODUCTION

The use of hypergolic systems as missile propellants has introduced handling problems not associated with ordinary fuel-oxidant systems. Of particular interest here are the hypergolic systems in which hydrazine fuels are combined with nitrogen tetroxide. The flammability characteristics of such systems have been studied rather extensively at the Bureau of Mines. This report contains the results obtained to date with hydrazine, monomethyl hydrazine, and unsymmetrical dimethyl hydrazine at the Explosives Research Laboratory.

II. EXPERIMENTAL RESULTS

A. NO_2^* - Air Mixtures

Minimum spontaneous ignition temperatures (S.I.T.) of liquid hydrazine, unsymmetrical dimethylhydrazine (UDMH), and monomethylhydrazine (MMH), were determined at 25°C. in contact with nitrogen tetroxide (NO_2^*)-air mixtures in a modified ASTM autoignition temperature apparatus (1, 2). These tests were conducted by injecting the liquid fuel into a heated atmosphere of NO_2^* and air contained in a uniformly heated 250 cc. pyrex erlenmeyer flask. The results of these tests are given in Figure 1 where the S.I.T. is plotted as a function of NO_2^* content. In every test the fuel and oxidant reacted on contact producing a white cloud of fine particles; however, as noted in the figure, this reaction did not always culminate in an ignition. Although 70 μ liters of liquid fuel was normally used in each test, preliminary studies showed that the S.I.T. was independent of the fuel volume down to at least 10 μ liters. Time delays between injection of the liquid and ignition, when it occurred, were imperceptible to the observer. The short horizontal lines appearing on the curves in Figure 1 indicate the uncertainty in the NO_2^* concentration (± 0.8 volume percent at 100°C.). Approximately 100 separate tests were conducted to establish each curve.

The results of Figure 1 show that at ambient temperature (25°C.) liquid UDMH ignites spontaneously in those NO_2^* -air mixtures containing more than about 8 volume percent NO_2^* ; similarly, MMH and hydrazine ignite in NO_2^* -air mixtures containing more than about 11 and 14 percent, respectively. At temperatures above 50°C. the MMH ignites in the presence of lower concentrations of NO_2^* than does UDMH.

In the first experiments, the liquid fuel temperature was maintained at 25°C.; however, since higher ambient temperatures are encountered in practice, we determined the effect of liquid temperature on the S.I.T. of the fuels. Figures 2, 3 and 4 show the results of this study. For both liquid hydrazine and UDMH at any fixed concentration of NO_2^* in air, the S.I.T. was found to increase with decreasing

\dagger NO_2^* represents the equilibrium mixture of NO_2 and N_2O_4 .

liquid temperature. This appears to be in agreement with the results predicted by the thermal theory of ignition since an increase in the fuel vapor concentration (due to an increase in the liquid temperature) increases the reaction rate at any specified oxidant temperature and concentration and thereby lowers the S.I.T. However, the corresponding results for liquid MMH at 36°, 55° and 67°C. appear to be anomalous and further study is indicated.

B. NO₂*-O₂-He Mixtures

To determine the effect of thermal conductivity of the oxidizer on the S.I.T. of UDMH, a series of ignition temperature tests was conducted with "air" (HeAir) in which the nitrogen was replaced with helium. The S.I.T. curve obtained under these conditions is given in Figure 5, curve a (upper branch). Comparison of this curve with curve a in Figure 1 shows that the S.I.T. of UDMH in NO₂*-HeAir is the same as that in NO₂*-Air.

The S.I.T. curves obtained in NO₂*-O₂, NO₂*-He and various NO₂*O₂-He mixtures are also given in Figure 5. One can see from these results that very small (0.3%) quantities of oxygen in helium have a substantial effect on lowering the S.I.T. One would therefore suspect that the oxygen acts as a third body in the kinetic mechanisms (3). The addition of further quantities of O₂ has a less pronounced effect on the S.I.T. of UDMH.

C. Effect of Pressure

In an effort to determine the effect of moderate oxidant pressure changes on the S.I.T. of these liquids, a series of experiments was conducted on UDMH in a pyrex-lined steel container at 15 and 45 psi. initial pressure; the container was equipped with suitable hardware for pressure measurement and introduction of the gases and liquids. The results obtained at these pressures are given in Figure 6. The results obtained here at 15 psia. agree with those obtained at atmospheric pressure in the modified ASTM apparatus (Figure 1). Normally the S.I.T. of a fuel is not affected appreciably by moderate changes in pressure. For example, an increase in pressure from 15 to 45 psia. lowers the S.I.T. of UDMH in air by 4°C. (Figure 6). However, as NO₂* is added to the air, the difference between the S.I.T. values at these two pressures increases and then eventually decreases again. Since a small increase in pressure shifts the NO₂* equilibrium towards N₂O₄, we would expect a change in the S.I.T. with changing N₂O₄/NO₂ ratio if the reactivity of the two species (NO₂ and N₂O₄) differ. This is illustrated in Figure 7 where the changes in the ratio $\frac{N_2O_4}{N_2O_4+NO_2}$ and in the NO₂* concentration (ΔNO_2^*) for a 30 psi. change

in pressure are plotted as a function of the S.I.T. This figure shows a direct correlation between the change in N₂O₄ concentration and the change in NO₂* concentration for the pressure change considered. In other words, for a given NO₂*-air mixture the S.I.T. decreases with increasing pressure because the NO₂* equilibrium shifts towards increasing concentration of the more reactive N₂O₄. If N₂O₄ had been the less reactive species the S.I.T. would probably have increased initially with increasing pressure.

D. Vaporized Fuel

The above investigations were conducted with liquid fuel; however, similar results can be obtained with gaseous fuel. Such data were obtained for UDMH by vaporizing a measured volume of liquid in air in the modified ASTM apparatus. NO₂* was then injected into this heated mixture to determine if an ignition would result.

Figure 8 shows the results of this study; the S.I.T. is given here as a function of the UDMH concentration in the UDMH-air mixture. From this figure we see that at 25°C. a UDMH-air mixture containing greater than 9 volume percent UDMH will ignite spontaneously on contact with NO_2^* at the same temperature.

The lower limit of flammability (L.L.) line of UDMH-air mixtures is included in Figure 8. Mixtures with UDMH concentrations below the L.L. line are considered nonflammable so that we would not expect them to ignite spontaneously on contact with NO_2^* . However, there is also a range of mixture compositions between the L.L. line and the S.I.T. curve that are not ignited in this manner; an external ignition source (flame, spark, etc.) would be required to ignite these mixtures.

III. CONCLUSIONS

1. At ambient temperature (25°C.) and pressure, liquid hydrazine, monomethylhydrazine and unsymmetrical dimethylhydrazine ignite spontaneously in NO_2^* -air atmospheres containing NO_2^* concentrations greater than about 8, 11 and 14 volume percent, respectively. These results appear to be independent of the fuel volume down to at least 10 μ liters. An increase in the liquid fuel temperature appears to decrease the NO_2^* -air mixture temperature required for spontaneous ignition.

2. The addition of small quantities (0.3%) of oxygen to an He- NO_2^* mixture lowers the S.I.T. of UDMH considerably (as much as 50°C.). This indicates that oxygen may be acting as a third body in the kinetic reactions leading to ignition.

3. A moderate increase in pressure tends to decrease the S.I.T. of UDMH in NO_2^* -air. The amount of decrease varies with addition of NO_2^* to the air in the same manner as the mole fraction of N_2O_4 .

4. At ambient temperature and pressure, mixtures of UDMH vapor and air ignite spontaneously on contact with NO_2^* provided the UDMH concentration in the UDMH-air mixture exceeds about 9 volume percent.

IV. ACKNOWLEDGMENT

This research was supported in part by the Department of the Navy under Order NAonr-11-60 (Office of Naval Research, Bureau of Ships, Bureau of Yards and Docks, Bureau of Weapons).

LITERATURE CITED

1. ASTM Standards on Petroleum Products and Lubricants. American Society for Testing Materials, Philadelphia, Pa., pp. 155-6, November 1956.
2. Zabetakis, M. G., Furno, A. L., and Jones, G. W., Minimum Spontaneous Ignition Temperatures of Combustibles in Air. Ind. Eng. Chem., Vol. 46, pp. 2173-78, October 1954.
3. Laidler, K. J., Chemical Kinetics, McGraw-Hill Book Company, Inc., New York, p. 70, 1950.

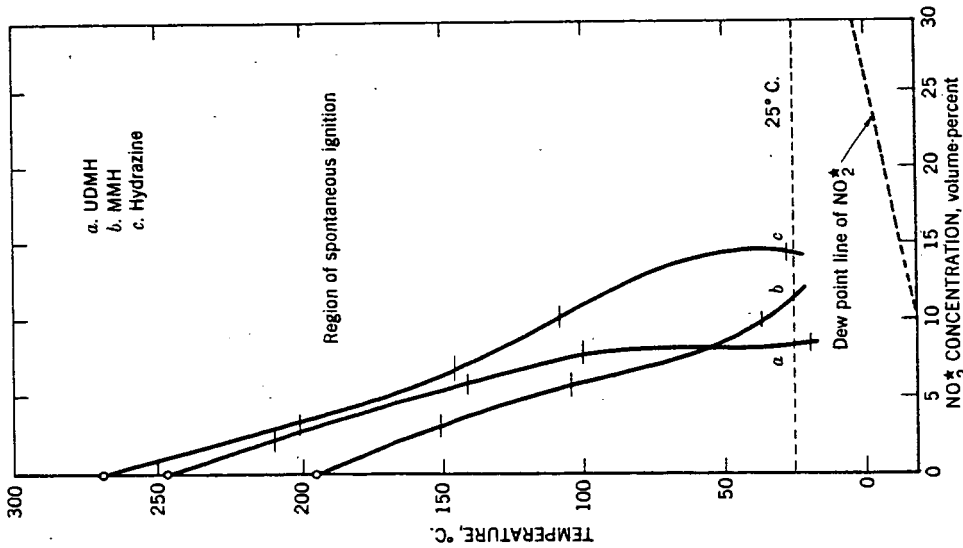


Figure 1.--Minimum spontaneous ignition temperatures of liquid hydrazine, MMH and UDMH at an initial temperature of 25°C, in contact with NO₂-air mixtures at 740±10 mm. of Hg pressure as a function of NO₂* concentration.

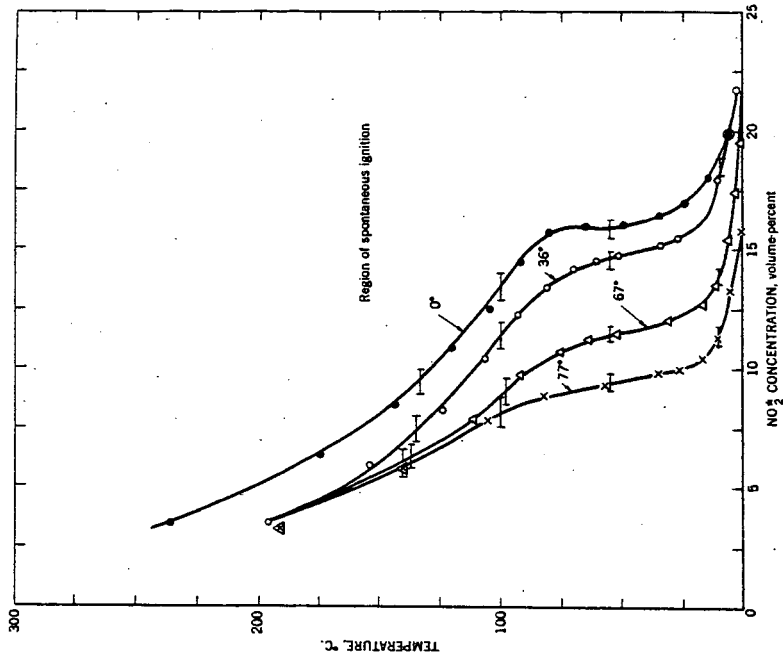


Figure 2.--Minimum spontaneous ignition temperatures of liquid hydrazine at various initial temperatures in NO₂*-air mixtures at 740±10 mm. of Hg pressure as a function of NO₂* concentration.

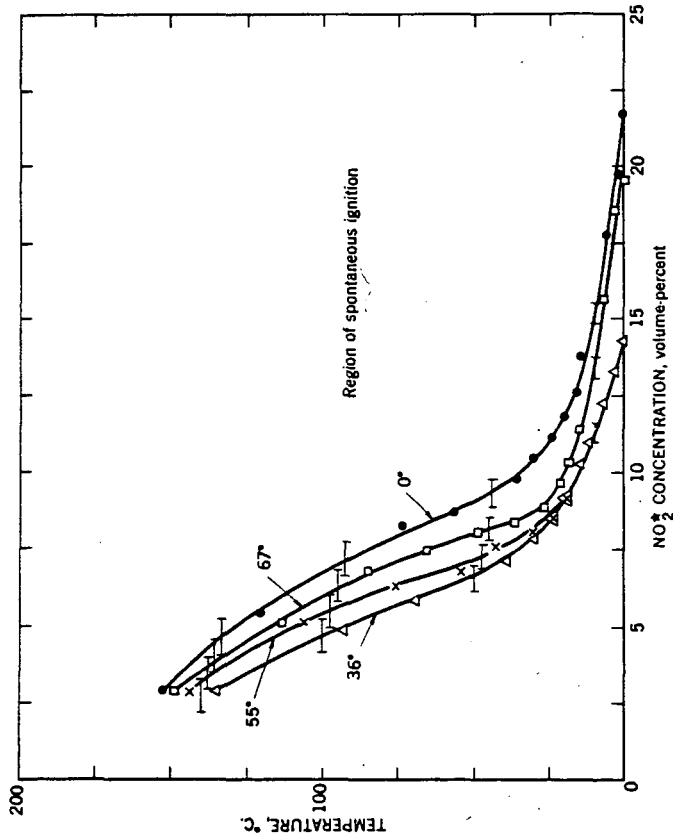


Figure 3.--Minimum spontaneous ignition temperatures of liquid MMH at various initial temperatures in NO₂*-air mixtures at 740±10 mm. of Hg pressure as a function of NO₂* concentration.

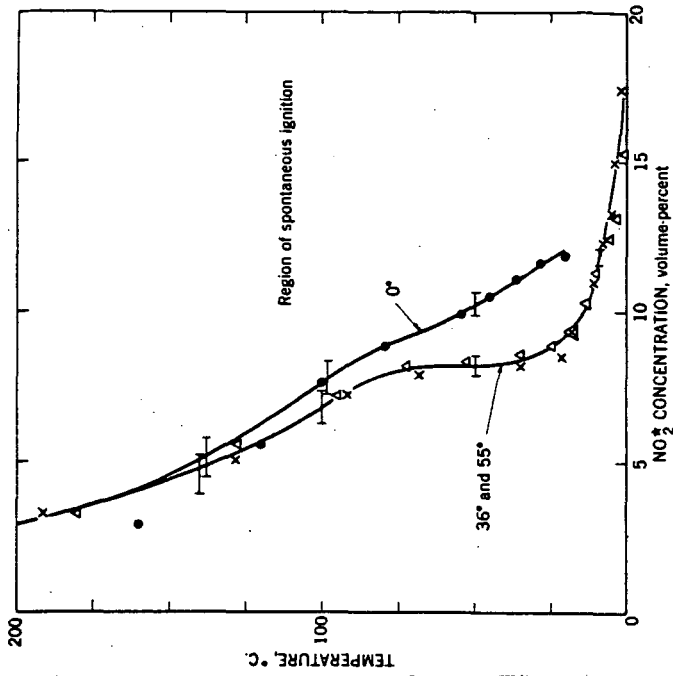


Figure 4.--Minimum spontaneous ignition temperatures of liquid UDMH at various initial temperatures in NO₂*-air mixtures at 740±10 mm. of Hg pressure as a function of NO₂* concentration.

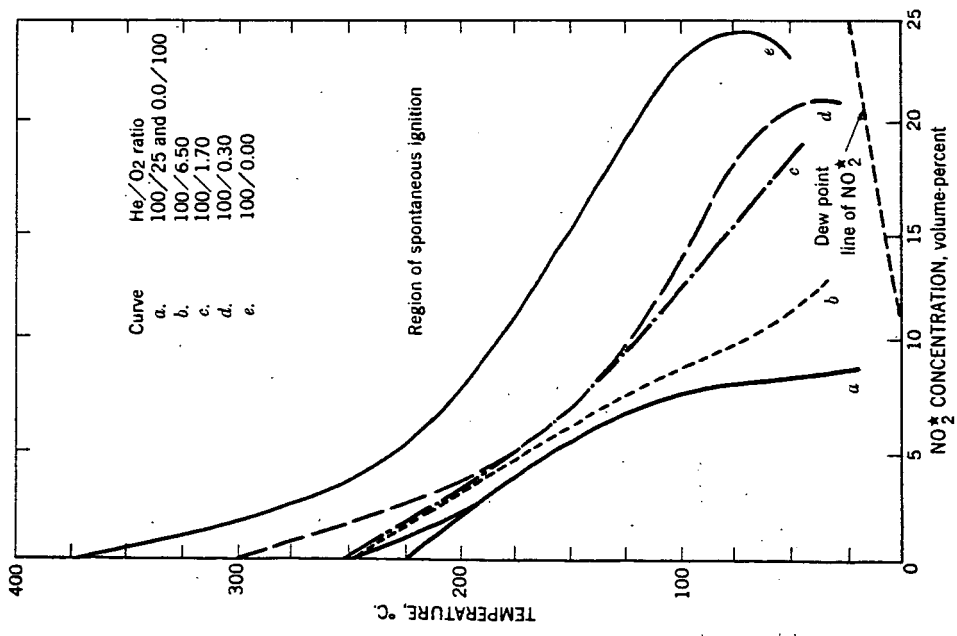


Figure 5.--Minimum spontaneous ignition temperatures of 0.05 cc. of liquid UDMH in He-O₂-NO₂* atmospheres at one atmosphere pressure for various He/O₂ ratios.

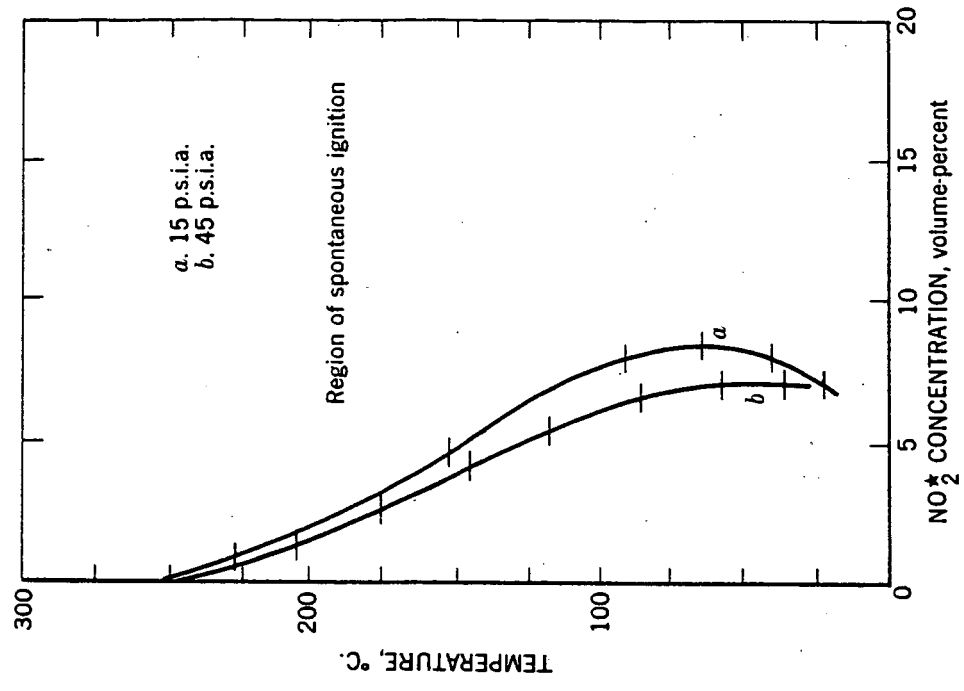


Figure 6.--Minimum spontaneous ignition temperatures of 0.05 cc. of liquid UDMH in NO₂*-air mixtures at 15 and 45 psia. pressure as a function of NO₂* concentration.

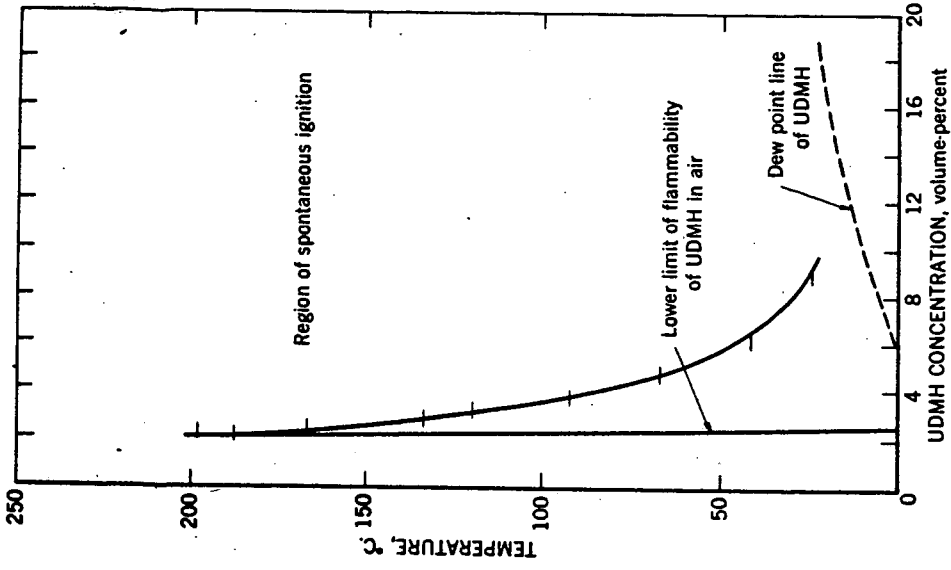


Figure 8.--Minimum spontaneous ignition temperatures of vaporized UDMH-air mixtures in contact with 100% NO₂* at 25°C, and 740±10 mm. of Hg Pressure as a function of UDMH concentration in air.

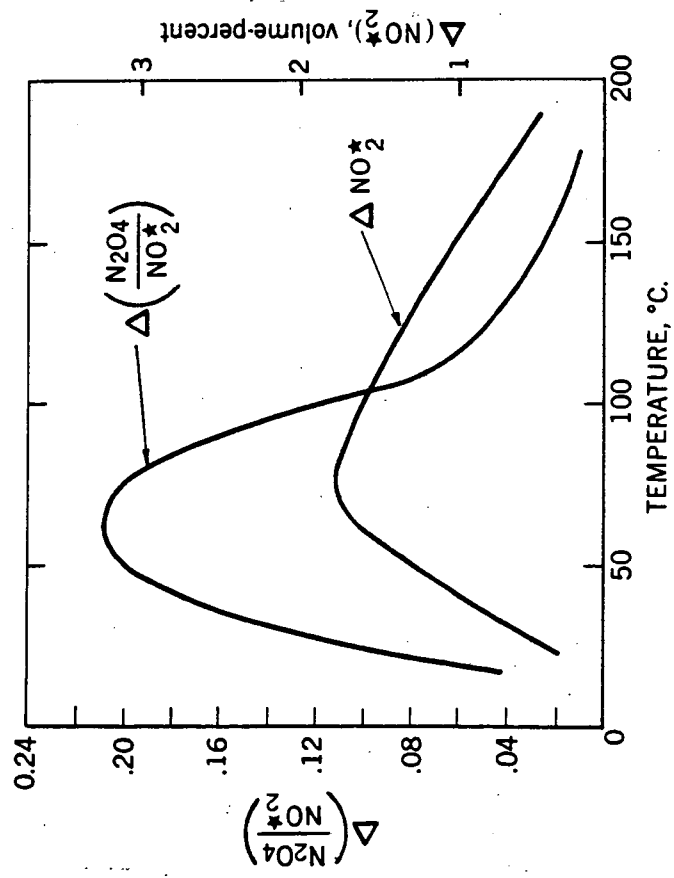


Figure 7.--Effect of temperature on the differences in NO₂* and in the mole fraction of N₂O₄ in NO₂* due to a change in pressure (45 to 15 psia.).

ABSTRACT

TITLE OF PAPER: The Reactions of Pentaborane-11 With Unsaturated Hydrocarbons

AUTHORS: A. Levy and E. A. Lawton

PLACE WORK WAS DONE: Battelle Memorial Institute
Columbus 1, Ohio

Conditions have been established for reacting pentaborane-11 with olefinic and acetylenic compounds. Depending upon the reaction conditions, gel-like and liquid products are obtained from reactions with olefins, while the acetylenes yield only gel-like products. The liquid products have been examined with respect to physical properties, molecular weight, elemental analysis, methanolysis, mass spectrographic and infrared analysis, thermal stability, pyrophoricity, and heat of combustion. A structure is proposed from this evidence for the new product.

Chemical Structure and Processing of Coal
George Richard Hill and Lloyd B. Lyon
Fuels Engineering Department, University of Utah
Salt Lake City, Utah.

During the past several years, much excellent work has been done which contributes to a more complete knowledge of the basic structure of coal. Smirnov (1) states in a comprehensive review article that there has been a development and deepening of our knowledge of coal structure, an increase in the number of investigations and a broadening of the circle of scientists from different countries occupied with these questions.

The Model for High Volatile Bituminous coal, suggested in Figure 1, takes into account the major observations reported in the literature as well as observations made in our laboratory (2).

The model suggests that coal consists of large heterocyclic nuclei (with alkyl side chains) monomers, held together by the three dimensional C-C groups suggested by Friedel (3), the functional oxygen groups of Van Krevelen (4), and the ether bonds of Kukhareenko (1), Roy (5), Blom (6), Brooks (7) and Orchin and Storch (8, 9, 10, 11). Sulfur is interchangeable with oxygen in some structures and the close relationship between the chemical properties of similar fractions suggests that sulfur and oxygen may be present in linking units. All researchers seem to agree that nitrogen occurs mainly in the heterocyclic ring structures. (12).

The functional oxygen groups in coal are best presented by Blom, Edelhausen, and Van Krevelen in their functional oxygen group diagram (6). Van Krevelen's method of calculating the functional oxygen groups by the amount of water, carbon dioxide and carbon monoxide derived from primary carbonization was applied to the gases obtained from low temperature carbonization of a Utah semi-coking coal (13). The results are as follow: OH = 6.4 to 7.8%, COOH = 0.5 to 1.0%, -O- and C = O = 1.3 to 2.6%. These percentages agree with the proposed model.

The nature of the "hydrocarbon" components of the coal structure has been discussed by Nelson (14). His evaluation of the work of Frolich and Fulton on coals heated to temperatures of 750°F to 1100°F is the partial basis for concluding that long chain, simple, aliphatic and alicyclic hydrocarbons groups predominate in the coal structure. Other evidence is found in the work of Goodman, Gomez and Parry (15, 16) who find high yields of olefins and paraffins in their low temperature carbonization distillates. The amount of olefins found in low temperature

tars may be as high as 50% of the neutral oil yield. Olefins and paraffins combined in a typical sample of distillate from a high volatile bituminous B coal from Spring Canyon Utah totalled 64% (Ibid.)

The normal and isoparaffin content of low temperature tars is reported by Lewis. He identified C₉ to C₂₂ normal paraffins and C₁₀ to C₁₇ isoparaffins in the products of low temperature distillation (17).

A sample of crystalline hydrocarbon from low temperature carbonization was furnished our laboratory by the Pacific Chemical Company of Wellington, Utah. The material had been assumed to be a pure aromatic fraction; infra-red analysis and other tests demonstrated it to be essentially a C₂₀ paraffin. The total distillate from this operation was atypical of coal tars; it resembled a waxy gas-oil-cresote oil mixture and was reddish-brown in color. Apparently little secondary cracking and polymerization had occurred in the process of its formation.

Friedel and Queiser, by ultra-violet and visible spectra studies concluded that aliphatic groups rather than poly nuclear condensed aromatics predominate in the coal structure (3,12). Given (18) and Brown (19, 20) present evidence for polycondensed aromatics. It may be that coals can vary in the relative amounts of hydrocarbon class constituents as do different crude oils.

The structures tying together the components constituting coal are considered by Given (18), Van Krevelen (1, 21, 22, 23) and Dryden (24) to be principally aliphatic (methylene) bridges. Friedel and Queiser (3) believe that tetrahedral bonds are the cross linking units required to give coal its three dimensional structure. Brown et al., from nuclear magnetic resonance studies and from infra-red studies on coal distillates, found little evidence for methylene bridge carbons (19, 20). The structure proposed in the present paper conforms to these observations.

There seems to be a general belief that the larger the organic molecule the more complex it becomes. This belief is probably a logical consequence of the increase in the number of theoretically possible isomers with increase in molecular weight and the difficulty of separating the large molecules. However, Hood and associates from mass spectrometric studies of heavy distillates of petroleum (e.g. C₂₀-C₄₀ oils and waxes) during the past several years present a different picture. They find the molecules contain essentially one long carbon-atom chain, to one or both ends of which a ring system or short branch may be attached. In paraffin waxes the molecules are predominantly n-alkanes along with some slightly branched iso-alkanes, cycloalkanes, and even traces of aromatics. In lubricating oils, the isoalkanes have slightly longer branches, and the monocycloalkanes and monoaromatics have several short methyl branches on the ring.

Polyaromatics generally appear to have all of their aromatic rings in a single condensed nucleus. Similarly, mass spectral evidence for polycyclic saturates suggests molecules with a condensed ring system at one end of a chain, but the interpretations are less clear and cannot yet exclude the possibility of a ring systems at both ends. Although it is recognized that a small percentage of complex molecules might be present, the authors consider the new picture to be one which, in general, is representative of the distillate range of petroleum ($< C_{40}$) (25). This concept of simplicity and lack of isomers of large molecules is probably true in the basic structure of coal as well. In coal the large condensed nuclei are hetrocyclics with the same simple aliphatic side chains.

Structure and Distillation

From the work of Orchin, Storch and associates (9, 10, 11, 26), Frankè, Crowley and Elder (27), Gomez, Goodman and Parry (15, 16), Berkowitz (28, 29) and Van Krevelen and associates (4), it can be seen that the yield of liquids from coal distillation is dependent upon the basic structure of the coal, particularly the functional groups, and the process used to convert the coal into liquids and coke. It has been observed that distillation under moderate pressures of hydrogen eliminates the oxygen bridges, increases the liquid yield and also increases coke quality (9, 10, 11, 26, 27).

It is apparent that total hydrogenation of coal is uneconomic. However, a distillation process in which the hydrogen rich portions of the coal are retained as relatively low molecular weight hydrocarbons by hydrogenation in the presence of suitable catalysts might be worth considering.

Most investigators agree that the functional oxygen and sulfur groups control the yield of liquid products from coal. Van Krevelen states that the secondary reactions (polymerization to high molecular weight products) are especially noticeable with phenolic model materials. The cleaving of non-hydrocarbon bonds such as those of nitrogen, oxygen and sulfur, by hydrogen treating methods has recently become well established in the petroleum industry. For example, Blue and Spurlock have worked with cobalt molybdenum catalysts (30). Commercial catalytic hydrocracking methods include the Gulf HDS process (31), the Union Oil Uni-cracking process (32), the Standard Oil of California Isocracking process and the Universal Oil Lomax process, among others. The trend of increased hydrogen processing in industry has been discussed by Olson and Schneider (33) who mention hydrocracking of residual oils, hydrogenation of shale oil and gilsonite, hydrogenation of low gravity, high sulfur crudes and hydrogenation of aromatics to form superior jet fuels.

Some of these methods have been and are being applied to coal and to coal liquids (9, 27, 34) for the removal of the functional cross bonding groups for the production of maximum yields of liquids and of high quality coke. Van Krevelen for example, has worked on model material pyrolysis using the hydrogen donor materials suggested by Orchin and Storch to increase liquid yields and to minimize the polymerization-condensation reactions promoted by hydroxyl groups (4). The Varga process (35) and the Lozovoi process (36) are two additional examples of the use of hydrocracking techniques to produce high octane gasoline and other liquids from coal, primary tars, shale oil and high asphalt crude oil residues. Catalytic methods discussed by Flinn (37), Haensel (38) and Topchiev (39) are applicable to coal and coal liquids.

The high liquid yields made possible by hydrocracking-hydrotreating distillation of high volatile coals plus the marketability of the residual coke make it apparent that there will be a smooth and gradual transition from conventional petroleum refining to coal refining as the economic picture becomes favorable.

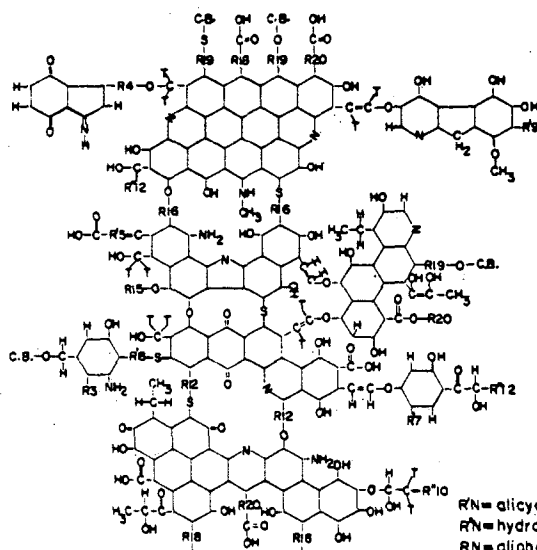
BIBLIOGRAPHY

- (1) Smirnov, R. N., "Contemporary Representation of Coal Structure," *Advances in Chemistry*, B. 28, No. 7, 1959, (Inst. Fossil Fuels, Moscow, A. Review with 113 references through 1958), Translated by V. Fredricks.
- (2) Lyon, Lloyd and Hill, George Richard, Ed., "The Structure and Chemistry of High Volatile Coals; The Catalytic Conversion of High Volatile Coals by Hydro-Catalytic Methods to Liquids and Coke". University of Utah Engineering Experiment Bulletin No. 109, Vol. 51, No. 26.
- (3) Friedel, R. A., Queiser, J. A., "Ultra-Violet-Visible Spectrum and the Aromaticity of Coal," *Fuel*, London, Vol. 38, 1959, pp. 369-79.
- (4) Van Krevelen, D. W., Waterman, H. I., Wolfs, P. M. J., Part I to VII - *Brennstoff-Chemie*, V. 40, 1959, Special Reference V - "Pyrolysis of Model Materials with Functional Groups," and VII - "Application to Mineral Coal of Understanding Attained," Translated by V. Fredricks.
- (5) Roy, M. M., "Chromatographic Analysis of Coal Extracts Prepared from Assam Coal," *Fuel*, London, Vol. 36, pp. 344-54.
- (6) Blom, L., Edelhausen, L., Van Krevelen, D. W., "Chemical Structure and Properties of Coal XVIII- Oxygen Groups in Coal and Related Products," *Fuel*, London, Vol. 36, 1957, pp. 135-58.
- (7) Brooks, J. D., Maher, T. P., "Acidic Oxygen-Containing Groups in Coal," *Fuel*, London, Vol. 36, pp. 51-62.
- (8) Golumbic, C., Anderson, J. B., Orchin, M., Storch, H. H., "Solvent Extraction of Coal by Aromatic Compounds at Atmospheric Pressure," U.S. Bureau of Mines, R. I. 4662, March 1950.

- (9) Orchin, M., Storch, H. H., "Solvation and Hydrogenation of Coal," *Ind. Eng. Chem.* Vol. 40, No. 8, August 1948, pp. 1385-89.
- (10) Orchin, M., Goldbach, G. L., Wolak, M., Storch, H. H., "Coal Hydrogenation. The Effect of Variations in the Coal-to-Vehicle Ratio," U. S. Bureau of Mines, R. I. 4499, July 1949.
- (11) Orchin, M., Columbic, C., Anderson, J. E., Storch, H. H., "Studies of the Extraction and Coking of Coals and Their Significance in Relation to its Structure," U. S. Bureau of Mines Bull., 505, 1951.
- (12) LeMaire, G. W., "A Study of Asphalt and Asphaltic Materials," *Quarterly of the Colo. Sch. of Mines*, Vol. 48, No. 2, April 1953.
- (13) State of Utah, "Low-Temperature Carbonization of Utah Coals," May 1939.
- (14) Nelson, W. L., *Petroleum Refining Engineering*, Fourth Edition, McGraw-Hill Book Company, Inc., New York, 1958.
- (15) Gomez, M., Goodman, J. B., Parry, V. F., "Low-Temperature Tar from Fluidized Carbonizing Reactors," U.S. Bureau of Mines, R. I. 5302, Feb. 1957.
- (16) Gomez, M., Goodman, J. B., Parry, V. F., "General Properties of Low-Temperature Tar," U. S. Bureau of Mines Bull. 569.
- (17) Lewis, H. R., "Paraffins in Low Temperature Tar From Fluidized Carbonization Process," *Chemical and Industry*, London, August 15, 1959, (National Coal Board, Stoke Orchard, England) pp. 1049-50.
- (18) Given, P. H., "The Distribution of Hydrogen in Coals and Its Relation to Coal Structure," *Fuel*, London, Vol. 39, 1960, pp. 147-53.
- (19) Brown, J. K., "Infra-red Spectra of Solvent Extracts of Coals," *Fuel*, London, Vol. 38, 1959, pp. 55-63.
- (20) Brown, J. K., Ladner, W. R., Sheppard, N., "A Study of the Hydrogen Distribution in Coal-like Materials by High-Resolution Nuclear Magnetic Resonance Spectroscopy I - The Measurement and Interpretations of the Spectra," *Fuel*, London, Vol. 39, 1960, pp. 79-86. "II - A Comparison With Infra red Measurements and the Conversion to Carbon Structure," *Fuel*, London, Vol. 39, 1960, pp. 87-95.
- (21) Van Krevelen, D. W., Ghermin, H. A. G., Schuyer, J., "XIX - Reevaluation of the Structural Parameters of Vitritines," *Fuel*, London, Vol. 36, pp. 313-20. (1957)
- (22) Fitzgerald, D., Van Krevelen, D. W., "XXI - The Kinetics of Coal Carbonization," *Fuel*, London, Vol. 38, 1959, pp. 17-37.
- (23) Wolfs, P. M. J., Van Krevelen, D. W., Waterman, H. I., "Chemical Structure and Properties of Coal XXV - The Carbonization of Coal Models," *Fuel*, London, Vol. 39, 1960, pp. 25-38.
- (24) Dryden, I. G. C., "Chemical Structure of Coals: A Method for Comparing Data of Different Origins and for Testing Sets of Data for Self-Consistency," *Fuel*, London, Vol. 37, 1958, pp. 444-68.

- (25) Hood, A., Clerc, R. J., O'Neal, M. J., "The Molecular Structure of Heavy Petroleum Compounds," Journal of the Institute of Petroleum, Vol. 45, No. 426, June 1959, pp. 168-73.
- (26) Pevere, E. F., Arnold, G. B., U. S. Patent 2,595,979, June 5, 1952.
- (27) Franke, N. W., Crowley, E. L., Elder, H. S., "Solvent Extraction of Lignite and Carbonization of Lignite Extracts," Ind. Eng. Chem., Vol. 49, No. 9, Sept. 1957, pp. 1402-8.
- (28) Berkowitz, N., "Dispersibility of Coal in a Supersonic Field," Nature, Vol. 163, May 21, 1949, pp. 809-10.
- (29) Berkowitz, N., "Mechanism of Coal Pyrolysis 1 - On the Nature and Kinetics of Devolatilization," Fuel, London, Vol. 39, 1960, pp. 47-58.
- (30) Blue, E. M., Spurlock, B., "Cobalt-Moly Catalyst," Chem. Eng. Prog., Vol. 56, No. 4, April 1960, pp. 54-9.
- (31) Beuther, H., Flinn, R. A., "Gulf HDS Turns Resid Into Cat Feed," Petroleum Refiner, Vol. 39, No. 4, April 1960, pp. 143-48.
- (32) Hansford, R. C., Reeg, C. P., Wood, F. C., Vaell, R., "Unicracking," Oil and Gas Journal, Vol. 58, No. 16, April 18, 1960, pp. 104-6.
- (33) Olson, H. N., Schneider, South West Engineering Co., "Big Future for Hydrogen Processing," Petroleum Refiner, Vol. 39, No. 4, April 1960.
- (34) Lyon, Lloyd B., Patents Pending.
- (35) Varga, J., Karolyi, J., Steingösznev, P., Zalai, A., Birthler, R., Rabo, Gy., Nagynyomasu Kieserleti Intezet, Budapest. "Hydrocracking Tried on Larger Scale," Petroleum Refiner, Vol. 39, No. 4, pp. 182-3.
- (36) Lozovoi, A. V., Muselevich, D. L., Blonskaye, A. I., Ravikovich, T. M., Titova, T. A., "High Octane Gasoline From Coal and Primary Tars," USSR 111, 769, June 25, 1958.
- (37) Flinn, R. A., Larson, O. A., Beuther, H., "The Mechanism of Catalytic Hydrocracking," Ind. & Eng. Chem., Vol. 53, No. 2, Feb. 1960, pp. 153-56.
- (38) Haensel, V., Berger, C. U., Advance Petroleum Chemistry and Refining, Interscience Publishers, Inc., Edited by K. A. Kobe and J. J. McKetta, Vol. 1, 1958.
- (39) Topchiev, A. V., "Boron Fluoride and Its Compounds as Catalysts in Organic Chemistry," International Series of Monographs on Organic Chemistry, Translated by J. T. Greaves, Pergamon Press, 1959.

TYPICAL CROSS BONDED STRUCTURE OF HIGH VOLATILE COALS



(High Volatile Coal Analyses)

H = 4 to 6% by wt.
 C = 70 to 93% by wt.
 N = .5 to 2% " "
 S = .5 to 3% " "
 O = 7 to 24% " "

CROSS BONDING TO MORE
 HETEROCYCLIC GROUPS

PROPOSED MODEL

Fig. I

RN = alicyclics of n carbons.
 RN = hydroaromatics of n carbons.
 RN = aliphatic side chain of n carbons.
 C.B. = cross bonding by O or S to new
 heterocyclic groups with long
 side chains.
 T = tetrahedral 3 dimensional CC bonds,
 C-O bonds and C-S bonds.

PYRITE REMOVAL FROM OIL-SHALE CONCENTRATES USING LITHIUM ALUMINUM HYDRIDE

Dale L. Lawlor, J. L. Fester, and W. E. Robinson

Bureau of Mines, U. S. Department of the Interior,
Laramie, Wyo.

A new technique has been developed by the Federal Bureau of Mines for removing pyrite from oil-shale concentrates. This was accomplished by treating concentrates with a tetrahydrofuran solution of lithium aluminum hydride at reflux temperature and extracting the resulting soluble sulfide with dilute acid. By this procedure, the pyrite content of a carbonate free oil-shale concentrate was reduced from 5.0 to 0.02 percent, without objectionable alteration of the organic material (kerogen) as indicated by elemental and infrared analyses. Concentrates obtained by this method will be useful in kerogen structural studies.

According to Bradley (1), oil shale of the Green River formation was deposited in shallow, fresh-water lakes during the Eocene period. The kerogen probably formed from microscopic algae and other aquatic organisms; the minerals formed from water-soluble salts and from deposition of stream-carried silt. A typical Green River oil shale contains more than 50 percent mineral, which includes carbonates, quartz, feldspar, illite clay, and pyrite. Pyrite forms in an alkaline and reducing medium and according to Rosenthal (3), may be formed in nature under similar conditions. It is desirable to remove most or all of the minerals from oil shale in order to have a suitable sample for structural study. Ordinary concentration techniques remove other minerals but concentrate pyrite with the kerogen. This presents a special problem.

Pyrite enters into many of the reactions of kerogen, and many physical-property measurements of kerogen cannot be made when pyrite is present. For example, pyrite enters into reduction, oxidation, and hydrolysis reactions; complicates functional group analysis; and causes high background and poor resolution in X-ray diffraction analyses. Organic sulfur analyses necessitate pyritic sulfur corrections.

Previously, quantitative removal of pyrite has not been possible without objectionable alteration to the kerogen. Nitric acid completely oxidizes the pyrite, but oxidizes and nitrates the kerogen. Nascent hydrogen does not entirely remove the pyrite (2). Pyrite can be oxidized by other reagents (5), but if they were used on oil shale, drastic alteration of the kerogen probably would result.

Lithium aluminum hydride treatment quantitatively removes pyrite from oil-shale concentrates. This treatment is rapid and simple, and causes predictable changes to the kerogen.

EXPERIMENTAL PROCEDURE

Sample Preparation. Two concentrates were used in this study and were prepared from the same raw shale. The first of these, designated as acid concentrate, was prepared in the following manner: A sample of Green River oil shale was ground to pass a 100-mesh screen and treated with one normal hydrochloric acid until free of carbonate minerals. The mixture then was filtered and the

residue washed with boiling water until the filtrate was neutral. The concentrate then was dried under vacuum at 60° C. for 12 hours.

The second concentrate, designated as attrited concentrate, was prepared (4) from the acid concentrate by the following procedure: Cetane was mixed with the sample to make a paste which was ground in a ball mill with an excess of water until a minimum ash was attained for the organic concentrate. The cetane then was extracted from the paste with benzene and the organic concentrate was dried under vacuum at 60° C. for 12 hours. The silicate minerals were removed by this concentration procedure, because they are preferentially wet by water.

A sample of an Illinois bituminous coal was ground to pass a 100-mesh screen and dried under vacuum at 60° C. for 12 hours.

Lithium Aluminum Hydride Treatment. Two-hundred grams of attrited concentrate and 40 grams of lithium aluminum hydride (LAH) were placed in a 3-liter flask, equipped with a reflux condenser to which a Caroxite drying tube was attached. One and one-half liters of tetrahydrofuran was slowly introduced. The reaction mixture was refluxed for one-half hour, cooled to room temperature, and vacuum filtered. The filtration was stopped while the residue was still wet. To destroy the unreacted LAH, the residue was transferred in small portions as rapidly as possible to a 4-liter beaker containing 1 liter of water. This mixture was acidified with 100 milliliters of 1 N hydrochloric acid, heated to boiling, and filtered. This acid treatment was repeated four times to insure complete removal of aluminum ions, as shown by testing the washings with ammonium hydroxide. The residue was washed with boiling water to remove the hydrochloric acid and then dried under vacuum at 60° C. for 12 hours.

The acid concentrate and the bituminous coal were treated using a similar procedure, except that 20-gram samples with 4 grams of LAH were used.

Nitric Acid Treatment. Pyrite was removed from the attrited concentrate by boiling the sample for one-half hour in 2 N nitric acid and filtering and leaching with boiling water until the filtrate was neutral. The product was dried under vacuum at 60° C. for 12 hours.

Sample Analyses. Pyrite content was determined by the modified Mott method (6). Qualitative evidence for the presence of pyrite was obtained from X-ray diffraction spectra using its 33° 2 theta peak. Ash content was determined at 1000° C. Elemental analyses were determined using the following methods: Carbon and hydrogen by combustion, nitrogen by Kjeldahl, total sulfur by Eschka, organic sulfur by subtraction of pyritic from total sulfur, oxygen by difference, and chlorine by Schoninger. Organic elemental composition was calculated on a mineral and chlorine free basis.

Infrared spectra were obtained using the potassium bromide pellet technique.

RESULTS AND DISCUSSION

Pyrite Removal. Pyrite is quantitatively removed from the oil-shale concentrates. Lithium aluminum hydride treatment lowers the pyrite content of the

attrited concentrate from 5.3 percent to 0.02 percent and the pyrite in the acid concentrate from 3.1 to 0.02 percent as shown in Table 1. Further evidence of

Table 1. - Decrease of pyrite and ash content due to LAH treatment

	Attrited Concentrate		Acid Concentrate		Bituminous Coal	
	Untreated	Treated	Untreated	Treated	Untreated	Treated
Pyrite, wt. %	5.3	0.02	3.1	0.02	1.8	0.2
Ash, wt. %	8.8	5.5	44.5	43.0	9.4	6.7
Pyrite, X-ray Peak Heights	16	0	4	0	6	0

pyrite removal is shown by disappearance of the X-ray diffraction pyrite peak in the LAH treated concentrates. Pyrite removal is also reflected by decrease of the ash in the attrited concentrate from 8.8 to 5.5 percent and in the acid concentrate from 44.5 to 43.0 percent. This ash reduction approximates the amount expected due to pyrite removal.

This method, which was developed for oil shale, reduced the pyrite content of the bituminous coal sample from 1.8 to 0.2 percent.

Effect on Kerogen. Examination of available data shows little change in the kerogen structure by LAH treatment. Organic elemental analyses (Table 2) reveal

Table 2. - Organic composition of various samples

	Attrited Concentrate		HNO ₃ Concentrate	Acid Concentrate		Bituminous Coal	
	Untreated	Treated		Untreated	Treated	Untreated	Treated
WT. % 1/							
H	10.2	10.9	9.0	10.2	10.8	5.7	5.7
C	77.5	79.9	70.1	77.5	78.6	77.6	78.0
N	2.6	2.7	4.3	2.5	2.6	1.4	1.4
S	1.4	1.5	1.0	1.3	1.5	2.7	3.2
O 2/	8.3	5.0	15.6	8.5	6.5	12.6	11.7
Total	100.0	100.0	100.0	100.0	100.0	100.0	100.0
ATOMIC RATIOS							
H/C	1.58	1.63	1.54	1.58	1.65	0.88	0.88
N/C	0.03	0.03	0.05	0.03	0.03	0.02	0.02
S/C	0.005	0.006	0.005	0.006	0.007	0.01	0.02
O/C	0.08	0.05	0.17	0.08	0.06	0.12	0.11

1/ Based on mineral and chlorine-free sample

2/ By difference

no significant differences, except for oxygen, between treated and untreated samples. The elemental analyses indicate a loss of 3.3 percent oxygen for the attrited concentrate and 2.0 percent for the acid treated concentrate. The atomic ratios of hydrogen to carbon, nitrogen to carbon, and sulfur to carbon for the LAH treated sample are approximately the same as the untreated concentrates. However, the oxygen to carbon ratios of the treated concentrates are lowered from 0.08 to approximately 0.05.

The overall infrared spectra (Figure 1) are much the same for the treated and untreated samples. Infrared spectra, however, show elimination of the 5.9 micron band which is attributed to carbonyl groups. The change noted in the 9 to 10 micron region presumably is due to better resolution of the silicate mineral bands. The carbonyl elimination and oxygen decrease may be explained by the reduction of a carboxyl group or an ester linkage to form alcohols.

Nitric acid treatment of the attrited concentrate for pyrite removal increases the nitrogen content from 2.6 to 4.3 percent and oxygen from 8.3 to 15.6 percent.

CONCLUSIONS

Pyrite has been quantitatively removed from concentrates by using lithium aluminum hydride.

The concentrate produced by LAH treatment is well suited for kerogen structural studies because the LAH reacts only with specific functional groups. Of the functional groups present in kerogen, LAH reduces carbonyl oxygen but does not attack other groups such as ethers, alkenes and amines. Since such changes can be evaluated, they do not interfere with structural studies. Hence, the lithium aluminum hydride method for the removal of pyrite is preferable to the use of strong oxidizing agents, such as nitric acid, which cause non-specific changes in the kerogen.

Since LAH treatment eliminates the pyrite from kerogen concentrates, further treatment with dilute hydrofluoric acid should produce a near mineral-free sample, which would be valuable for future studies on kerogen structure.

ACKNOWLEDGMENT

This work was conducted under a cooperative agreement between the Bureau of Mines, U. S. Department of the Interior, and the University of Wyoming.

LITERATURE CITED

- (1) Bradley, W. H., Geol. Survey Prof. Paper 168 (1931) 58 pp.
- (2) Dancy, T. E. and Giedroyc, V., Jour. Inst. Petrol. 36 (1950) 593-603.
- (3) Rosenthal, G., Heidelberger Beitr. Mineral. u. Petrog. No. 6 (1956) 146-64.
- (4) Smith, J. W. and Higby, L. W., Anal. Chem., 32 (1960) 1718.
- (5) Swift, E. H., Introductory Quantitative Analysis, Prentice-Hall, Inc., New York, N. Y., (1950) p. 349.
- (6) van Hees, W. and Early, E., Fuel, 28 (1959) 425-8.

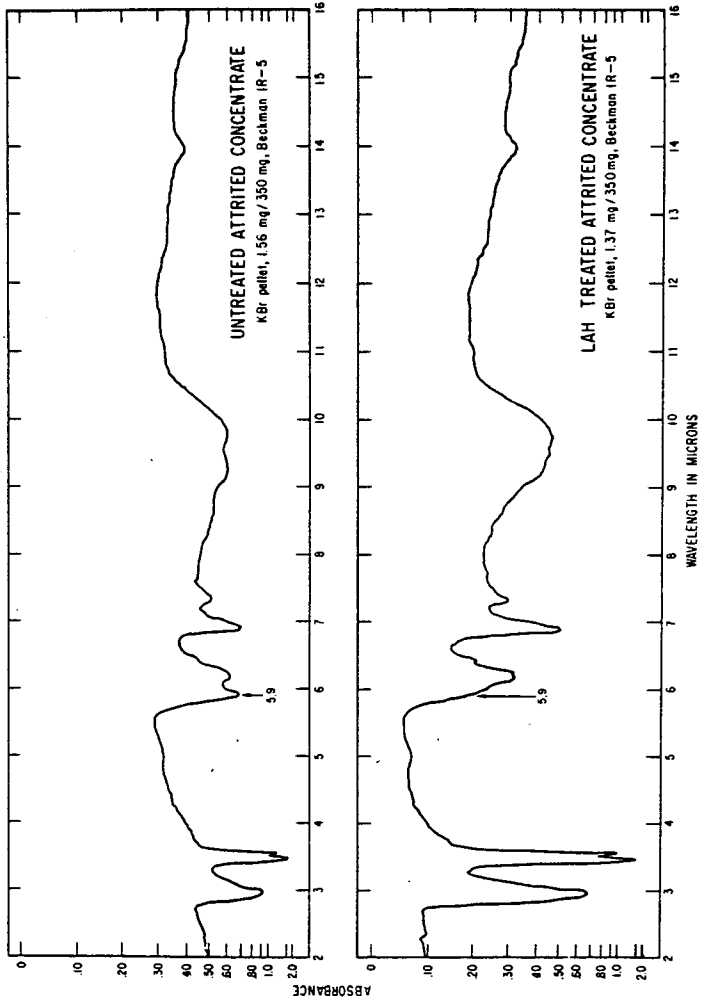


FIGURE 1 - INFRARED SPECTRA OF CONCENTRATES.

50A-334 P

Fundamental Properties of Green River Oil Shale
as Determined from Nitrogen Adsorption and
Desorption Isotherms

P. R. Tisot

Laramie Petroleum Research Center
Bureau of Mines, U. S. Department of the Interior
Laramie, Wyoming

Oil shale, a major potential source of liquid fuels, consists of a complex mixture of organic and inorganic constituents in variable proportions. Understanding of its fundamental properties and structure may aid in improving existing methods for converting the organic matter to useful liquid and gaseous products and in devising new methods (7,8,9,10,12).

A previous publication (14) presented data on particle size, particle-size distribution, and particle-size classification of the primary inorganic particles. Included were photomicrographs showing the geometric form of many of these particles. The paper also described the method used in preparing the organic-free mineral constituents for that work and the current study.

The present paper presents information on surface area, pore structure, and pore volume of oil shale and its mineral constituents, and the manner in which the organic matter is distributed through the shale. Based on the surface area of the mineral constituents and some logical assumptions, the maximum amount of organic matter in contact with the surface of the inorganic matrix is calculated.

EXPERIMENTAL

Preparation of Oil-Shale Samples

Two samples of approximately 200 pounds each were prepared by compositing random samples of EF and B bed shales from the Bureau of Mines experimental oil-shale mine near Rifle, Colorado (13). The composite sample from EF bed assayed 28.6 gallons a ton and that from B bed 75 gallons a ton. These were crushed to pass a 2-mesh-per-inch screen. A representative sample from each of the crushed oil shales was reduced to pass a 0.375-inch screen and a representative portion of this reduced further to pass a 200-mesh screen. The particles smaller than 44 microns were removed using a screening and washing technique. The remaining particles, 44 to 77 microns, were used to determine surface area, micropore structure, and pore volume. This particle-size range was selected to obtain a representative sample of the initial shale within a 4 to 5 gram sample, limited by the size of the adsorption bulb; to expose any naturally existing micropore structure, and to eliminate the surfaces of the extremely fine particles created during crushing. The 44 to 77 micron particles represented 53.4 and 42.6 weight percent of the respective 28.6- and 75-gallon-per-ton shales ground to pass 200-mesh. Chemical analyses indicated that their organic-inorganic ratios were quite similar to those of the 200-mesh shales prior to removing the particles smaller than 44 microns.

Apparatus

The low-temperature adsorption apparatus and technique employed for this study were similar to those described by Emmett (4), Joyner (1), and Reis (11). The

Pyrex-glass adsorption apparatus, fabricated in this laboratory, consisted of an adsorption bulb, calibrated gas burettes, mercury manometer, McLeod gauge, nitrogen-vapor-pressure thermometer, high vacuum system capable of 10^{-6} mm. of Hg., purification trains for nitrogen and helium, and reservoirs for the purified gases. The purity of the two gases exceeded 99.9 mole percent as determined by mass spectrometer.

Procedure

Oil Shale, 44 to 77 Microns. A sample of known weight was packed tightly into the adsorption bulb and degassed at 220°F. for 72 to 96 hours to attain a constant pressure of 10^{-6} mm. Hg. This degassing temperature was selected to clean the shale's surfaces without significantly changing its chemical or physical structure. To determine the effect of degassing time, runs as short as 8 hours were made. After degassing, the dead-space volume within the adsorption bulb was measured with helium at the temperature of liquid nitrogen. Subsequently the helium was pumped from the adsorption bulb and the sample again degassed at 220°F. for 30 minutes before determining its adsorption isotherm.

A complete adsorption isotherm at the temperature of liquid nitrogen was obtained by measuring the quantity of nitrogen adsorbed at pressures from a few millimeters to the saturation pressure of the nitrogen. Adsorption equilibrium was reached rapidly below a relative pressure of 0.35. Fifteen minutes was allowed for equilibrium before each successive known volume of nitrogen was admitted into the adsorption bulb. Above 0.35, two hours were allowed for equilibrium to be attained. This appeared ample time for the heat of adsorption to dissipate and for equilibrium to be established. To determine if equilibrium had occurred, the time was extended to six hours at several different relative pressures. No significant differences were noted when compared with two hours time. After completing the adsorption isotherm, the data for the desorption isotherm were obtained by removing a known volume of nitrogen and allowing the system to come to equilibrium before removing the next known volume of nitrogen. This was continued until the relative pressure dropped to 0.2. Equal time was allowed for desorption at the different relative pressures as was allowed for adsorption. Several adsorption-desorption runs were made for each of the two shales using different representative samples for each run. The loss in weight, probably due to decarboxylation and loss of volatile organic matter, ranged from 0.20 to 0.34 weight percent of the samples charged to the adsorption bulb.

Inorganic Constituents. Previous work (14) indicated that a high percentage of the primary inorganic particles were smaller than 44 microns. The term "primary" refers to the initial size of the particles. To retain their initial size and to maintain representation of the initial shales, a composite sample consisting of several hundred pieces, 0.25 to 0.375 inch, was selected from each of the two shales crushed to pass a 0.375-inch screen. The organic matter was removed from these samples by a thermal treatment which did not exceed 750°F. (14), and then each organic-free shale residue was blended to give two uniform samples before their respective adsorption and desorption isotherms were determined.

New inorganic particles, mainly calcium sulfate, were formed when the organic matter was removed. Because the calcium sulfate could exist as extremely fine particles and hence have an appreciable surface area, it was leached from a portion of each residue. Adsorption isotherms were determined on the water-soluble-free residues to compare their surface areas with those of the initial residues. The leached material represented 1.7 and 8.4 weight percent of the initial residues from the 28.6- and 75-gallon-per-ton shales. Because the residue from the rich shale contained such a high percentage of water-soluble material, both its adsorption and desorption isotherms were determined.

A sample, 5 to 6 grams, from each of the residues was packed tightly into separate adsorption bulbs, degassed at 600°F. for 16 hours, and then the dead-space volume determined. The sample was again degassed at 600°F. under high vacuum for 30 minutes before determining the respective isotherms. The time allowed for equilibrium to be

attained after each addition of nitrogen was 15 to 30 minutes for relative pressures below 0.35 and two to three hours for those above 0.35. In obtaining the desorption data, the reverse time intervals were used for desorption to attain equilibrium. In a number of instances, the time between addition or removal of nitrogen was increased to 10 hours in the relative pressure region above 0.75. Comparison of these data with those from the shorter periods indicated that two to three hours was ample time for either adsorption or desorption to occur at the higher relative pressures.

INTERPRETATION OF RESULTS

The experimental data can be expressed in graphic form as adsorption and desorption isotherms. These relate volume of nitrogen adsorbed or desorbed per gram of sample as a function of the relative pressure, P/P_0 , where P is the measured pressure within the adsorption bulb and P_0 is the liquefaction pressure of nitrogen. The adsorption-desorption isotherms of the two oil shales, the primary inorganic particles from each shale, and those from the rich shale free of water-soluble material are presented in Figures 1, 2, 3, 4, and 5.

As classified by Brunauer (2), all of the adsorption isotherms are of the sigmoid or S-shaped type, also referred to as Type II, with an asymptotic approach to the P_0 line. They were interpreted according to the method of Brunauer, Emmett, and Teller (3) who showed that S-shaped adsorption isotherms can be plotted according to the equation:

$$\frac{P}{V(P_0 - P)} = \frac{1}{V_m C} + \frac{(C - 1)P}{V_m C P_0} \quad \text{where}$$

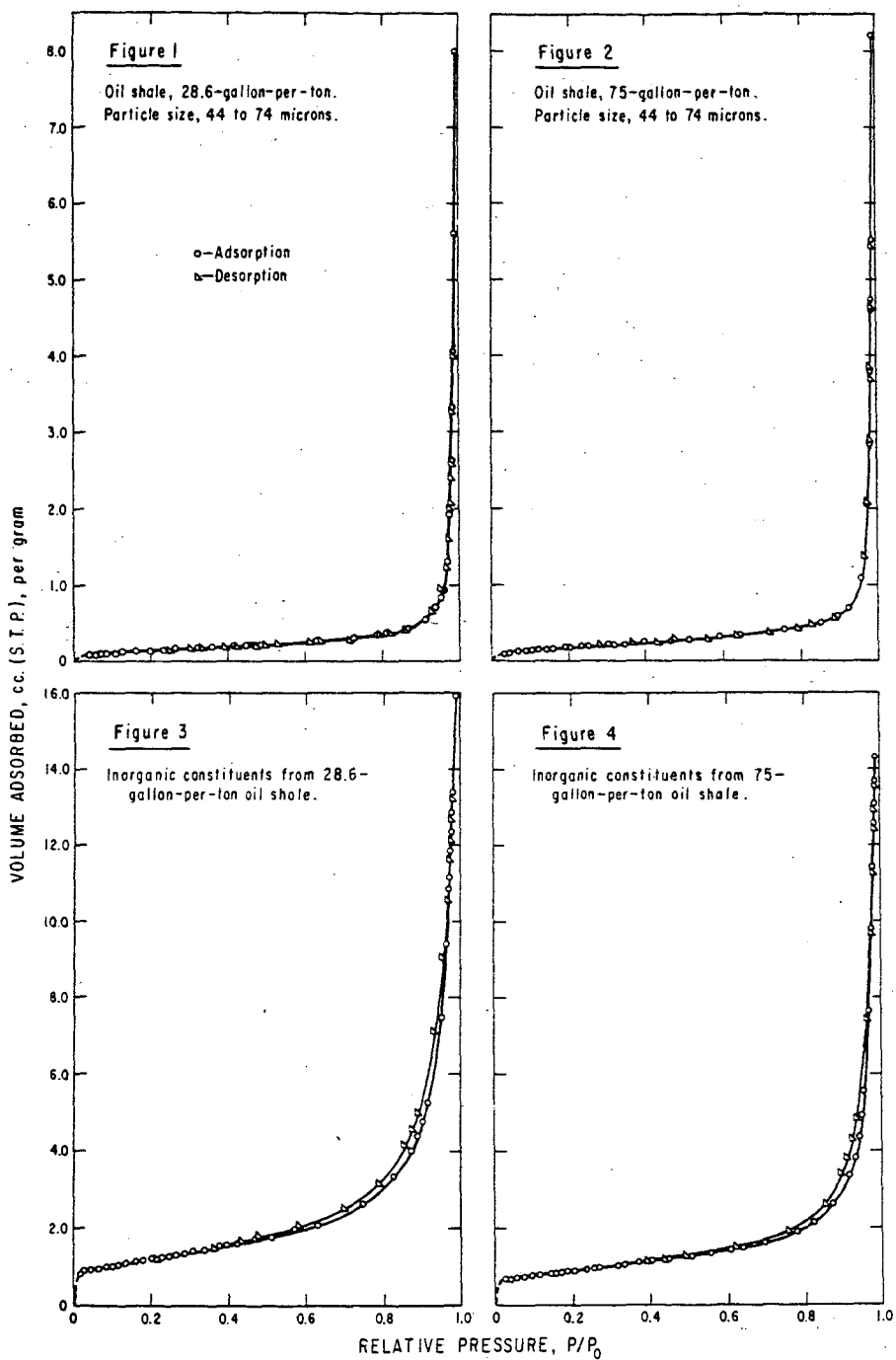
- P = measured pressure
- P_0 = liquefaction pressure of the adsorbate
- V = volume of gas adsorbed at pressure P
- V_m = volume of gas required to form a monolayer
- C = constant relating to heat of adsorption

A plot of $P/V (P_0 - P)$ as a function of P/P_0 is linear within the relative pressure range of 0.05 to about 0.35 provided the adsorption isotherm is of the sigmoid or S-shaped type. Deviations from linearity occur below and above this relative pressure range. They are negative up to 0.05 and positive above 0.35.

The experimental data for the two shales and the primary inorganic particles were plotted according to the BET equation and they are presented in Figures 6, 7, and 8. These adsorption isotherms are in excellent agreement with the BET theory. The volume of nitrogen, V_m , required to form a monolayer was calculated from the slope and intercept of these isotherms and then translated into area units, sq. meters per gram, using 16.2 \AA . (6) as the area of the adsorbed nitrogen molecule.

Oil Shale

Surface Area. The surface areas of the two shales are presented in Table I. That of the rich oil shale remained essentially constant with respect to degassing time while that from the leaner shale differed by about 0.14 sq. meter per gram. Why the surface area dropped was not known because the samples did not appear to be completely degassed before 96 hours. The values selected to represent the shale particles, 0.75 and 0.58 sq. meter per gram, were those after degassing for 96 hours. These values when converted to surface areas per cubic centimeter, were very close, 1.22 and 1.24 sq. meters per cc. respectively. They are about 20 times the surface area of nonporous spheres with a diameter midway between 44 to 74 microns when packed in a rectangular pattern and each successive layer resting in the depressions provided by the previous layer.



NITROGEN ADSORPTION-DESORPTION ISOTHERMS.

Table I. - Surface Area of Oil Shale, Particle Size, 44 to 74 Microns

Oil Shale	Weight, gms.	Degassing Temp., °F.	Degassing Time, hrs.	V _m cc./g.	Surface Area, Sq. M/g.	Surface Area, Sq. M/cc.
28.6 GPT ^{1/}	5.056	220	8	0.850	0.73	1.57
"	5.271	220	24	0.838	0.70	1.50
"	5.080	220	96	0.690	0.59	1.27
"	4.885	220	96	0.646	0.58	1.24
75 GPT	3.609	220	8	0.616	0.75	1.22
"	3.609	220	60	0.594	0.72	1.17
"	3.930	220	96	0.616	0.75	1.22

^{1/} Gallons per ton

Much of the surface area of the shale particles was probably contributed by surface roughness, induced fractures in the inorganic crystals exposed at the surfaces of these particles, and induced fractures in the organic matter itself brought about when the shale particles were prepared. Some of the surface area may be attributed to naturally occurring pores or capillaries with diameters less than 10 Å. If such exist, their surface area could not be determined directly from the adsorption-desorption isotherms nor their presence detected, because within the relative pressure region, 0.05 to 0.35 capillary condensation presumably does not occur and hysteresis therefore would not be evident. The coverage of nitrogen on the adsorbate within this region varies from less than a monolayer up to about 1.5 monolayers (5). The small measured surface area of the shale particles indicates that surfaces attributed to capillaries or pores accessible through openings less than 10 Å., if they occur, are not very large.

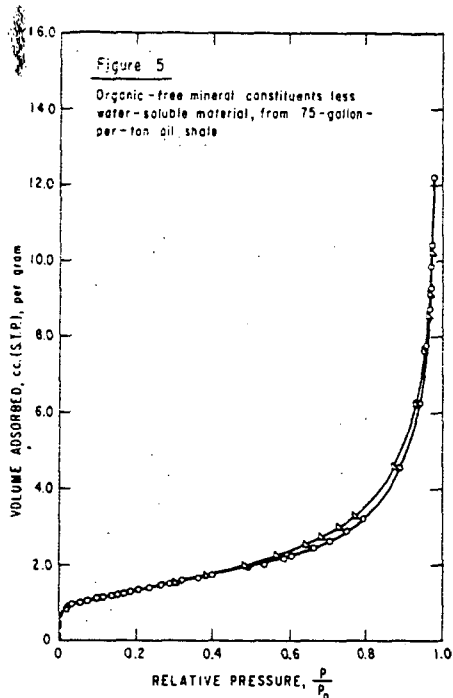
Pore Structure. Pore size, pore-size distribution, and pore volume of the adsorbent is obtained from adsorption-desorption isotherms and Kelvin's equation which relates the radius of a capillary to the relative pressure at which condensation takes place (11). Kelvin's equation is expressed as follows:

$$\ln \frac{P}{P_0} = \frac{-2\sigma V \cos \theta}{rRT}$$

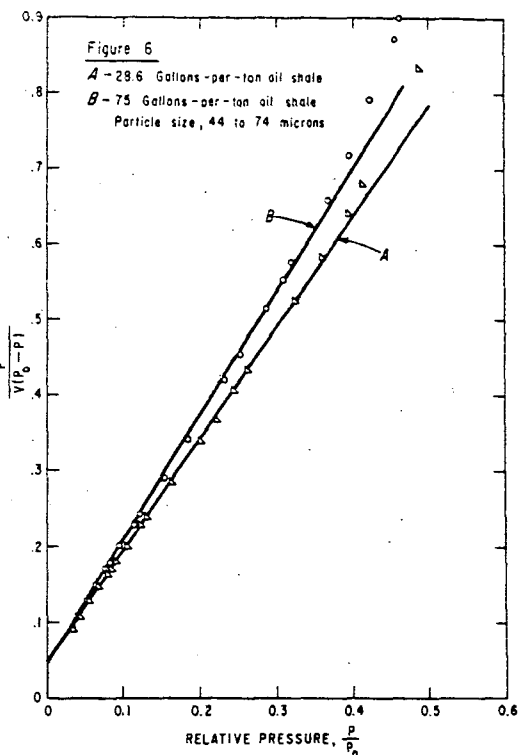
where

$\frac{P}{P_0}$	=	relative pressure
r	=	capillary radius
σ	=	surface tension of the adsorbate
V	=	molar volume of liquid adsorbate
θ	=	angle of contact
R	=	gas constant
T	=	absolute temperature

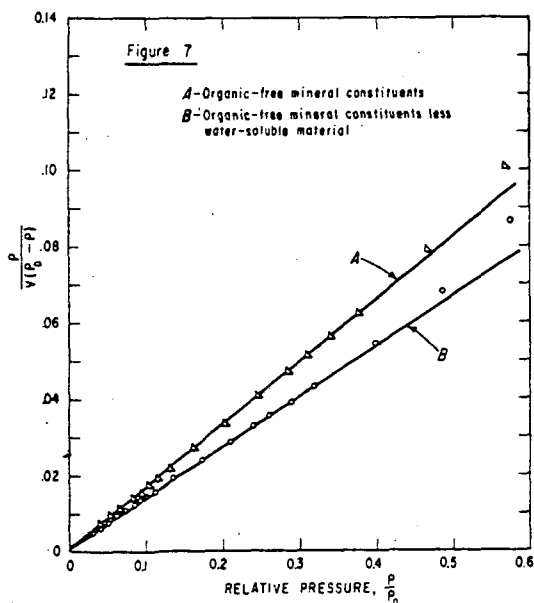
When capillary condensation occurs, the desorption isotherm usually lies well above the adsorption isotherm down to a relative pressure, near 0.4, which corresponds to the thickness of two monolayers of adsorbate. The nature of the pore structure determines the contour of the hysteresis loop in the desorption isotherm. Those which have hysteresis loops with plateaus followed by steep portions in the isotherm indicate a narrow pore-size distribution whereas curves free of inflection points indicate a broad pore-size distribution.



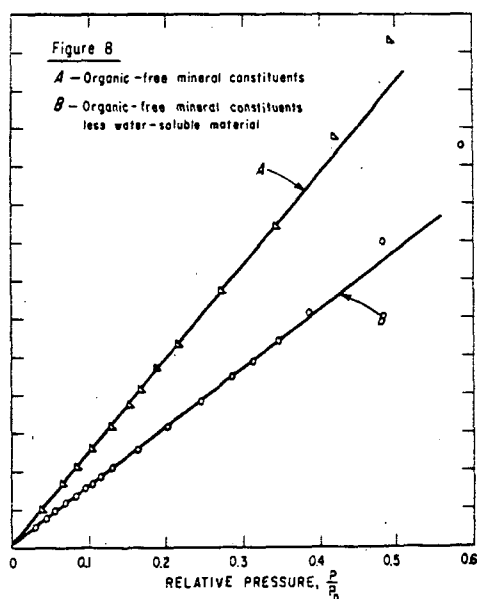
NITROGEN ADSORPTION-DESORPTION ISOTHERM.



NITROGEN ADSORPTION ISOTHERMS ACCORDING TO THE BET EQUATION.



NITROGEN ADSORPTION ISOTHERMS ACCORDING TO THE BET EQUATION.



The isotherms in Figures 1 and 2 show practically no hysteresis therefore little, if any, capillary condensation and evaporation. Deposition and removal of nitrogen apparently involved similar physical forces. This phenomenon indicates that the shale particles contained no appreciable amount of pores and/or capillaries with radii of the pore openings ranging from 10.5 to 235 A. as determined by Kelvin's equation.

Pore Volume. The pore volume can be calculated, from the quantity of nitrogen adsorbed between the relative pressure of 0.4 to 1.0. In Type II adsorption isotherms, however, which approach P_0 asymptotically; the relative pressure at which capillary condensation is complete and interparticle condensation begins is not readily discernible. In Figures 1 and 2 the relative pressure selected for calculating pore volume was the intercept between the extrapolated near linear portions of each adsorption isotherm. In both isotherms the intercept occurred at 0.96. At this point all capillary condensation should be completed and all pores accessible through openings with radii up to 235 A. should be filled with liquid nitrogen. Reis (11) points out that there is reason to believe that in Type II isotherms, adsorption above a relative pressure of 0.90 may be interparticle condensation principally.

The pore volumes of the shale particles calculated from two different relative pressures, 0.96 and 0.90, are given in Table II. The value 0.808 was used as the density of nitrogen at the liquefaction pressure. As noted in Table II, the relative pressure selected to represent completion of capillary condensation significantly influences the calculated pore volume. The actual value may be somewhere between these two limits.

Table II. - Pore Volume of Oil-Shale Particles, 44 to 77 Microns

	Weight, gms.	Pore Volume			
		$\frac{P}{P_0} = 0.96$		$\frac{P}{P_0} = 0.90$	
		cc./gm.	Vol. %	cc./gm.	Vol. %
Oil Shale					
28.6 GPT	4.885	0.0013	0.28	0.0005	0.11
75 GPT	3.930	0.0013	0.21	0.0006	0.10

The pore volumes calculated from either relative pressure are small. These values, although small, may be higher than the true pore volume. Induced minute fractures in the shale particles as result of crushing and interparticle condensation probably contribute to these volumes. Because the isotherms in Figures 1 and 2 exhibit practically no hysteresis, they indicate absence of pore volume accessible through pore openings with radii smaller than 100 A.

Inorganic Constituents

Surface Area. The surface area of the primary inorganic particles free of organic matter and those free of both organic matter and water-soluble material were calculated from their respective BET plots, Figures 7 and 8, and presented in Table III. The particles free of water-soluble material had the higher value. This was not expected because of the calcium sulfates present. The increase in surface area over the initial inorganic particles may be attributed to separation of the platelet structure of some clay minerals, etching on the surface of minerals slightly soluble in water, removal of material other than calcium sulfate or a combination of these factors.

Pore Structure. In Figures 3, 4, and 5 the desorption isotherms exhibit hysteresis characteristic of porous materials yielding Type II isotherms. The hysteresis loops in

Table III. - Surface Area of Primary Inorganic Particles

Primary Inorganic Particles	Weight, gms.	Degassing Temp., °F.	Degassing Time, hrs.	V _m cc./g.	Surface Area Sq. M./g.
28.6 GPT Oil Shale <u>1/</u>	6.261	600	16	0.969	4.24
75 " " <u>1/</u>	6.915	600	16	1.081	4.73
28.6 " " <u>2/</u>	5.711	600	16	0.713	3.12
75 " " <u>2/</u>	6.323	600	16	1.029	4.15

1/ Initial2/ Free of water-soluble material

the respective figures begin at relative pressures near 0.96, 0.97, 0.97 and all join the adsorption isotherms near 0.4. The smooth contours indicate that the pore openings in the primary inorganic particles have random pore-size distribution. Calculated from Kelvin's equation, the pore radii extend from 10.5 A. to 235 A. within the relative pressure region of 0.4 to 0.96 and 10.5 A. to 312 A. within 0.4 to 0.97. However, if condensation above a relative pressure of 0.90 is considered to be interparticle principally (11), the upper limit of the pore radii would be about 100 A.

Pore Volume. Pore volume per gram and percent porosity of the primary inorganic particles calculated from their respective isotherms, Figures 3, 4, and 5, are presented in Table IV. The volume occupied by the organic matter in 28.6- and 75-gallon-per-ton

Table IV. - Pore Volume of Primary Inorganic Particles

Primary Inorganic Particles	Weight, gms.	Pore Volume			
		P/P ₀ at 0.96		P/P ₀ at 0.90	
		cc./g	Vol.%	cc./g.	Vol.%
28.6 GPT Oil Shale <u>1/</u>	6.261	0.0096	2.66	0.0050	1.39
75 " " <u>1/</u>	5.711	0.0086	2.36	0.0029	0.80
75 " " <u>2/</u>	6.232	0.0079	2.16	0.0048	1.31

1/ Initial2/ Free of water-soluble material

oil shales is 0.151 and 0.417 cc. per gram respectively. The maximum amount of the organic matter in the respective shales that could exist within the pores or capillaries of the primary inorganic particles is 6.36 and 2.06 volume percent based on the pore volumes obtained at a relative pressure of 0.96. The corresponding volume percents with respect to 0.90 relative pressure are 3.31 and 0.70. The pore volumes presented in Table IV show that the primary inorganic particles are not very porous and that the distribution of the organic matter in the shales appear to be essentially interparticle and not intraparticle.

Organic Matter in Contact with the Mineral Constituents.

Using surface area data and some logical assumptions an estimate can be made of the amount of organic matter in contact with the mineral constituents. The assumptions were: The organic molecules were spheres, 10 or 20 A. in diameter; the total surface of the mineral constituents was accessible for contact; and the spherical molecules formed a rectangular pattern on the surface. Based on the organic matter's density, 1.07, the approximate molecular weights of the 10 A. and 20 A. molecules would be 340 and 2700 respectively. The amount of organic matter represented by one monomolecular layer in contact with the surface is presented in Table V. This table also presents the number of monolayers the total organic could form if evenly distributed over the surface. These estimates suggest that only a small part of the organic matter is bonded either chemically or physically to the surface of the mineral constituents.

Table V. - Estimated Amount of Organic Matter in Contact with the Mineral Constituents

Mineral Constituents	Surface Area, Sq. M./g.	Dia. of Organic Molecule, A.	Organic Matter Represented by One Monolayer, Wt. %	No. of Monolayers from Total Organic Matter
28.6 GPT Oil Shale	4.24	10	3.11	32
" "	4.24	20	1.57	64
75 GPT	3.12	10	0.57	175
" "	3.12	20	0.29	345

SUMMARY

Data from low-temperature nitrogen adsorption-desorption isotherms on Green River oil shale and its mineral constituents provide a better understanding of its basic physical structure. These data indicate that oil shale is a highly consolidated material with no significant micropore structure, pore volume, or internal surface. This type of physical structure is not favorable to surface dependent chemical or physical processes as it restricts reactive fragments or molecules to the interface. It appears that access to the interior must be preceded by removing, either chemically or physically, successive monolayers or molecules of organic or inorganic matter.

The primary inorganic particles contain pores and/or capillaries with random pore-size distribution. Their pore radii extend from 10.5 A. to 235 A. The pore volume accessible through these pore openings is about 0.01 cc. per gram and the amount of organic matter in the 28.6- and 75-gallon-per-ton oil shales that could exist within these pore spaces was calculated as 6.36 and 2.06 volume percent respectively. These values are considered as maximum volumes. If condensation above a relative pressure of 0.90 was interparticle condensation principally, the volume percents would be about one half. The data show that the distribution of the organic matter within the inorganic matrix is essentially interparticle and not intraparticle.

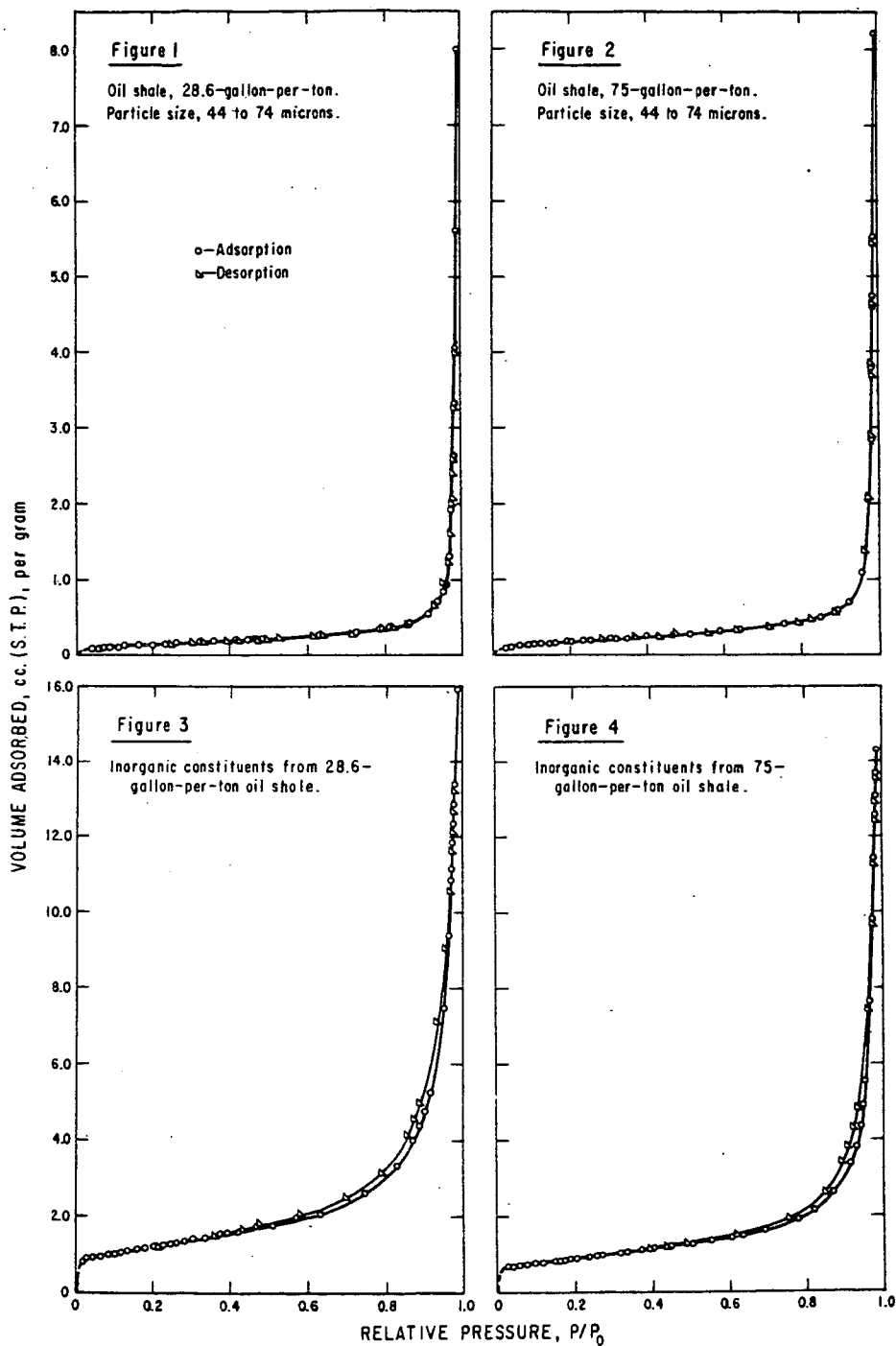
The primary inorganic particles contain no extensive micropore structure as evidenced by the surface area, about 4 sq. meters per gram. Estimates made from surface area values and logical assumptions suggest that only a small percentage of the organic matter is in direct contact with the surfaces of the mineral constituents.

ACKNOWLEDGMENT

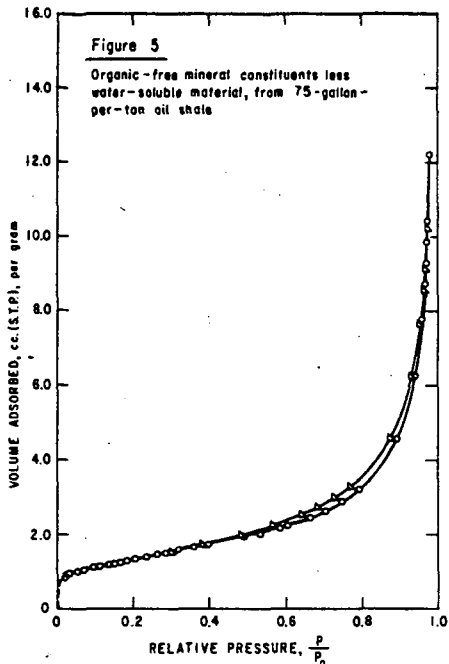
This work was done under a cooperative agreement between the Bureau of Mines, U. S. Department of the Interior, and the University of Wyoming.

Literature Cited

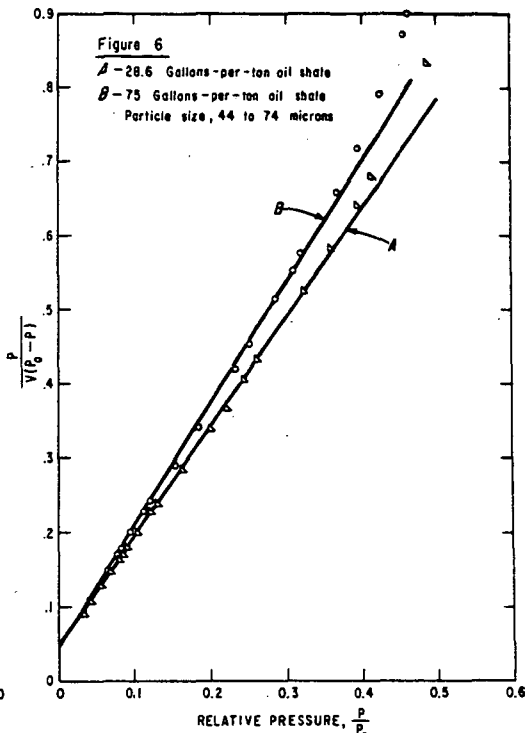
1. Barr, W. E., and Anhorn, V. J., "Scientific and Industrial Glass Blowing and Laboratory Techniques," p. 257, Industrial Publishing Co., Pittsburgh, Pa., 1949.
2. Brunauer, S., "The Adsorption of Gases and Vapors," p. 95, Princeton University Press, Princeton, N. J., 1943.
3. Brunauer, S., Emmett, P. H., Teller, E. J., J. Am. Chem. Soc. 60, 309 (1938).
4. Emmett, P. H., "Catalysis," Vol. 1, p. 31, Reinhold Publishing Corp., New York, 1954.
5. Emmett, P. H., Ind. Eng. Chem., 37, 639 (1945).
6. Emmett, P. H., Brunauer, S., J. Am. Chem. Soc., 59, 1553 (1937).
7. Hull, W. Q., Guthrie, B., Sippelle, E. M., Ind. Eng. Chem. 43, 2 (1951).
8. Matzick, A., Ruark, J. R., Putman, M. W., U. S. Bur. of Mines Rept. Invest. 5145, November 1955.
9. McKee, R. H., "Shale Oil," p. 150, The Chemical Catalog Co., Inc., New York, 1925.
10. "Oil Shale and Cannel Coal," Vol. 2, p. 345, The Institute of Petroleum, Mason House, 26 Portland Place, London, W 1, 1951.
11. Reis, H. E., Jr., "Advances in Catalysis," Vol. 4, p. 87, Academic Press Inc., Publishers, New York, 1952.
12. Ruark, J. R., Berry, K. L., Guthrie, B., U. S. Bur. of Mines Rept. Invest. 5279, November 1956.
13. Stanfield, K. E., Frost, I. C., McAuley, W. S., Smith, H. N., U. S. Bur. of Mines Rept. Invest. 4825, p. 18, November 1951.
14. Tisot, P. R., Murphy, W. I. R., J. Chem. Eng. Data, Vol. 5, No. 4, 558 (1960).



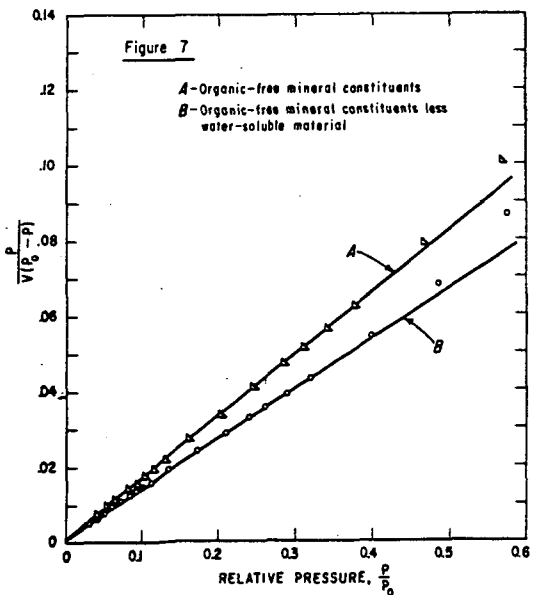
NITROGEN ADSORPTION-DESORPTION ISOTHERMS.



NITROGEN ADSORPTION-DESORPTION ISOTHERM.



NITROGEN ADSORPTION ISOTHERMS ACCORDING TO THE BET EQUATION.



NITROGEN ADSORPTION ISOTHERMS ACCORDING TO THE BET EQUATION.

